



Martin, Emily (2025) *A convergent route towards marine polycyclic ethers via a novel centrosymmetric approach*. PhD thesis.

<https://theses.gla.ac.uk/85174/>

Copyright and moral rights for this work are retained by the author

A copy can be downloaded for personal non-commercial research or study, without prior permission or charge

This work cannot be reproduced or quoted extensively from without first obtaining permission from the author

The content must not be changed in any way or sold commercially in any format or medium without the formal permission of the author

When referring to this work, full bibliographic details including the author, title, awarding institution and date of the thesis must be given

Enlighten: Theses

<https://theses.gla.ac.uk/>
research-enlighten@glasgow.ac.uk

A Convergent Route Towards Marine Polycyclic Ethers via a Novel Centrosymmetric Approach

Emily Martin

Thesis submitted in the fulfilment of the requirements for the Degree of
Doctor of Philosophy

School of Chemistry
College of Science and Engineering
University of Glasgow

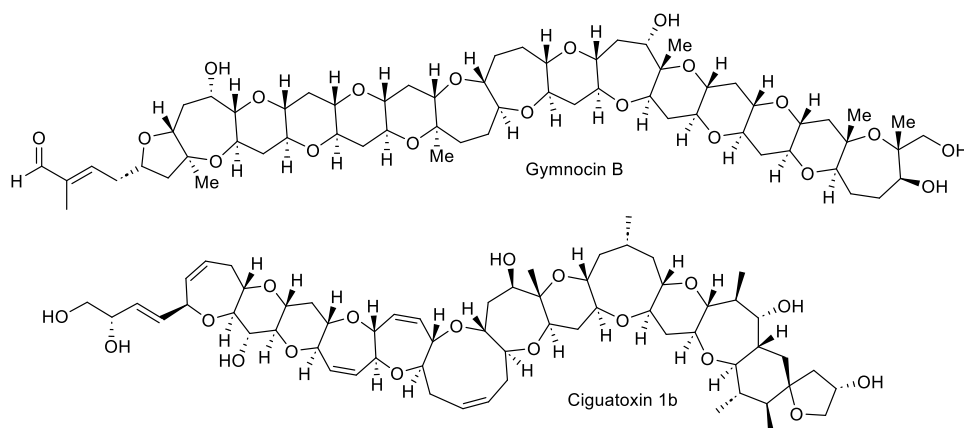
December 2024



**University
of Glasgow**

Abstract

Marine ladder polyether (MLP) toxins are a family of toxins produced by various dinoflagellates species. These natural products exhibit a wide array of toxic and pharmaceutical effects. Their complex structures and potentially useful bioactivities make them an attractive total synthesis target. Previous total syntheses of the MLP toxins suffer from large step counts and low overall yields, which presents a challenge for investigating their biological effects.



This project exploits the hidden symmetry within the MLP toxins. This project demonstrates a bidirectional synthetic approach to MLP toxins with a key desymmetrisation step in order to diverge fragments when necessary. This bidirectional approach increases synthetic efficiency by decreasing overall step count.

This thesis focuses on two main aims; attempts towards the total synthesis of gymnocin B, and the synthesis of various MLP fragments. A convergent bidirectional route to gymnocin B has been developed and efforts have been made at its completion. To fully demonstrate the versatility of this approach, fragments from an assortment of MLPs have been synthesised from a single key symmetric intermediate.

Table of Contents

Acknowledgements	iv
Author's Declaration	v
Abbreviations	vi
1. Introduction	1
1.1 Polycyclic ether toxins	1
1.1.1 Biosynthesis	2
1.1.2 Toxicology	4
1.1.3 Therapeutic Potential	5
1.2 Strategies for MLP synthesis	6
1.2.1 Biomimetic strategies	7
1.2.2 Reductive etherification	13
1.2.3 Yamaguchi esterification/lactonization	15
1.2.4 Iterative polypyran synthesis	18
1.2.5 Ring-closing metatheses	21
1.3 Gymnocins	22
1.3.1 Previous total synthesis of gymnocin B	23
1.4 Bi-directional syntheses and desymmetrisation techniques	26
1.5.1 First non-enzymatic desymmetrisation	27
1.5.2 Synthesis of the AB fragment of hemibrevetoxin B	28
1.5.3 Desymmetrisation of a centrosymmetric bis-aldehyde	30
1.5.4 Synthesis of enyne 188 and elatenyne 187	32
2. Project aims and strategy	36
3. Previous Work in Clark Group	40
3.1 Synthesis of diketone 210	40
3.2 Desymmetrisation	45
3.2.1 CBS reduction	45
3.2.2 Metal-catalysed hydrosilylation	46
4. Results and Discussion	48
4.1 Synthesis of diketone 210	48
4.2 Desymmetrisation of diketone 210	56
4.2.1 Background	56
4.2.2 Previous mechanistic studies	58
4.2.3 Results of desymmetrisation of diketone 210	61

4.3 Towards the total synthesis of gymnocin B	64
4.3.2 Attempts towards gymnocin B	65
4.4 Introduction of methyl groups	67
4.4.1 C-H insertion	67
4.4.2 α -Carbon functionalisation	73
4.5 Synthesis of fragments	75
4.5.1 Ring expansions in MLP synthesis	78
4.5.1 Synthesis of fragments via TMS-diazomethane ring expansion	81
4.5.2 Other single-carbon ring expansion methods	83
4.5.3 [2+2] cycloaddition/rearrangement	85
5. Conclusion	92
5.1 Summary of work	92
5.1.1 Synthesis of diketone 210	92
5.1.2 Desymmetrisation of diketone 210	93
5.1.3 Synthesis of MLP fragments	94
5.2 Future work	96
5.2.1 Synthesis of fragments	96
5.2.2 Total synthesis of gymnocin B	98
6. Experimental	100
6.1 Synthesis of reagents	101
6.2 Experimental procedures	106
7. References	133
8. Appendix	145
8.1 ^1H and ^{13}C NMR Data	145
8.2 X-ray crystal structure data	159

Acknowledgements

Firstly, I would like to give thanks to my supervisor, Professor J. Stephen Clark, for giving me the opportunity to work on this project. His guidance and support over the last four years has been invaluable.

To my second supervisor, Dr. Alistair Boyer, I would like to say thank you for the advice and encouragement over the first three years of my PhD. Thank you for welcoming me into the lab, teaching me the rules to a variety of card games, and all of the lunchtime chats.

I would like to thank the Schmidt group, Niamh and Iona, for your friendship over the last year. You have made a stressful final year a lot easier, and I am so grateful to have met you both. The Prunet group; Hollie and J.B., thank you for making the lab such a fun place for the last couple of years. It wouldn't have been the same without you. Sophie, Justin, Jess, and Matt W., thank you for all of the lunches, card games, board games, and pub quizzes. Thank you to the rest of the Clark group for making the lab and office such a great place to work. To the postdocs, Myron, Venky, Jimmy, and Jordan, thank you for teaching me so much and always being willing to give advice. I would also like to thank all of the technical staff at the university and Karen and Finlay from stores for keeping everything running so smoothly.

I would like to thank my family for the encouragement and support over these last four years. A special thank you to my grandad Noel, who saw me begin this journey but sadly isn't here to see me finish it. I hope I've done you proud.

The most important thank you of all goes to my fiancé, James. Thank you for your unwavering love, support, and patience throughout this whole experience. Thank you for believing in me even when I didn't believe in myself. I genuinely couldn't have done this without you.

Author's Declaration

I declare that the thesis presented here is solely my own work, except where explicit reference is made to the contribution of others. This thesis has not been submitted, nor is currently being submitted, in candidature for any other degree.

Emily Martin

Abbreviations

Ac	acetyl
AIBN	azobisisobutyronitrile
APCI	atmospheric pressure chemical ionisation
aq.	aqueous
Ar	aryl
BINAP	(2,2'-bis(diphenylphosphino)-1,1'-binaphthyl)
BINOL	1,1'-Bi-2-naphthol
Bn	benzyl
Boc	<i>tert</i> -butyloxycarbonyl
Bz	benzoyl
Calcd	calculated
CBS	Corey-Bakshi-Shibata
CFP	Ciguatera fish poisoning
COD	cyclooctadiene
COPD	chronic obstructive pulmonary disease
CSA	camphorsulfonic acid
DABCO	1,4-diazabicyclo[2.2.2]octane
DBU	1,8-diazabicyclo[5.4.0]undec-7-ene
DCE	dichloroethane
DMAP	4-dimethylaminopyridine
DMDO	dimethyl dioxirane
DMP	Dess-Martin periodinane
DMSO	dimethyl sulfoxide

<i>dr</i>	diastereomeric ratio
<i>ee</i>	enantiomeric excess
ESI	electrospray ionisation
h	hour(s)
HLADH	horse liver alcohol dehydrogenase
HMDS	hexamethyldisilazane
HPLC	high performance liquid chromatography
HRMS	high resolution mass spectrometry
IBX	2-iodoxybenzoic acid
IR	infrared
KIE	kinetic isotope effect
LD ₅₀	Median lethal dose
LDA	lithium diisopropylamide
LHMDS	lithium hexamethyldisilazane
LRMS	low resolution mass spectrometry
<i>m</i> CPBA	<i>meta</i> -chloroperbenzoic acid
min	minute(s)
MLP	Marine ladder polyether
MS	molecular sieves
NMDAR	<i>N</i> -methyl-D-aspartate receptor
NMO	<i>N</i> -methylmorpholine <i>N</i> -oxide
NMR	nuclear magnetic resonance
NSP	neurotoxic shellfish poisoning
P	protecting group

Ph	phenyl
PPTS	pyridinium <i>p</i> -toluensulfonate
<i>p</i> -TSA	<i>para</i> -toluene sulfonic acid
Quant.	Quantitative
RCM	ring closing metathesis
rt	room temperature
TBAB	tetra- <i>n</i> -butylammonium bromide
TBAF	tetra- <i>n</i> -butylammonium fluoride
TBAI	tetra- <i>n</i> -butylammonium iodide
TBDPS	<i>tert</i> -butyldiphenylsilane
TBS	<i>tert</i> -butyldimethylsilane
TES	triethylsilane
TIS	triisopropyl silane
Tf	Triflate
THF	tetrahydrofuran
THP	tetrahydropyran
TLC	thin layer chromatography
TMS	trimethylsilane
TPAP	tetrapropylammonium perruthenate

1. Introduction

1.1 Polycyclic ether toxins

Marine ladder polyether (MLP) toxins are a family of complex biotoxins, produced by dinoflagellate species, which possess a range of biological activities. The common structural feature within this family of toxins is a *trans*-fused polycyclic ether skeleton. The majority of ring junction atoms in MLPs are hydrogens, although these can also include methyl groups (Figure 1). The first reported member of this family was brevetoxin B **4** (Figure 1),¹ and, as of now, more than 50 members have been isolated.²

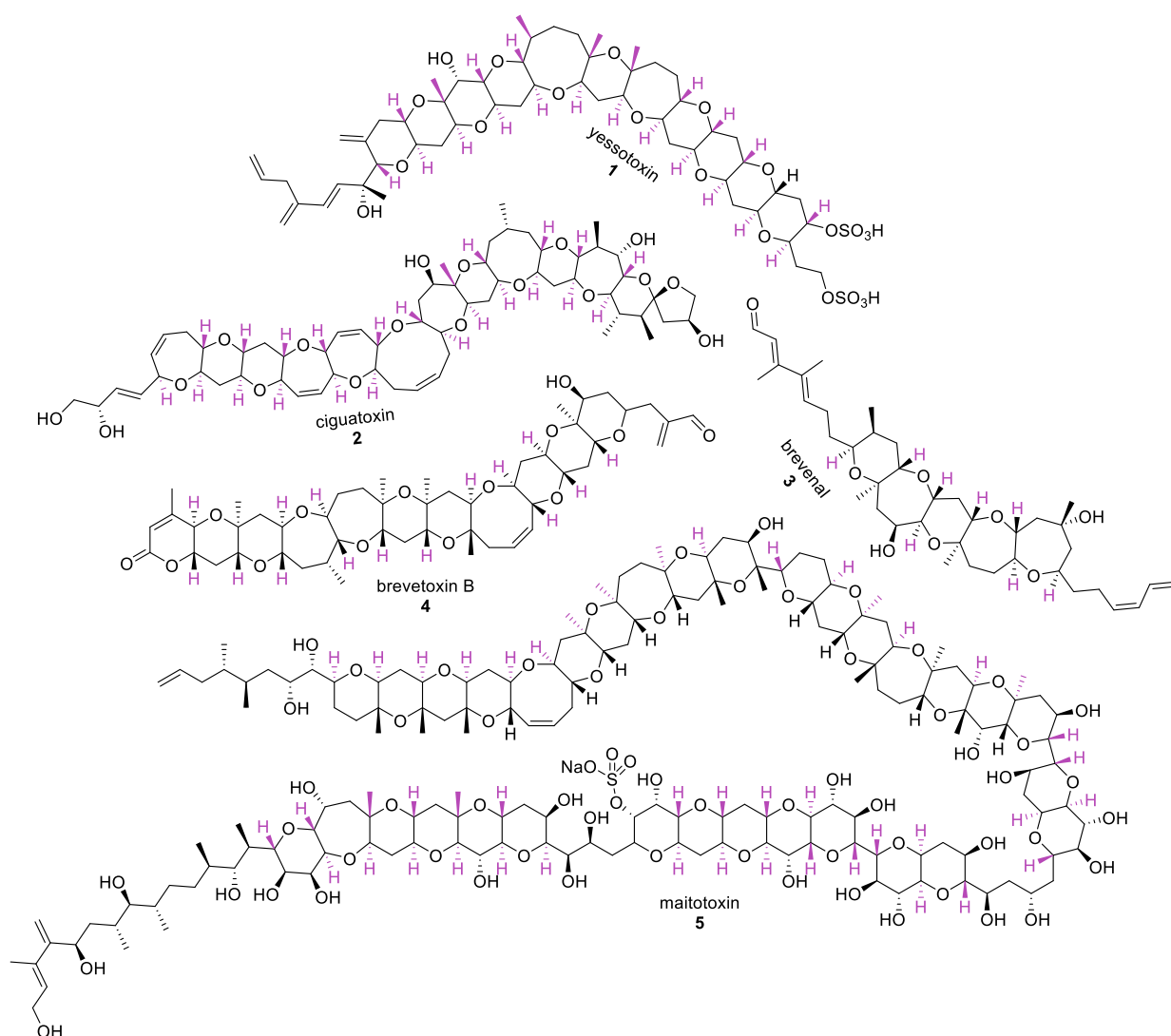


Figure 1. Examples of some MLP toxins

Notable sociological and environmental impacts of these toxins include food poisoning and harmful algal blooms known as ‘red tides’. Red tides are harmful algal blooms that lead to mass loss of marine life as a result of hypoxic conditions and biotoxins released by the algal species. MLP toxins are a major cause of the death of

marine life during these algal blooms, being produced by *Karenia brevis* and *Karenia mikimotoi* during red tide events.³ Red tides have a great impact on marine life, and this can occur from direct contact with the toxins in the water or consumption of toxin-contaminated prey. It has been reported that these red tides cause mass death to various fish species, while also causing smaller die-offs of sea turtles, sharks, and dolphins.⁴ A bloom which occurred on the United States Atlantic coast from June 1987 – May 1988 led to the death of approximately 700 bottlenose dolphins. Along with their impact on marine life, MLP toxins can cause disease in humans from consumption of contaminated seafood. Maitotoxin **5** and ciguatoxin **2** are the most common MLP toxins involved in seafood poisoning, known as ciguatera fish poisoning (CFP).⁵ CFP occurs when toxin-contaminated seafood is ingested, and can cause a wide-range of symptoms, including nausea, vomiting, and diarrhea.⁶ Though rarely fatal, CFP symptoms can sometimes persist for months or years.⁷ These toxins are also involved in the negative impacts of red tides.

Interestingly, brevisin **6** deviates from the rest of the MLP family in both structure and toxicity; it consists of an ‘interrupted’ structure, made up of two polycyclic ether fragments connected by a methylene group, (Figure 2). Brevisin **6** is non-toxic, with the ability to act as a brevetoxin antagonist.⁸

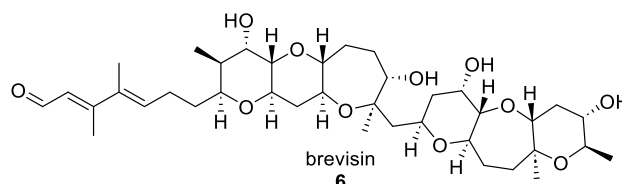
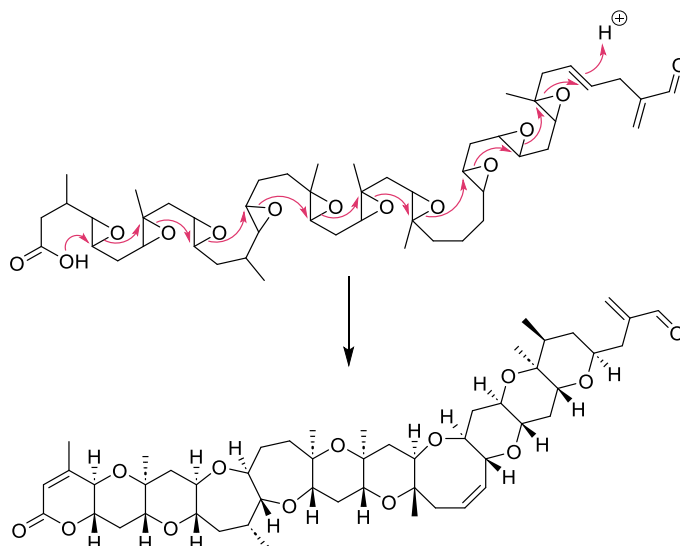


Figure 2. Structure of brevisin **6**

1.1.1 Biosynthesis

In 1984, Nakanishi reported a proposed biosynthesis of hemibrevetoxin B,⁹ in which the cyclic backbone is formed via an epoxide-opening cascade, (Scheme 1). Hemibrevetoxin B contains eight methyl groups along the cyclic backbone; he suggested that these could either originate from *S*-adenosylmethionine, propionate, or acetate, depending on their position on the backbone.



Scheme 1. Proposed biosynthesis of brevetoxin B⁹

Further investigations were conducted and in 1986, Nakinishi and coworkers reported the ¹³C assignments of brevetoxin B **4**.¹⁰ In order to do this, *Gymnodinium breve* was fed with [1-¹³C]-, [2-¹³C]-, [1,2-¹³C₂]acetates and methyl-¹³C-methionine. It was determined that 16 carbons were enriched from [1-¹³C]acetate, 30 carbons were enriched from [2-¹³C]acetate, and 4 carbons were enriched from methyl-¹³C-methionine, (Figure 3). From this data, it was clear that the backbone of brevetoxin B was not a simple polyketide, as can be seen from the various C-C bonds.

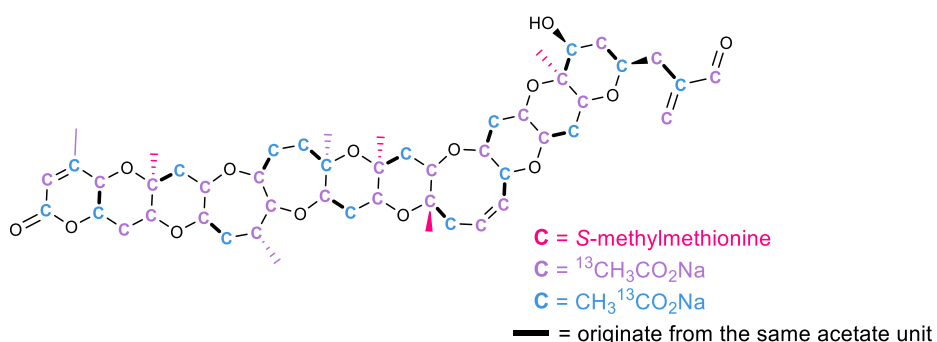
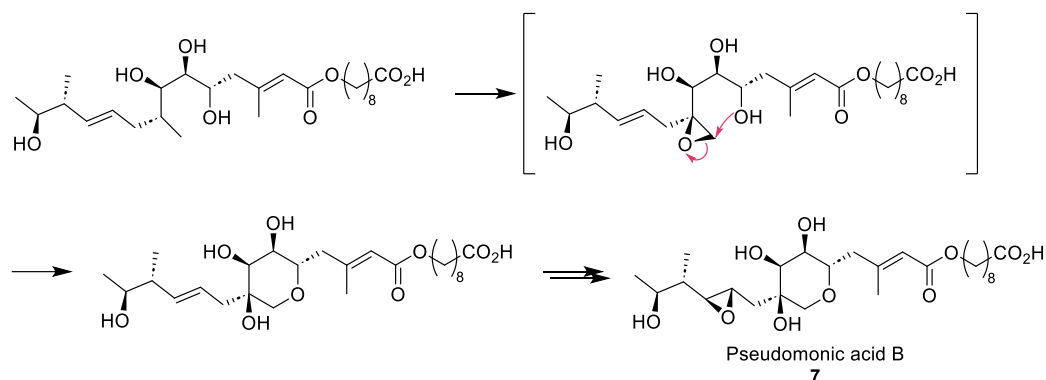


Figure 3. Origin of each carbon in brevetoxin B

A major flaw in the epoxide-opening cascade hypothesis is that it relies on the disfavoured 6-*endo-tet* cyclisation, as opposed to the more favourable 5-*exo-tet* cyclisation, in accordance with Baldwin's rules.^{11,12} However, there is precedent for such a transformation occurring in nature as an enzymatically controlled process. For examples, pseudomonic acid B **7** (PA-B) contain a tetrahydropyranyl (THP) unit which is key to its antibiotic properties. Willis and coworkers identified a tandem oxygenase/hydrolase enzyme which catalyses both the formation of the epoxide and

the subsequent nucleophilic attack of the hydroxy group onto the epoxide by 6-*endo-tet* cyclisation (Scheme 2).¹³ This process should be disfavoured according to Baldwin's rules. Thus, it could be imagined that such an enzyme exists for the biosynthesis of MLPs.



Scheme 2. 6-*endo-tet* cyclisation to form PA-B 7

1.1.2 Toxicology

As mentioned previously, the MLP toxin family shows an expansive range of bioactivities. The ciguatoxins are a class of MLPs which are sodium channel agonists, giving them neurotoxic effects. Their binding prevents normal channel activation and leads to changes in neurotransmitter release. They have shown LD₅₀ values (intraperitoneal injection) of 0.3 – 4 µg/kg,¹⁴ and so they are ‘category 1’ toxic as recognised by the European Union.¹⁵ These toxins can accumulate along the food chain, contaminating the seafood that humans consume.¹⁶ Ingesting ciguatoxin-containing seafood can lead to ciguatera fish poisoning, which affects up to 50,000 people per annum¹⁷ and is the most common type of seafood-related food poisoning.¹⁸ These toxins are such a concern that the European Union has organised the EuroCigua project I and II, in order to better understand the risks associated with CFP in Europe.

Along with CFP, there are other illnesses associated with the ingestion of MLP contaminated seafood. Neurotoxic shellfish poisoning (NSP) is linked to the consumption of shellfish that is contaminated with brevetoxins. Similar to ciguatoxins, brevetoxins are sodium channel agonists. They induce neurotoxicity by binding to voltage-gated sodium channels¹⁸ and have the ability to pass through cell membranes, including the blood-brain barrier. Interestingly, another polycyclic ether known as brevenal **3** has been suggested as a treatment for NSP. Brevenal **3** is a non-toxic compound produced by *Karenia brevis*, the same dinoflagellate species responsible

for the production of the brevetoxins. Brevetoxins bind to site 5 of voltage-gated sodium channels. Brevenal **3** has been shown to bind to a different, unknown site, and its binding has the ability to displace PbTx-3, reducing its toxic effects.¹⁹ An *in vivo* assay showed that pre-treatment of *Gambusia affinis* with brevenal increased their survival time after PbTx-3 exposure by almost three-fold.²⁰

Yessotoxins are calcium modulators; they target calcium channels, and can both increase and inhibit calcium influx in cells. The presence of sulfate groups makes it difficult for yessotoxins to be absorbed via the digestive tract, and so they are non-toxic when ingested.²¹ As a result of their impact on calcium channels, yessotoxins **1** exhibit cardiotoxic effects.²²

It is evident that MLP toxins demonstrate a wide-range of toxicities, and they have significant implications for human health as a consequence of their ability to cause food poisonings. Further research into MLPs is necessary in order to understand their toxic effects and develop treatments.

1.1.3 Therapeutic Potential

Despite their generally toxic effects, many of the MLP toxins have demonstrated therapeutic potential. The E-cadherin-catenin system is typically involved in tumour suppression, but it has been shown that alterations to this system contribute to tumour proliferation in breast, prostate, and intestinal cancers.²³ Ronzitti *et al.* examined the impact of yessotoxin **1** on MCF-7 breast cancer cells. They found that yessotoxin selectively disrupts the E-cadherin-catenin system (with no effect on the N- and K-cadherin systems), leading to suppression of MCF-7 cell proliferation.²⁴ However, the disruption of the E-cadherin-catenin system also leads to a reduction in cell adhesion, indicating yessotoxin **1** may also have the potential to facilitate metastasis. Protoceratins are cytotoxic MLPs produced by *Protoceratium reticulatum* which were first isolated in 2004 (Figure 4).²⁵ They are reported to be highly cytotoxic against human cancer cell lines with IC₅₀ values of < 0.0005 µM.²⁵

As well as their anti-cancer effects, there has been interest in the yessotoxins as anti-allergics. Blank *et al.* investigated these effects and demonstrated that yessotoxins have the ability to reduce the allergy response.²⁶

N-methyl-D-aspartate receptor (NMDAR) functioning has shown to be increased after incubation with brevetoxin-2. NMDARs are calcium-channels which enhance neuronal plasticity. The ability of brevetoxin-2 to upregulate NMDARs indicates their potential to improve stroke recovery.²⁷

Gambieric acids A-D (Figure 4) were isolated from *Gambierdiscus toxicus*, and have been shown to have extremely potent fungicidal effects. These compounds have only shown moderate toxicity towards mammalian cells, leading to interest in them as potential antifungal therapeutics.²⁸

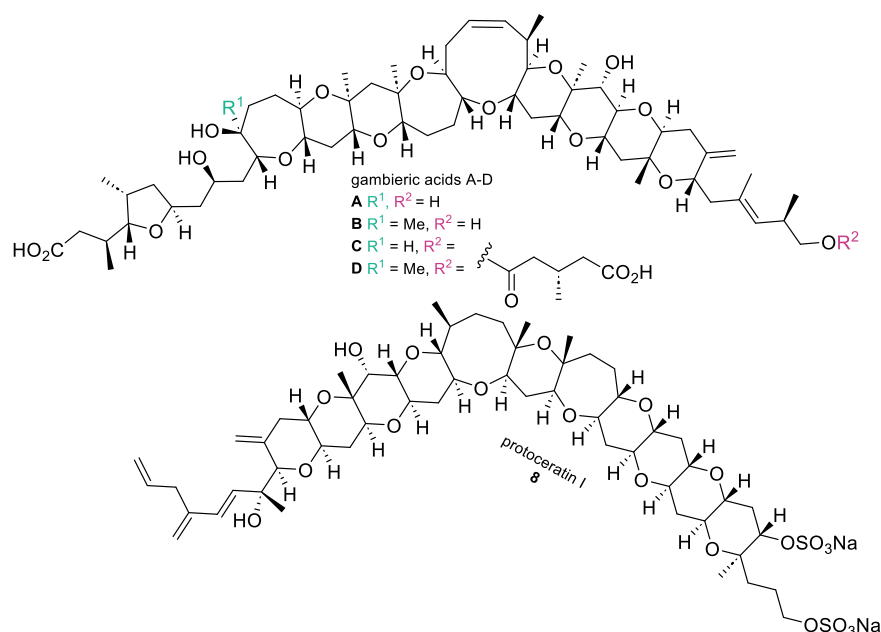


Figure 4. Structure of gambieric acids and protoceratin I

Brevenal **3** (Figure 1) is a non-toxic polycyclic ether produced by *Karenia brevis*, and despite its lack of toxicity, it shares many structural similarities with brevetoxins A and B. Interestingly, brevenal **3** reduces brevetoxin **4** cytotoxicity²⁰ and has shown promise as an anti-inflammatory therapeutic to treat diseases such as chronic obstructive pulmonary disease (COPD), cystic fibrosis, and asthma.²⁹ It is non-toxic towards human cells, and in *in vitro* studies it has decreased levels of proinflammatory chemokine IL-8 from human lung epithelial cells.²⁹ It also caused a reduction in TNF α production in MH-S lung macrophages.

1.2 Strategies for MLP synthesis

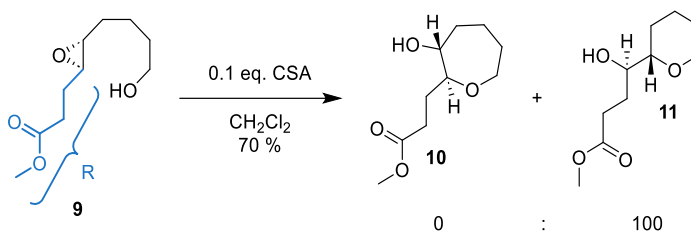
Evidently, MLPs demonstrate strong therapeutic potential for an extensive list of ailments. In order to further investigate their therapeutic abilities, it is imperative to

develop reliable and efficient synthetic methods. To date, there have been significant efforts in the literature towards developing synthetic strategies for MLPs.

1.2.1 Biomimetic strategies

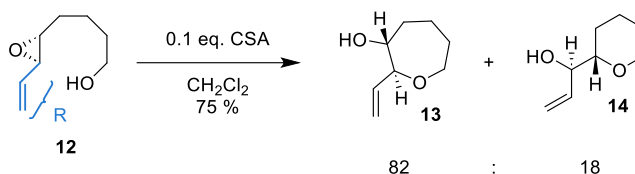
Many researchers have taken inspiration from the epoxide-opening cascade of the proposed biosynthesis to devise strategies for the synthesis of MLPs. Nicolaou *et al.* developed a reliable synthetic method to prepare both oxepane and tetrahydropyran systems *via* epoxide-opening ring-closure.³⁰

By tuning the **R group**, they were able to selectively produce oxepane rings over tetrahydropyran rings. When subjected to acidic conditions, epoxide **9** underwent 6-*exo* cyclisation to exclusively give the tetrahydropyran system **11** (Scheme 3).



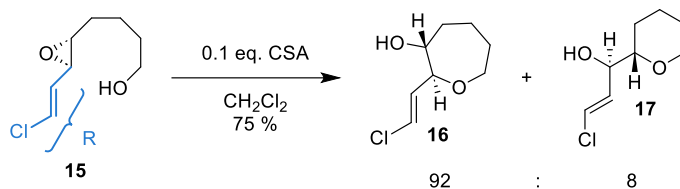
Scheme 3. 6-*exo* cyclisation to form tetrahydropyran **11**

However, when epoxide **12** was subjected to the same acidic conditions, it underwent a 7-*endo* cyclisation to give oxepane system **13** as the major product (Scheme 4). Nicolaou and coworkers postulated that this was due to the more electron-rich double bond which directs the cyclisation reaction.



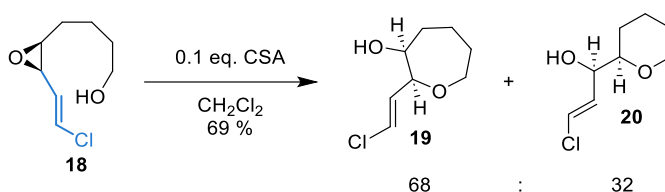
Scheme 4. 7-*endo* cyclisation to form oxepane **13**

Introduction of a vinyl chloride substituent in epoxide **15** provided the ability to tune the regioselectivity of the cyclisation even further. This was due to the increased electron-withdrawing nature of the chloride. This system gave oxepane system **16** with the undesired tetrahydropyran system **17** in an impressive 92:8 ratio (Scheme 5).



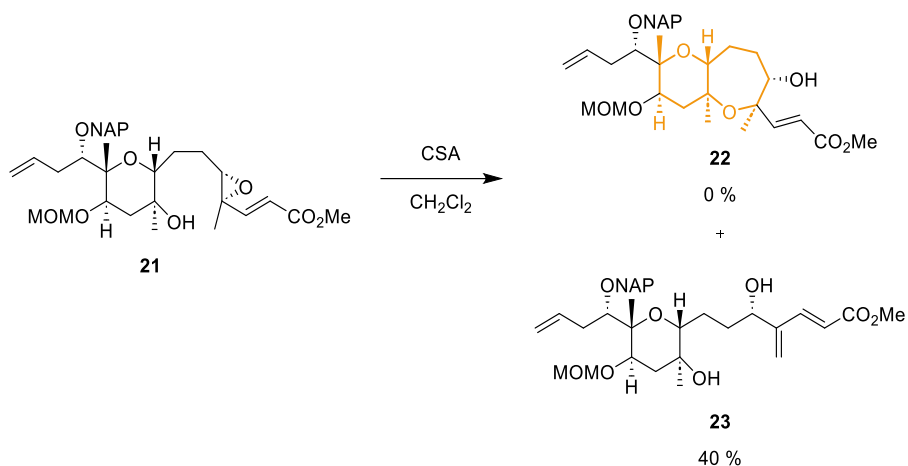
Scheme 5. 7-*endo* cyclisation of chloride **15** to form oxepane **16**

The scope of this method was expanded to include *cis* epoxides, although cyclisation reactions of these substrates were less selective towards the oxepane systems than reactions of the previously used *trans* epoxides (Scheme 6).



Scheme 6. Cyclisation of *cis* chloride **18**

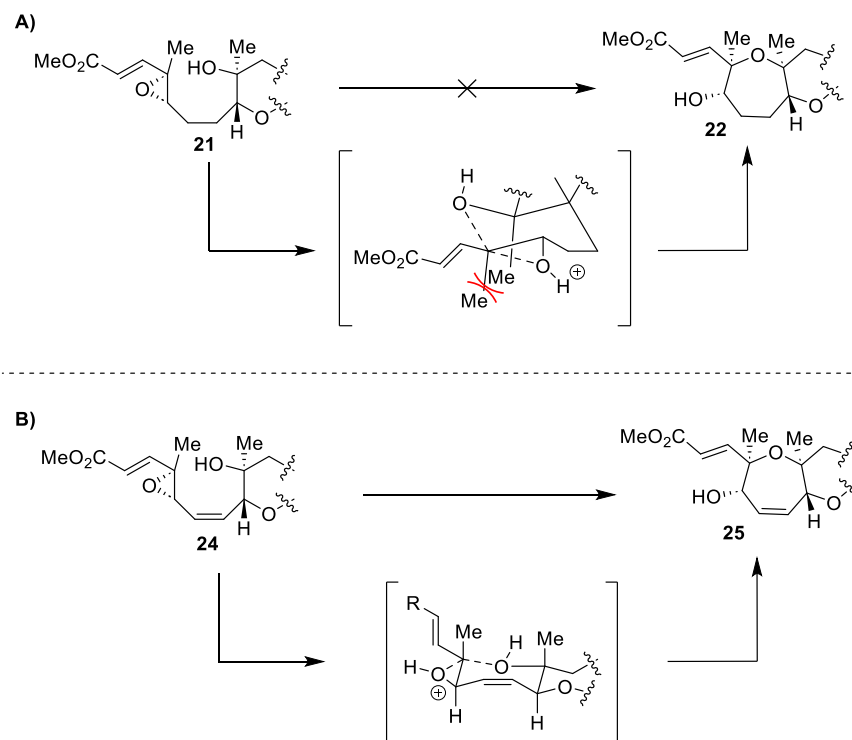
Despite the success of synthesising oxepane ring systems *via* a biomimetic 7-*endo* cyclisation reaction, previous attempts to produce *syn*-2,7-dimethyloxepane rings had been unsuccessful. In their synthesis of the LMN fragment of ciguatoxin C-CTX-1, Hirama and co-workers envisioned that they could use the method developed by Nicolaou to synthesise the M ring. Unfortunately, this reaction afforded none of the desired *syn*-2,7-dimethyloxepane system **22**, and the elimination product **23** was formed instead (Scheme 7).³¹



Scheme 7. Failed synthesis of *syn*-2,7-dimethyloxepane **22**

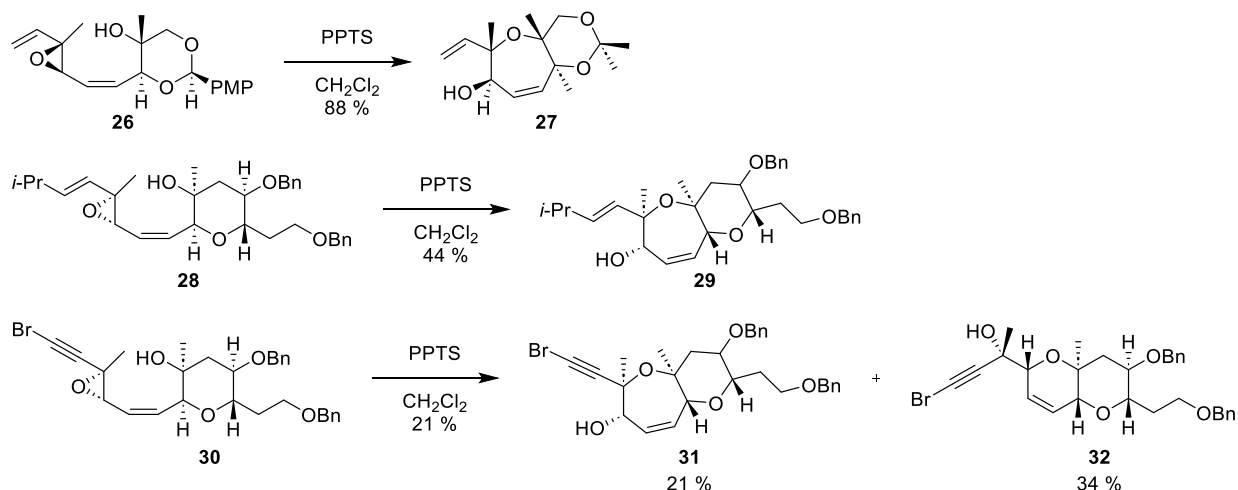
Mori *et al.* postulated that the failure of this reaction might have been due to the cycloheptane-type transition state that is required, which leads to both eclipsing strain and 1,3-dimethyl repulsion, thus disfavouring the cyclisation and leading to the

elimination product. They anticipated that the transition state for a cycloheptene-type transition state would be significantly more favourable, due to the adoption of a chair-like conformation in which the eclipsing strain and 1,3-dimethyl repulsion are reduced (Scheme 8).³²



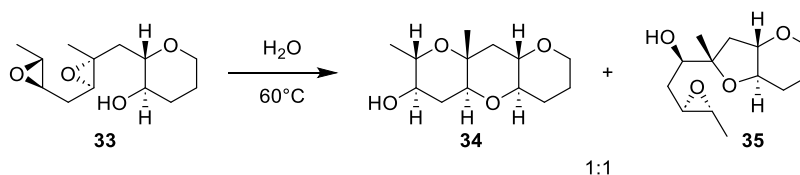
Scheme 8. A) Transition for cyclisation of **21** to form *syn* dimethyl oxepane **22**, B) transition state for cyclisation of **24** to form *syn* dimethyl oxepane **25**

In order to access the *syn*-2,7-dimethyloxepane system, a *cis* alkene was introduced between the ether and epoxide functionalities of the vinyl epoxides. Through a biomimetic epoxide-opening, the authors synthesised a variety of *syn*-2,7-dimethyloxepanes via a 7-*endo* cyclisation reaction (Scheme 9).



Scheme 9. Synthesis of *syn*-2,7-dimethyloxepanes **27**, **29**, and **31**

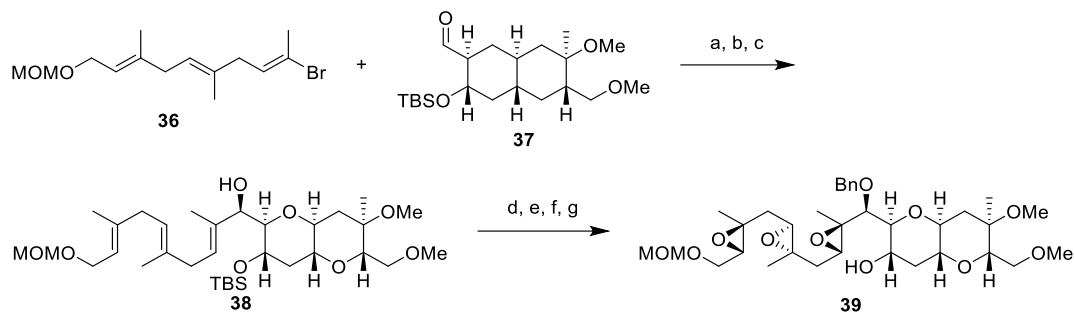
In their work towards the synthesis of the C-G fragment of brevisulcenal F, Jamison and coworkers employed a late-stage epoxide-opening cascade on a triepoxide intermediate.³³ In the past, cyclisation of a similar bis-epoxide had afforded the 6-*endo* cyclisation product **34** tetrahydropyran and undesired 5-*exo* cyclisation product tetrahydrofuran **35** in a 1:1 mixture (Scheme 10).



Scheme 10. Previous attempt at epoxide-opening cascade under neutral pH

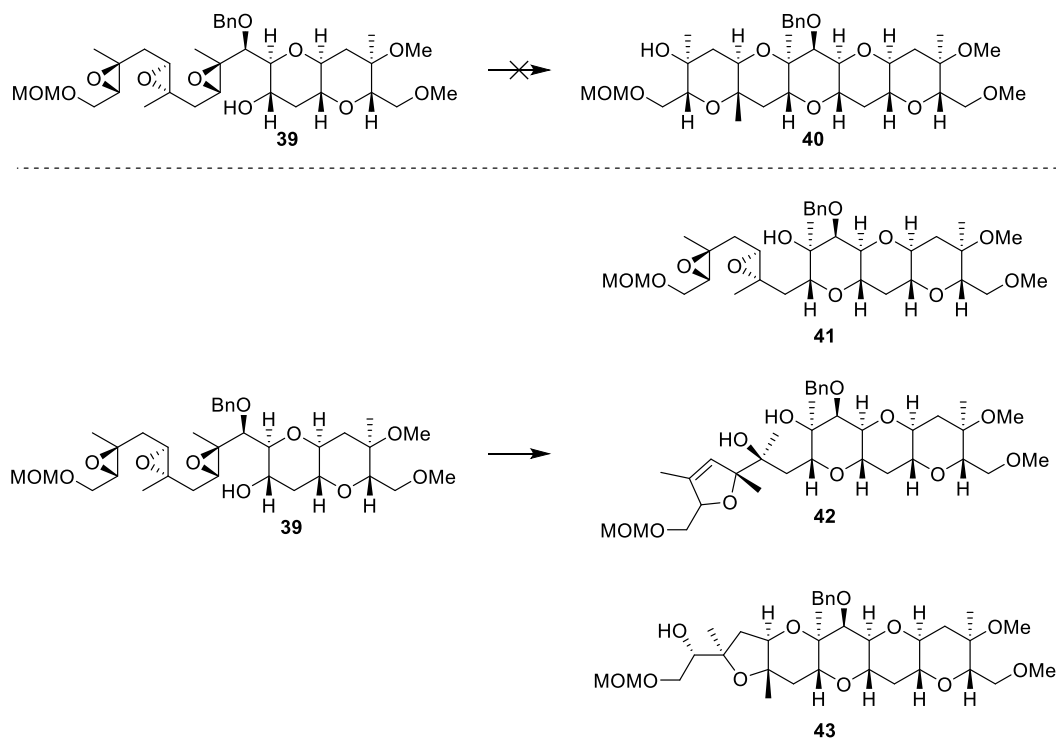
It is known that the pH of the reaction medium has a great impact on regioselectivity of epoxide-opening reactions.³⁴ Under basic conditions, the nucleophile will almost exclusively attack at the least hindered carbon, and this can be attributed to steric effects. However, under acidic conditions, there is a tendency for the nucleophile to attack at the more hindered carbon. Jamison and co-workers hypothesised that the use of a strong base would favour the *endo* cyclisation, as this would be a result of attack on the least hindered carbon.

Coupling of bicyclic aldehyde **37** and triene **36** followed by inversion of hydroxy group stereochemistry afforded the epoxidation precursor **38**. A two-step epoxidation sequence was necessary because the olefin proximal to the ring system was unreactive when tri-epoxidation was attempted in a single step (Scheme 11).



Scheme 11. Synthesis of triepoxide **39**. a) *t*-BuLi, Et₂O, -78 °C; then ZnBr₂; then **37**, Tol, 0 °C → rt, 78 %, *dr* >20:1, b) DMP, NaHCO₃, CH₂Cl₂, rt, c) NaBH₄, CeCl₃·7H₂O, MeOH, -40 °C, 76 %, *dr* 10:1, d) TBHP, Ti(O*i*-Pr)₄, L-(-)-DET, CH₂Cl₂, -20 °C, 92 %, *dr* >20:1, e) Shi epoxidation catalyst, oxone, (*n*-Bu)₄NHSO₄, K₂CO₃, pH 10.5, DMM/CH₃CN, 0 °C, 85 %, *dr* 5:1, f) BnBr, Ag₂O, TBAI, rt, g) TBAF, THF, rt

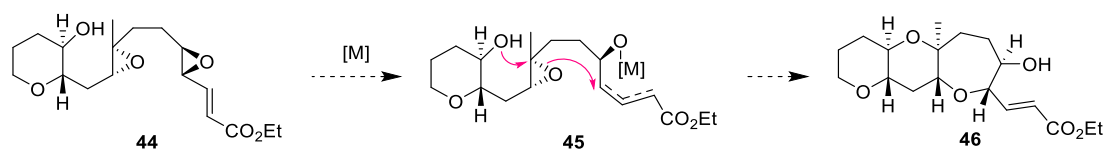
Unfortunately, attempted epoxide-opening reactions did not afford the desired product **40**. Different ratios of **41**, **42**, and **43** were instead produced depending on reaction conditions (Scheme 12). KHMDS at room temperature and NaHMDS at 80 °C produced **41** and **42**, and LHMDS at 80 °C gave almost exclusively **43** with a small amount of **42**.



Scheme 12. Results of attempted epoxide-opening cascade

Inspired by the above synthesis of oxepane rings, Jamison *et al.* imagined that an alkenyl-substituted epoxide with an activator might react with high *endo* selectivity and produce oxepane rings.³⁵ The chosen activator was a transition metal catalyst, which

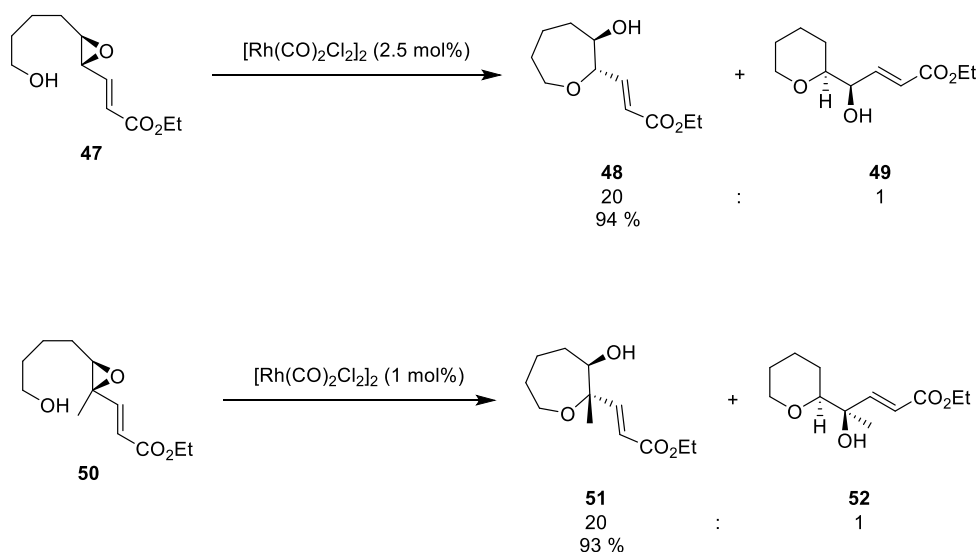
they expected to complex with the alkenyl side-chain of the epoxide, activating the epoxide for an *endo* cyclisation reaction (Scheme 13).



Scheme 13. Proposed cyclisation mechanism of bis-epoxide **44**

Even though application of Pd catalysis to activated alkenyl epoxides is a well-known technique, the authors decided to avoid the use of a Pd catalyst due to lack of examples of its use with oxygen nucleophiles. They discovered that $[\text{Rh}(\text{CO})_2\text{Cl}]_2$ had been used to activate alkenyl epoxides for opening by alcohols and amines. For this reason, they settled on $[\text{Rh}(\text{CO})_2\text{Cl}]_2$ as their chosen transition metal catalyst.

High *endo* selectivity was achieved, along with impressive yields for the synthesis of oxepanes **48** and **51**, from both di- and tri-substituted alkenyl epoxides **47** and **50** (Scheme 14).



Scheme 14. Successful Rh-catalysed *endo*-cyclisation of epoxides **47** and **50**

This procedure was then successfully implemented during a total synthesis of brevisin **6**. The ABC **61** and EF **56** fragments of brevisin **6** were synthesised, both of which contain an oxepane (Scheme 15).

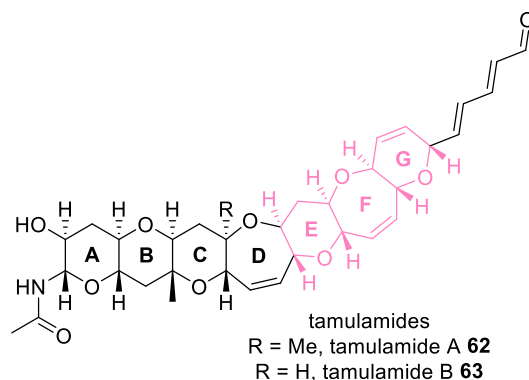
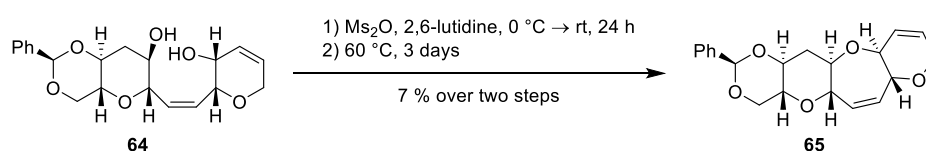


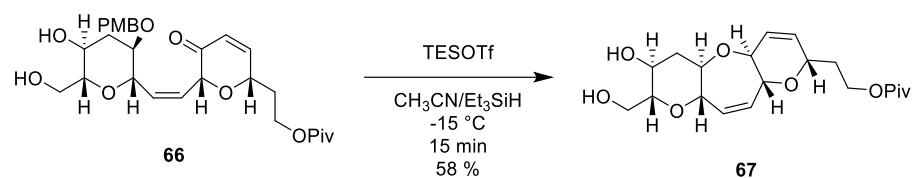
Figure 5. Structure of tamulamides A and B

Accessing 7-membered rings has been a significant challenge for synthetic chemists, and ring-closing metathesis (RCM) or ring-expansion reaction are often used to prepare oxepenes in polyether synthesis. In this work, a new method for the synthesis of 7-membered rings was reported. Initial attempts at etherification in order to close the D ring provided some challenges, with initial attempts using Mitsunobu conditions or activation of the allylic alcohol proving to be unsuccessful. The desired product **65** was accessed *via* mesylation and S_N2 ring-closure under elevated temperatures. Unfortunately, this product could only be accessed in a 7 % yield over two steps (Scheme 16), and so the researchers decided to explore a reductive etherification method in order to avoid the problems associated with the use of a reactive allylic alcohol.



Scheme 16. Low-yielding formation of E ring

The use of reductive etherification as a method for ring construction is not a new concept in polyether synthesis, but a major challenge that it presents is the stereoselectivity of the reaction. Jamison and Kelley attempted reductive etherification on enone **66**, including a pivaloyl protected ethyl alcohol in an attempt to easily access the dienal side chain of the EFG ring system after ring closure. The reductive etherification proceeded smoothly and afforded desired tricycle **67** in a 58 % yield, exclusively as a *trans* isomer (Scheme 17).



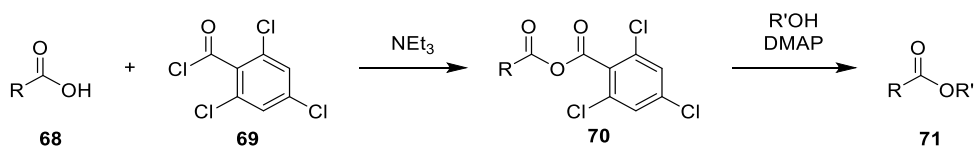
Scheme 17. Reductive etherification to form E ring

This method provides a reliable route for the synthesis of 7-membered rings in a single step under mild conditions. However, it is not compatible with substrates containing functional groups that are sensitive to reductive conditions.

1.2.3 Yamaguchi esterification/lactonization

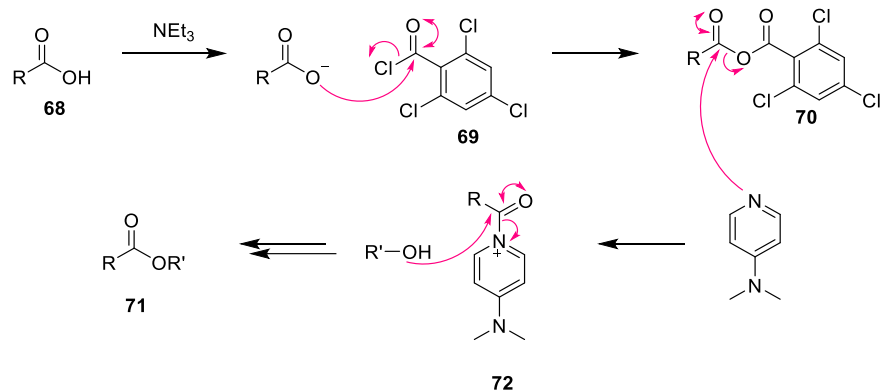
In their synthesis of gambieric acid, Sasaki and Fuwa employed the use of Yamaguchi's esterification and lactonisation techniques in order to both couple fragments and to form the larger ring systems.³⁷

The Yamaguchi esterification is a method for the production of esters under mild conditions in the presence of 2,4,6-trichlorobenzoyl chloride **69** and 4-dimethylaminopyridine (DMAP) (Scheme 18).³⁸



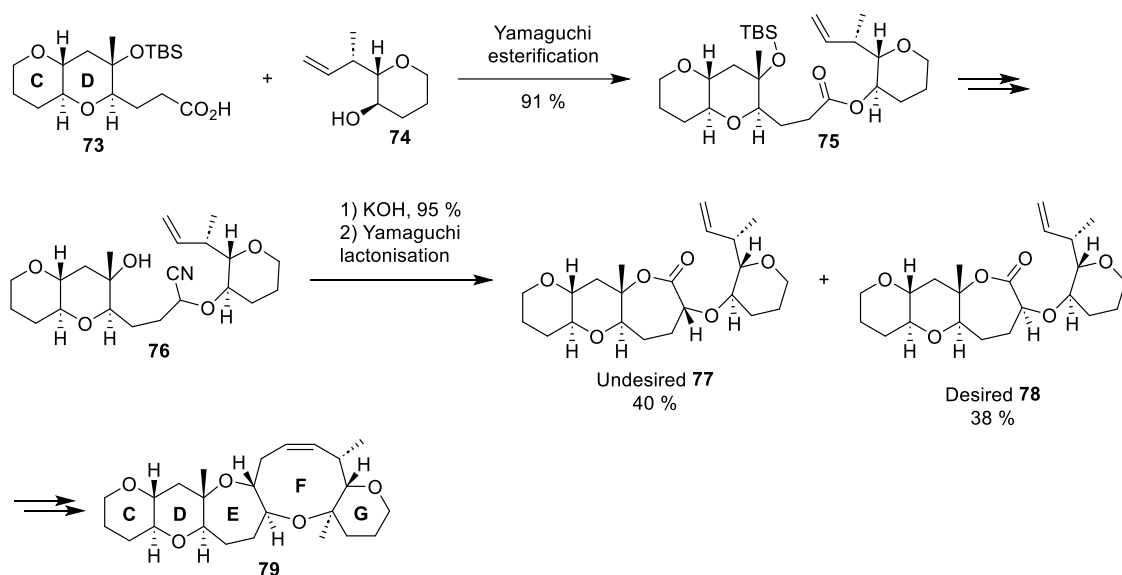
Scheme 18. General Yamaguchi esterification reaction

Deprotonation of the carboxylic acid by triethylamine allows attack of the carboxylate onto the aryl acid chloride, forming a mixed anhydride. Being a better nucleophile than the alcohol, the DMAP attacks the mixed anhydride, forming species **72**. This species is a better electrophile than the previous mixed anhydride, allowing for attack of the alcohol. The DMAP acts as a leaving group and the desired ester **71** is formed (Scheme 19).



Scheme 19. Mechanism of the Yamaguchi esterification

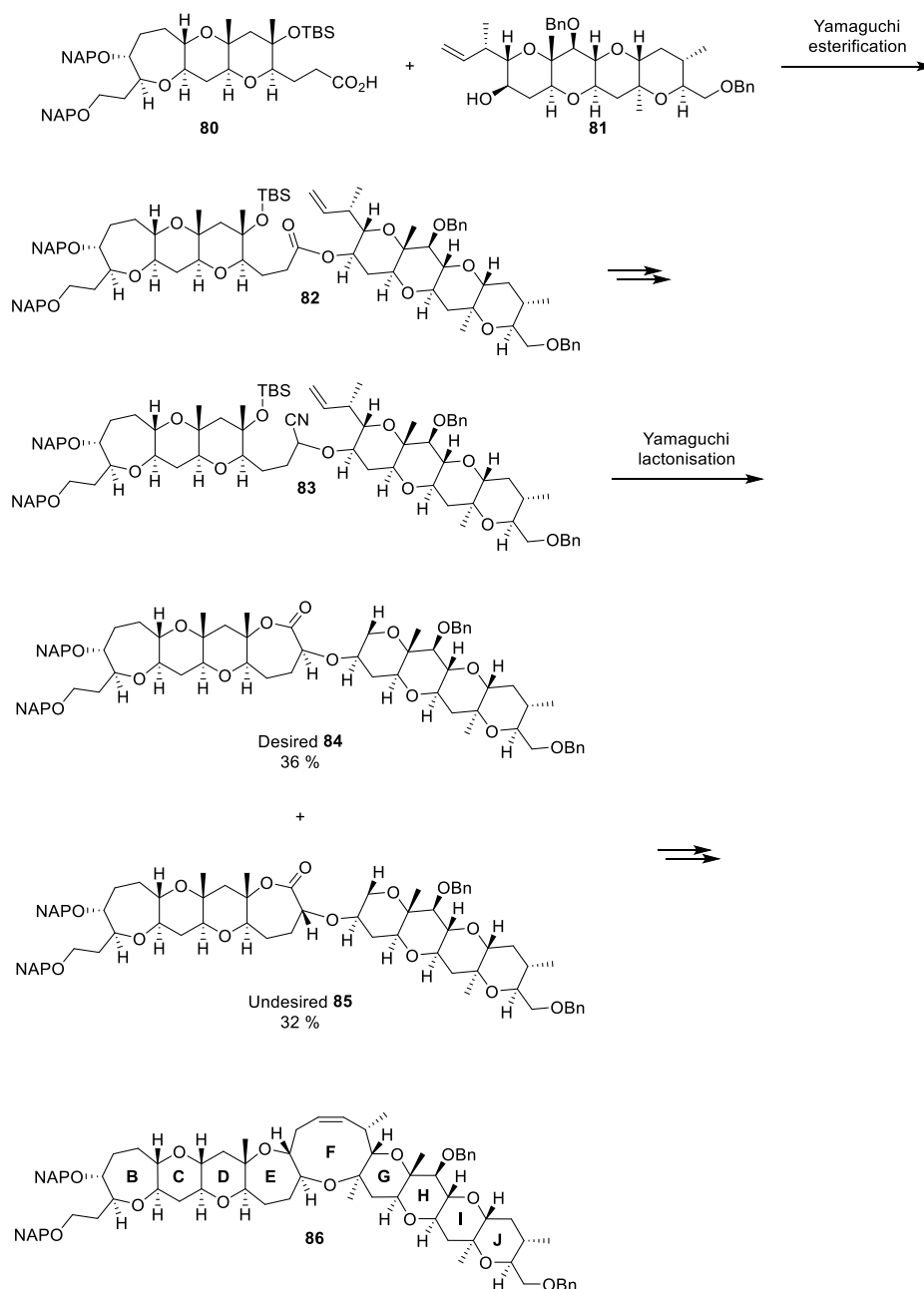
In their synthesis of the CDEFG fragment **79** of gambieric acid, Sasaki and Sato began with a Yamaguchi esterification to couple the CD **73** and G **74** fragments.³⁹ The resulting ester **75** was converted into nitrile **76**, which then underwent hydrolysis. **76** was converted to a hydroxy acid, and subsequently underwent Yamaguchi lactonisation in order to form the seven-membered E ring (Scheme 20). In their original publication, Yamaguchi and coworkers demonstrated the utility of this technique to form ring systems.³⁸ Lactonisation afforded both the desired **78** and undesired **77** diastereomers in a ~1:1 ratio, and attempts at epimerisation of **77** were unsuccessful. However, they continued with **78** and successfully synthesised the CDEFG fragment **79** of gambieric acid.



Scheme 20. Synthesis of the CDEFG fragment of gambieric acid via a Yamaguchi esterification technique

With evidence that this was a viable route for the synthesis of polycyclic ethers, they decided to apply it to their total synthesis of gambieric acid.³⁷ Coupling of fragments

80 and **81** via Yamaguchi esterification afforded ester **82**. This was converted into nitrile intermediate **83**, which was then hydrolysed to give the corresponding hydroxy acid. Yamaguchi lactonisation formed the seven-membered E ring. However, as with the synthesis of the CDEFG fragment, diastereomers **84** and **85** were produced in roughly equal amounts and attempts to epimerise **85** were unsuccessful. They decided to complete the B-J fragment **86** but later abandoned the route due to the lack of stereocontrol (Scheme 21).

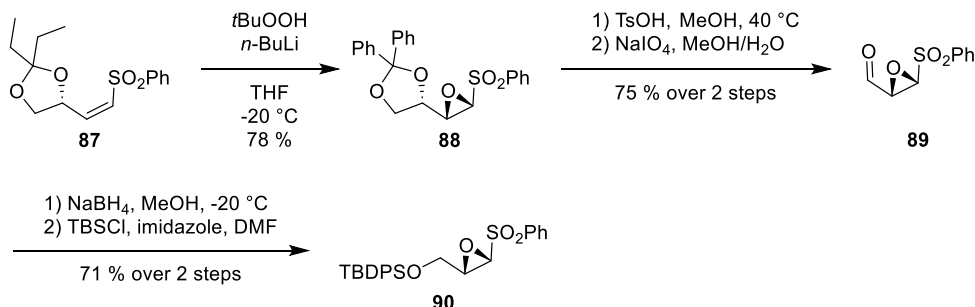


Scheme 21. Synthesis of the B-J fragment **86** of gambieric acid *via* a Yamaguchi esterification technique

1.2.4 Iterative polypyran synthesis

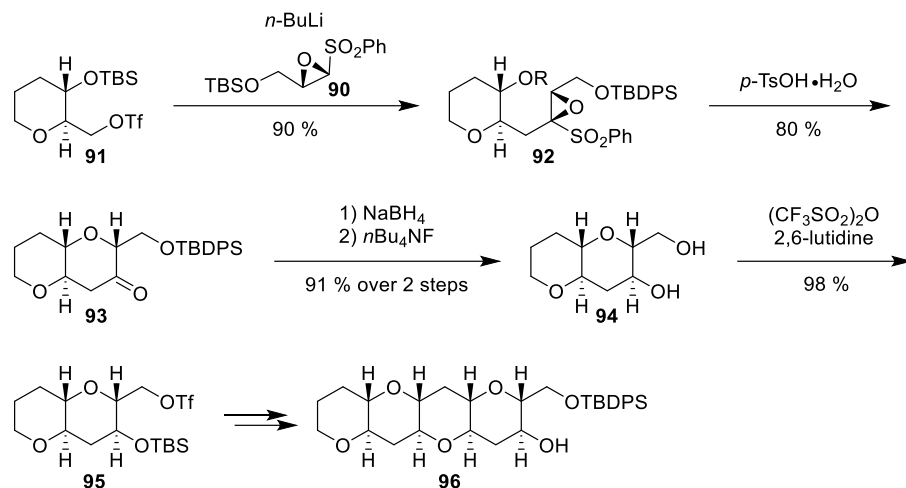
Iterative syntheses are those which involve repetition of a cycle of reactions, allowing the production of molecules which consist of repeating units. Iterative strategies benefit from a small number of unique reactions needed to build up complexity, allowing maximum optimisation of the few reactions used.

In their development of an iterative synthesis of *trans*-fused tetrahydropyrans, Mori *et al.* also took inspiration from the proposed biosynthesis in that they used an epoxide-opening strategy.⁴⁰ However, this method is distinct from others because an epoxide nucleophile is used in order to build up the epoxide-opening precursor. Their use of this epoxide nucleophile, known as the oxiranyl anion, is the first time that the alkylation of this anion has been studied. They use epoxy sulfones as precursors to the oxiranyl anion, and found that alkyl triflates can be used as electrophilic coupling partners. Epoxidation of sulfone **87** gave the protected sulfone **88**. Deprotection of the acetonide under acidic conditions followed by oxidative cleavage of the diol gave aldehyde **89**. Sodium borohydride reduction and TBDPS protection of the resulting free hydroxy group gave key epoxy sulfone **90** (Scheme 22).



Scheme 22. Synthesis of epoxy sulfone **90**

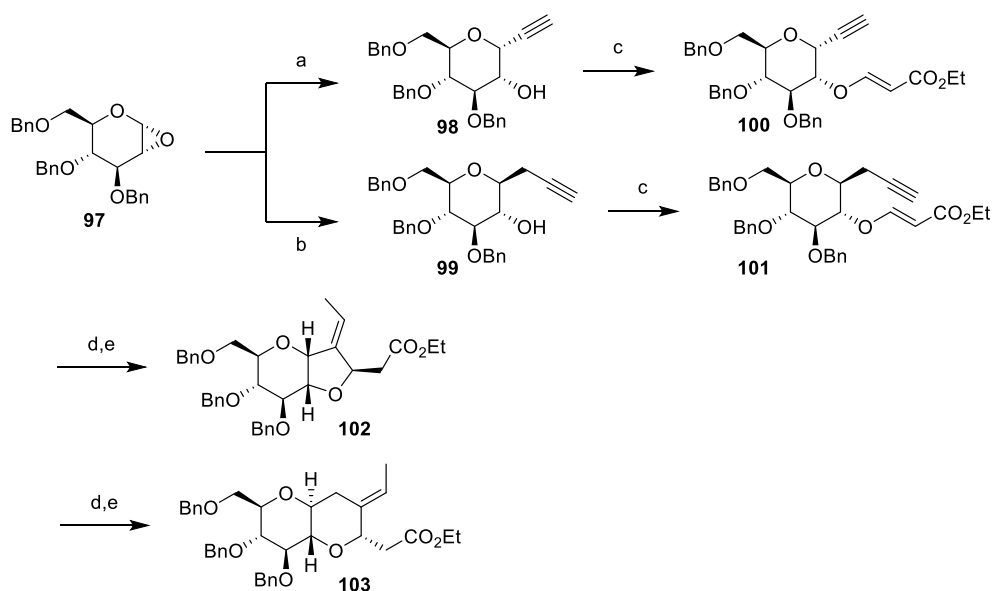
Coupling of triflate **91** with epoxy sulfone **90** gave coupling product **92**. Acid-mediated epoxide-opening with a free hydroxyl group resulted in ring closure to give bicyclic compound **93**. Sequential ketone reduction, removal of the TBDPS group and reaction with triflic anhydride gave triflate **95**. This could then undergo the same sequence of reactions, allowing a tetracyclic system to be built up relatively simply (Scheme 23).



Scheme 23. Synthesis of tetracycle **96** via use of oxiranyl anion

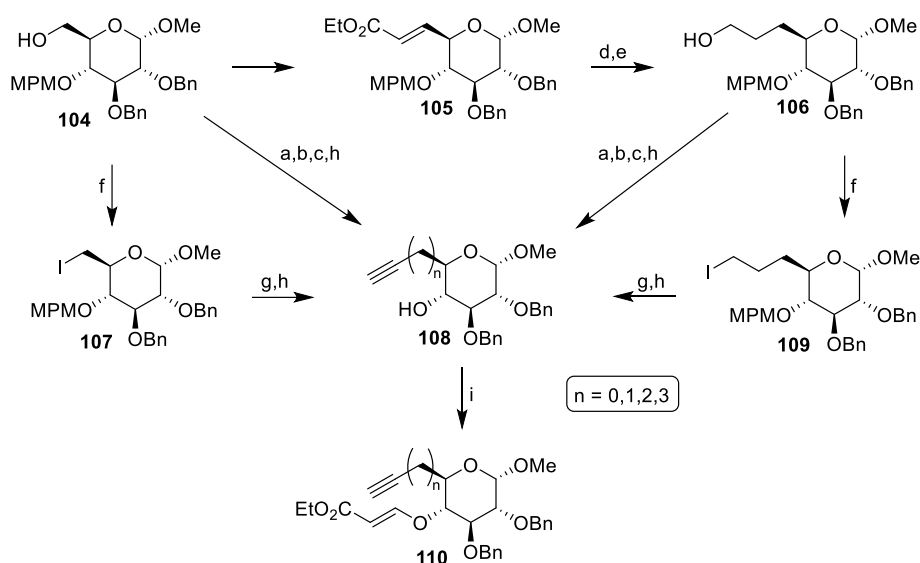
Van Boom *et al.* reported iterative polyether synthesis based on radical cyclisation of β -(alkynyloxy)acrylates.⁴¹ The β -(alkynyloxy)acrylates were derived from carbohydrates. This method offers a versatile method for the formation of various ring sizes, as the alkyl chain of the enyne is readily modified.

In their synthesis, carbohydrate-derived epoxide **97** is converted to enynes **98** and **99** via epoxide-opening with a nucleophilic alkynyl species. The ring size of the product resulting from the cyclisation reaction is dependent on the length of the alkyl chain installed (Scheme 24).



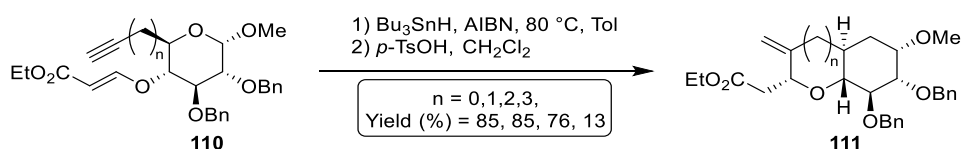
Scheme 24. Synthesis of bicyclic fragments **102** and **103**. a) NaCCH, ZnCl₂, 85 %, b) Bu₃SnCHCCH₂, *n*BuLi, then ZnCl₂, 72 %, c) ethyl propiolate, NMM, 98 %/95 %, d) Bu₃SnH, AIBN, 59 %/72 %, e) *p*TsOH, 97 %/99 %

The authors then explored the synthesis of β (alkynyloxy)acrylates from partially protected methyl α -D-glucoside. They successfully synthesised alkyl chains of length $n = 0, 1, 2, 3$ (Scheme 25).



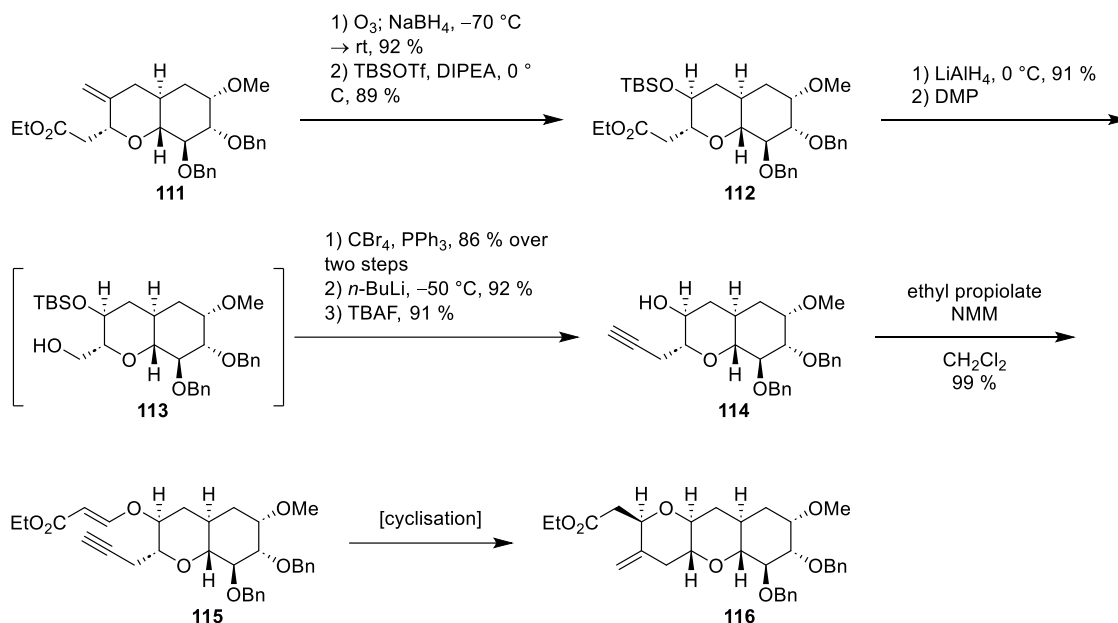
Scheme 25. Synthesis of cyclic fragment **110** with various alkyl chain lengths. a) DMP, b) PPh_3 , CBr_4 , 82 % over 2 steps, c) $t\text{BuLi}$, 76 – 92 %, d) H_2 , PtO_2 , e) LiAlH_4 , 76 % over 2 steps, g) HCCLi ethylenediamine complex, 74 – 82 %, h) DDQ, H_2O , 77 – 88 %, i) ethyl propiolate, NMM, 94 – 99 %

Radical cyclisation of all alkyl chain lengths was successful, though $n = 3$ afforded a disappointing yield of 13 % (Scheme 26).



Scheme 26. Cyclisation of β (alkynyloxy)acrylate **110** to form bicyclic fragment **111**

Bicyclic compound **111** could be converted to a bicyclic compound with the same functionalities as **110**, allowing further rings to be constructed (Scheme 27). Ozonolysis in the presence of sodium borohydride followed by hydroxyl group protection afforded ester **112**. Reduction of the ester was carried out with lithium aluminium hydride, and the resulting alcohol was oxidised with Dess-Martin periodinane (DMP). A Corey-Fuchs reaction and TBS deprotection produced alkyne **114**. Addition of ethyl propiolate afforded **115**, which now contained the necessary functionality for cyclisation. Cyclisation under the previously mentioned conditions produced tricyclic compound **116**.

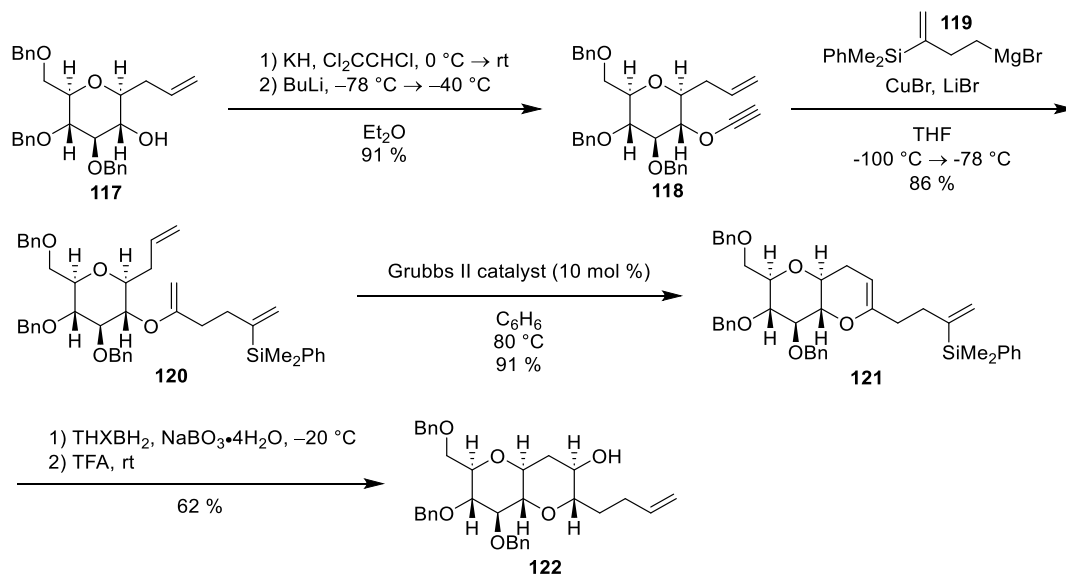


Scheme 27. Regeneration of functionality and synthesis of tricyclic compound **116**

Though this was a successful method for the formation of various ring sizes, the synthesis of the cyclisation precursors involves a high step count, and only a single ring is formed at a time.

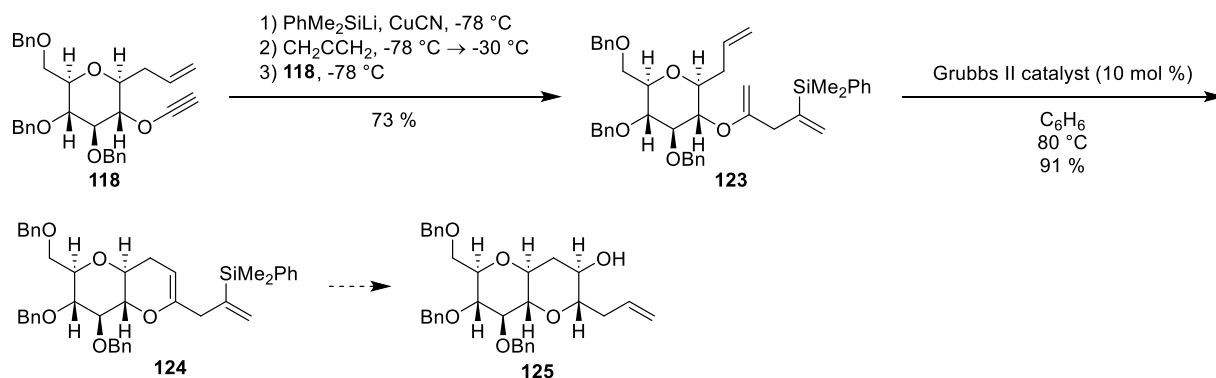
1.2.5 Ring-closing metatheses

Much like Mori and coworkers, Clark *et al.* used an iterative synthesis of fused polyethers in order to improve synthetic efficiency and reliability.⁴² This method uses alkynyl ethers to produce RCM precursors. Reaction of the alkynyl ether with an organocopper reagent produces RCM precursor **120**. The side chain includes a masked alkene, which can easily be unmasked and thus ready to perform another round of the same reactions to further elaborate the polyether backbone. The length of the carbon chain can be tuned to match the desired ring size. The alcohol **117** was first converted into an alkynyl ether **118**, and then subjected to reaction with the organocopper reagent formed from Grignard reagent **119**. RCM with Grubbs 2nd generation catalyst gave bicyclic compound **121**. Hydroboration and oxidation of both the alkene and silyl group followed by Peterson's elimination gave the desired bicyclic compound **122** with an unmasked alkene side chain. This intermediate could undergo the same series of reactions to form a seven-membered ring (Scheme 28).



Scheme 28. Clark's iterative sequence for the formation of polycyclic ethers

To introduce a propenyl side chain instead of a butenyl side chain, slight modifications were made to the synthetic sequence (Scheme 29). The organocopper reagent was formed from phenyldimethylsilyl lithium and copper (I) cyanide which was then reacted with allene. This organocopper reagent was then subjected to reaction with alkynyl ether **118** to give desired masked alkene **123**. RCM with Grubbs 2nd generation catalyst produced bicyclic compound **124**. **124** could potentially be subjected to the same hydroboration/oxidation and Peterson elimination sequence as previously mentioned to afford bicyclic compound **125** with an unmasked alkene side chain.



Scheme 29. Synthesis of bicyclic compound **125**

1.3 Gymnocins

The gymnocin toxins which have so far been isolated from *Karenia mikimotoi* are known as gymnocin A **126** and B **127**. Gymnocin A **126** and B **127** consist of 14 and 15 contiguous polycyclic ether rings, respectively, with a 2-methyl-2-butenal side-chain.

Gymnocin A **126** was successfully isolated by Satake *et al.* in 2002,⁴³ followed by the first successful total synthesis by Tsukano and Sasaki in 2003.⁴⁴ Satake *et al.* went on to isolate gymnocin B **127** in 2005,⁴⁵ although it wasn't until 2019 that Jamison *et al.* reported the first and only successful total synthesis.²

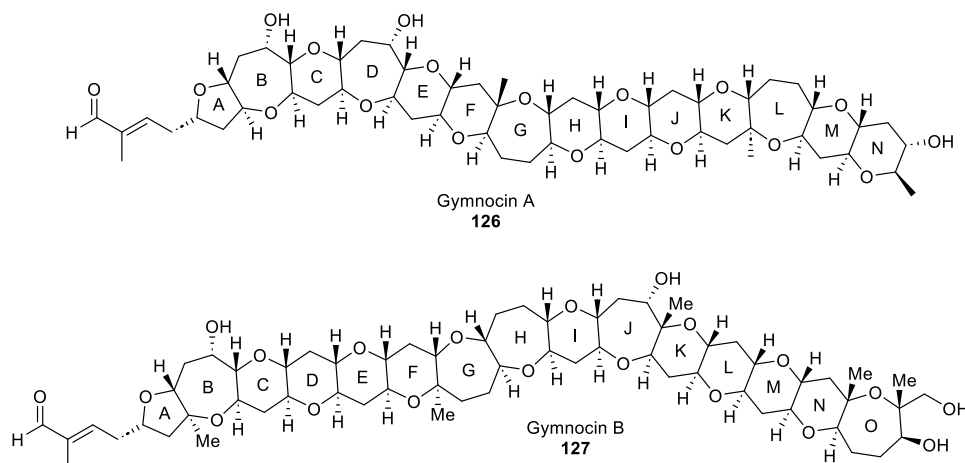
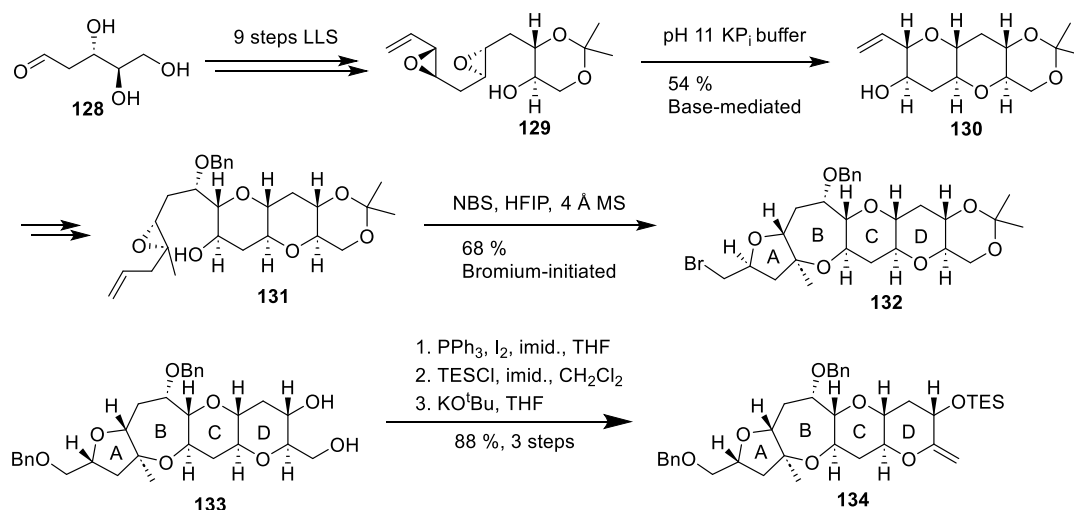


Figure 6. Gymnocin A **126** and B **127**

1.3.1 Previous total synthesis of gymnocin B

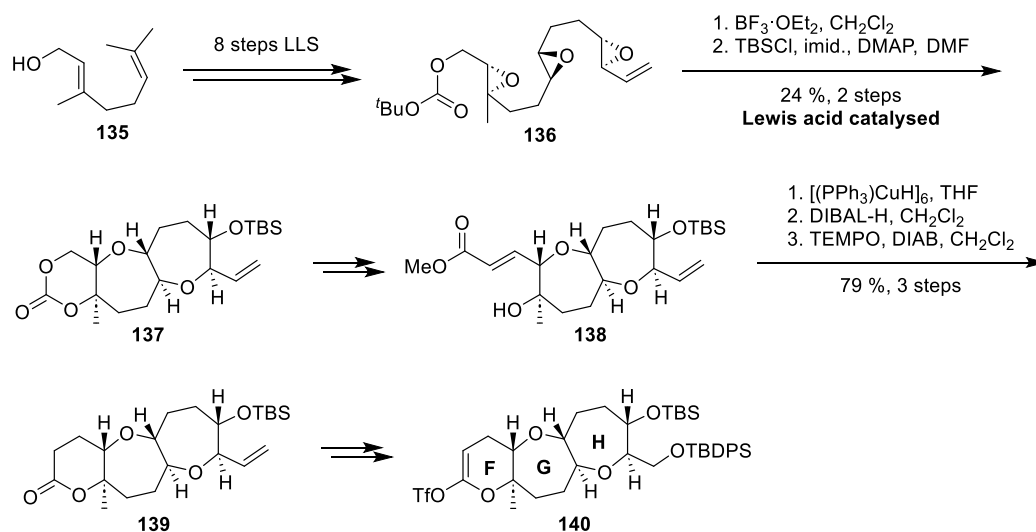
Jamison and coworkers employed a convergent, biomimetic approach to their total synthesis of gymnocin B.² They produced the ABCD fragment **134** via a series of epoxide-opening cascades to form the ring systems (Scheme 30).



Scheme 30. Jamison *et al.*'s synthesis of the A-D fragment **134** of gymnocin B

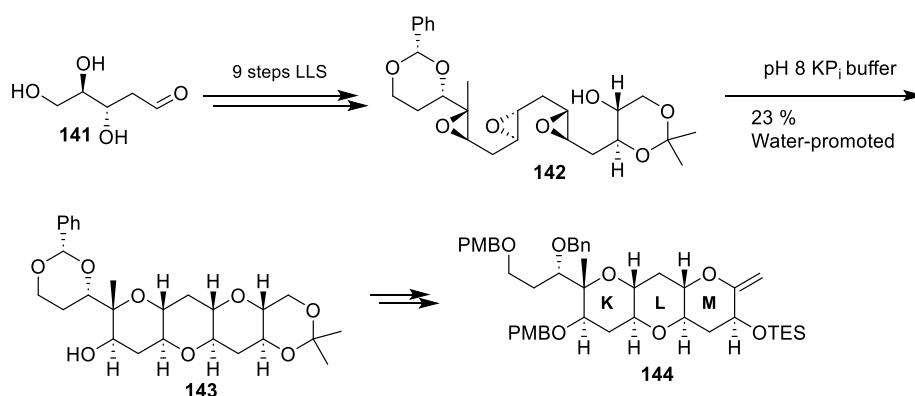
They then focused on the synthesis of the FGH fragment **140**. Again, an epoxide-opening cascade of **136** was employed to form the seven membered rings of **138**. In order to construct the six membered ring, conjugate reduction of ester **138** followed by

DIBAL-H reduction of the ester allowed spontaneous cyclisation to occur, forming the six-membered ring (Scheme 31).



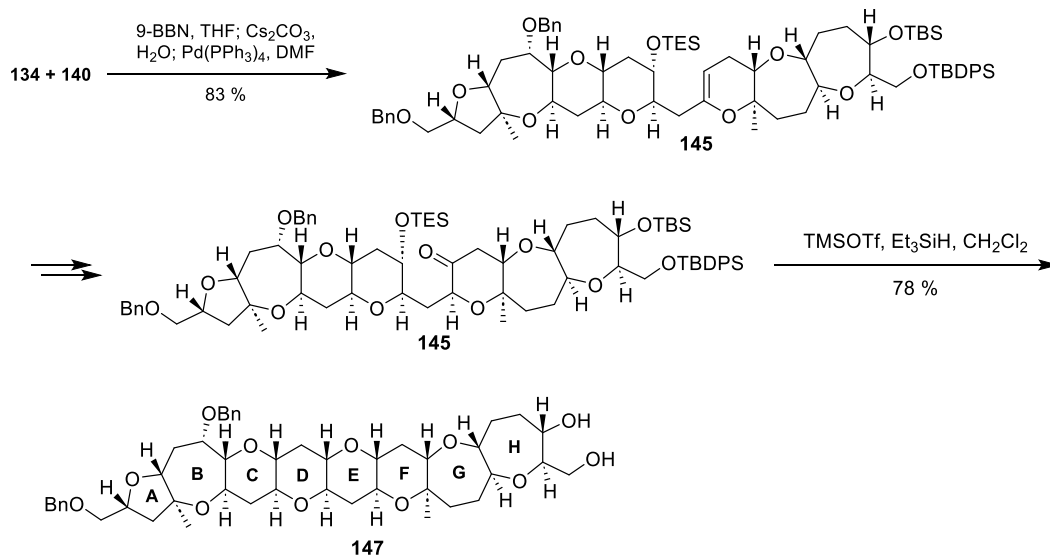
Scheme 31. Jamison *et al.*'s synthesis of the FGH fragment **140** of gymnocin B

Triepoxide **142** was produced from a multi-step synthesis starting with aldehyde **141**. An epoxide-opening cascade of **142** constructed the rings of the KLM fragment **144** (Scheme 32).



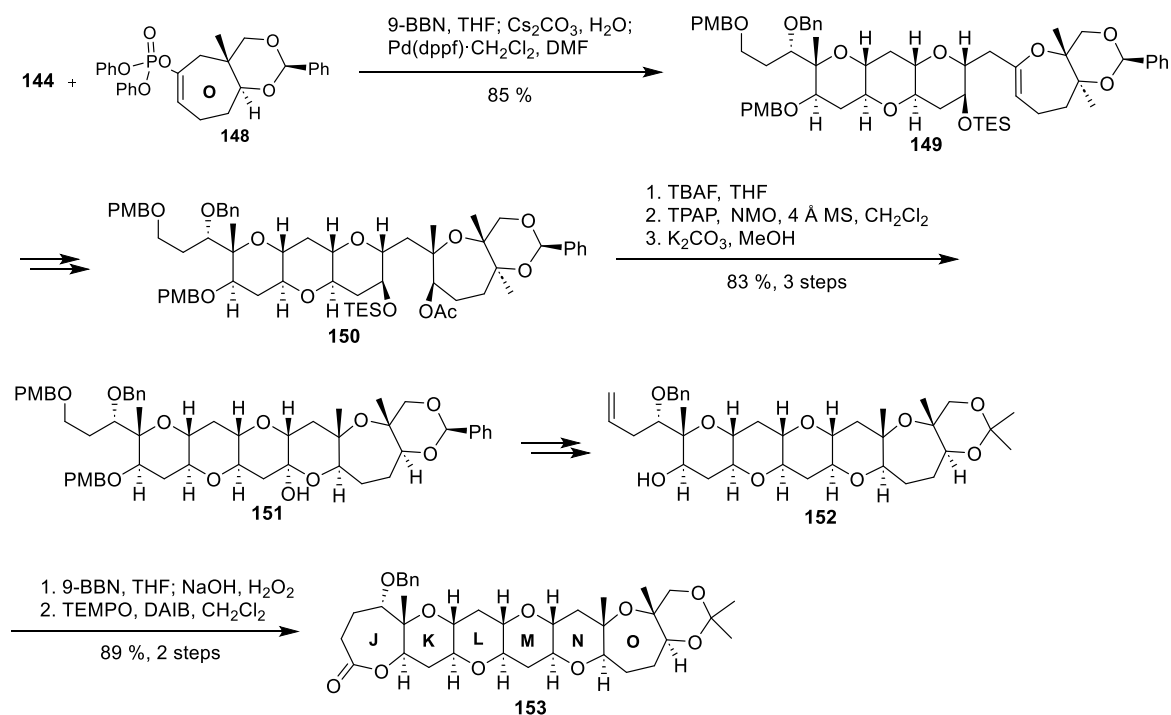
Scheme 32. Jamison *et al.*'s synthesis of the KLM fragment **144** of gymnocin B

The ABCD fragment **134** was subjected to a hydroboration, and was then coupled with the FGH fragment **140** via a Suzuki-Miyaura coupling. The E ring was formed by ring-closing via reductive etherification (Scheme 33).



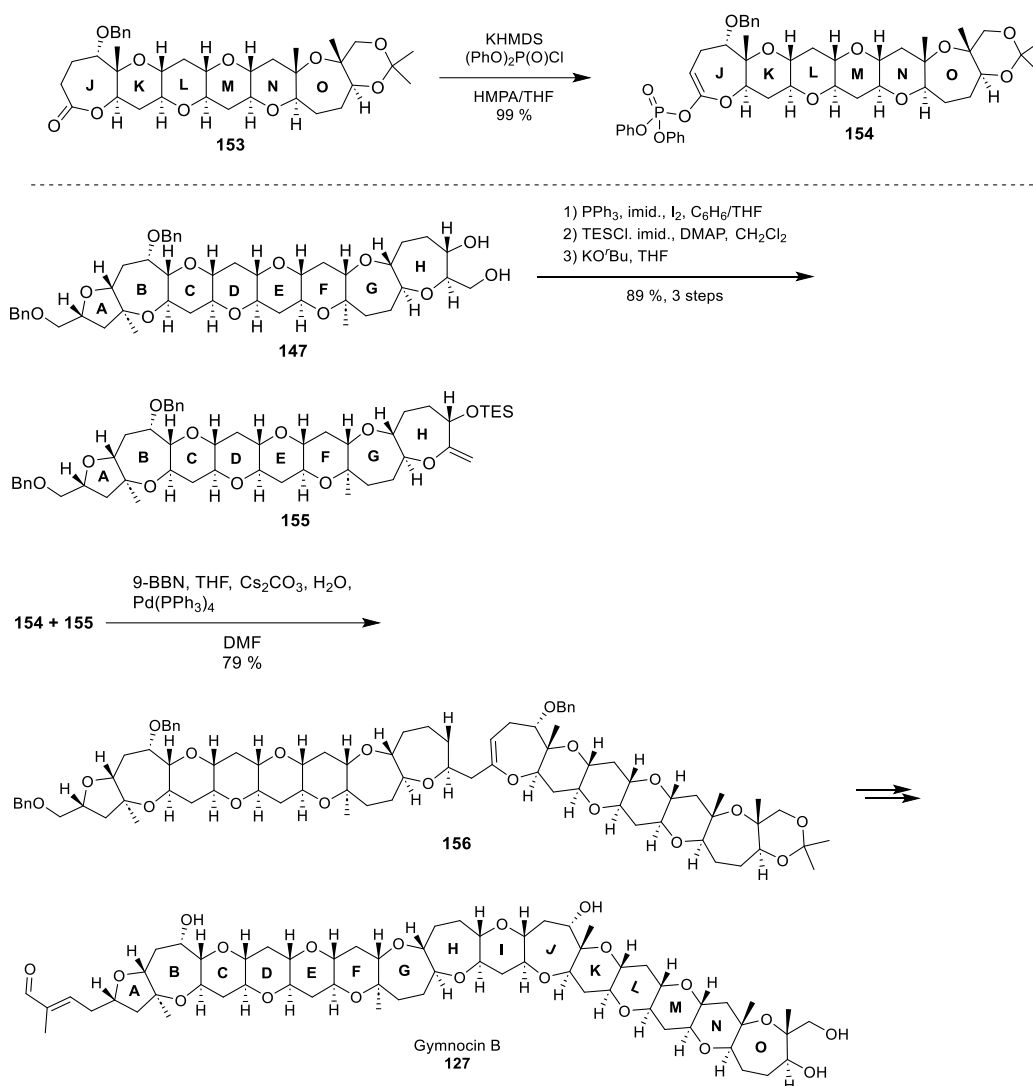
Scheme 33. Jamison et al.'s synthesis of the A-H fragment **147** of gymnocin B

Again, the KLM fragment **144** was subjected to hydroboration and then coupled with known fragment **148** via a Suzuki-Miyaura coupling. Removal of the TES group, oxidation of the resulting alcohol, and base-catalysed deacetylation led to spontaneous ring-closed to form the N ring (Scheme 34).



Scheme 34. Jamison et al.'s synthesis of the J-O fragment **153** of gymnocin B

The A-H fragment **147** was converted to enol ether **155**, and the J-O fragment **153** was converted to phosphate **154**. These two fragments were coupling via Suzuki-Miyaura coupling. Further functionalisation produced desired gymnocin B **127** (Scheme 35).



Scheme 35. Completion of gymnocin B **127** by Jamison *et al.*

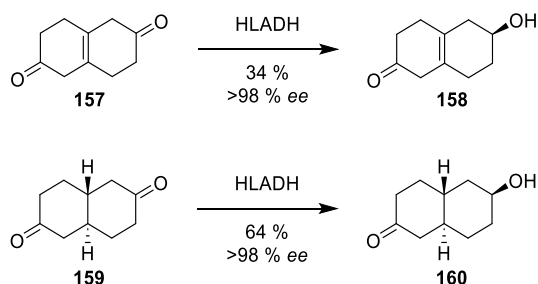
This synthesis has a large step count, and we believed that we could significantly reduce the number of steps through the use of the centrosymmetric/desymmetrisation strategy.

1.4 Bi-directional syntheses and desymmetrisation techniques

In a bi-directional synthesis, reactions happen on both sides of a symmetric molecule concurrently, leading to a highly efficient synthesis. Often, a point is reached where different functionalities must be installed on either side of the molecule, and thus a desymmetrisation reaction must be employed. A desymmetrisation reaction is simply one which leads to the breaking of symmetry in a molecule. These reactions are performed asymmetrically, and they produce an enantioenriched pool of a key molecule from a *meso* starting material.

Many members of the marine ladder polyether (MLP) family contain hidden elements of symmetry within their polycyclic ether skeleton. If this can be exploited in their synthesis, it lends itself to a more efficient bidirectional synthesis of the key fragments.

In 1988, Jones and Dodds reported the first asymmetric desymmetrisation of a centrosymmetric molecule through the use of enzymatic catalysis.⁴⁶ Symmetrical diketones **157** and **158** were reduced with horse liver alcohol dehydrogenase (HLADH), to afford ketones **159** and **160** in high ee (Scheme 36).



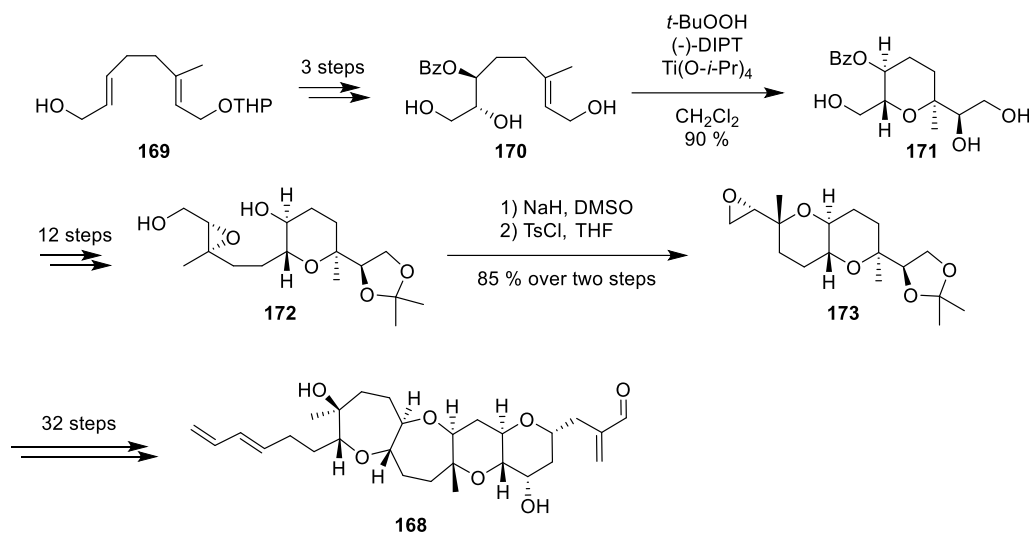
Scheme 36. First asymmetric desymmetrisation of a centrosymmetric molecule

Enzymes can be powerful tools in organic synthesis. Enzymatic reactions often benefit from impressive ee values, mild conditions, and are considered to be ‘green’ as they can be performed in aqueous conditions. However, the use of enzymes also presents with significant challenges.⁴⁷ Enzymes tend to have high substrate specificity, and thus may not act on a desired unnatural substrate. While performing reactions in physiological aqueous conditions is beneficial from an environmental standpoint, many organic substrates will not be soluble in these conditions, and the enzyme may not be compatible with the organic solvents required. Many enzymatic systems require the use of cofactors, and this further complicates their application. If whole cell systems cannot be utilised (e.g. due to cell penetration issues), then considerations for regeneration of the cofactor will need to be made.⁴⁸ And lastly, enzymes may not be cost-effective, as some commercially available enzymes can be highly expensive.

1.5.1 First non-enzymatic desymmetrisation

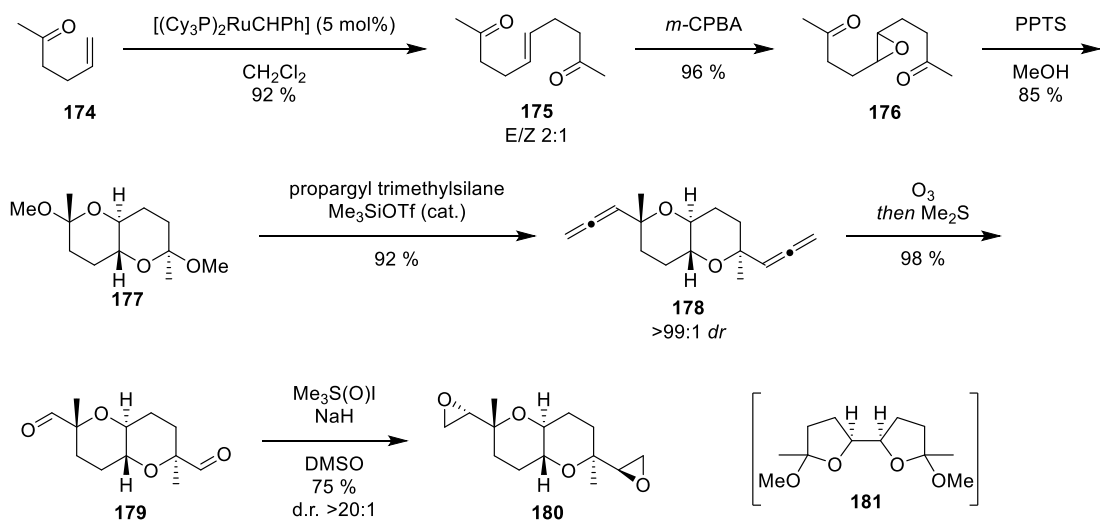
In 1981, Hirao and coworkers reported the first asymmetric reduction of ketones with alkoxy-amine-borane complexes.⁴⁹ Corey, Bakshi, and Shibata further expanded on this work and reported the first asymmetric reduction of ketones using a chiral oxazaborolidine catalyst in 1987.⁵⁰ This reaction and catalyst became commonly known as the ‘CBS reduction’ and the ‘CBS catalyst’ (Scheme 37).

In 1998, Nakata reported a total synthesis of hemibrevetoxin B. In this synthesis, intermediate **173** was produced in a traditional, non-bidirectional manner. Intermediate **173** was then converted into hemibrevetoxin B **168** in 32 steps (Scheme 39).⁵⁵



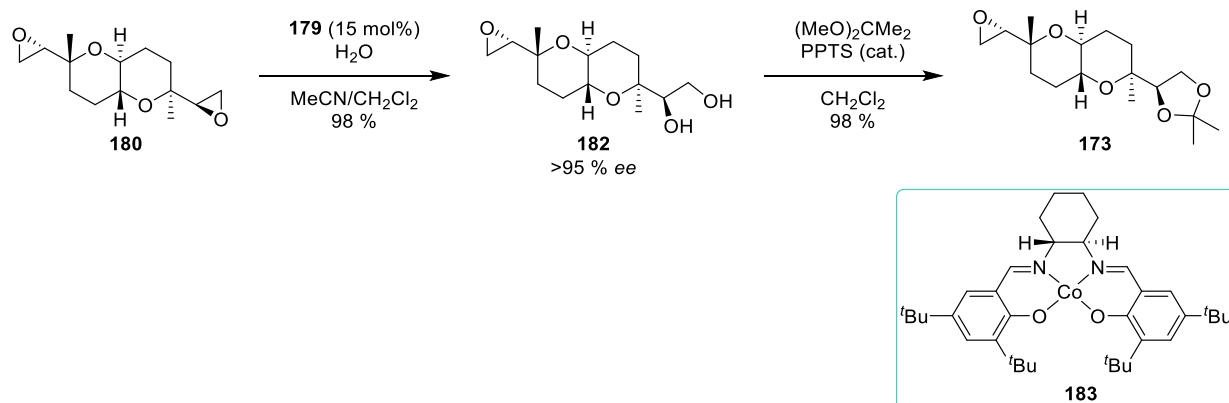
Scheme 39. Synthesis of hemibrevetoxin B **168** via key intermediate **173**

Nelson and co-workers recognised that intermediate **173** could be produced via a bidirectional synthesis followed by a desymmetrisation of centrosymmetric intermediate **180**, which would significantly reduce the amount of steps required to produce hemibrevetoxin B (Scheme 40).⁵² The synthesis began with cross-metathesis of commercially available 5-hexen-2-one **174** using the Grubbs 1st generation catalyst. The cross-metathesis product **175** was obtained in a 92 % yield and a 2:1 *E/Z* ratio. Enedione **175** was epoxidised with *m*-CPBA afforded epoxide **176**. Cyclisation of epoxide **176** in the presence of PPTS and MeOH gave bicyclic system **177**. Interestingly, the product of this reaction is initially **181**, which equilibrates to afford the fused bicyclic structure. Bicyclic acetal **177** was subjected to nucleophilic substitution with propargyl trimethylsilane to produce di-allene **178**. This reaction demonstrated excellent stereocontrol and the di-axially substituted product was isolated in >99:1 *dr*. Bis-aldehyde **179** was accessed *via* ozonolysis followed by reductive work-up. Sulfur ylide-mediated epoxidation afforded bis-epoxide **180** in >20:1 *dr*.



Scheme 40. Bidirectional synthesis of bis-epoxide **180**

In order to desymmetrise the molecule and develop each side of the molecule individually, they decided to perform an enantioselective epoxide hydrolysis with Jacobsen's salen catalyst **183**. Jacobsen's enantioselective epoxide hydrolysis is attractive as the only required reagents are water and a recyclable cobalt catalyst. Diol **182** was isolated in a 98 % yield and >95 % ee. Diol **182** was converted to acetone **173** by acid-catalysed reaction with 2,2-dimethoxypropane (Scheme 41). Epoxide **173** could be subjected to the 32-step synthesis of hemibrevetoxin B **168** reported by Nakata *et al.* as discussed above.

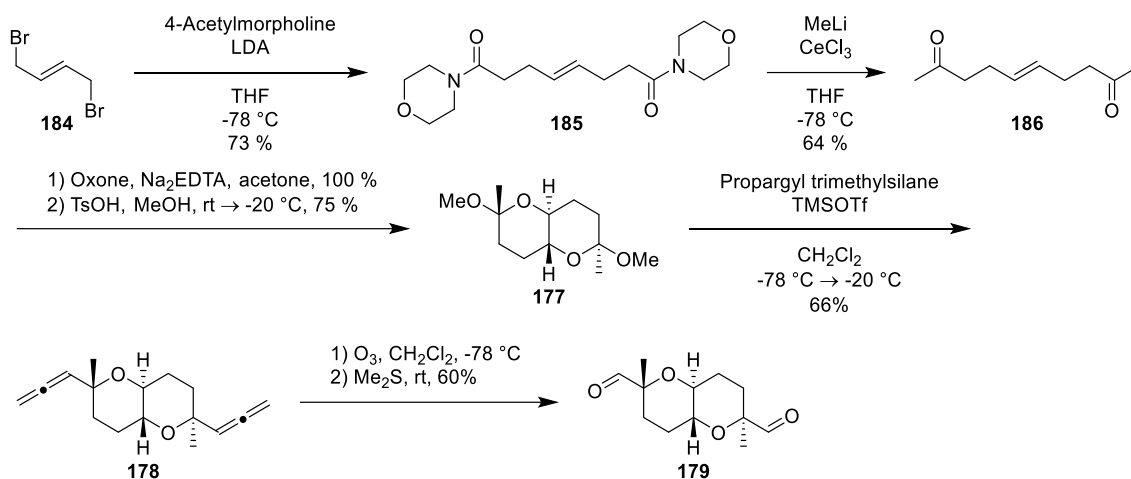


Scheme 41. Desymmetrisation of bis-epoxide **180** via enantioselective hydrolysis

1.5.3 Desymmetrisation of a centrosymmetric bis-aldehyde

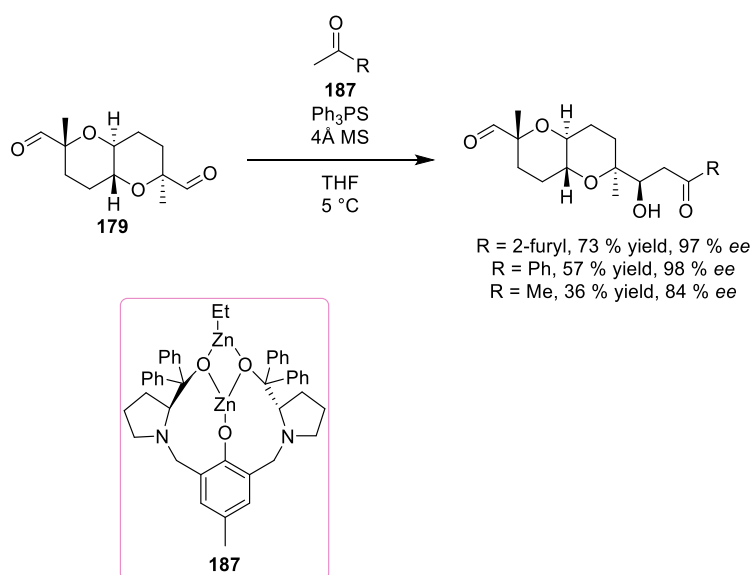
In 2007, Nelson *et al.* developed a new desymmetrisation procedure for bis-aldehyde **179**, which had previously been desymmetrised via the enantioselective epoxide hydrolysis discussed in Section 1.4.2. This desymmetrisation method involved carbon-carbon bond formation.⁵⁶

They reported a new synthesis of bis-aldehyde **179** which began with commercially available *trans*-1,4-dibromo-2-butene **184**. Reaction with 4-acetylmorpholine afford bis-acetylmorpholine **185**. **185** was converted to diketone **186** in the presence of MeLi and CeCl₃. Epoxidation with oxone led to cyclisation, and then formation of bis-acetal **177** in the presence of acidic methanol. Allene formation followed by ozonolysis produced desired bis-aldehyde **179** (Scheme 42).



Scheme 42. Bi-directional synthesis of the centrosymmetric bis-aldehyde **179**

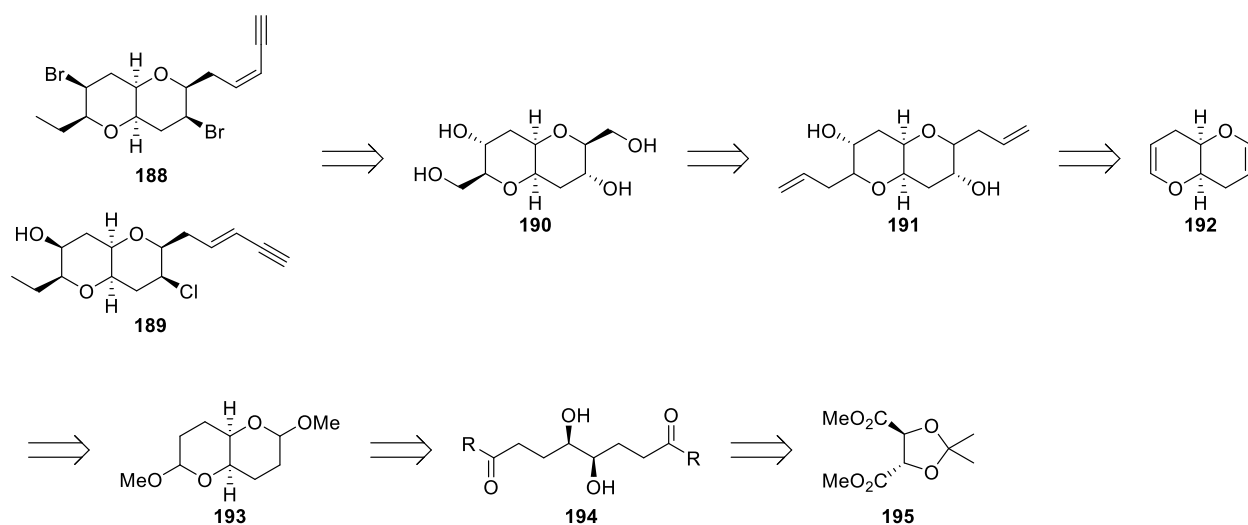
Bis-aldehyde **179** was desymmetrised via an asymmetric aldol reaction with Zn catalyst **187** (Scheme 43). This reaction achieved good ee with moderate to good yields for most of the ketones used. This is a useful method for asymmetric desymmetrisation of compounds as it desymmetrises and increases the complexity of the molecule in a single step.



Scheme 43. Desymmetrisation of bis-aldehyde **179**

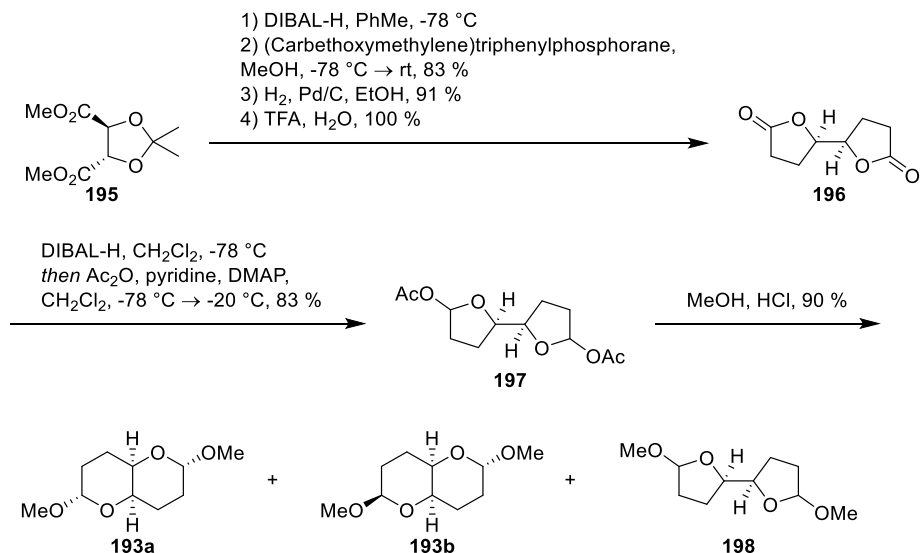
1.5.4 Synthesis of enyne **188** and elatenyne **187**

Burton and coworkers demonstrated the effectiveness of bidirectional elaboration of a fused bicyclic ether during their synthesis of elatenyne and an enyne produced by *Laurencia majuscula*.⁵⁷ *Laurencia majuscula* is an algal species that has been the source of many isolated natural products. Elatenyne **188** was isolated in 1986 and the structure was determined by ¹H and ¹³C NMR spectroscopic analysis. The enyne **189** was isolated more recently in 1993 and its structure was also assigned via NMR spectroscopy. In their synthesis of these two natural products, Burton *et al.* decided to take advantage of the C₂ symmetry within the molecule and use a bidirectional approach (Scheme 44). They envisioned that the side chains could be installed via functionalisation and manipulation of tetrol **190**. Tetrol **190** would be accessed from ozonolysis of diene **191**, which itself would be synthesised via epoxidation of enol ether **192** and epoxide-opening with a nucleophilic allyl species. Enol ether **192** was postulated to be produced from acetal **193**, which would be synthesised from the diol **194**. Bis-ester **195** would be converted to diol **194**.



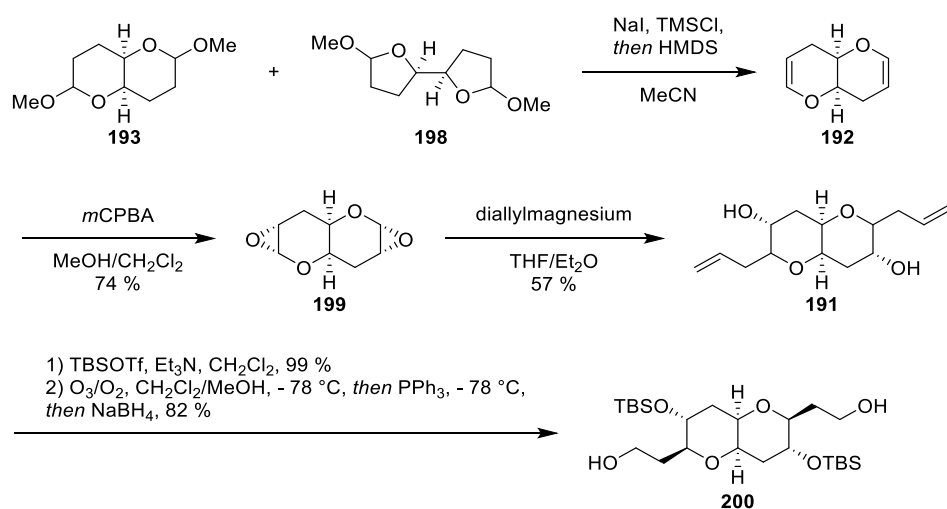
Scheme 44. Retrosynthesis of elatenyne **188** and enyne **189**

In order to synthesise acetal **193**, first a four-step procedure partially reported by Sasaki and coworkers to lactone **196** was followed,⁵⁸ giving the desired lactone in a 75 % yield over four steps. Reduction of the lactone **196** and acetyl protection with acetic anhydride afforded the bis-acetate **197** in an 83 % yield. Finally, treatment of bis-acetate **197** with acidic methanol produced a mixture of acetals **193a**, **193b**, and **198** (Scheme 45). Acetals **193a** and **193b** were obtained as a separable 1.3:1 mixture, along with diastereomers of **198** (ca 17% of mixture).



Scheme 45. Synthesis of acetals **193a**, **193b**, and **198**

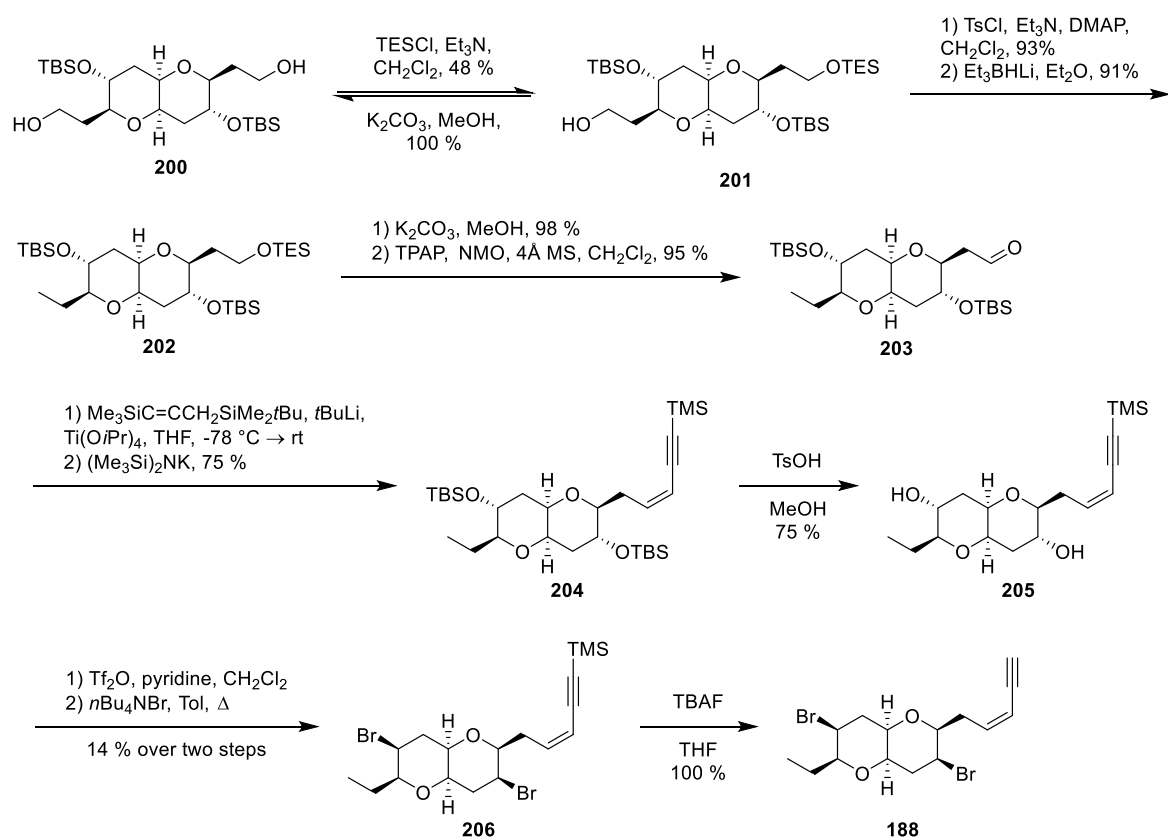
Initially, they imagined that enol ether **192** could be accessed from elimination of both methoxy groups from acetals **193a** and **193b**, but they discovered that all of the acetals **193a**, **193b**, and **198** produced enol ether **192** when subjected to the reaction conditions. Epoxidation of enol ether with *m*CPBA afforded epoxide **199**. Epoxide-opening with diallylmagnesium installed the allyl side chains in **191** as a mixture of diastereomers. The free hydroxyl groups were TBS-protected and ozonolysis of the terminal alkenes afforded diol **200** (Scheme 46).



Scheme 46. Bi-directional synthesis of diol **200**

With desired diol **200** in hand, they now focused effort on the desymmetrisation reaction. In order to install the desired ethyl side chain, they aimed to perform monotosylation of the diol **200**. Unfortunately, all efforts to perform monotosylation resulted in disappointing yields of 30 % or less. They also found that mono-oxidation of

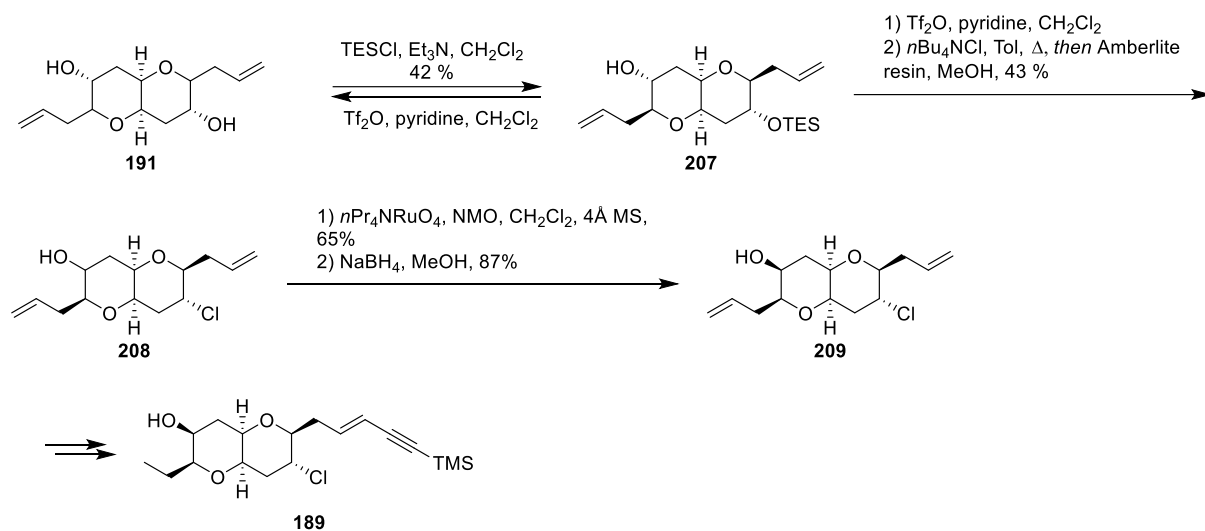
diol **200** resulted in discouraging yields. For this reason, they instead attempted to perform monosilylation. They took inspiration from Schreiber *et al.*, who reported monosilylation as a successful method for the desymmetrisation of C₂-symmetric molecules.⁵⁹ Diol **200** was subjected to silylation with 1 eq. of TESCl to afford alcohol **201** in a 48 % yield. The unwanted bis-silylated product could undergo selective TES deprotection by treatment with potassium carbonate and methanol, and the resulting diol **200** could be resubjected to monosilylation conditions. Alcohol **201** was tosylated and reduced with lithium triethylborohydride to afford **202** with the desired ethyl side chain. TES deprotection followed by TPAP oxidation afforded aldehyde **203**. A Yamamoto-Peterson reaction was then used to couple mono-aldehyde **203** and the silyl alkyne to give a Z-enyne **204**. Removal of the TBS groups under acidic conditions produced diol **205** which was converted to a bis-triflate. Di-bromination with tetrabutylammonium bromide (TBAB) afforded bis-bromide **206**. Removal of the TMS group in the presence of TBAF afforded desired natural product elatenyne **188** (Scheme 47).



Scheme 47. Synthesis of elatenyne **188**

With the synthesis of elatenyne **188** successfully completed, the authors focused their efforts on the synthesis of enyne **189**. To do this, a diastereomeric mixture of diol **191**

was subjected to the desymmetrisation procedure, which delivered alcohol **207** in a 42 % yield. Triflation of **207** followed by reaction with tetrabutylammonium chloride afforded the desired chloride **208**. The stereochemistry of the hydroxyl-bearing carbon was incorrect, and was inverted through an oxidation/reduction sequence to afford alcohol **209**. Alcohol **209** was converted to enyne **189** in seven steps (Scheme 48).



Scheme 48. Desymmetrisation of diol **191** and synthesis of enyne **189**

2. Project aims and strategy

A key focus of the work in the Clark group over the last several years has been the synthesis of MLPs.⁶⁰⁻⁶² As discussed in Section 1, the current reported syntheses of MLPs have high step counts with low overall yields. The work in the Clark group has attempted to develop shorter, more efficient syntheses. In her efforts towards the total synthesis of hemibrevetoxin B, Dr Jessica Elwood decided to employ a bidirectional synthesis with a desymmetrisation step. A bidirectional synthesis allows both sides of a symmetric molecule to be built up at the same time, and the desymmetrisation step removes the symmetry and allows each side to be functionalised individually when necessary. Dr Jessica Elwood identified diketone **210** as the key symmetric intermediate which would undergo desymmetrisation (Figure 8).⁶³

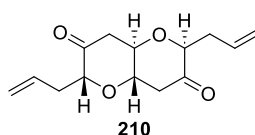


Figure 8. Structure of key symmetric intermediate **210**

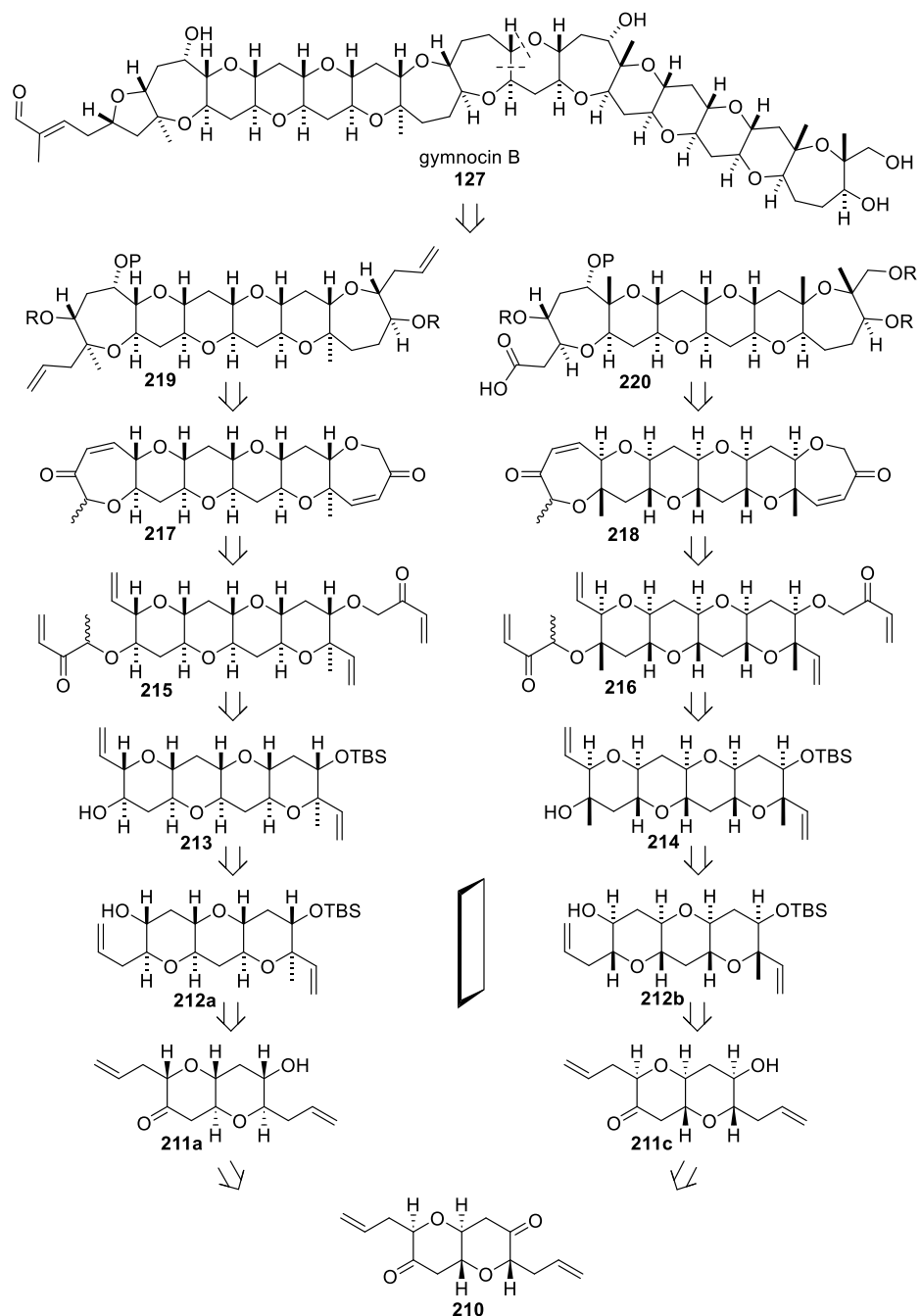
While her work focused on the synthesis of hemibrevetoxin B, it was noted the diketone **210** could potentially be a key intermediate in the total synthesis of several MLPs, making this bidirectional/desymmetrisation strategy a general strategy in the synthesis of MLPs. Desymmetrisation of diketone **210** would allow functionalisation to occur on one side of the molecule and this would give the ability to access a wide-range of molecules from this one intermediate. If a desymmetrising reduction of diketone **210** could be performed, a hydroxyl group on one side of the molecule could be exploited to perform a ring formation, providing access to a tricyclic compound. Another option would be ring expansion of one of the six-membered rings in order to synthesis [6,7]- or [6,8]-fused bicyclic systems.

This project aims to provide a general and efficient route to MLP synthesis via bidirectional synthesis of diketone **210** with a key desymmetrisation reaction. This allows both sides of a molecule to be developed at the same time, significantly reducing the number of synthetic steps. The desymmetrisation of diketone **210** will break the symmetry and allow each side of the molecule to be functionalised separately when necessary. This approach could be applied to multiple intermediates

which could be coupled together in the final steps of the synthesis, allowing for a highly efficient convergent synthesis.

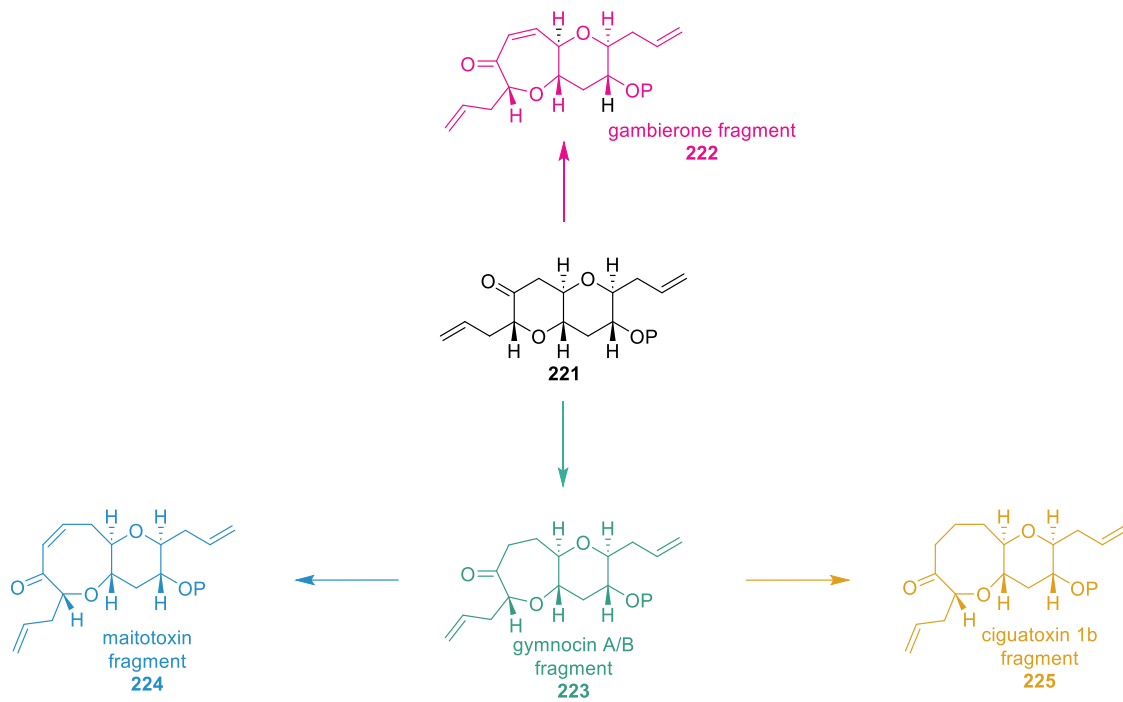
In order to prove the applicability of this approach, it was decided to use this approach in the total synthesis of gymnocin B. The retrosynthetic analysis of gymnocin B **127** is outlined below (Scheme 49). Gymnocin B **127** could be synthesised via coupling of fragments **219** and **220** followed by a further ring closure and introduction of the 2-methyl-2-butenal side chain. Fragments **219** and **220** would be accessed from various functionalisations of fragments **217** and **218**. Fragments **217** and **218** could be produced by RCM of fragments **215** and **216**. Addition of an α,β -unsaturated ketone to **213** and **214** was proposed to give fragments **215** and **216**. *O*-vinylation of **212a** and **212b** followed by RCM would afford a tetracyclic enol ether. This enol ether would undergo a similar series of reaction as shown below in Section 3.1 (epoxidation, epoxide-opening, vinylation) to afford the vinylated alcohol **213**. Oxidation of the alcohol and nucleophilic attack of a methyl group onto the ketone would produce the desired methylated compound **214**. Fragments **212a** and **212b** were envisaged to be accessed from **211a** and **211c**. Fragments **211a** and **211c** result from desymmetrisation of diketone **210**.

This largely bidirectional synthesis allows for complexity to be built up very quickly. For example, RCM of fragment **215** produces a hexacyclic molecule from a tetracyclic starting material. This strategy is highly advantageous as it significantly reduces the steps necessary to access gymnocin B. Another advantage to this approach is the use of the key desymmetrisation step; coupling partners **219** and **220** can be traced back to the same centrosymmetric diketone **210**. This significantly simplifies the synthesis, as the first eight steps produce the intermediate needed for both coupling partners. Additionally, diketone **210** is itself produced in an efficient bidirectional manner.



Scheme 49. Retrosynthetic analysis of gymnocin B **127**

In order to prove that this approach is more general than just the total synthesis of gymnocin B, fragments of various MLPs will be synthesised (Scheme 50). These fragments can be accessed from ring expansions of **221**, which comes from desymmetrisation and protection of diketone **210**.

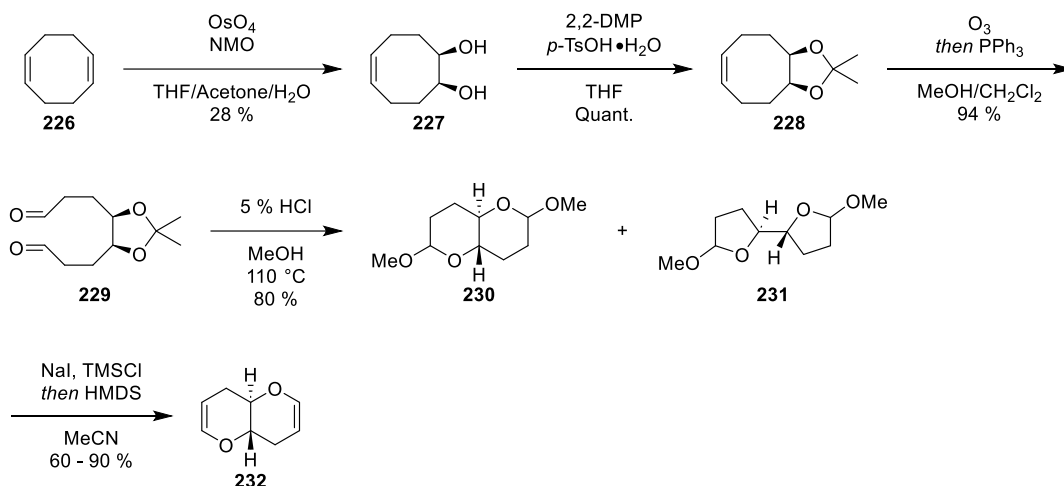


Scheme 50. Proposed synthesis of various MLP fragments

3. Previous Work in Clark Group

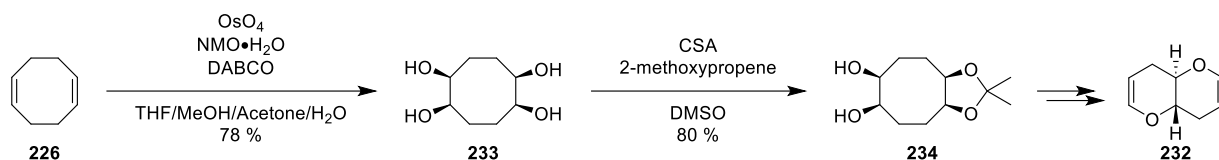
3.1 Synthesis of diketone **210**

As discussed above, Dr Jessica Elwood identified diketone **210** as a key intermediate in her synthesis of hemibrevetoxin B, and so she developed a synthetic route for diketone **210**. Initially, the synthesis of diketone **210** began with an Upjohn dihydroxylation of 1,5-cyclooctadiene **226** to afford diol **227** in a poor yield. This was followed by acetonide protection of the diol and then ozonolysis with reductive work-up to afford bis-aldehyde **229**. When the acetonide was cleaved under acidic conditions in the presence of methanol, the deprotected product underwent spontaneous cyclisation to afford a mixture of acetals **230** and **231**. Following Burton's conditions for the synthesis of the *cis*-fused bis-enol ether,⁵⁷ the *trans*-fused enol ether **232** was produced in good yield (Scheme 51).



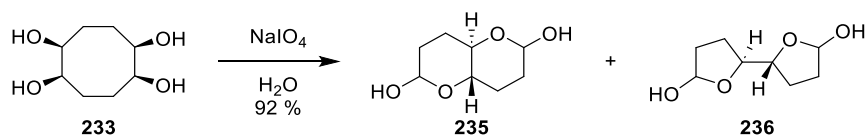
Scheme 51. Original synthesis of enol ether **232**

Due to a low-yielding first step, a new synthetic route was developed. In this route, a bis-dihydroxylation of 1,5-cyclooctadiene was performed to afford tetrol **233**. Addition of DABCO significantly improved the reaction rate. Acetonide protection of one of the diol functionalities followed by oxidative cleavage with sodium metaperiodate produced bis-aldehyde **234**. As before, acetonide deprotection and reaction under Burton's conditions gave enol ether **232**. This new synthetic route afforded enol ether **232** in a 37 % overall yield, significantly improved compared to the 16 % overall yield achieved by use of the first route (Scheme 52).



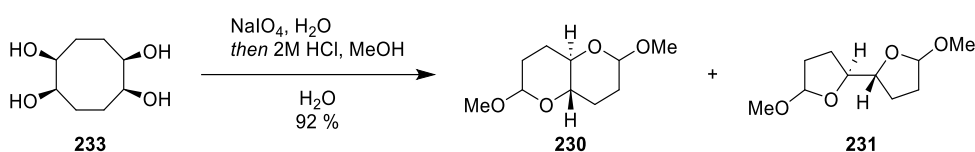
Scheme 52. Improved synthesis of **232**

It was then discovered that treatment of tetrol **233** with careful consideration of equivalents of sodium metaperiodate in water led to cleavage of one diol, followed by spontaneous intramolecular cyclisation to produce a mixture of lactols **235** and **236** (Scheme 53). This removed the need for protection of one of the diols.



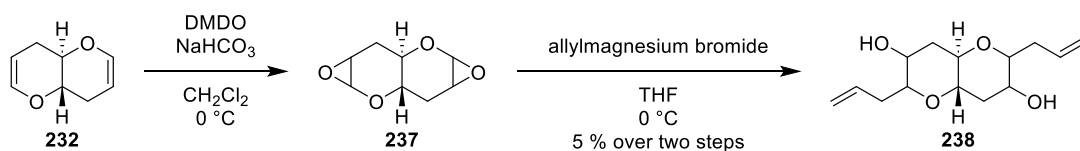
Scheme 53. One-step synthesis of lactols **235** and **236** from tetrol **233**

If this reaction was performed in the presence of acidic methanol, desired acetals **230** and **231** could be produced in just two steps from commercially available 1,5-cyclooctadiene **226** (Scheme 54).



Scheme 54. One-step synthesis of acetals **230** and **231** from tetrol **233**

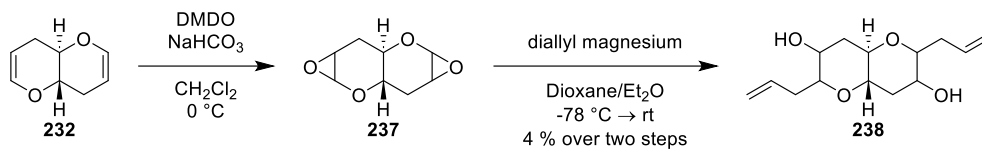
With a reliable route to enol ether **232** now established, efforts moved to functionalisation of this enol ether. The first method that was explored was epoxidation followed by epoxide-opening with an allyl Grignard reagent. Unfortunately, epoxidation with DMDO followed by epoxide-opening of bis-epoxide **237** with allylmagnesium bromide resulted in a disappointing 5% yield of diol **238** (Scheme 55).



Scheme 55. Synthesis of diol **238** via epoxide-opening with allylmagnesium bromide

Burton and coworkers had been successful in epoxidation of their *cis*-fused bis-enol ether followed by epoxide-opening with diallyl magnesium. Disappointingly, using the

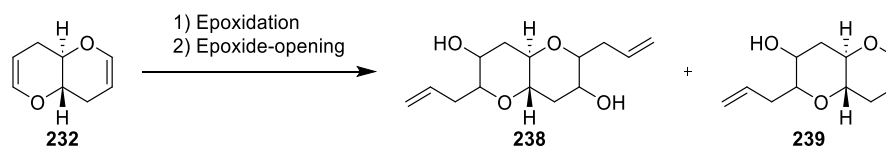
same conditions on the *trans*-fused system afforded diol **238** in just 4 % yield over two steps (Scheme 56).



Scheme 56. Synthesis of diol **238** via epoxide-opening with diallyl magnesium

Extensive testing of conditions gave a disappointing maximum yield of 10 % (Table 1).

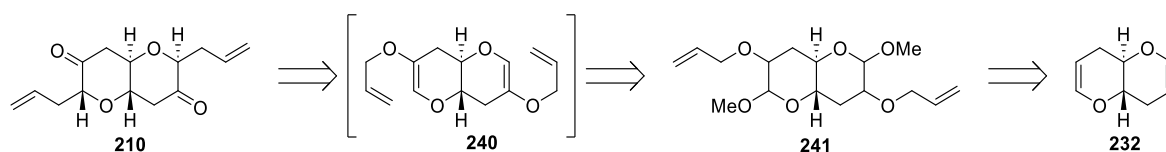
Table 1. Conditions used for epoxide-opening



Entry	Epoxidation conditions	Epoxide-opening conditions	Yield 238 (%)	Yield 239 (%)
1	<i>m</i> CPBA, CH ₂ Cl ₂ , 0 °C, 30 min	AllylMgBr, THF, 0 °C to rt, 3 h	2	5
2	<i>m</i> CPBA, KF, CH ₂ Cl ₂ , 0 °C to rt, 4 h	AllylMgBr, THF, 0 °C to rt, 4 h	5	-
3	<i>m</i> CPBA, KF, CH ₂ Cl ₂ , 0 °C to rt, 4 h	AllylMgBr, THF, -78 °C to rt, 4 h	8	-
4	<i>m</i> CPBA, KF, CH ₂ Cl ₂ , 0 °C to rt, 4 h	AllylMgBr, THF, 0 °C to rt, 18 h	10	-
5	<i>m</i> CPBA, KF, CH ₂ Cl ₂ , 0 °C to rt, 18 h	AllylMgBr, THF, 0 °C to rt, 2 h	Decomp.	Decomp.
6	<i>m</i> CPBA, KF, Et ₂ O, 0 °C, 4 h	AllylMgBr, Et ₂ O, 0 °C to rt, 18 h	8	6

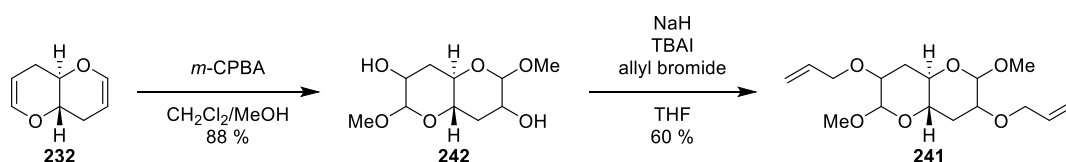
These poor yields were attributed to significantly reduced stability of the *trans*-fused bis-epoxide compared to the *cis*-fused isomer used by Burton and coworkers. It was evident that any strategy that involved isolation of epoxide **238** would not be viable.

The next approach involved a Claisen rearrangement. The Claisen rearrangement precursor targeted was **240**, which was expected to undergo elimination to produce **241**, followed by a Claisen rearrangement to afford diketone **210** (Scheme 57).



Scheme 57. Claisen rearrangement-based retrosynthesis of diketone **210**

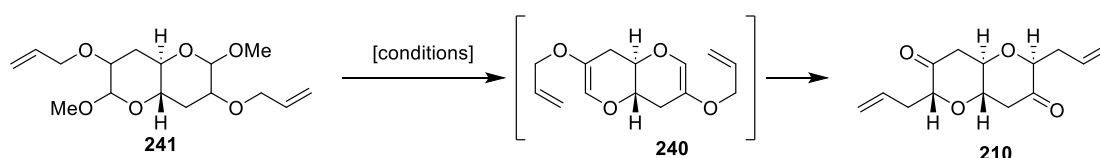
Bis-acetal **242** was accessed via epoxidation/in-situ epoxide-opening with methanol. An in-situ epoxide-opening avoided the issue of epoxide-instability, and bis-acetal was accessed in an 88 % yield. With acetal **242** in hand, O-allylation with allyl bromide afforded Claisen precursor **241** in a 60 % yield (Scheme 58).



Scheme 58. Synthesis of Claisen rearrangement precursor **241**

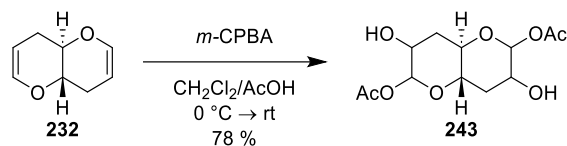
Unfortunately, all reaction conditions used for the Claisen rearrangement failed to deliver the desired diketone **210** (Table 2).

Table 2. Attempted Claisen rearrangement conditions



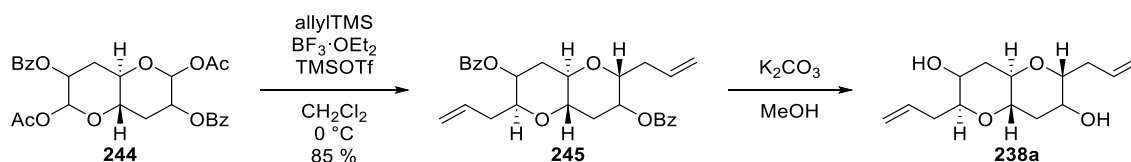
Entry	Conditions	Result
1	PPTS, pyridine, toluene, 130 °C	241 recovered
2	<i>p</i> -TsOH, quinoline, 190 °C	241 recovered
3	TMSCl, NaI, HMDS, MeCN, rt	Decomp.

The next route explored involved formation of acetate **243** followed by C-allylation to introduce the allyl groups. Enol ether **232** was epoxidised using *m*CPBA in the presence of acetic acid as a co-solvent. The acetic acid acted as a nucleophile and opened the epoxide, producing bis-acetate **243** (Scheme 59).



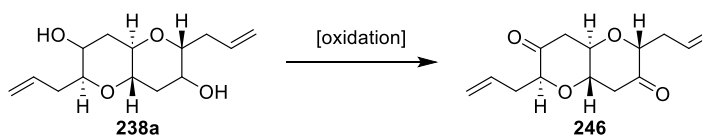
Scheme 59. Synthesis of bis-acetate **243**

The free hydroxy groups were protected with benzoyl groups in order to improve solubility. Benzoyl protected compound **244** was then subjected to C-allylation in the presence of allylTMS and a mixture of Lewis acids $\text{BF}_3 \cdot \text{OEt}_2$ and TMSOTf. Interestingly, this reaction did not proceed if either Lewis acid was used individually. Aggarwal and coworkers have reported that, when combined, $\text{BF}_3 \cdot \text{OEt}_2$ and TMSOTf produce $\text{BF}_2\text{OTf} \cdot \text{OEt}_2$, a significantly more powerful Lewis acid.⁶⁴ In the presence of $\text{BF}_2\text{OTf} \cdot \text{OEt}_2$, the desired bis-allylated product **245** was obtained in good yields. Debenzoylation with potassium carbonate in methanol afforded diol **238a** (Scheme 60).



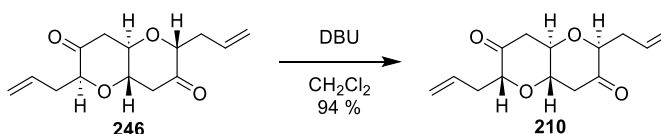
Scheme 60. C-allylation to produce diol **238a**

It was now necessary to oxidise diol **238a** to afford diketone **246** (Scheme 61). Both Swern and DMP oxidation reactions were attempted; the Swern oxidation afforded diketone **246** in a 50 % yield, whereas the DMP oxidation afforded diketone **246** in a 79 % yield.



Scheme 61. Oxidation of diol **238a**

Disappointingly, the major diastereomer obtained from both oxidation reactions was the undesired diastereomer in which both allyl groups were located in axial positions. Thus, epimerisation with DBU was necessary to access the desired diketone **210** (Scheme 62).



Scheme 62. Epimerisation of diketone **246** to desired diketone **210**

3.2 Desymmetrisation

3.2.1 CBS reduction

The first attempt to desymmetrise diketone **210** involved the use of the Corey-Bakshi-Shibata (CBS) reduction protocol. Three different CBS catalysts were used; (*R*)-Me-CBS **247**, (*R*)-*n*Bu-CBS **248**, and (*R*)-H-CBS **249** (Figure 9).

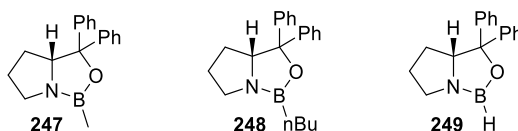
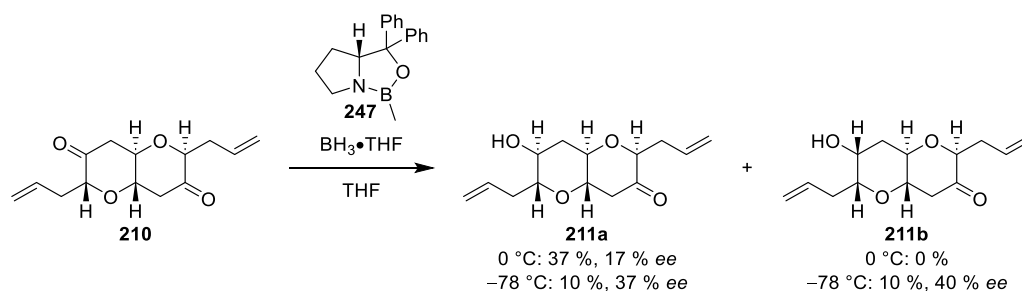


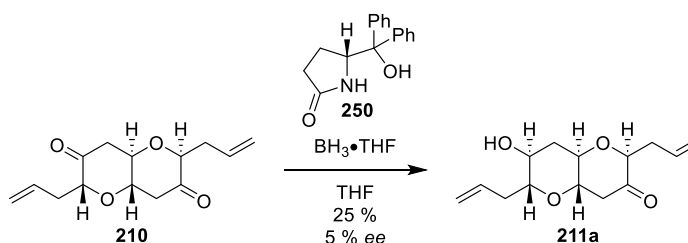
Figure 9. Structure of CBS catalysts **247**, **248**, and **249**

Desymmetrisation to mono-alcohol **211a** was attempted. The (*R*)-Me-CBS **247** was used at 0 °C and -78 °C. At 0 °C, it afforded both poor yields and product with low *ee*. When the reaction was performed at -78 °C, the *ee* was improved but the yield was significantly reduced. Additionally, production of the undesired diastereomer **211b** was observed when the reaction was performed at -78 °C (Scheme 63).



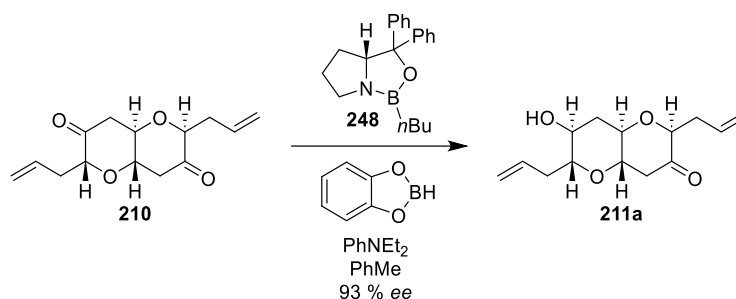
Scheme 63. Reduction of diketone **210** with (*R*)-Me-CBS

The (*R*)-H-CBS catalyst **249** was generated in-situ from lactam **250** and $\text{BH}_3 \cdot \text{THF}$. This catalyst gave the best yield at 25 %, but it also gave the lowest *ee* of just 5 % (Scheme 64).



Scheme 64. Asymmetric reduction of diketone **210** with (*R*)-H-CBS catalyst **234**

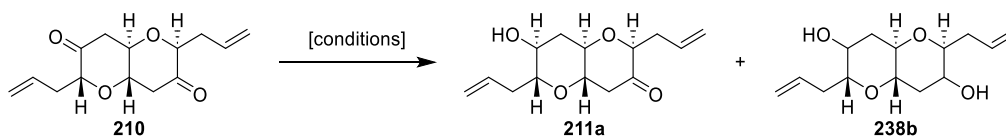
Unfortunately, although good *ee* values were obtained when the (*R*)-*n*Bu-CBS catalyst **248** was used, the very low yield (of 8 %) prevented this from being a viable method for desymmetrisation (Scheme 65).



Scheme 65. Reduction of diketone **210** with (*R*)-*n*Bu-CBS catalyst **248**

3.2.2 Metal-catalysed hydrosilylation

Hydrosilylation is a reaction in which Si-H bonds are added across C=C or C=O bonds. This can be used as a method for ketone reduction, because the silyl group can easily be removed, to give a free hydroxyl group. After the lack of success with the CBS reduction, an asymmetric metal-catalysed hydrosilylation reaction was chosen as the desymmetrisation method. Riant and coworkers reported an efficient system for the asymmetric hydrosilylation of ketones.⁶⁵ This technique employed the use of a CuF_2 /*S*-BINAP system with phenylsilane as the silane source. Riant and coworkers reported quantitative yields with *ee* values of up to 92 %. Unfortunately, when this system was applied to diketone **210**, low *ee* values and significant amounts of over-reduction to the diol **238b** were observed (Scheme 66).



Scheme 66. Asymmetric reduction of diketone **210**

Although the yields were significantly improved compared to those obtained when using the CBS catalysts, modest *ee* values meant this approach was not viable (Table 3). The best result achieved by use of this method was a 60 % yield with a product *ee* of 70 %, and significant amounts of diol **238b** were obtained (Table 3, Entry 4).

Table 3. Attempted conditions for the Cu-catalysed reduction of diketone **210**

Entry	Conditions	Result
1	BINAP (5 mol%), CuF ₂ (5 mol%), PhSiH ₃ (2.5 eq.), toluene, air, 23 °C	10 % 211a , 75 % ee, 238b major product
2	BINAP (10 mol%), CuF ₂ (10 mol%), PhSiH ₃ (1.1 eq.), toluene, air, 0 °C	62 % 211a , 50 % ee, trace 238b
3	BINAP (3 mol%), Cu(OAc) ₂ ·H ₂ O (6 mol%), PhSiH ₃ (1.5 eq.), toluene, Ar, 0 °C	Trace 211a , 70 % ee, 238b major product
4	BINAP (3 mol%), Cu(OAc) ₂ ·H ₂ O (6 mol%), PhSiH ₃ (1.0 eq.), toluene, Ar, 0 °C	60 % 211a , 70 % ee, 20 % 238b

A rhodium-based catalytic system developed by Nishiyama and coworkers was then explored (Table 4).⁶⁶ This method delivered product with high ee values, but conversion was poor initially. It was decided to take this method forward based on impressive ee values, and attempt to optimise the reaction conditions to improve conversion.

Table 4. Attempted conditions for the Rh-catalysed reduction of diketone **210**

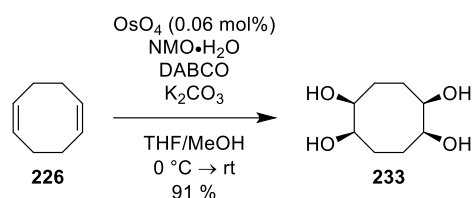
Entry	Conditions	Yield 211a	Yield	ee
			238b	211a
			(%)	(%)
1	[(S)-iPrPybox]RhCl ₃ (5 mol%), (S)-iPrPybox (20 mol%), AgBF ₄ (10 mol%), Ph ₂ SiH ₂ (1.2 eq.), THF, Ar, rt	71 % brsm (10 % conversion)	Trace	>95
2	[(S)-iPrPybox]RhCl ₃ (5 mol%), (S)-iPrPybox (20 mol%), iPrOH, piperidine, Ph ₂ SiH ₂ , THF, Ar, 96 h	52	35	>95

4. Results and Discussion

4.1 Synthesis of diketone **210**

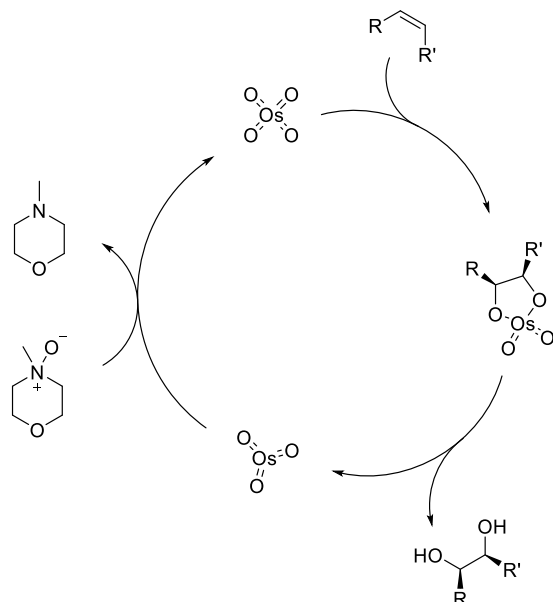
As discussed in Section 2 and Section 3, diketone **210** is a common functionality found within the MLP family. Dr. Jessica Elwood synthesised it in her work towards hemibrevetoxin B. It is also found in gymnocins A and B, and could potentially provide access to other key ring systems (e.g. ring expansion to a fused [7,7]-ring system).

Initially, the synthesis of diketone **210** was carried out using Dr Jessica Elwood's synthetic route.⁶³ The synthesis of diketone **210** began with Upjohn bis-dihydroxylation of 1,5-cyclooctadiene **226** (Scheme 67). This reaction afforded desired tetrol **233** in a 91 % yield.



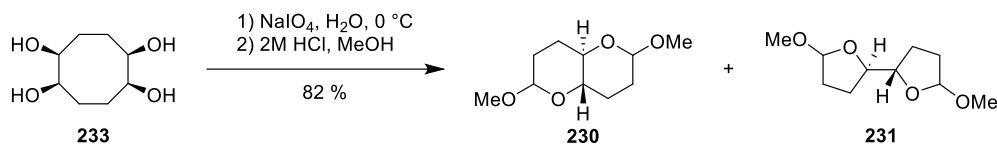
Scheme 67. Bis-dihydroxylation of 1,5-cyclooctadiene **226** to produce tetrol **233**

The Upjohn dihydroxylation was developed in 1976 as a modification to the standard dihydroxylation reaction at the time. In the original procedure, stoichiometric amounts of the highly toxic and expensive osmium tetroxide were required. In the Upjohn dihydroxylation reaction conditions, the additive *N*-methylmorpholine *N*-oxide (NMO) is used as a stoichiometric oxidant to regenerate the osmium tetroxide after dihydroxylation is complete, allowing the use of catalytic amounts of osmium tetroxide (Scheme 68).⁶⁷



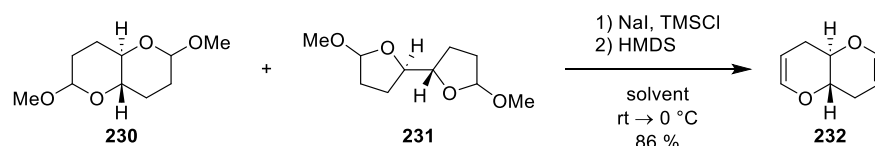
Scheme 68. Catalytic cycling of the Upjohn dihydroxylation

With decagram quantities of tetrol **233** in hand, the mixture of acetals **230** and **231** was produced via oxidative cleavage of one of the 1,2-diols present in the substrate, followed by cyclisation in the presence of acidic methanol (Scheme 69). This reaction gave a mixture of the fused bicyclic bis-acetal **230** and the linearly conjoined bis-acetal **231** in good yield.



Scheme 69. Synthesis of acetals **230** and **231**

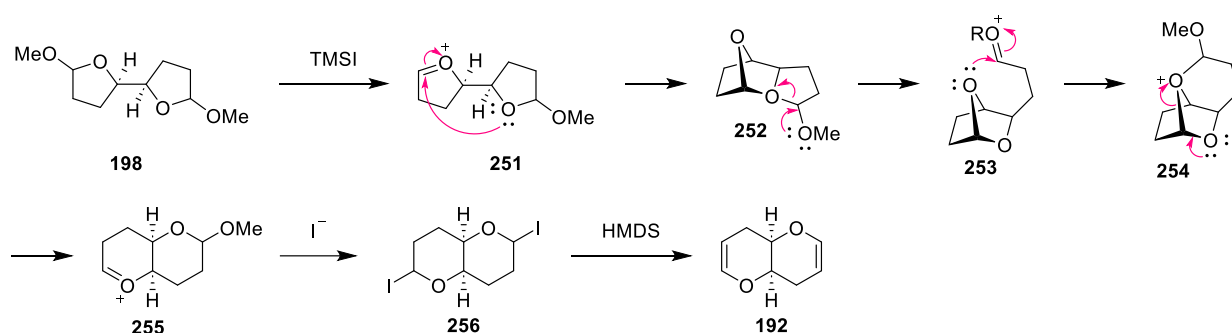
The mixture of bis-acetals **230** and **231** was converted into the fused bicyclic bis-enol ether **232** by subjecting it to conditions reported by Burton and coworkers (Scheme 70).⁵⁷ The methoxy groups were replaced by iodide groups upon the addition of sodium iodide and TMSCl. The addition of base led to deprotonation and displacement of the iodide groups to form enol ether **232**.



Scheme 70. Synthesis of enol ether **232**

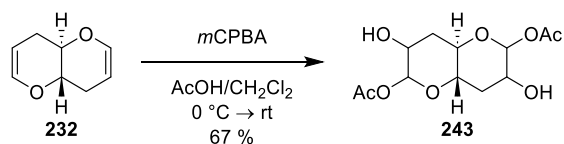
Burton and coworkers reported that both acetals **193** and **198** undergo the transformation to enol ether **192**, and they proposed a mechanism for this reaction

(Scheme 71). Exchange of one methoxy group with an iodide followed by spontaneous loss of the iodide produces oxocarbenium ion **251**. Cyclisation of **251** affords a tricyclic intermediate **252**. This intermediate opens to form second oxocarbenium ion **253**, which also undergoes cyclisation to form second tricyclic intermediate **254** which undergoes ring-opening to afford third oxocarbenium ion **255**. Nucleophilic attack of an iodide to the oxocarbenium ion and exchange of the remaining methoxy group with an iodide affords bis-iodide **256**. Addition of base (HMDS) affords desired enol ether **192**.



Scheme 71. Proposed mechanism for the formation of enol ether **192**⁵⁷

Enol ether **232** was epoxidised with *m*CPBA and then underwent in-situ epoxide opening using acetic acid to afford bis-acetate **243** (Scheme 72). This reaction was performed under anhydrous conditions as significant amounts of the tri- or tetrol may be produced if water is present. Initial attempts at this reaction suffered from purification difficulties due to the high polarity of bis-acetate **243**, leading it to become ‘stuck’ on the silica gel during flash column chromatography. It was found that the use of wide, short pads of silica for flash column chromatography were sufficient to remove *m*CPBA and its byproducts while avoiding loss of product.

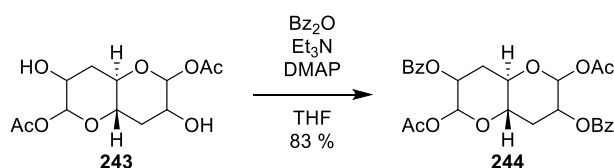


Scheme 72. Synthesis of bis-acetate **243**

This reaction produces multiple diastereomers as there is no stereocontrol in the epoxidation or epoxide-opening. Epoxidation can occur from either face of the molecule, producing diastereomers. Attack of acetic acid onto these diastereomers can also occur from either side of the molecule. It is possible that some interactions such as hydrogen bonding between the acetic acid and the epoxide oxygen may bias

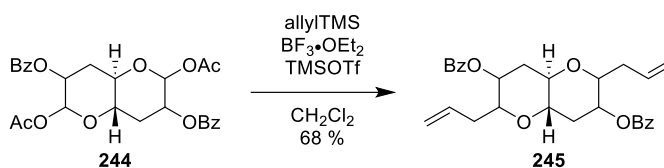
the *dr* towards one of the diastereomers, however the ratio of diastereomers was not investigated. Ultimately, the stereochemical outcome of this reaction is not of concern as the hydroxyl groups are later oxidised and the anomeric position can be altered by epimerisation.

Due to the insolubility of bis-acetate **243** in the solvent required for C-allylation, it was necessary to benzoyl protect the free hydroxyl groups. Benzoylation with benzoic anhydride, triethylamine, and DMAP afforded the desired protected bis-benzoate **244** in good yield (Scheme 73).



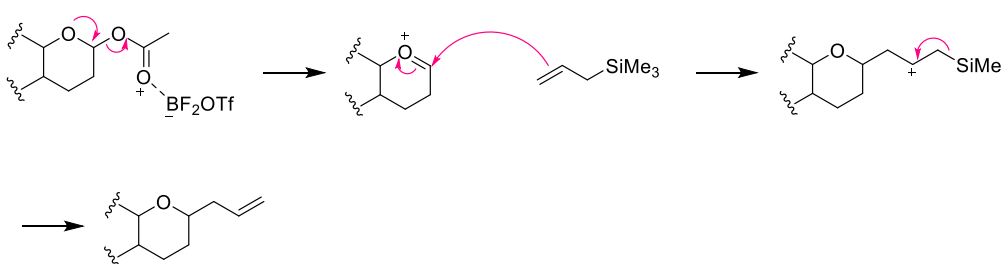
Scheme 73. Benzoyl protection of bis-acetate **243**

Upon successful dissolution of **244** in CH_2Cl_2 , C-allylation was accomplished by a Sakurai reaction with allylTMS to produce bis-allylated compound **245** (Scheme 74).



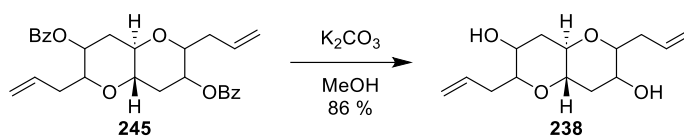
Scheme 74. C-allylation of **244**

This allylation is a Sakurai-type C-allylation. Allylation by allylTMS and activation of the electrophile by a Lewis acid are key components of the Sakurai allylation reaction. Loss of one acetate group affords an oxocarbenium ion. Nucleophilic attack by allylTMS followed by loss of the TMS group affords the desired allylated product (Scheme 75). The β -silicon effect allows the allylTMS to act as a nucleophile and stabilise the primary carbocation.



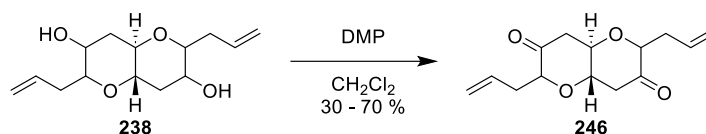
Scheme 75. Mechanism of C-allylation

Following C-allylation, the benzoyl groups were removed by treatment of **245** with potassium carbonate and methanol to afford diol **238** (Scheme 76).



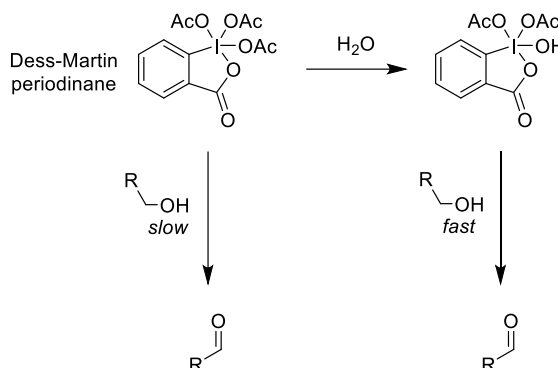
Scheme 76. Benzoyl deprotection of **245**

With both hydroxyl groups deprotected, the next step was to oxidise them to afford diketone **246**. Oxidation of diol **238** with Dess-Martin periodinane was performed (Scheme 77), but reliability issues were encountered with this reaction.



Scheme 77. DMP oxidation of diol **238**

It is known that the presence of water can improve the yield and rate of reaction of the DMP oxidation. This is a result of water reacting with DMP and producing a more powerful oxidant in situ (Scheme 78).⁶⁸

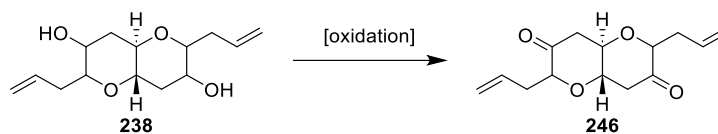


Scheme 78. Proposed explanation for the water-induced rate increase of DMP oxidations⁶⁸

Addition of water to the oxidation reaction was attempted, but no significant changes were noticed. It was then postulated that the diastereomers of **238** could have different rates of reactions in the oxidation, thus contributing to the variability in the outcome from the oxidation reaction.

The isolated diastereomers were individually subjected to the same oxidation conditions, but no significant differences in yields or rates of reaction were observed between the comparable reactions. Thus, it was decided to explore a variety of different oxidation methods. These attempted reactions are outlined in Table 5.

Table 5. Attempted oxidations for the synthesis of diketone **246**



Oxidation	Yield (%)
Freshly synthesised DMP	30
IBX	38
Parikh-Doering	Decomposition
<i>Attempted by co-workers:</i>	
Jones	36
PCC	50
TPAP	0 – 50
Oppenauer	0
TEMPO	Decomposition
NaOCl	Decomposition
Albright-Goldman	64

The Albright-Goldman oxidation was selected as the most successful oxidation method. This oxidation was reported in 1965 and it uses an ‘activated DMSO’ species as the oxidant (Figure 10).⁶⁹ DMSO reacts with acetic anhydride to produce an intermediate which is sufficiently electrophilic to be attacked by the alcohol. This method afforded improved and more reliable yields in comparison to the DMP oxidation when applied to diol **246**.

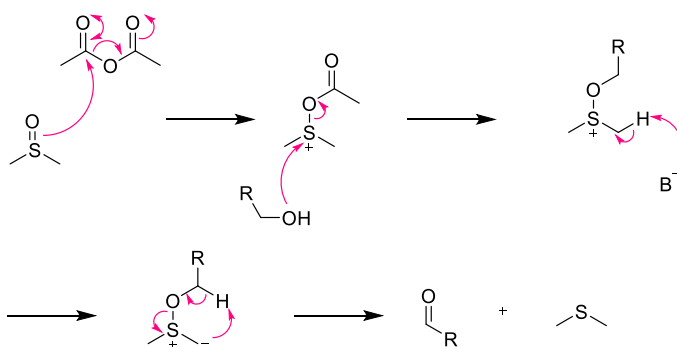
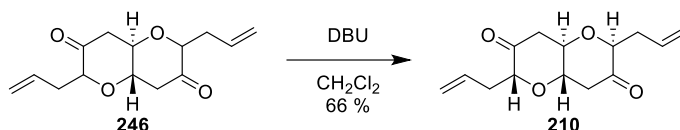


Figure 10. Mechanism of the Albright-Goldman oxidation

Unfortunately, the major diastereomer from the C-allylation possesses allyl groups in the axial position of each ring, whilst the desired diketone **210** requires them to be in the equatorial position. In order to obtain the correct diastereomer **210**, an epimerisation reaction of diketone **246** was performed with diazabicycloundecane (DBU) (Scheme 79). This method routinely afforded diketone **210** in a 6-10:1 ratio of desired epimer **210** to undesired epimer **246**.



Scheme 79. Epimerisation of diketone **246**

The epimerisation could be clearly observed by ^1H NMR spectroscopy. The protons at C_1/C_2 display an upfield shift in the spectrum of the required diastereomer as compared to the spectrum of the undesired epimer, and the protons at C_3/C_4 display a downfield shift (Figure 11).

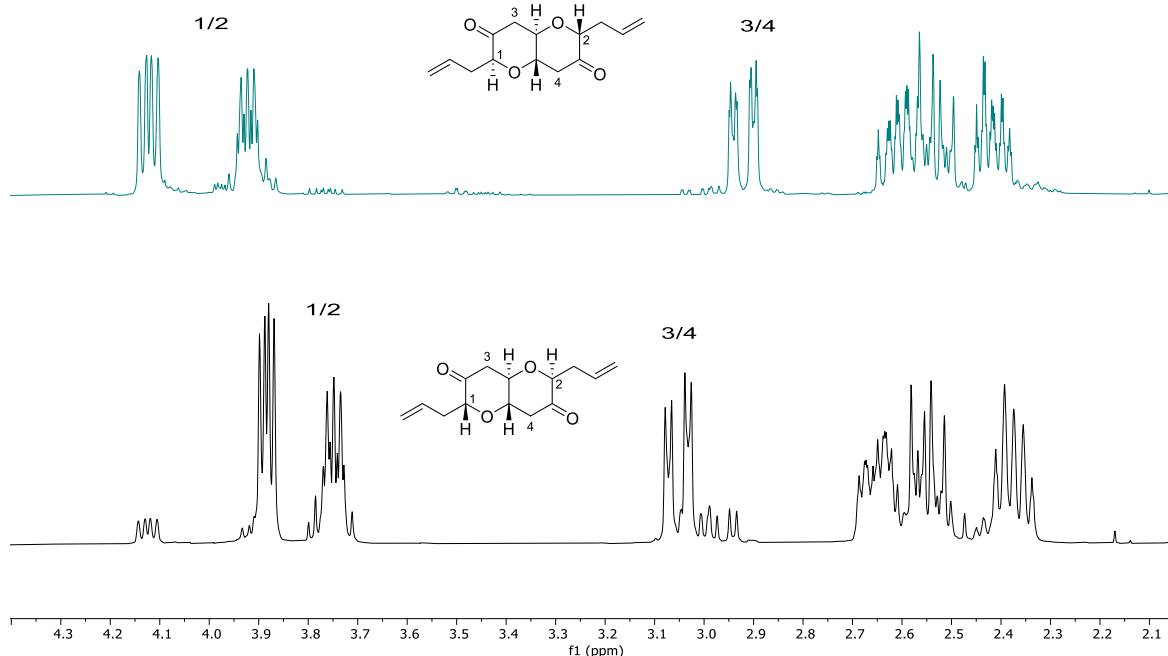


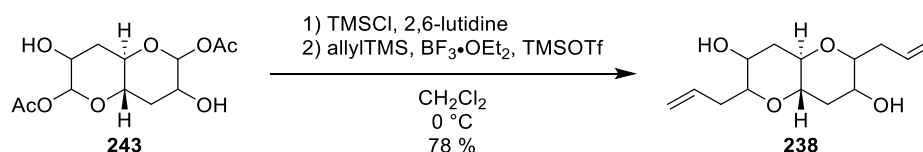
Figure 11. Comparison of ^1H NMR spectra of diketone **246** and epimerised diketone **210**

An X-ray crystal structure of desired epimer **210** was obtained (Figure 12).



Figure 12. X-Ray crystal structure of diketone **210**

Though diketone **210** could now reliably be accessed in 9 steps, the need for protection of the hydroxyl groups to improve solubility of diol **238** was not particularly elegant and required two extra steps. A one-pot allylation method was developed to circumvent this issue. This method involved in situ TMS protection of the hydroxy groups, increasing the solubility of the starting material in the reaction solvent. Subsequent addition of the Lewis acids and allylTMS resulted in in situ removal of the TMS groups and provided the allylated diol in a single operation (Scheme 80).



Scheme 80. One-pot C-allylation of bis-acetate **243**

When monitoring C-allylation progress by TLC, three major products were observed. The diastereomers were separated, and a crystal structure of one of the isomers was obtained (Figure 13).

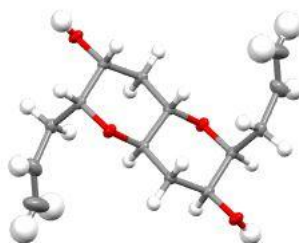
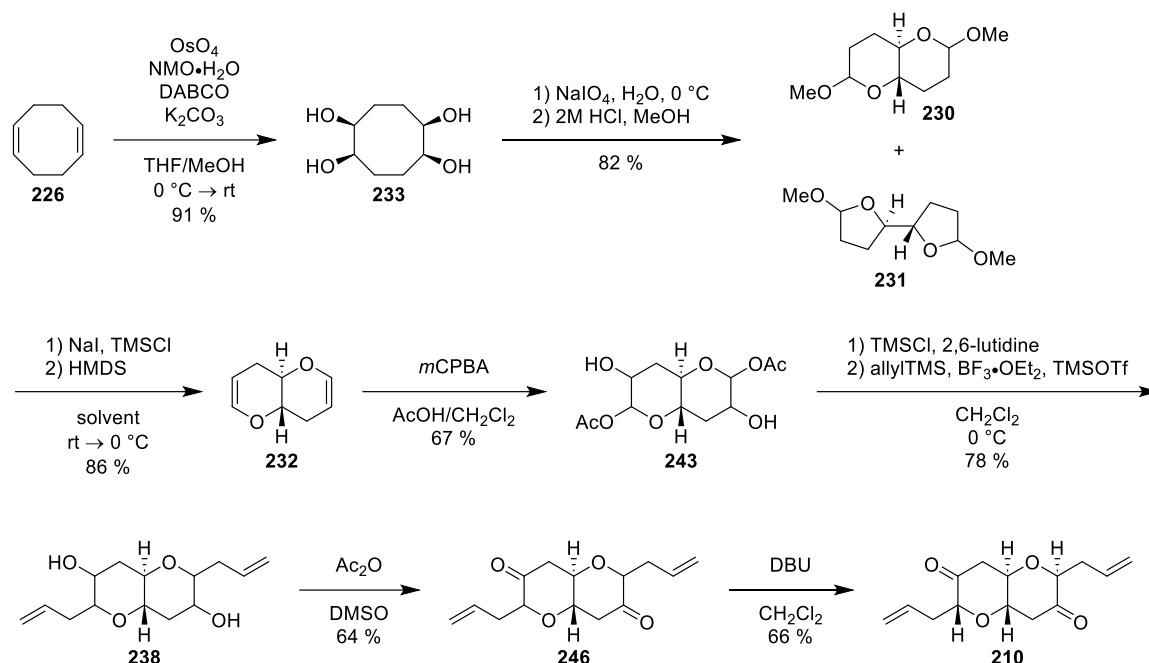


Figure 13. X-ray crystal structure of diol **238**

Diketone **210** could now be accessed on a multigram scale in six steps and with an overall yield of 14 % (Scheme 81).

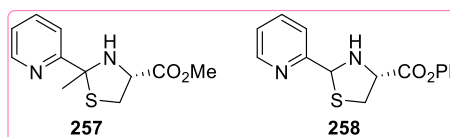
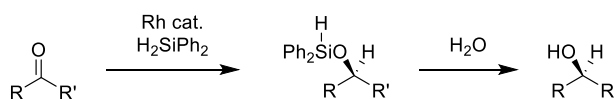


Scheme 81. 7-step synthesis of diketone **210** from 1,5-cyclooctadiene **226**

4.2 Desymmetrisation of diketone **210**

4.2.1 Background

Brunner and Kürzinger reported the enantioselective hydrosilylation of ketones with $[\text{Rh}(\text{COD})\text{Cl}]_2$ and pyridinethiazolidine ligands.⁷⁰ They successfully produced fifty-eight unique silyl ethers using this new method, and these silyl ethers were subsequently hydrolysed to the corresponding secondary alcohol (Scheme 82). The most successful ligands used were **257** and **258**.



Scheme 82. First reported enantioselective Rh-catalysed hydrosilylation of ketones and subsequent hydrolysis

Brunner and Kürzinger explored the reaction scope using a wide range of substrates and noted that functional groups appeared to have a large impact on ee values. Aryl and heterocyclic ketones were reduced to give alcohols with ee values of $\geq 80\%$, but linear alkyl ketones could only be reduced to give products with a maximum ee of 50%. In 35 of the 58 cases, ligand **258** provided better ee values than ligand **257** (Table 6).

Table 6. Substrate scope of the first reported enantioselective Rh-catalysed hydrosilylation of ketones

Entry	R	R'	Yield (%)	ee (%) (ligand 257)	ee (%) (ligand 258)
1	Ph	Me	90	79	85
2	2-chlorophenyl	Me	95	78	83
3	Phenyl	Et	90	61	74
4	2-pyridyl	Me	90	73	88
5	Butyl	Me	80	44	52
6	Heptyl	Et	85	11	19

Nishiyama *et al.* further developed this work on asymmetric rhodium-catalysed hydrosilylation reactions. In 1992, they reported a novel rhodium catalyst bearing a bis(oxazolanyl)pyridine ligand (commonly known as PyBox) (Figure 14).⁶⁶ Treatment of $\text{RhCl}_3(\text{H}_2\text{O})_3$ with PyBox **259** afforded the catalyst (PyBox)RhCl₃.

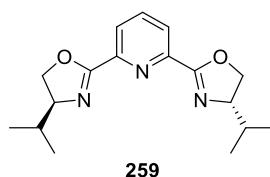
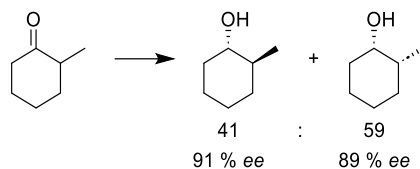


Figure 14. PyBox ligand **259**

They reported the reduction of 16 different aliphatic and aromatic ketones mediated by this complex. The best ee values were achieved with aromatic ketones, and lower ee values were observed with aliphatic ketones.

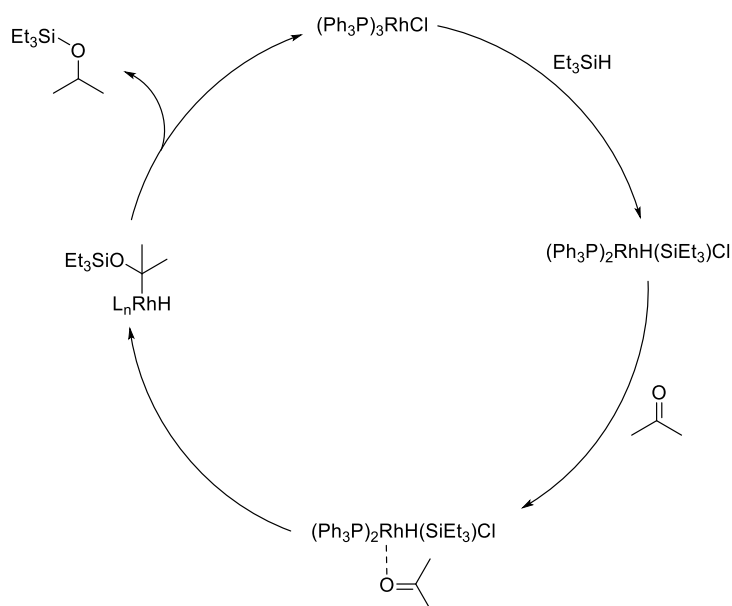
The reduction of cyclohexanone and its derivatives was also investigated (Scheme 83).⁷¹ It was expected that due to the bulky nature of the ligand, *cis* alcohol (corresponding to equatorial attack) would be the major product. However, a *trans:cis* ratio of 67:33 was observed. When the same conditions were used with substituted cyclohexanone derivatives, a roughly 50:50 ratio of *trans:cis* was observed. However, each product was isolated in high ee, thus demonstrating the *Re/Si* face selectivity of the catalyst, as opposed to axial/equatorial selectivity.



Scheme 83. Results of Rh-catalysed hydrosilylation of cyclohexanone with a PyBox catalyst

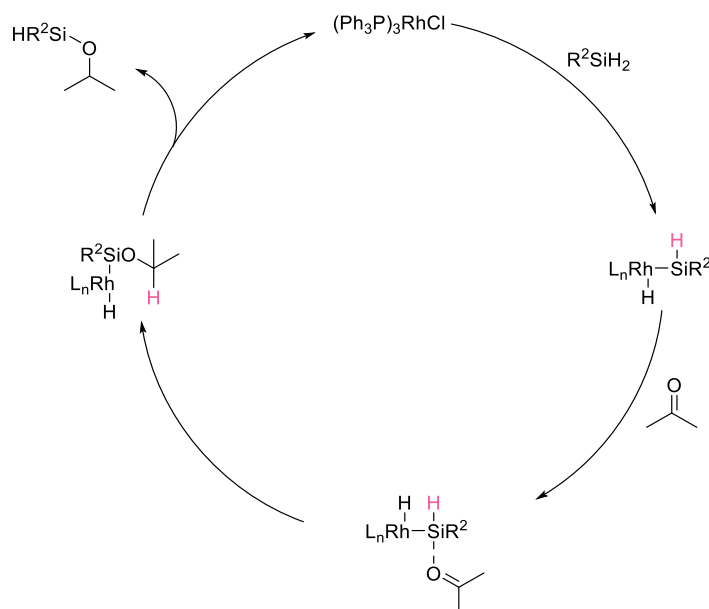
4.2.2 Previous mechanistic studies

There has been much debate regarding the mechanism of the rhodium-catalysed hydrosilylation of ketones. In 1975, Ojima *et al.* proposed the catalytic cycle below.⁷² Oxidative addition of the monohydrosilane to the rhodium catalyst forms Rh(III) species $(\text{Ph}_3\text{P})_2\text{RhH}(\text{SiEt}_3)\text{Cl}$. Co-ordination of a ketone to the rhodium followed by insertion into the Rh-Si bond forms the metallocarbene. The metallocarbene undergoes reductive elimination to release the product hydrosilane and regenerate the catalyst (Scheme 84).



Scheme 84. Ojima catalytic cycle for the Rh-catalysed hydrosilylation of ketones

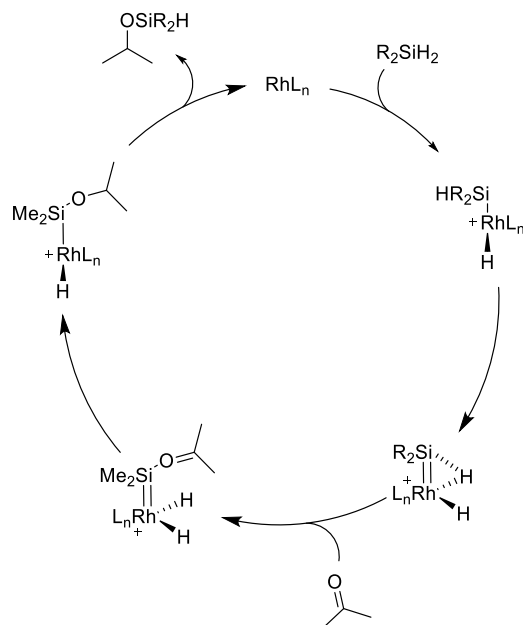
This mechanism was supported by the isolation of the $(\text{Ph}_3\text{P})_2\text{RhH}(\text{SiEt}_3)\text{Cl}$ intermediate. However, this mechanism does not explain the increase in reaction rate observed when a dihydrosilane is used instead of a monohydrosilane. As well as this, Chan *et al.* observed that, when applied to α,β -unsaturated systems, monohydrosilanes exclusively produce the 1,4-addition products, whereas dihydrosilanes exclusively produce the 1,2-addition products.⁷³ This cannot be explained by the mechanism proposed by Ojima and coworkers, and so Chan and coworkers proposed an alternative mechanism (Scheme 85).



Scheme 85. Chan catalytic cycle for the Rh-catalysed hydrosilylation of ketones

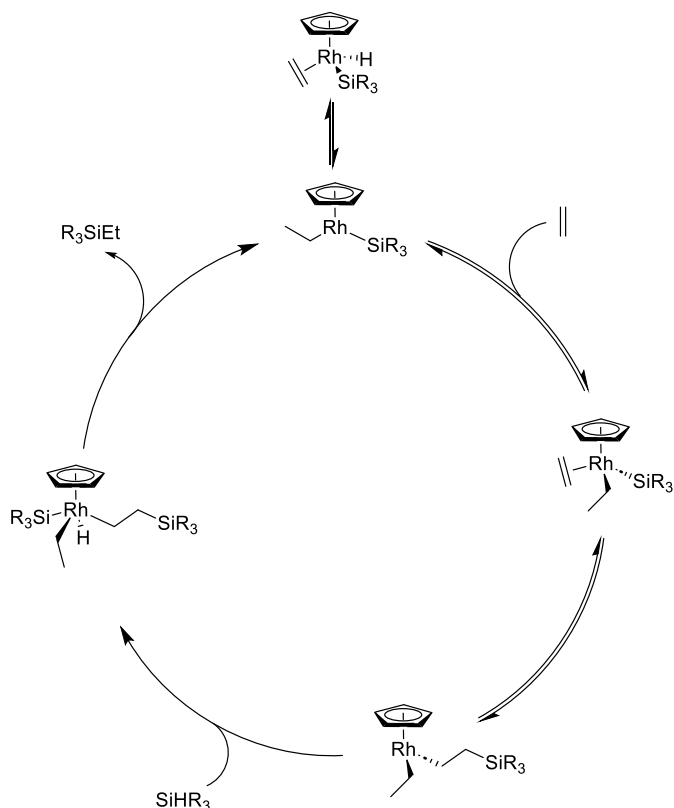
In this mechanism, it is the hydrogen on the silicon which is transferred onto the carbon of the carbonyl species. This hydrogen is not available when a monohydrosilane is used.

Gade and coworkers noted an inverse kinetic isotope effect (KIE) when dihydrosilanes were used in the enantioselective hydrosilylation of ketones. This KIE could not be explained by the previously discussed Chan mechanism, and thus Gade and coworkers put forth another possible mechanism (Scheme 86).⁷⁴ Computational studies suggested that the formation of a silylene intermediate provided a lower-energy pathway to the product, compared to the Ojima and Chan mechanisms.



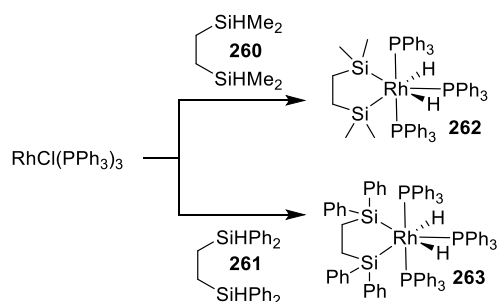
Scheme 86. Gade mechanism for the Rh-catalysed hydrosilylation of ketones

Aside from these three mechanisms, other hypotheses have been put forward with regard to the mechanism. Perutz *et al.* proposed a mechanism for the Rh-catalysed hydrosilylation of alkenes which involves a Rh(V) species (Scheme 87).⁷⁵ This species results from a second oxidative addition of a silane. Through deuterium labelling studies, it was found that incorporation of deuterium from Et₃SiD into CpRh(C₂H₄)(SiEt₃)H occurred. The amount of deuterated hydrosilylation product increased with the ratio of Et₃SiD to C₂H₄.



Scheme 87. Rh(V) mechanism for the Rh-catalysed hydrosilylation of ketones

Itoh *et al.* reported unusual rate increases during hydrosilylation reactions of carbonyl compounds when bifunctional organosilanes were used.⁷⁶ NMR studies found that the reaction of $\text{RhCl}(\text{PPh}_3)_3$ with **260** and **261** led to the production of disilyl Rh species **262** and **263** (Scheme 88). They postulated that since the second oxidative addition is intramolecular, it occurs much more rapidly and thus allows reductive elimination to occur more rapidly. In contrast, in the case of monofunctional silanes, oxidation addition is an intermolecular process.

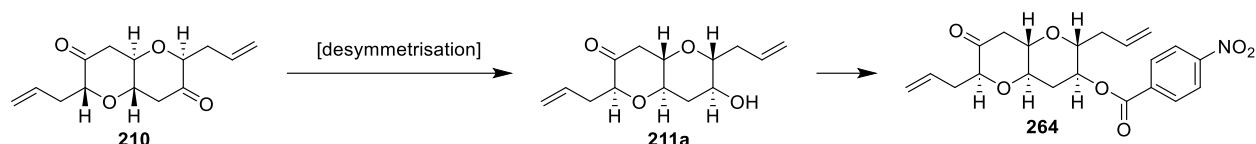


Scheme 88. Formation of Rh(V) species **262** and **263** from bifunctional organosilanes

4.2.3 Results of desymmetrisation of diketone **210**

As mentioned in Section 3.2, Nishiyama's conditions for asymmetric hydrosilylation were chosen based on impressive *ee* values obtained, though poor conversion

continued to be an issue. The reported procedure involved the use of catalytic [(S)-*i*PrPybox]RhCl₃ (5 mol%) with an extra 20 mol% of ligand present in solution. AgBF₄ was used as an additive to activate the catalyst (though it was found that the addition of *i*PrOH/piperidine could be used instead as a more cost-effective alternative), and diphenylsilane was used as the silane source. The ee of the product was measured by conversion into the *p*-nitrobenzoate ester **264** which was detected by UV on HPLC (Scheme 89).



Scheme 89. Desymmetrisation of diketone **210** and formation of UV-active **264**

Following the reported procedure, a decent ee could be seen although the exact ratio was difficult to determine due to a messy HPLC trace despite attempts at purification (Figure 15).

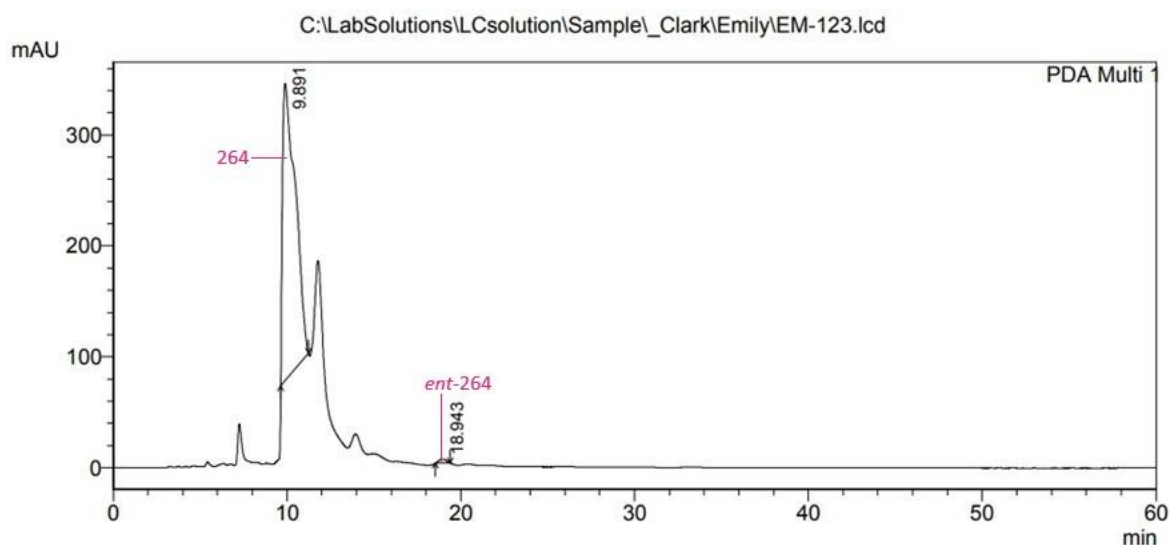


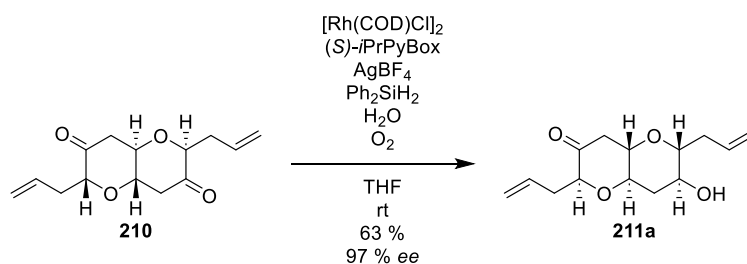
Figure 15. HPLC trace of diketone **210** desymmetrisation using Rh(III) catalyst

Across all polycyclic ether project team members, both poor conversion and significant variations in conversion presented themselves as issues. Various reaction conditions were screened by Dr. Sophie Woolford (previous PhD student) and, surprisingly, the addition of water was found to significantly increase the rate of reaction; considerable amounts of mono-alcohol **211** were visible on TLC after 18 hours, whereas no mono-alcohol **211** was present within the same timeframe when dry conditions with 4Å MS were used.⁷⁷ These results were reproducible across all team

members. These results were unanticipated because Nishiyama had reported that exclusion of water was required. It is hypothesised that the hygroscopic nature of AgBF_4 led to the accidental incorporation of water into the reaction in Nishiyama's case.

It was also discovered that sparging the solvent and catalyst mixture with oxygen prior to reagent addition increased the rate of reaction, and also provided a cleaner crude product. Barnett and coworkers reported an increase in reaction rate of Rh-catalysed ring openings of bicycloalkanes when oxygen was introduced to the system.⁷⁸ In a later publication, $[(\text{PPh}_3)_2\text{RhCl}(\text{O}_2)]_2$ was isolated and shown to catalyse ring-opening of bicycloalkanes, thus leading the authors to hypothesise that this is the catalytically active species in the reaction.⁷⁹ Though these observations were regarding Wilkinson's catalyst and not $[\text{Rh}(\text{COD})\text{Cl}]_2$, it is still noteworthy that a rhodium catalyst is known to benefit from the presence of oxygen. It may be the case that a rhodium-dioxygen species may be produced which is a more effective catalyst, thus causing the observed increase in reaction rate.

In the catalytic cycle for this reduction reaction, the active species is a Rh(I) complex. This Rh(I) species is generated from the Rh(III) catalyst that is initially added to the reaction. It was thought that if the reaction began with a Rh(I) source instead of a Rh(III) source, an improved reaction rate might be observed. This proved to be correct, and ~50 % conversion could be achieved after 18 hours with an impressive ee and cleaner HPLC trace (Figure 16). Unfortunately, one problem remained, and that is the over-reduction of diketone **210**. The reaction cannot go to completion, as the mono-alcohol **211** will begin to be reduced to diol **240** and so it is necessary to stop the reaction before full conversion is achieved. However, usable amounts of mono-alcohol **211** can be produced in high ee, making this a viable route for the desymmetrisation of diketone **210** (Scheme 90).



Scheme 90. Desymmetrisation of diketone **210**

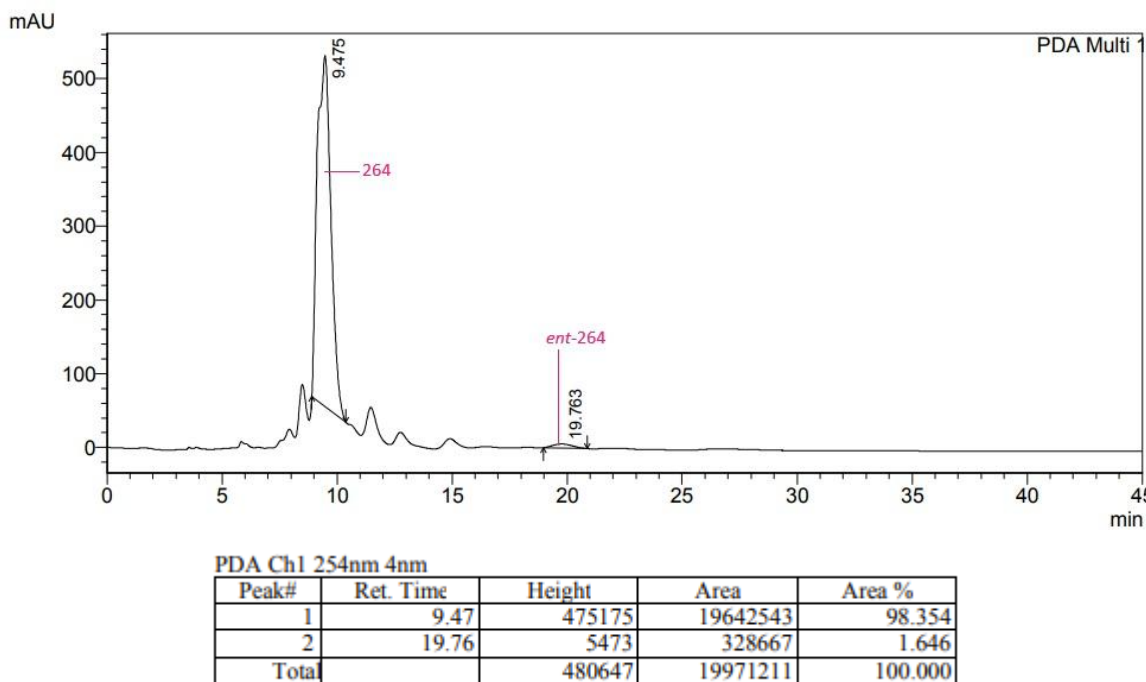


Figure 16. HPLC trace of diketone **210** desymmetrisation using Rh(I) catalyst

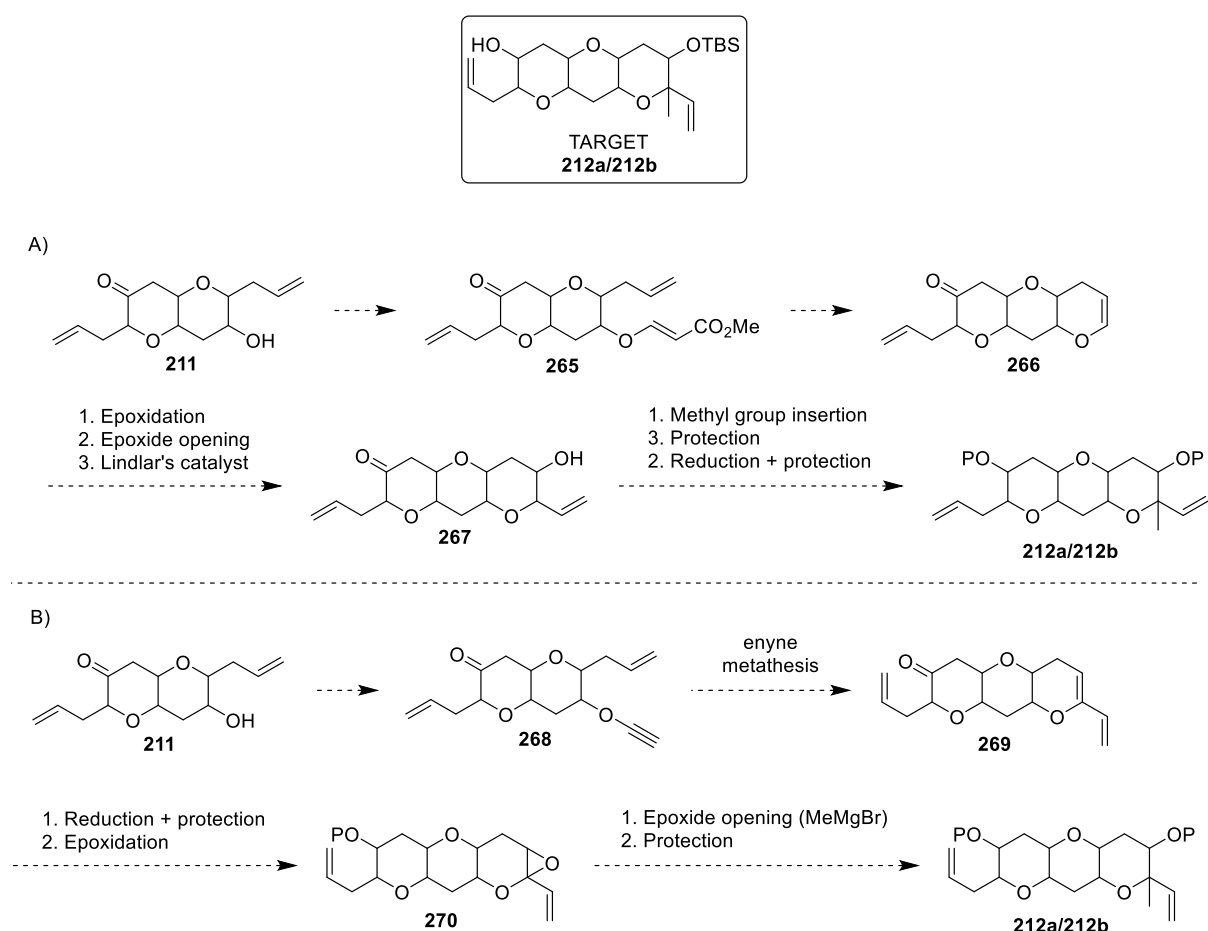
As discussed in Section 4.2.2, the exact mechanism for the reduction reaction is not obvious, which makes it difficult to propose a reason for the rate increase observed when water is introduced. As a dihydrosilane is used, it is likely that the reaction proceeds through the mechanism proposed by Chan and coworkers.⁷³ It could be postulated that water displaces the product from the rhodium centre, thus increasing catalyst turnover. Though their work concerned a Rh-catalysed carbonylation reaction and not hydrosilylation, it is interesting to note that Gomes da Rosa and coworkers observed an enhancement effect upon the addition of water.⁸⁰ Further studies showed that water was acting as a ligand in the active species, which provides some evidence that the same may be happening in our system.

4.3 Towards the total synthesis of gymnocin B

With a reliable synthesis of diketone **210** and a desymmetrisation procedure to **211** developed, this method could now be applied to the total synthesis of gymnocin B as discussed earlier.

The two proposed routes to produce fragments **212a** and **212b** are outlined below (Scheme 91). The first route follows an *O*-vinylation and RCM procedure that was previously developed in the Clark group for a similar compound to access enol ether **266**. Enol ether **266** could be epoxidised and subjected to epoxide opening with acetylenemagnesium bromide. The resulting alkyne could be reduced with Lindlar's

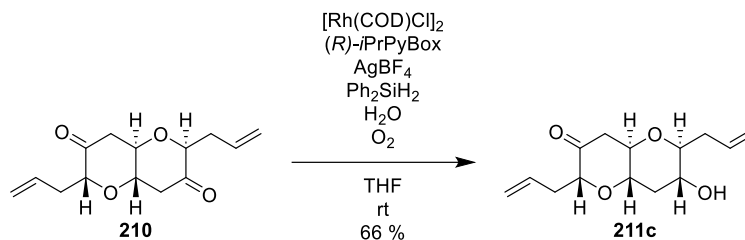
catalyst to afford vinylated product **267**. This product was envisaged to be subjected to a methylation procedure which will be discussed in Section 4.4 (Scheme 91A). The second route proposes that alkynyl ether **268** can be produced from either enantiomer of desymmetrised product **211**. Enyne metathesis of **268** would afford triene **269**. Triene **269** could undergo epoxidation and epoxidation with methylmagnesium bromide to afford the desired methylated products **212a** or **212b** (Scheme 91B). In their total synthesis of gambierol, Rainier *et al.* reported success in opening a similar bicyclic polyether epoxide by attack of the Grignard onto the carbon adjacent to the oxygen.⁸¹



Scheme 91. A) Synthesis of target fragment via *O*-vinylation route, B) synthesis of target fragment via enyne metathesis route

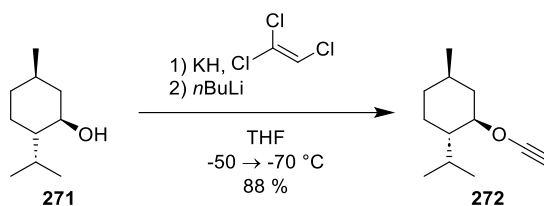
4.3.2 Attempts towards gymnocin B

It was decided to follow the synthesis outlined in Scheme 91B to access **212a/212b**. First, diketone **210** was desymmetrised to fragment **211c** following standard desymmetrisation conditions (Scheme 92).



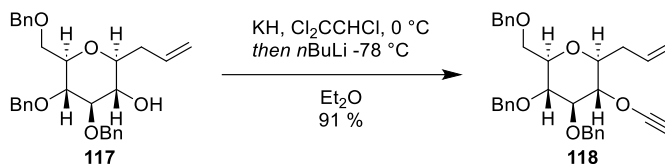
Scheme 92. Desymmetrisation of diketone **210**

To synthesise alkyne ether **268**, Greene's conditions were followed. In 1986, Greene and coworkers reported a method for the synthesis of alkyne ethers. They successfully produced alkyne ether **272** by treating alcohol **271** with trichloroethylene and *n*-butyllithium (Scheme 93).⁸²



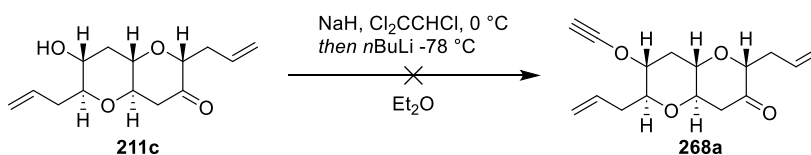
Scheme 93. Greene *et al.*'s procedure for alkyne ether synthesis

As mentioned in Section 1.2.4, Clark *et al.* applied this hydroxyl alkylation technique to the synthesis of an MLP intermediate **118** (Scheme 94).



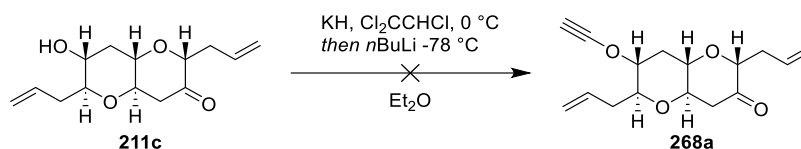
Scheme 94. Clark *et al.*'s synthesis of alkyne ether **118**

These conditions were applied to **211c**. However, as a result of availability in the lab, sodium hydride was first used as a replacement for potassium hydride, and freshly distilled trichloroethylene was used. Unfortunately, there was no reaction observed and alcohol **211c** was reisolated (Scheme 95).



Scheme 95. Unsuccessful synthesis of alkyne ether **268a** with sodium hydride

The reaction was repeated with potassium hydride instead of sodium hydride. Unfortunately, no desired product was observed (Scheme 96).



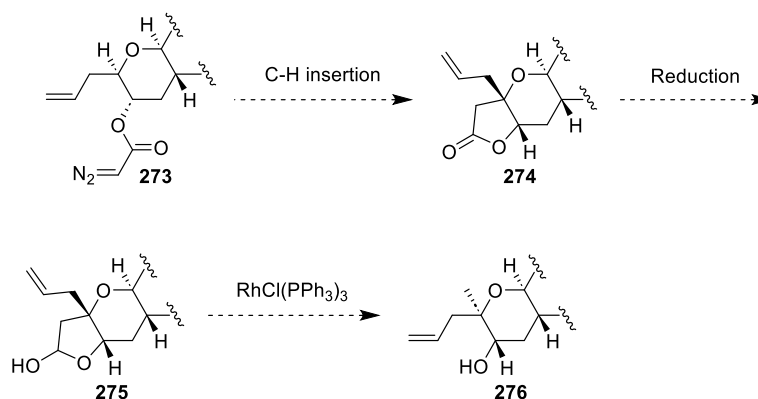
Scheme 96. Unsuccessful synthesis of alkynyl ether **268a** with potassium hydride

It is possible that the ketone functionality of **211c** was being converted to an enolate in the presence of potassium hydride. This enolate may have reacted with different reagents present in the reaction mixture, leading to the complex mixture that was observed. In future attempts, this ketone could be protected as an acetal, which should be stable to the reaction conditions. Due to time constraints this reaction could not be pursued any further.

4.4 Introduction of methyl groups

4.4.1 C-H insertion

Methyl groups at bridgehead positions are a common structural feature across the MLP family of natural products. The ability to introduce these methyl groups in the correct position with the correct stereochemistry is a crucial requirement for their total syntheses. It was hypothesised that reduction and decarbonylation of lactone **274** would afford the desired methylated product **276** (Scheme 97). This lactone would be produced via rhodium-catalysed C-H insertion reaction of diazoacetate **273**.



Scheme 97. Proposed synthesis of methylated compound **276**

It was decided to optimise all of these reactions on a model system, and acetonide **277** was chosen (Figure 17). This is a model system that has been used extensively in the Clark group in other studies.^{83,84}

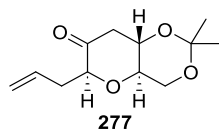
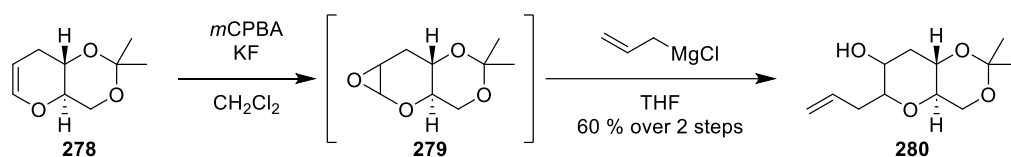


Figure 17. Model system for diketone **210**

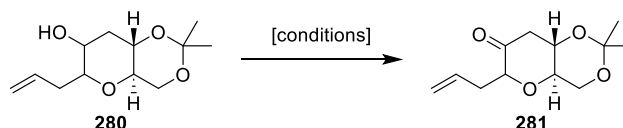
The synthesis of **277** begins with enol ether **278**, which was available in the lab from previous syntheses by other group members.⁸⁴ Enol ether **278** was epoxidised with *m*CPBA and the epoxide **279** was opened with allylmagnesium chloride to afford the allylated product **280** in a 60 % yield over two steps (Scheme 98).



Scheme 98. Synthesis of alcohol **280**

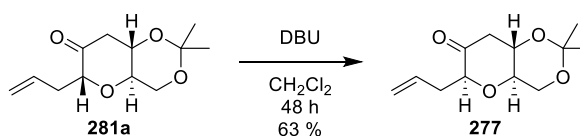
Alcohol **280** was then oxidised to afford ketone **281**. Several oxidation conditions were explored and the Albright-Goldman oxidation (Table 7, entry 2) was chosen as the preferred method.

Table 7. Attempted oxidations of alcohol **280**



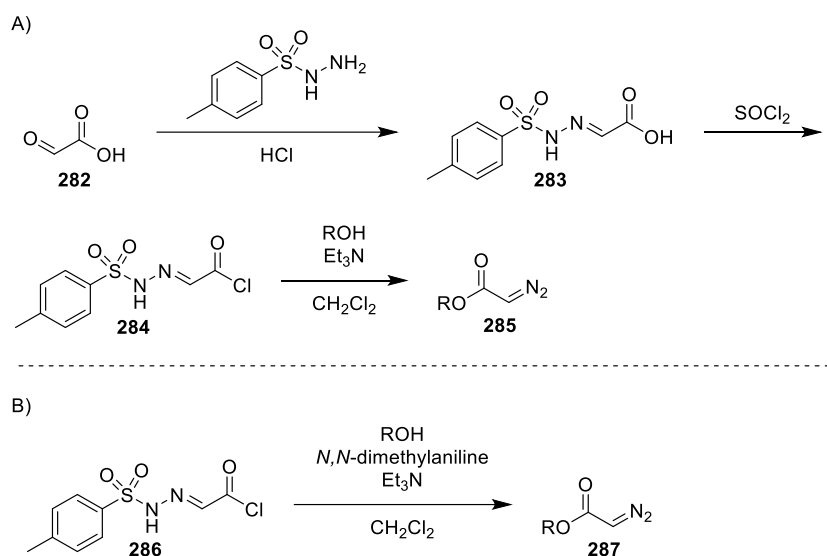
Entry	Conditions	Result
1	SO ₃ ·pyr, DMSO, Et ₃ N, CH ₂ Cl ₂ , 0 °C, 4 h	Decomp.
2	Ac ₂ O, DMSO, rt, 18 h	73 %
3	DMP, NaHCO ₃ , CH ₂ Cl ₂ , rt, 18 h	No reaction after 24 h

Unfortunately, the major isomer of the oxidation was the undesired diastereomer **281a**. Ketone **281a** was subjected to epimerisation with DBU to afford desired diastereomer **277** (Scheme 99).



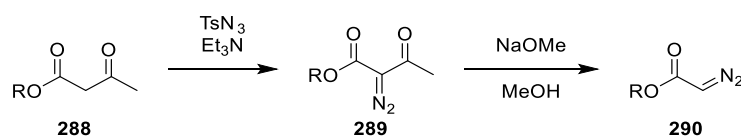
Scheme 99. Epimerisation of ketone **281a** to desired isomer **277**

In 2007, Fukuyama and coworkers reported a simple and efficient method for the synthesis of diazoacetates.⁸⁵ Until this point, the two major methods for diazoacetate synthesis had significant drawbacks. House *et al* reported the synthesis of diazoacetates from the *p*-toluenesulfonylhydrazone of glyoxylic acid.⁸⁶ This reaction was then modified and improved by Corey *et al*.⁸⁷ The reaction of an alcohol with the *p*-toluenesulfonylhydrazone of glyoxylic acid affords the desired diazoacetate in good yield (Scheme 100). However, the synthesis of the *p*-toluenesulfonylhydrazone of glyoxylic acid is a two-step procedure (Scheme 100A).



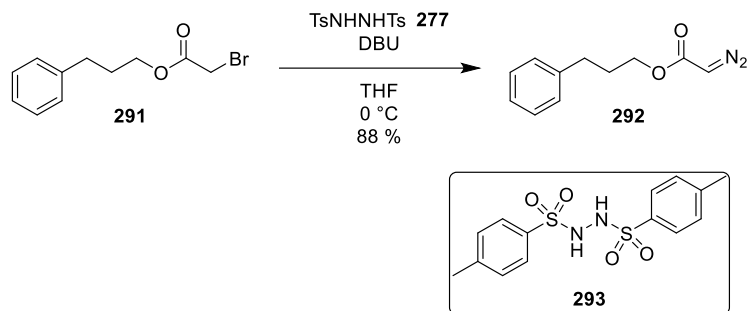
Scheme 100. A) House procedure for diazoacetate synthesis and B) the improved procedure by Corey *et al*.

Regitz *et al*. reported a two-step procedure for the production of diazoacetates from sulfonyl azides (Scheme 101).⁸⁸ However, this method requires an activating group which is removed under basic conditions. This excludes the use of any base-sensitive groups in the final diazoacetate product.



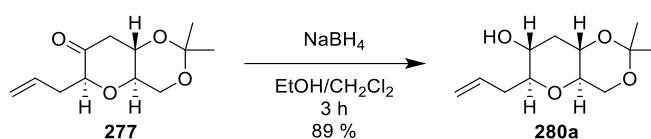
Scheme 101. Regitz procedure for diazoacetate synthesis

Fukuyama *et al*. reported a one-step procedure for the conversion of bromoacetates to diazoacetates using *N,N'*-ditosylhydrazine **293** (Scheme 102).⁸⁵ This simple method made the synthesis of diazoacetates more widely applicable.



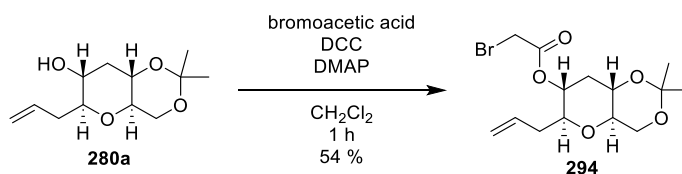
Scheme 102. Fukuyama's procedure for the synthesis of diazoacetates

Fukuyama's diazoacetate synthesis was chosen as the method to synthesise diazoacetate **273**. Ketone **277** was subjected to sodium borohydride reduction to afford alcohol **280a** as a single isomer in an 89% yield (Scheme 103).



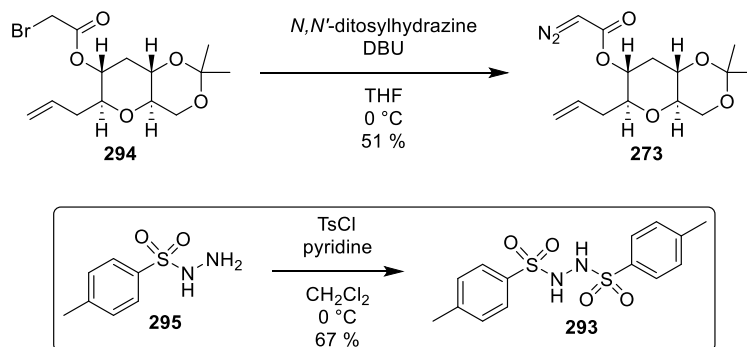
Scheme 103. Reduction of ketone **277** to alcohol **280a**

Alcohol **280a** was converted to bromoacetate **294** following a procedure reported by Feng *et al.*⁸⁹ This afforded bromoacetate **294** in a 54% yield (Scheme 104).



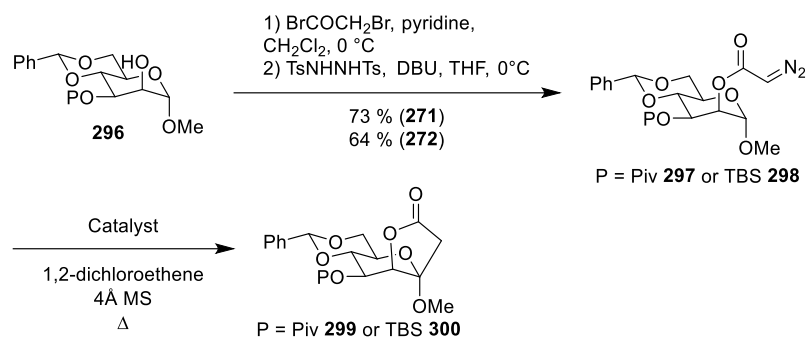
Scheme 104. Conversion of alcohol **280a** to bromoacetate **294**

With bromoacetate **294** in hand, Fukuyama's conditions were followed to produce diazoacetate **273** (Scheme 105). *N,N'*-Ditosylhydrazine **293** was synthesised from *p*-toluenesulfonyl hydrazide **295** and tosyl chloride, following the procedure reported by Fukuyama and coworkers.⁸⁵ This afforded diazoacetate **273**.



Scheme 105. Application of Fukuyama's diazoacetate synthesis to bromoacetate **294**

Focus now shifted to synthesis of lactone **274**, and this was expected to be doing following conditions reported by Lecourt *et al.* They reported a method for the carbene-mediated functionalisation of anomeric C-H bonds.⁹⁰ They investigated the insertion of metal-carbene species into the anomeric C-H bond of sugars; catalyst screening results are outlined in Table 8. This metal-carbene was synthesised from a diazoacetate-functionalised sugar. Fukuyama's diazoacetate synthesis was employed in order to access these diazoacetate sugars (Scheme 106).

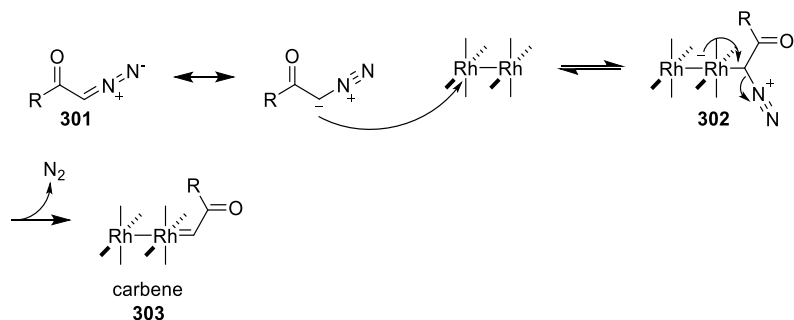


Scheme 106. Lecourt's procedure for anomeric C-H insertion

Table 8. C-H insertion catalyst screening by Lecourt *et al.*

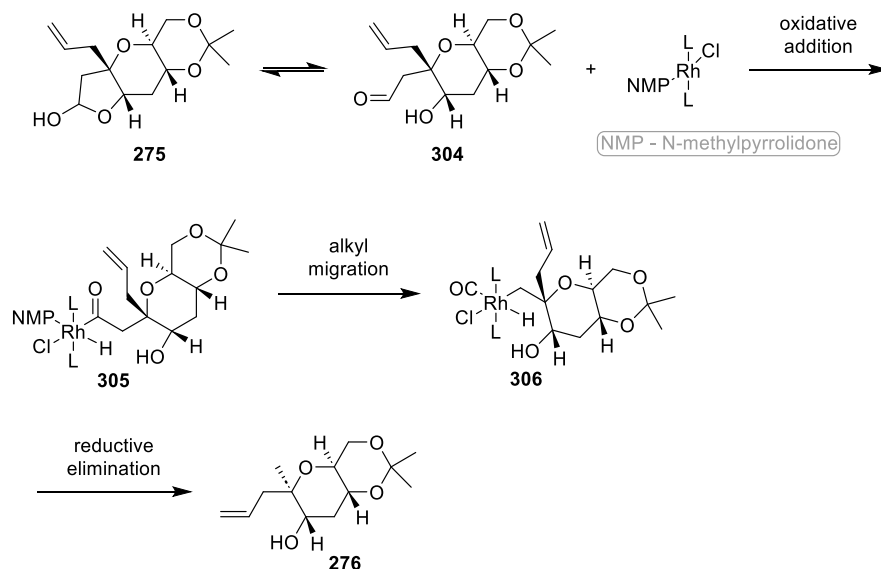
Entry	Diazosugar	Catalyst (mol%)	Yield (%)
1	297	Rh ₂ (OAc) ₂ (2)	77
2	297	Rh ₂ (oct) ₄ (2)	49
3	297	Rh ₂ (cap) ₄ (2)	9
4	297	Cu(acac) ₂ (2)	20
5	298	[RuCl ₂ (p-cym)] ₂ (2)	0
6	298	Rh ₂ (OAc) ₂ (1)	94

The mechanism for the rhodium carbenoid generation is outlined below (Scheme 107).⁹¹ The carbanion of the diazoacetate attacks the rhodium catalyst, forming the organometallic product **302**. Loss of nitrogen leads to formation of the metalcarbene **303**. This carbene species is then capable of inserting into a C-H bond, which would form lactone **274** if applied to diazoacetate **273**.



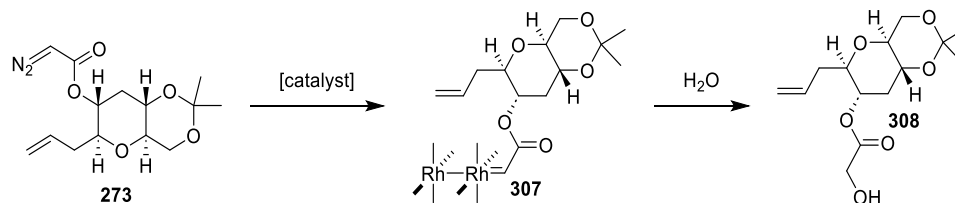
Scheme 107. Mechanism for the formation of metallocarbene **303**⁹¹

If lactone **274** could be accessed, it was hoped that reduction to lactol **275** would produce a species which behaved similarly to sugars in that it would undergo ring opening. It was imagined that application of the decarbonylation procedure reported by Andrews *et al.* to lactol **275** would produce the desired methylated product **276**. Andrews *et al.* developed a one-step conversion of C_n aldose sugars to their corresponding C_{n-1} without the use of protecting groups.⁹² Reduction of the lactone affords lactol **275**. This would allow ring-opening to aldehyde **304**. Oxidative addition of Wilkinson's catalyst is expected to afford species **305**. Migration of the CO group affords **306**. Reductive elimination produces desired methylated compound **276** (Scheme 108).



Scheme 108. Mechanism of Rh-catalysed decarbonylation

Rhodium-mediated C-H insertion was attempted with three different Rh(II) catalysts (Table 9). Unfortunately, with all three catalysts, the only product seen was the product from the reaction of water with the metallocarbene **307**, despite care being taken to maintain anhydrous conditions (Scheme 109).



Scheme 109. Reaction of metallocarbene **307** with water to form undesired side-product **308**

Table 9. Catalyst screening for C-H insertion

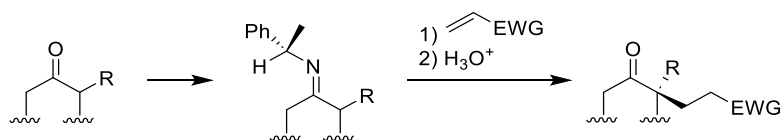
Catalyst	Result
$Rh_2(OAc)_2$	Only 308 observed
$Rh_2(TFA)_2$	Only 308 observed
$Rh_2(HFB)_4$	Only 308 observed

Lecourt and coworkers had noted that the addition of water was an issue in their original publication, but this problem was circumvented just by the slow addition of substrate to the catalyst. This was the procedure that had been followed, and yet the addition of water persisted as the only product. However, several years later, they reported on the impact of molecular sieves in this reaction and the prevention of side-reactions.⁹³ They noted that, on large scale, the reaction with water had become a significant issue. They experimented with differing amounts and types of 4Å molecular sieves and found that the best results were obtained with 1g/mg of catalyst, and it was crucial that vigorous stirring was applied.

This new procedure was followed, again with the same three catalysts as described previously. Unfortunately, the only product observed was the product of the reaction with water **308**. In future, it may be beneficial to explore performing this reaction in a glove box, or potentially drying the catalysts overnight under high vacuum to avoid any potential of water being introduced to the reaction.

4.4.2 α -Carbon functionalisation

A different option for inserting bridgehead methyl groups is following the α -carbon functionalisation strategy reported by D'Angelo *et al.*⁹⁴ This technique involves the conversion of the carbonyl group into an imine, followed by a Michael-type alkylation of the imine, and then hydrolysis to regenerate the carbonyl group (Scheme 110).



Scheme 110. D'Angelo *et al.*'s α -functionalisation of carbonyl compounds⁹⁴

By performing deuterium labelling studies, they determined that the reactive species is the corresponding enamine, and the formation of the C-C bond is concerted with a proton transfer to the α -position from the nitrogen. They proposed an 'aza-ene' type mechanism (Figure 18). This reaction proceeds with complete regioselectivity, with alkylation only occurring at the most substituted position of the enamine. Thus, with both of these requirements, the reaction must occur from enamine **311**, as this position holds the N-H bond and the enamine double bond *syn* to each other, allowing concerted proton transfer with C-C bond formation. With regards to the other possible enamine isomer **309**, the concerted proton transfer is not possible (Scheme 111).

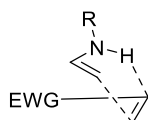
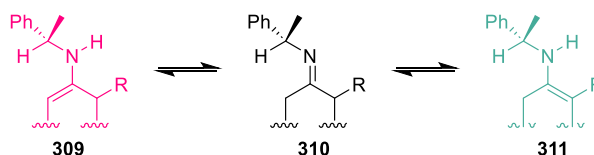


Figure 18. Proposed aza-ene transition state



Scheme 111. Allowed (**311**) and disallowed (**309**) product of the reaction

This reaction proceeds with impressive stereoselectivity, and this can be rationalised by the figure below (Figure 19). The phenyl group blocks the front face of the molecule, forcing back-side attack of the electrophile. In the case of an electrophile with non-bulky substituent, *endo* approach is favoured due to steric interactions between the R group and the EWG experienced in *exo* approach. In the case of an electrophile with a bulky substituent, the *endo* approach is disfavoured.

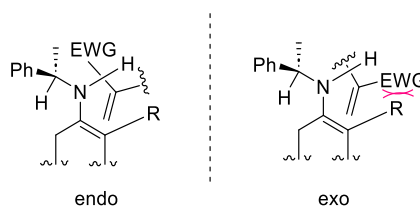
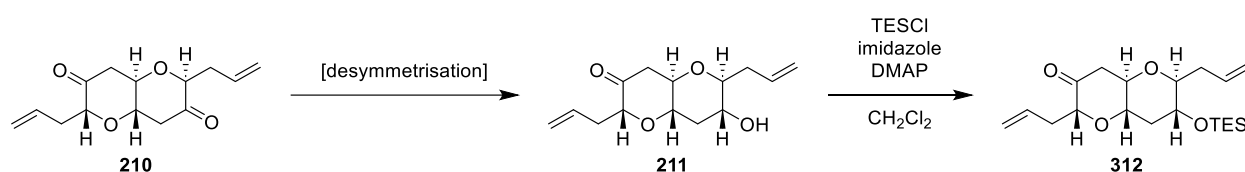


Figure 19. Explanation for stereoselectivity of the reaction

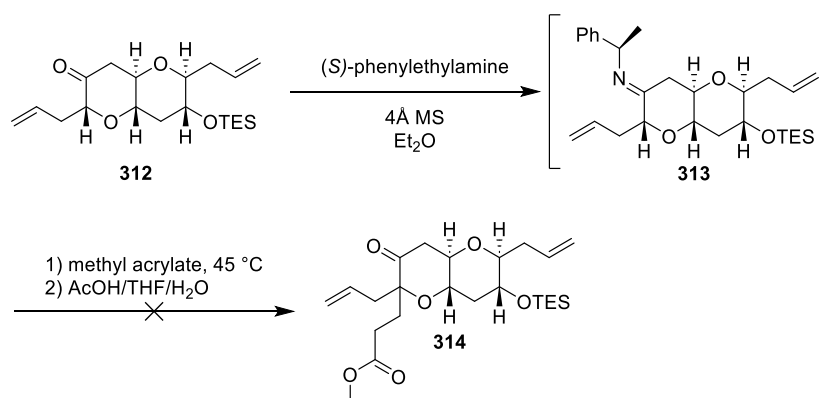
It was postulated that this technique could be used to functionalise the α position of diketone **210**. This would be achieved by synthesis of a diazoacetate in the α position. As in Section 4.4.1, Rh-catalysed C-H insertion followed by reduction and decarbonylation would afford the methylated product.

Initially, the original conditions provided in the article were used in order to determine if this procedure was compatible with our system. Diketone **210** was desymmetrised via standard desymmetrisation conditions discussed in Section 4.2. Once desymmetrised, the free hydroxyl was protected with a TES group to afford ketone **312** (Scheme 112).



Scheme 112. Desymmetrisation of diketone **210** and protection of the free hydroxyl

Ketone **312** was then converted to imine **313** following the conditions reported by D'Angelo *et al.*⁹⁵ Due to the unstable nature of imines, purification of imine **313** was not possible and it was used crude in the next reaction. Imine **313** was subjected to the conditions reported by D'Angelo *et al.* for α -functionalisation, but no product was observed (Scheme 113).



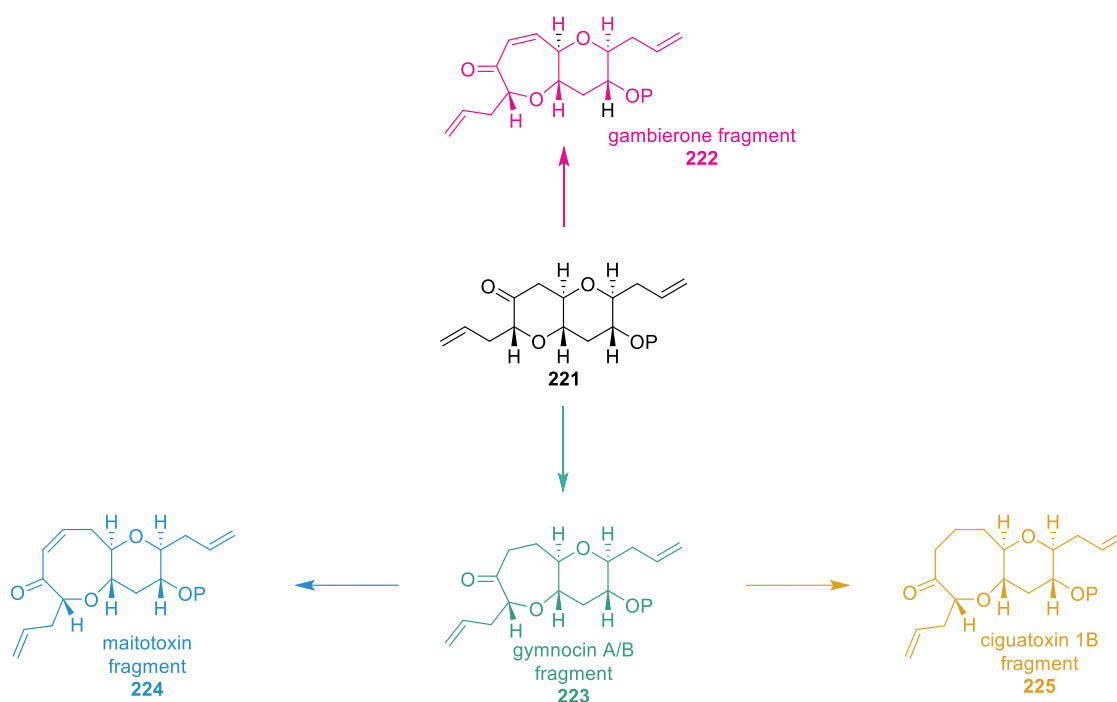
Scheme 113. Unsuccessful α -functionalisation of **313**

Due to time constraints, this procedure was not investigated any further.

4.5 Synthesis of fragments

Although this project focused on gymnocin B as a target natural product, this bidirectional/desymmetrisation approach could be applicable to a wide variety of additional MLPs. In order to demonstrate the utility of this method, we decided to

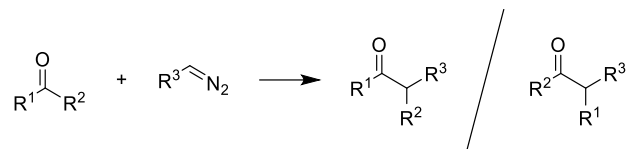
produce fragments from a range of MLPs. Once protected desymmetrised ketone **221** has been accessed, various other MLP fragments can be synthesised. Ring-expansion of the six-membered ring produces the [7,6]-system **223** that is found in both gymnocin A and gymnocin B. If, instead of TMS removal after ring-expansion, a Saegusa-Ito oxidation is performed on the ring-expansion product, the α,β -unsaturated enone **222** found in gambierone can be accessed. Further ring-expansion of the seven-membered ring of **223** could provide the [8,6]-system **225** found in ciguatoxin 1B. As before, a Saegusa-Ito oxidation of the ring-expansion product gives access to the α,β -unsaturated enone **224** found in maitotoxin. These fragments easily demonstrate the generality of this method (Scheme 114).



Scheme 114. Proposed fragments to be synthesised from ketone **221**

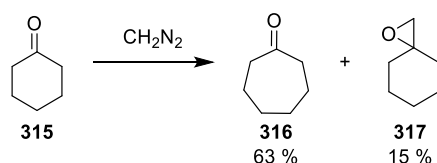
Ring expansion strategies are commonly employed in the synthesis of medium-sized (7- to 11-membered) ring systems. In traditional intramolecular cyclisation reactions to form these rings, loss of entropy coupled with transannular strain in the final product present a significant challenge. Using ring-expansion techniques, it's possible to offset these thermodynamic costs in some other way.

The Büchner-Curtius-Slotterbeck reaction is a popular homologation used for carbonyl compounds, employing the use of a diazoalkanes (Scheme 115).^{96,97} Although initially reported as a method for the synthesis of ketones from aldehydes, it has found extensive use as a ring-expansion technique for cyclic ketones.



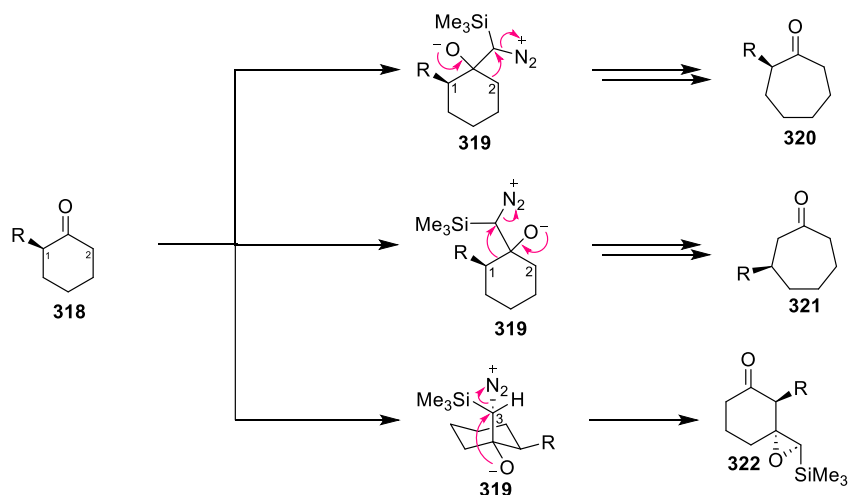
Scheme 115. Originally reported Büchner-Curtius-Schlotterbeck reaction

Mosettig and Burger were the first to apply this technique to cyclic ketones and demonstrated that it could be used for a single carbon ring-expansion.⁹⁸ In 1930, they described the conversion of cyclohexanone **315** to cycloheptanone **316**. They also observed the formation of an epoxide side product **317** (Scheme 116).



Scheme 116. Mosettig and Burger's ring expansion using the Büchner-Curtius-Schlotterbeck reaction

Though diazomethane provided useful ring expansion reactions, its use is limited by its toxicity and explosivity. TMS-diazomethane is a common alternative to diazomethane, because it maintains the reactivity of diazomethane while presenting a lower explosion risk. Upon formation of the tetrahedral intermediate **319**, rearrangement can occur from either C₁ or C₂, leading to the possible formation of two regioisomers **320** and **321**. The epoxide product **322** can be formed from attack of the oxygen onto C₃ (Scheme 117).⁹⁹

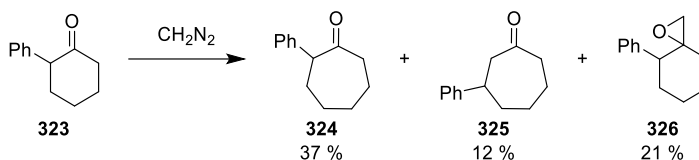


Scheme 117. Explanation for the three possible products of the TMS-diazomethane ring expansion

Electronic effects of substituents in the α position can significantly impact the outcome of the reaction. Electron-withdrawing groups increase the relative amount of

epoxide that is formed; the corresponding epoxide is formed in a 90 % yield in the reaction of 2-chlorocycloheptanone.¹⁰⁰

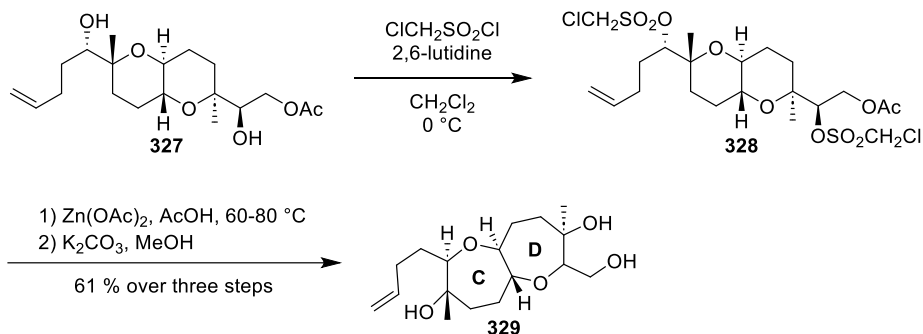
The presence of an alkyl or aryl group has been found to reduce the yield of the reaction, and two regioisomers of the product can be formed during the rearrangement. The ring-expansion of 2-phenylcyclohexanone **323** yields 37 % of regioisomer **324**, 12 % of regioisomer **325**, and 21 % of epoxide **326** (Scheme 118).¹⁰¹



Scheme 118. Diazomethane ring expansion of 2-phenylcyclohexanone **323**

4.5.1 Ring expansions in MLP synthesis

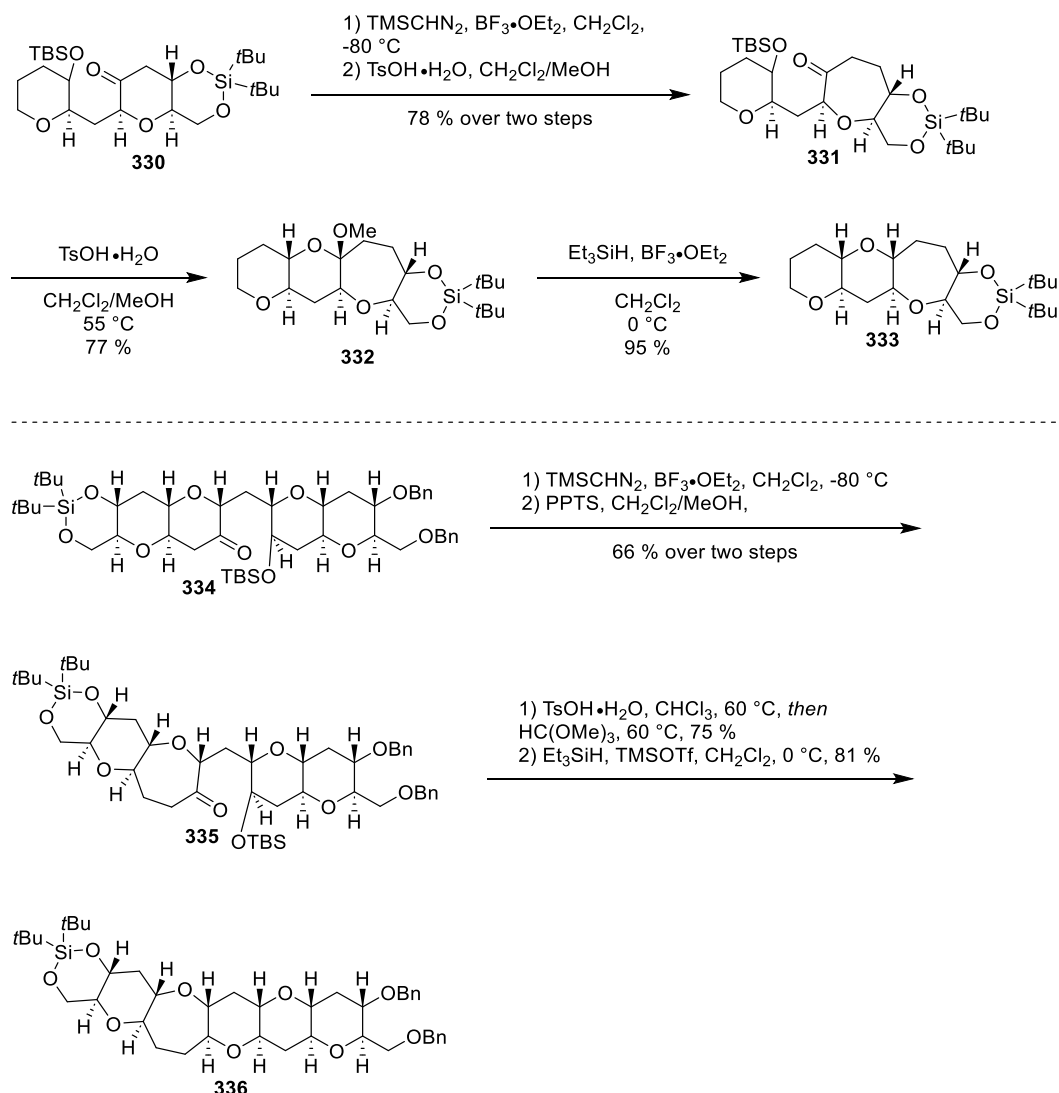
The use of ring expansion strategies in MLP synthesis is well-documented in the literature. In their synthesis of hemibrevetoxin B, Nakata and coworkers used ring expansion reactions in order to construct the CD rings (Scheme 119).⁵⁵ A double ring expansion of the [6,6]-system with $\text{Zn}(\text{OAc})_2$ afforded the CD fragment **329** in a 61 % yield over three steps.



Scheme 119. Ring expansion reaction in Nakata's synthesis of hemibrevetoxin B

In their directed synthetic studies towards the synthesis of polycyclic ethers, Mori *et al.* demonstrated the utility of ring-expansion reactions.¹⁰² In order to do this, they first synthesised the six-membered ring **330** which contained the desired functionality. This six-membered ring was then subjected to ring-expansion in the presence of TMSCHN_2 and $\text{BF}_3 \cdot \text{OEt}_2$ to afford the desired seven-membered cyclic fragment **331**. The ability to easily transform a six-membered ring to a seven-membered ring broadens the scope of this approach significantly, as MLPs generally have variable ring sizes along their polycyclic ether skeleton. They also employed the ring-expansion methodology on a

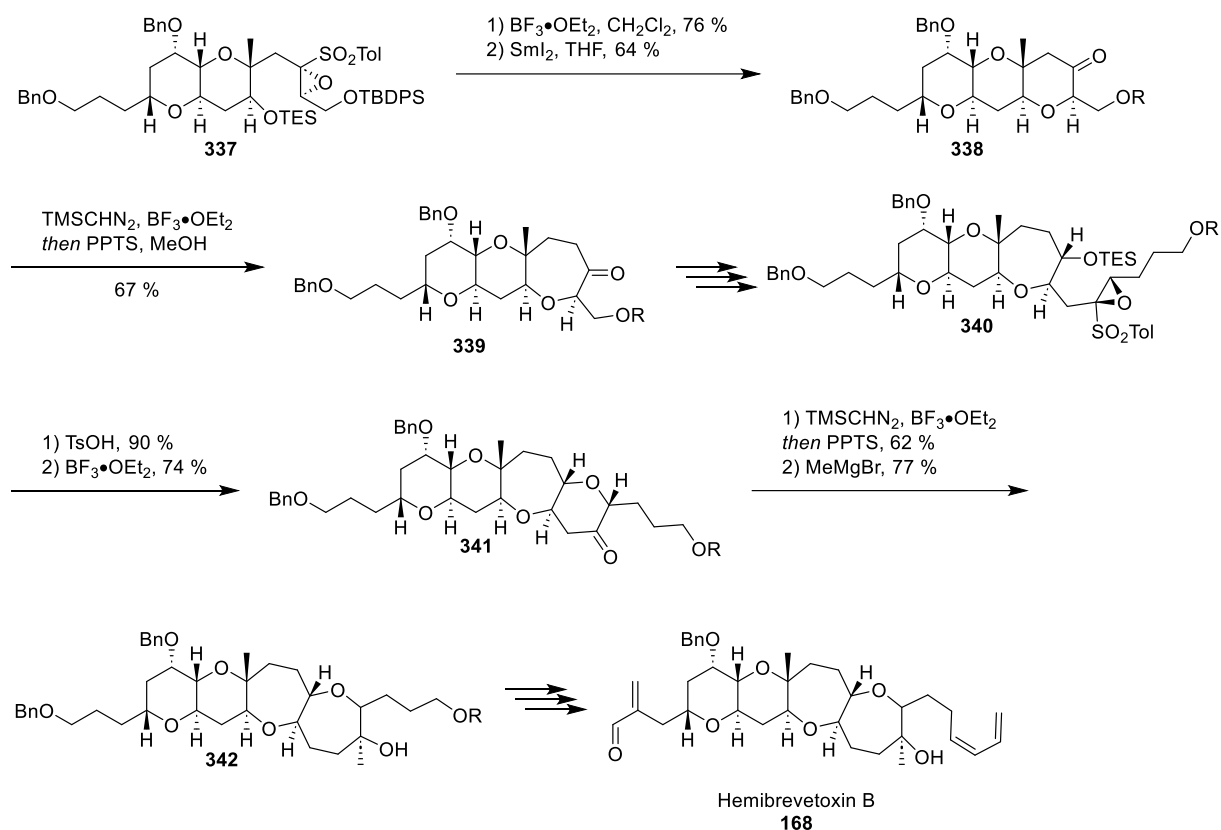
later stage pentacyclic fragment **334**, demonstrating that this technique can also be applied to larger, more complex polyether arrays (Scheme 120).



Scheme 120. TMS-diazomethane ring expansion reaction used in the synthesis of polycyclic ethers

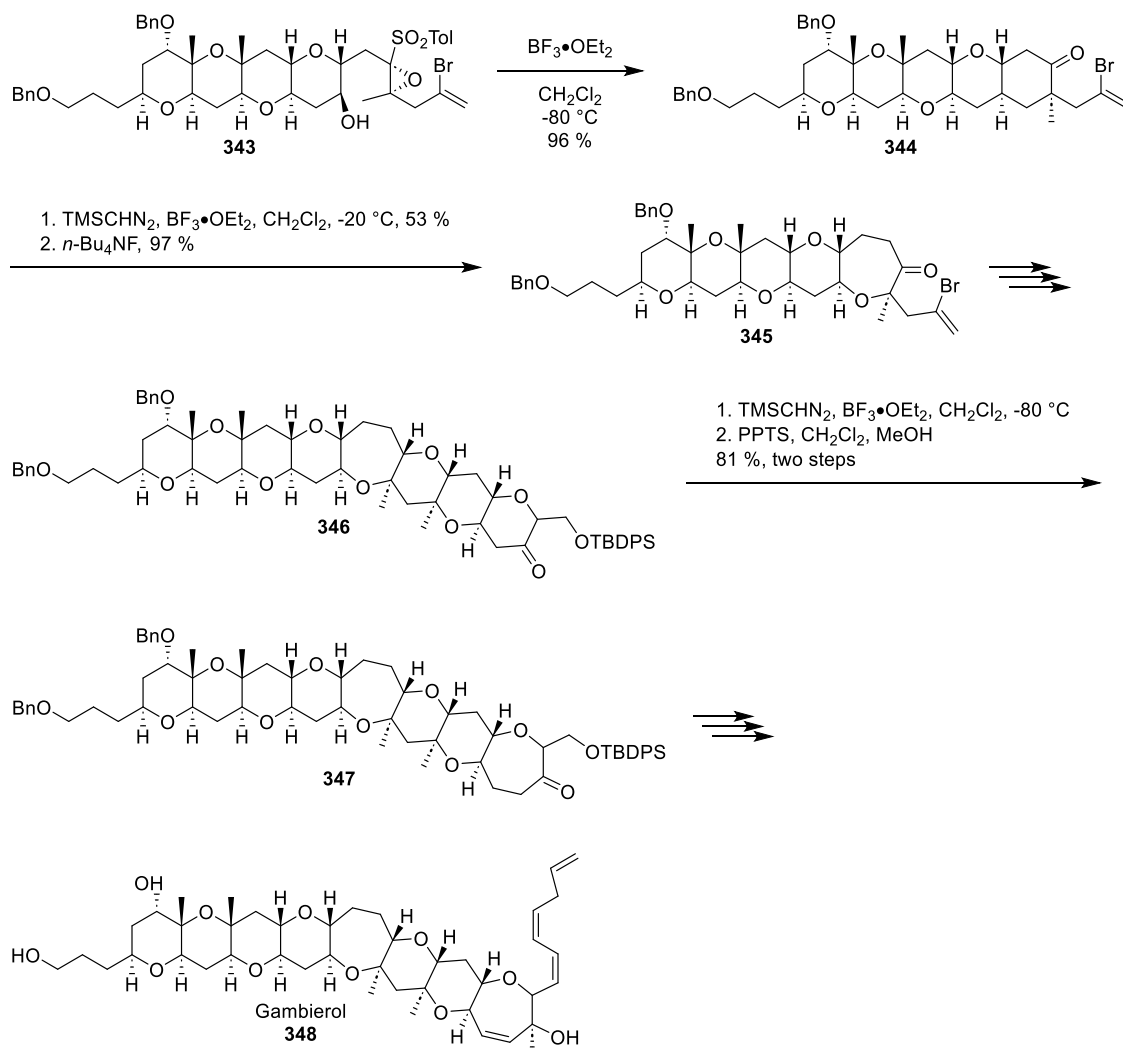
While in the previous work they focused on the synthesis of general polycyclic ethers, Mori *et al.* applied ring-expansion strategies to the total synthesis of MLPs. They used a biomimetic approach combined with ring-expansion strategies in the total synthesis of hemibrevetoxin **168**¹⁰³ and gambierol **337**.¹⁰⁴ In their synthesis of hemibrevetoxin B, they synthesised tricyclic fragment **338** and performed a ring expansion with TMSCHN₂ to afford the [6,6,7]-fragment **339**. Fragment **339** was converted to epoxide **340**, and a 6-*endo* cyclisation was carried out to afford tetracyclic ketone **341**. This tetracyclic ketone was also subjected to a TMSCHN₂-mediated ring-expansion to afford [6,6,7,7]-

tetracyclic fragment **342**. Further functionalisation afforded desired hemibrevetoxin B **168**.



Scheme 121. Mori *et al.*'s biomimetic/ring expansion approach to the total synthesis of hemibrevetoxin B **168**

In their synthesis of gambierol **337**, a 6-*endo* cyclisation of epoxide **343** afforded pentacyclic ketone **344**. Pentacyclic fragment **344** was subjected to a single-carbon ring-expansion to afford fragment **345**. After several more steps, they obtained the octacyclic ketone **346**. TMSCHN₂-mediated ring-expansion afforded fragment **347** and further functionalisation afforded the desired gambierol **348** (Scheme 122).

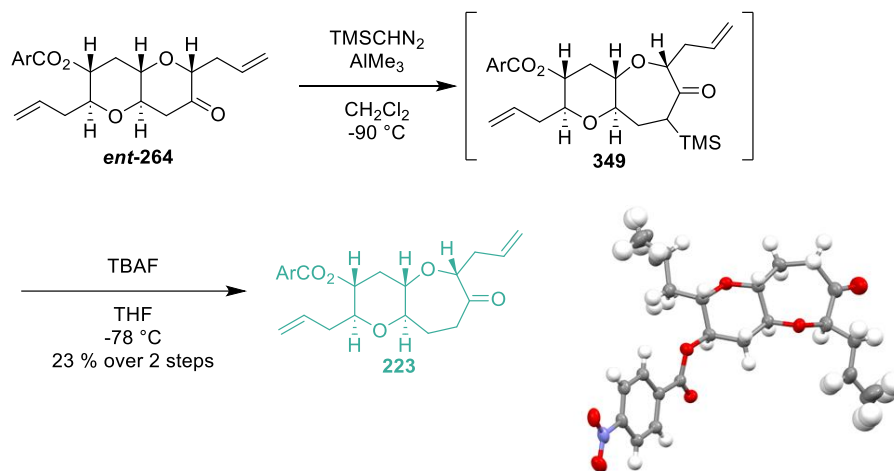


Scheme 122. TMS-diazomethane ring expansions used in Mori *et al.*'s synthesis of gambierol

348

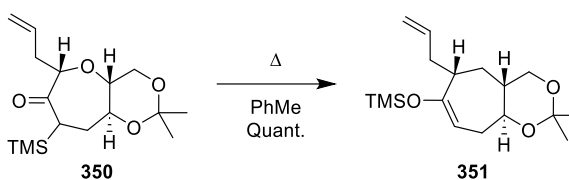
4.5.1 Synthesis of fragments via TMS-diazomethane ring expansion

With all of this information in mind, TMS-diazomethane was chosen as the reagent for the six- to seven-membered ring-expansion. Initially, $\text{BF}_3 \cdot \text{OEt}_2$ was used as the Lewis acid promoter, but it was found that AlMe_3 gave a cleaner reaction with improved the level of conversion. Following ring expansion, crude product **349** was subjected to silyl deprotection in the presence of TBAF to afford desired **gymnocin A/B fragment 223** (Scheme 123). An X-ray crystal structure of **ketone 223** was obtained and it showed the desired product.



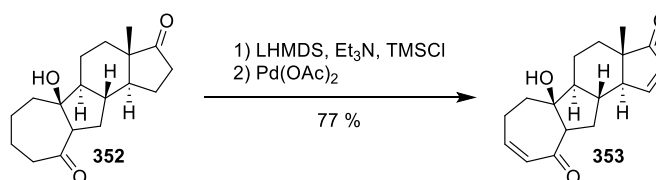
Scheme 123. Synthesis of gymnocin A/B fragment **223**

Initially, it was envisioned that silyl enol ether **354** could be accessed via a Brook-type rearrangement of **349**.¹⁰⁵ A similar transformation had been performed previously in the group, where ketone **350** was converted to silyl enol ether **351** (Scheme 124).



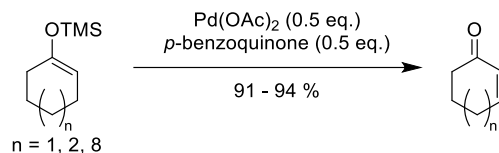
Scheme 124. Brook-type rearrangement previously done in the Clark group⁸³

Unfortunately, application of these reaction conditions to **349** afforded no reaction. As an alternative, the α,β -unsaturated ketone was produced by application of the conditions reported by Li *et al.*¹⁰⁶ In their total synthesis of bufogargarizins A and B, they produced α,β -unsaturated ketone **353** from bis-ketone **352**, which bore some similarities to our ketone **248** in that it was a seven-membered cyclic ketone that was part of a fused cyclic system (Scheme 125).



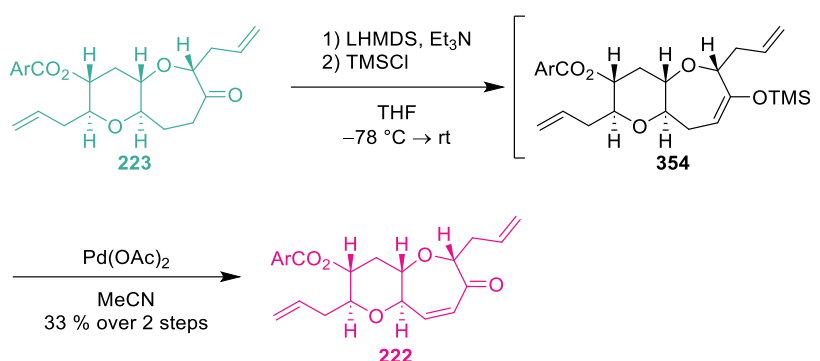
Scheme 125. Li *et al.*'s synthesis of α,β -unsaturated ketone **353**

This sequence of reactions involves producing the silyl enol ether, which is then subjected to a Saegusa-Ito oxidation. This reaction was first reported in 1978 as a way to access α,β -unsaturated carbonyl compounds from their saturated counterparts (Scheme 126).¹⁰⁷



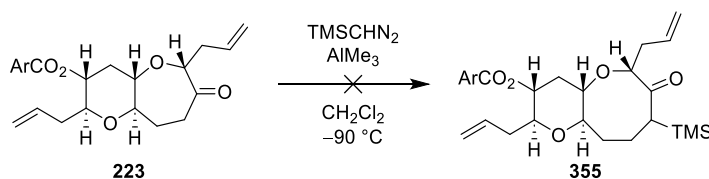
Scheme 126. Saegusa-Ito oxidation

The silyl enol ether was produced from ring expanded product **223** following the conditions reported by Li *et al.*¹⁰⁶ Unpurified silyl enol ether **354** was used in the Saegusa-Ito oxidation, where stoichiometric amounts of palladium acetate afforded α,β -unsaturated gambierone fragment **222** (Scheme 127).



Scheme 127. Synthesis of gambierone fragment **222**

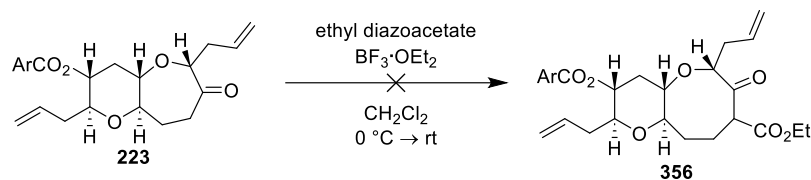
The next challenge to tackle was the expansion of the seven-membered ring to the eight-membered ring found in the maitotoxin and ciguatoxin fragments. The first attempt was performed using the same conditions as before, but unfortunately reaction was not observed and only starting material was recovered (Scheme 128).



Scheme 128. Unsuccessful ring expansion of **223**

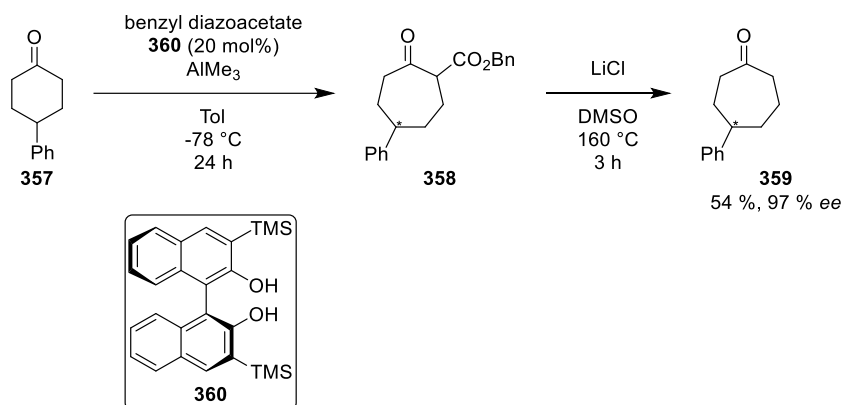
4.5.2 Other single-carbon ring expansion methods

Ethyl diazoacetate is another diazo compound which can be employed in a ring expansion reaction. Unfortunately, treatment of ketone **223** with ethyl diazoacetate and $\text{BF}_3 \cdot \text{OEt}_2$ gave no reaction after 24 h and led to eventual decomposition (Scheme 129).



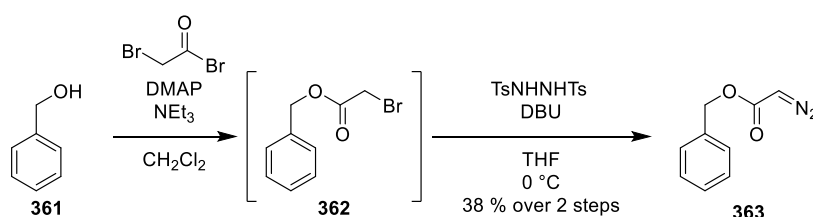
Scheme 129. Unsuccessful ring expansion of ketone **223**

In 2024, Maruoka *et al.* reported a method for asymmetric ring expansions of cyclic ketones using a BINOL-based ligand **360** and benzyl diazoacetate (Scheme 130).¹⁰⁸



Scheme 130. Maruoka *et al.*'s asymmetric ring expansion of **357**¹⁰⁸

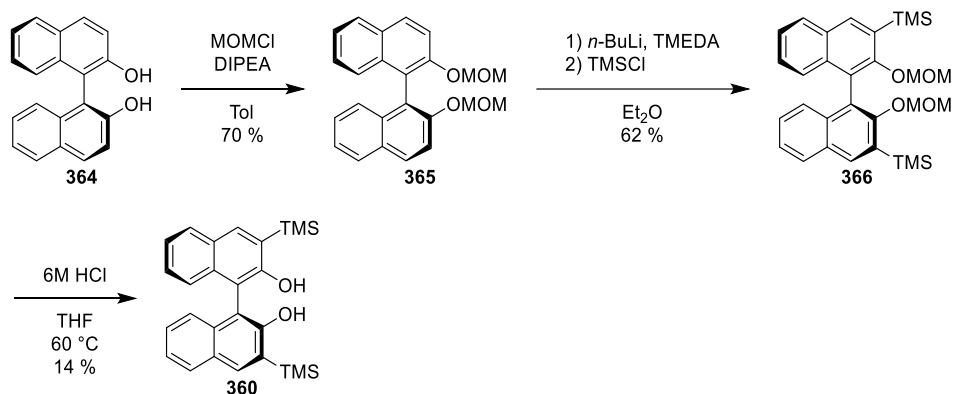
Before this reaction could be attempted, benzyl diazoacetate and ligand **360** had to be synthesised. Benzyl diazoacetate was synthesised following a procedure reported by Wang and coworkers.¹⁰⁹ Starting from benzyl alcohol **361**, α -bromo ester **362** was produced after reaction with bromoacetyl bromide, DMAP, and triethylamine. α -Bromo ester **362** was then converted into benzyl diazoacetate **363** by reaction with TsNHNHTs (Scheme 131).



Scheme 131. Synthesis of benzyl diazoacetate **363**

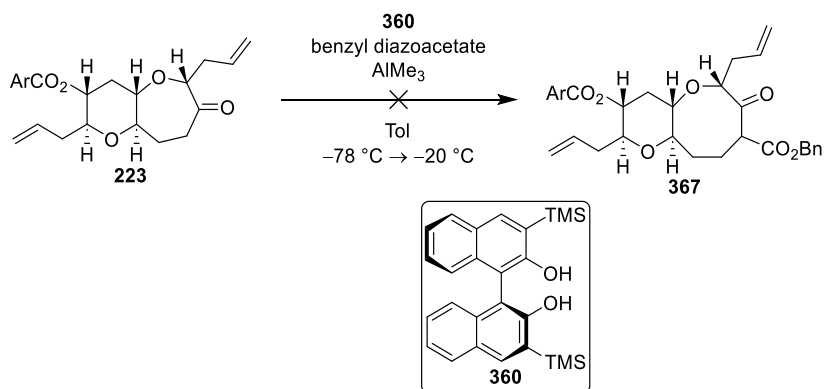
Ligand **360** was synthesised following a procedure reported by Maruoka *et al.*¹⁰⁸ The synthesis of ligand **360** began with MOM protection of (*S*)-binol **364** to produce MOM-protected product **365**. The TMS groups were then installed by treatment with *n*-BuLi, TMEDA, and TMSCl to afford intermediate **366**. Finally, MOM deprotection afforded the desired ligand **360**. Unfortunately, final MOM deprotection also led to partial removal

of the TMS groups, but enough of ligand **360** was produced to carry out the reaction (Scheme 132).



Scheme 132. Synthesis of ligand **360**

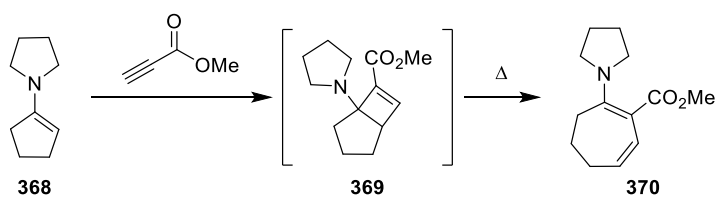
Unfortunately, when this methodology was applied to our system, no reaction occurred and starting material was reisolated (Scheme 133).



Scheme 133. Unsuccessful ring expansion of **223**

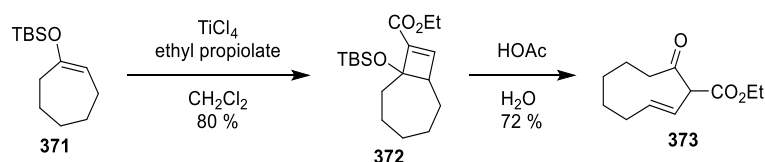
4.5.3 [2+2] cycloaddition/rearrangement

In 1963, Thweatt *et al.* reported the first use of a cyclobutene ring-opening as a method for a two-carbon ring expansion.¹¹⁰ They demonstrated that enamines will react readily with propiolates to form cyclobutene intermediates. These cyclobutene intermediates can undergo ring-opening when heated to reflux to form the desired ring expanded product (Scheme 134).



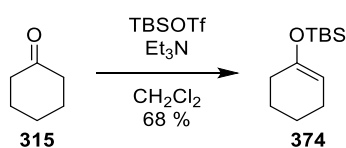
Scheme 134. Thweatt *et al.*'s two-carbon ring expansion via cyclobutene intermediate **369**¹¹⁰

Although this technique has been used in several total syntheses, it has some drawbacks. Namely, the synthesis of enamines from sterically hindered ketones is not a trivial task. For this reason, Untch and Clark explored a similar technique using silyl enol ethers. ¹¹¹ They demonstrated that, like enamines, silyl enol ethers undergo a [2+2] cycloaddition with propiolates to form cyclobutene intermediates. When exposed to mildly acidic conditions, the cyclobutene intermediates open to form the two-carbon ring expanded product (Scheme 135).



Scheme 135. Untch and Clark's application of Thweatt *et al.*'s two-carbon ring expansion to carbonyl systems¹¹¹

Due to the difficulties encountered when trying to perform a single-carbon ring expansion, it was decided to attempt a two-carbon ring expansion from the six-membered ring to the desired eight-membered. As mentioned above, Untch and Clark demonstrated an effective two-carbon ring expansion of silyl enol ether substrates. Before applying this methodology to the real system, it was decided to attempt the reaction on cyclohexanone **315** as a model compound. Employing the methodology reported by Untch and Clark, silyl enol ether **374** was produced from cyclohexanone in a 68 % yield (Scheme 136).



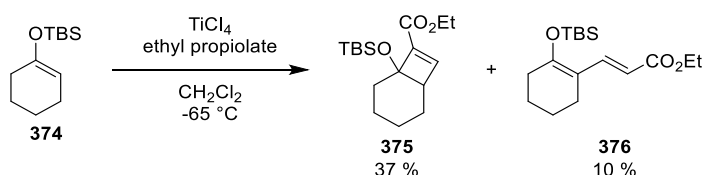
Scheme 136. Synthesis of silyl enol ether **374**

When consulting the literature, it was found that several conditions for the [2+2] cycloaddition of ether propiolate have been reported. The results of reactions performed under these various conditions attempted are outlined in Table 10.

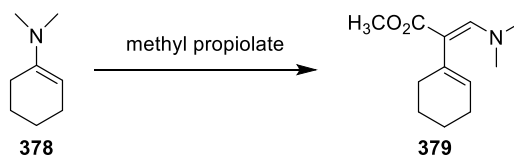
Table 10. Attempted reaction conditions for [2+2] cycloaddition of **374**

Conditions	Result
ZrCl ₄ (1 eq.), ethyl propiolate (1.5 eq.), CH ₂ Cl ₂ /Et ₂ O, -78 °C	Complex mixture
ZrCl ₄ (2 eq.), ethyl propiolate (2.2 eq.), CH ₂ Cl ₂ /Et ₂ O, -78 °C	Complex mixture
TiCl ₄ (1 eq.), ethyl propiolate (1.5 eq.), CH ₂ Cl ₂ , -65 °C	Complex mixture
TiCl ₄ (1 eq.) (freshly distilled), ethyl propiolate (1.5 eq.), CH ₂ Cl ₂ , -65 °C	Complex mixture
Tf ₂ NH (1 eq.), ethyl propiolate (1.1 eq.), CH ₂ Cl ₂ , rt	Complex mixture

Due to these unexpected failures, the literature was consulted once again. Interestingly, it became evident that this struggle with six-membered rings was not an isolated incident. In their report of this methodology, Untch and Clark had reported disappointing yields when the reaction was performed on the six-membered ring system. While they did manage to produce cyclobutene **375**, it was obtained with a yield of only 37 % yield, with a significant quantity of side-product **376** (Scheme 137).

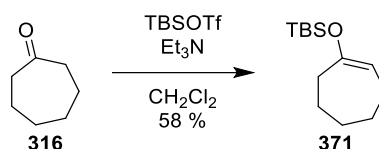
**Scheme 137.** Untch and Clark's [2+2] cycloaddition/rearrangement of **374**

As discussed above, the original [2+2] cycloaddition/ring-expansion methodology was performed on enamines, as reported by Thweatt *et al.* They also experienced difficulties with the cyclohexanone-derived enamine **378**, with unexpected side-product **379** being formed (Scheme 138).

**Scheme 138.** Thweatt *et al.*'s [2+2] cycloaddition/rearrangement of **378**

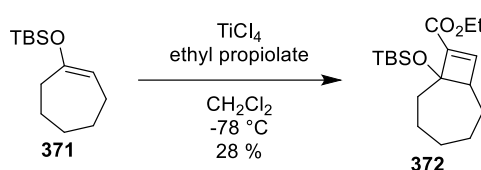
As the cyclohexanone-derived systems seemed to behave anomalously, it was decided to attempt Untch and Clark's conditions on one of the systems that worked

best for them. Cycloheptanone **316** was chosen as a substrate because they reported an 80 % yield with no significant side-products. Silyl enol ether **371** was produced in a 58 % yield using the same conditions as before (Scheme 139).



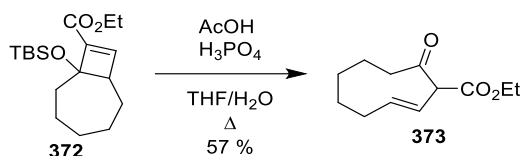
Scheme 139. Synthesis of seven-membered silyl enol ether **371**

With silyl enol ether **371** in hand, the [2+2] cycloaddition was attempted following the conditions reported by Untch and Clark.¹¹¹ Gratifyingly, the cyclobutene intermediate was successfully produced, albeit in a disappointing 28 % yield (Scheme 140).



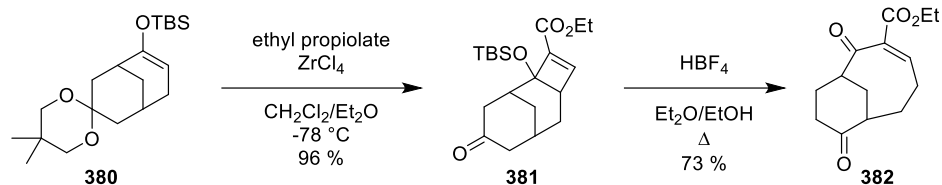
Scheme 140. [2+2] cycloaddition to form cyclobutene **372**

Following the conditions reported by Untch and Clark, hydrolysis of the cyclobutene **372** to the desired nine-membered cyclic ketone **373** was performed (Scheme 141). This time, the achieved yield of product (57 %) did not differ from the reported yield (80 %) as drastically as that of the [2+2] cycloaddition.



Scheme 141. Rearrangement of **372** to produce **373**

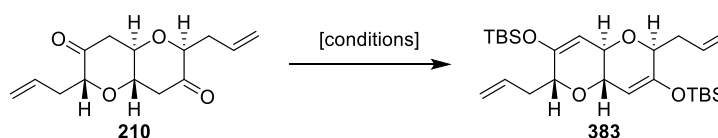
While these results highlighted the potential challenge to perform this ring expansion on a six-membered cyclic ketone, some encouraging results were found in the literature. In their work towards the synthesis of bicyclo[5.3.1]undecadiene ring systems, Miesh *et al.* decide to employ this [2+2] cycloaddition/hydrolysis methodology to form the larger ring systems.¹¹² This involved the synthesis of the cyclobutene intermediate **381** from the fused [6,6]-system **380**, which they achieved in an impressive 96 % yield. Exposing cyclobutene **381** to acidic conditions at reflux produced the desired bicyclo[5.3.1]undecane ring system **382** (Scheme 142).



Scheme 142. Successful [2+2] cycloaddition/rearrangement of **380** to produce [6,8]-system **382**

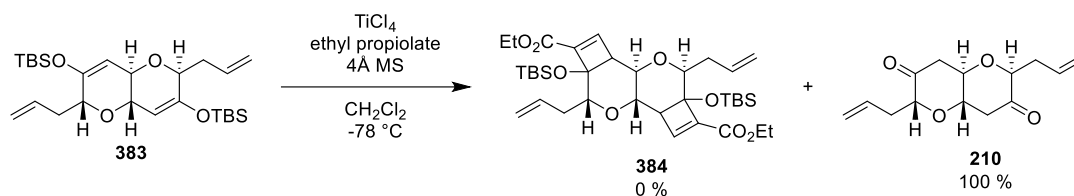
Our system is also a fused [6,6]-system, and so we were reassured by these results. The first step in applying the reaction to our system involved producing silyl enol ether **383**. Unsurprisingly, applying the same results as used for cyclohexanone/cycloheptanone was unsuccessful. However, the conditions used for producing Saegusa-Ito precursor **354** discussed in Section 4.5.1 were also unsuccessful. It was found that it was necessary to stir diketone **210** with TBSOTf before addition of the bases. With these reagents and this order of addition, silyl enol ether **383** was successfully produced (Table 11).

Table 11. Attempted reaction conditions for the synthesis of silyl enol ether **383**



Conditions	Result
TBSOTf, Et ₃ N, CH ₂ Cl ₂ , 4Å MS	NR after 48 h
1) LHMDS, Et ₃ N 2) TBSCl, THF, -78 °C	Decomposition
1) TBSOTf 2) LHMDS, Et ₃ N, THF, -78 °C	31 %

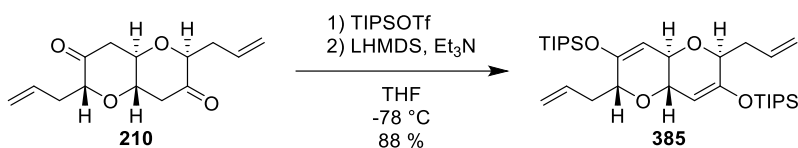
Unfortunately, when silyl enol ether **383** was subjected to the [2+2] cycloaddition conditions, full conversion to the original diketone **210** was observed after 10 min (measured by ¹H NMR) (Scheme 143).



Scheme 143. Unsuccessful [2+2] cycloaddition of **383**

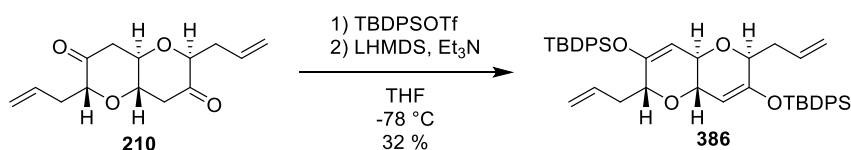
It was assumed that the TBS groups were incompatible with the acidic conditions produced by TiCl₄. Thus, more acid-stable silyl enol ethers were produced in the hopes that they would be under the reaction conditions. The first acid-stable silyl group

chosen was the triisopropylsilyl (TIPS) group. The TIPS enol ether **385** was produced similarly to before (Scheme 144).



Scheme 144. Synthesis of TIPS enol ether **385**

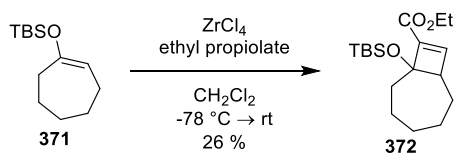
Unfortunately, upon addition of silyl enol ether **385** to the mixture of TiCl_4 and ethyl propiolate, immediate conversion back to diketone **210** was observed. It was then decided to produce the TBDPS enol ether **386** (Scheme 145), as this should provide more acid stability than the corresponding TIPS enol ether.



Scheme 145. Synthesis of TBDPS enol ether **386**

However, as before, silyl enol ether **386** did not survive the reaction conditions, and full conversion to diketone **210** was observed. Evidently, this [6,6]-fused system is not behaving as expected. It would be interesting to attempt the [2+2] cycloaddition on a [7,6]-silyl enol ether similar to **354**, to determine if it is the ring size which is impacting the reactivity.

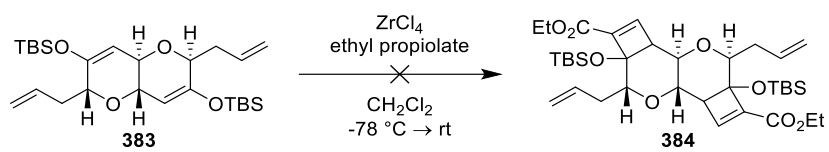
When it became obvious that the use of TiCl_4 was simply too harsh for the [6,6]-fused silyl enol ethers, milder conditions were investigated. As mentioned previously, Miesch *et al.* successfully performed the [2+2] cycloaddition with ZrCl_4 as the Lewis acid and so we decided to explore the use of these milder conditions. These conditions were first performed on the model silyl enol ether **371**, and cyclobutene intermediate **372** was obtained in a 26% yield (Scheme 146).



Scheme 146. Synthesis of cyclobutene **372** with ZrCl_4

The yield of the ZrCl_4 -catalysed reaction was similar to that of the TiCl_4 -catalyst, and so this result was encouraging. More importantly, Miesch *et al.* had achieved this

transformation on a [6,6]-fused system. Unfortunately, when silyl enol ether **383** was subjected to these conditions, no reaction was observed (Scheme 147).



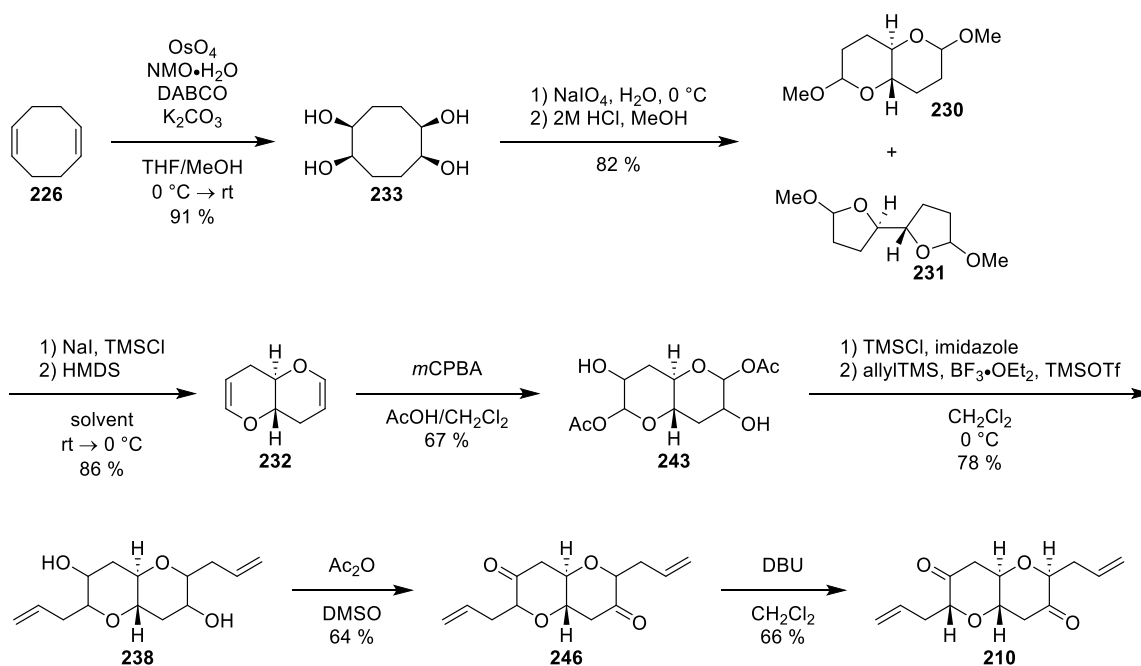
Scheme 147. Unsuccessful attempt at synthesis of cyclobutene **384**

5. Conclusion

5.1 Summary of work

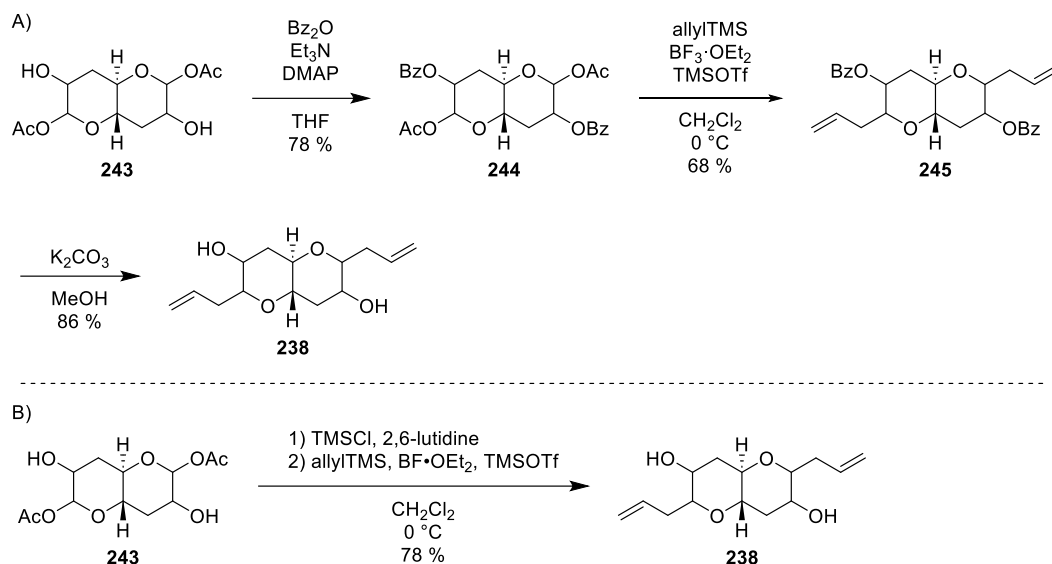
5.1.1 Synthesis of diketone **210**

The aim of this project was to develop a desymmetrisation strategy for a key symmetric intermediate in the synthesis of MLPs. This key symmetric intermediate was identified as diketone **210**. A multigram synthesis of diketone **210** was completed (Scheme 148).



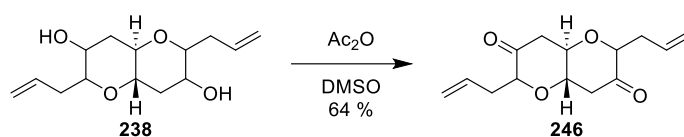
Scheme 148. Synthetic route to diketone **210**

This synthetic route was streamlined from that previously developed in the group. An updated one-pot allylation reaction to produce diol **240** was introduced, and this removed the need for protection/deprotection of free hydroxyl groups, as protection of these hydroxyl groups was only necessary for solubility reasons (Scheme 149).



Scheme 149. A) Initial route towards diol **238**, B) one-pot allylation procedure to produce diol **238**

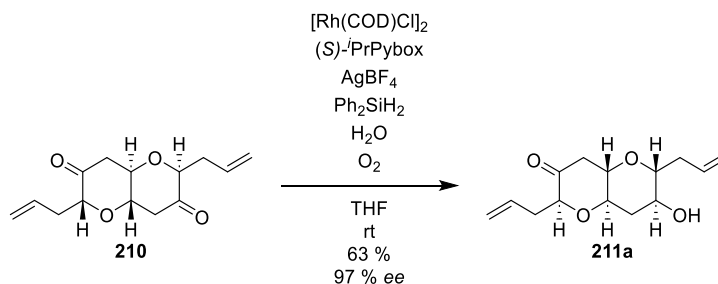
The oxidation of diol **238** to diketone **246** proved to be unreliable, and so various oxidation reactions were explored to find optimal reaction conditions. The Albright-Goldman oxidation was found to provide the best and delivered the most reliable yields (Scheme 150).



Scheme 150. Albright-Goldman oxidation of diol **238**

5.1.2 Desymmetrisation of diketone **210**

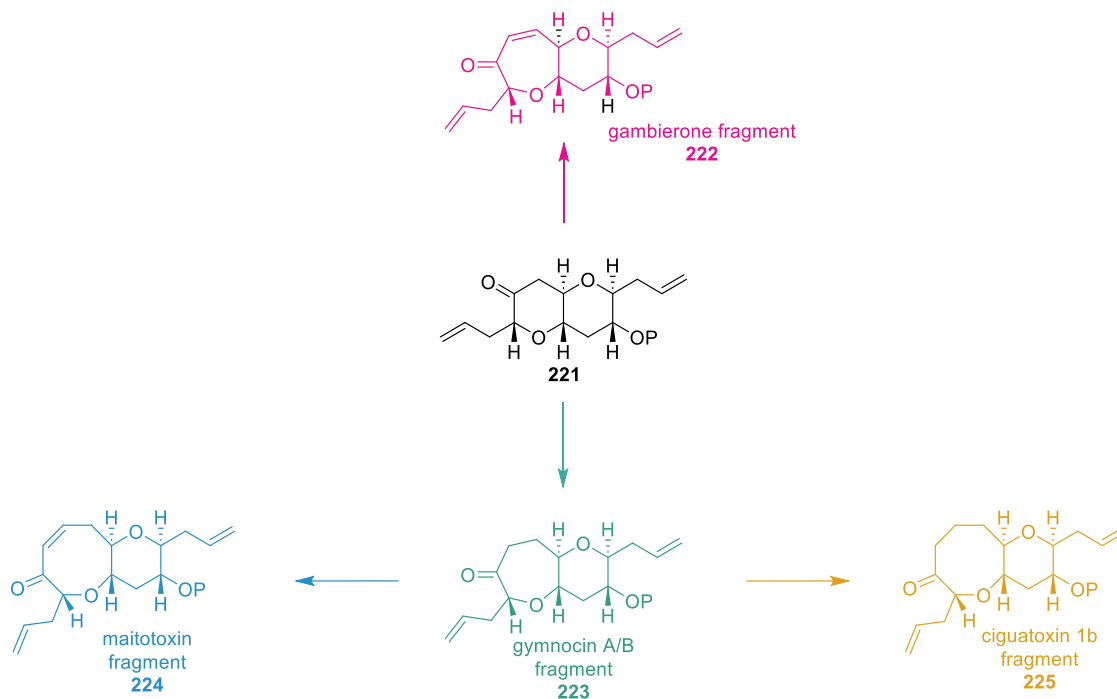
The key feature of this project is the ability to desymmetrise a centrosymmetric molecule. The desymmetrisation of diketone **210** via Rh-catalysed hydrosilylation was completed. Initial reaction conditions provided a slow reaction with unreliable yields. Condition screening performed by other team members was verified and it was found that all team members obtained an increased yield and higher rate of reaction when oxygen and water were introduced (Scheme 151).



Scheme 151. Desymmetrisation of diketone **210**

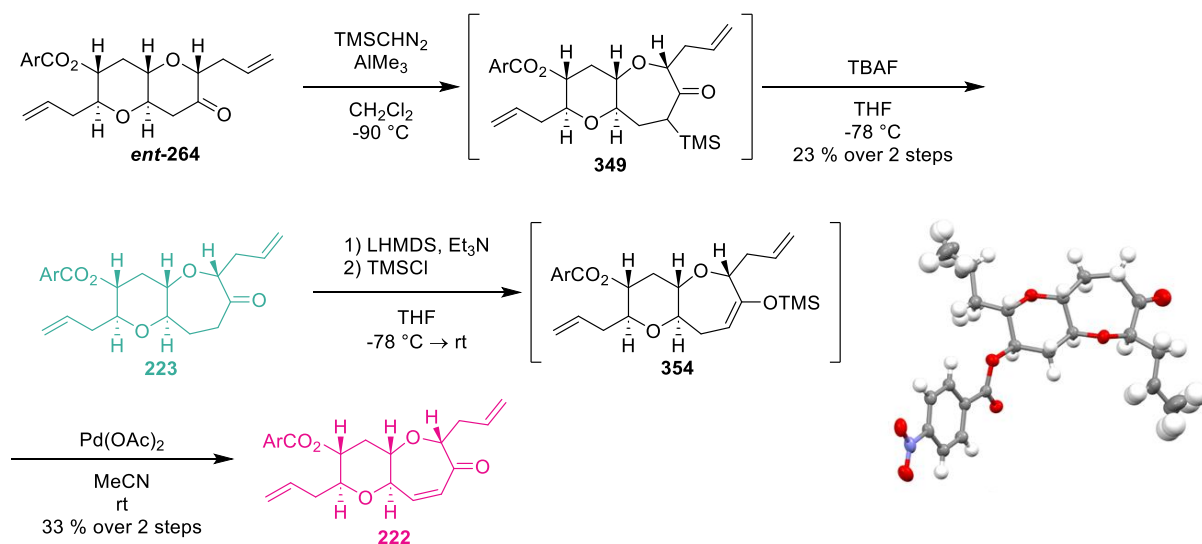
5.1.3 Synthesis of MLP fragments

A selection of MLP fragments were chosen as synthetic targets to demonstrate the versatility of this procedure. **Gymnocin A/B fragment 223**, **gambierone fragment 222**, **ciguatoxin 1b fragment 225**, and **maitotoxin fragment 224** were all expected to be accessed from key desymmetrised intermediate **221** (Scheme 152).



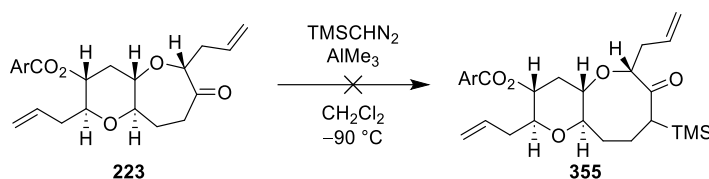
Scheme 152. Proposed fragments to be synthesised from ketone **221**

TMSCHN₂-mediated ring expansion of **ent-264** followed by TMS removal readily afforded **gymnocin A/B fragment 223**, and an X-ray crystal structure was obtained. Conversion of **gymnocin A/B fragment 223** into the silyl enol ether **354** followed by Saegusa-Ito oxidation produced **gambierone fragment 222** (Scheme 153).



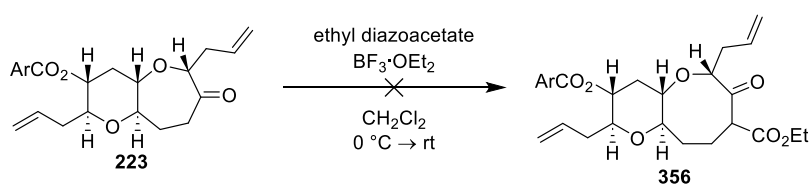
Scheme 153. Synthesis of fragments **222** and **223**

TMSCHN₂-mediated ring-expansion of **gymnocin A/B fragment** to access the 8-membered ring was unsuccessful. No reaction was observed and starting material was reisolated (Scheme 154).



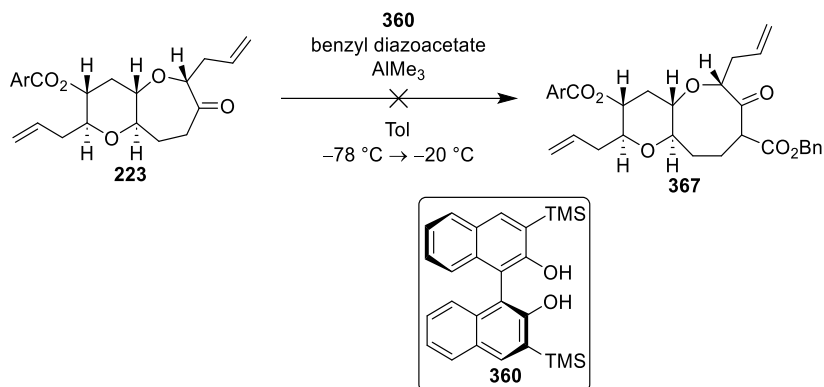
Scheme 154. Unsuccessful ring expansion of **223**

An ethyl diazoacetate-mediated ring expansion reaction of **223** was attempted, but these conditions led to decomposition (Scheme 155).



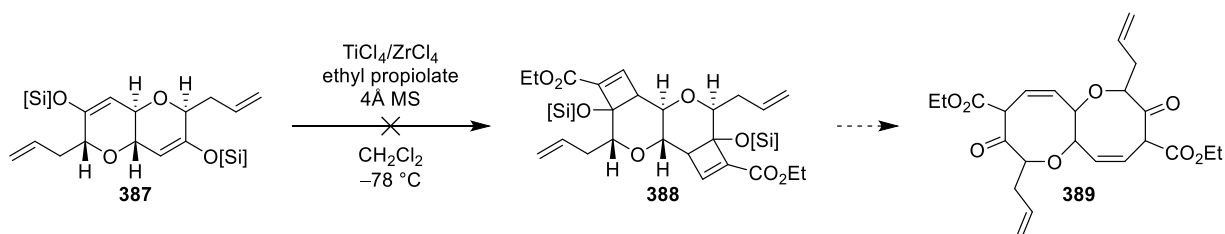
Scheme 155. Unsuccessful ring expansion of **223**

Asymmetric ring expansion conditions reported by Maruoka et al. were attempted, but no reaction was observed and starting material was reisolated (Scheme 156).



Scheme 156. Unsuccessful ring expansion of **223**

The [6,7]-system exhibited low reactivity, and so it was decided to attempt a two-carbon ring expansion on the 6-membered ring to access the 8-membered ring. Untch and Clark reported a two-carbon ring expansion by [2+2] cycloaddition of ethyl propiolate to a silyl enol ether followed by hydrolysis of the resulting cyclobutene. Unfortunately, attempts to perform the TiCl_4 -mediated [2+2] cycloaddition reaction on the [6,6]-silyl enol ether **387** was unsuccessful because the reaction conditions were too harsh, and silyl enol ether **387** was converted to diketone **210**. Reactions of TBS, TIPS, and TBDPS enol ether substrates were all unsuccessful. ZrCl_4 was used as a milder alternative to TiCl_4 , but this gave no reaction (Scheme 157).



Scheme 157. Unsuccessful [2+2] cycloaddition of **387**

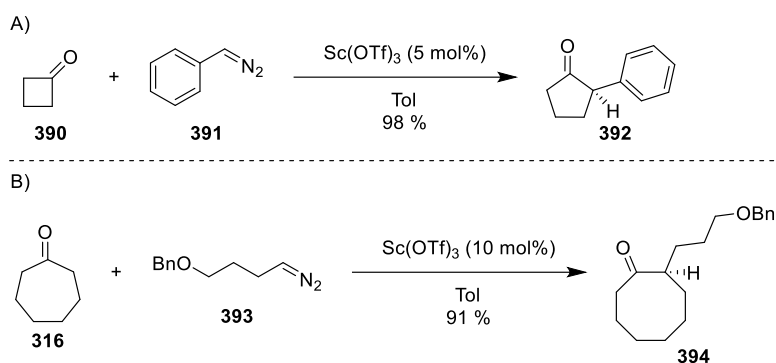
5.2 Future work

Future work on this project should be focused on both the synthesis of MLP fragments and the completion of the total synthesis of gymnocin B.

5.2.1 Synthesis of fragments

As discussed in Section 4.5, the largest obstacle to synthesising fragments **250** and **251** is accessing the 8-membered ring via ring expansion. While diazomethane-mediated ring expansions are extremely common in the literature, the TMSCHN_2 -mediated ring expansion of **223** to **355** was unsuccessful.

Traditionally, diazomethane-mediated ring expansions are performed in the presence of boron- or aluminium-based Lewis acids. However, Kingsbury and coworkers recognised that the presence of these Lewis acids can lead to decomposition of the diazo species. To circumvent this issue, they developed a protocol which uses Sc^{3+} salts as catalysts for diazoalkyl insertion reactions.¹¹³ Where boron- and aluminium-based Lewis acids provided no reaction, $\text{Sc}(\text{OTf})_3$ resulted in high turnover with low catalyst loading (Scheme 158A). They then applied this reaction to the ring expansion of cyclic ketones, and they were successful in producing an 8-membered ring **394** (Scheme 158B)



Scheme 158. A) Sc-catalysed ring expansion where B and Al Lewis acids were unsuccessful, B) synthesis of 8-membered ring by Sc-catalysis

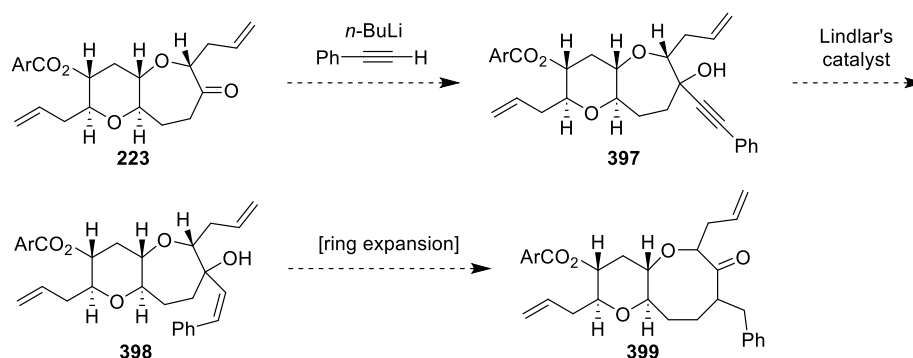
It is possible that 7-membered fragment **223** has lower reactivity than 6-membered fragment **ent-264**, leading to slow ring expansion and thus decomposition of TMSCHN_2 in the presence of AlMe_3 before ring expansion can occur. The use of $\text{Sc}(\text{OTf})_3$ in place of AlMe_3 may allow ring expansion to proceed.

In the event that the ring expansion in the presence of $\text{Sc}(\text{OTf})_3$ is unsuccessful, Knowles *et al.* developed a protocol that may be useful.¹¹⁴ This protocol employs an Ir catalyst to ring expand cyclic allylic alcohols and was used to ring expand the fused polycyclic androsterone **395** (Scheme 159). The phenyl side chain was found to be necessary in all starting materials.



Scheme 159. Ir-catalysed ring expansion of androsterone **395**

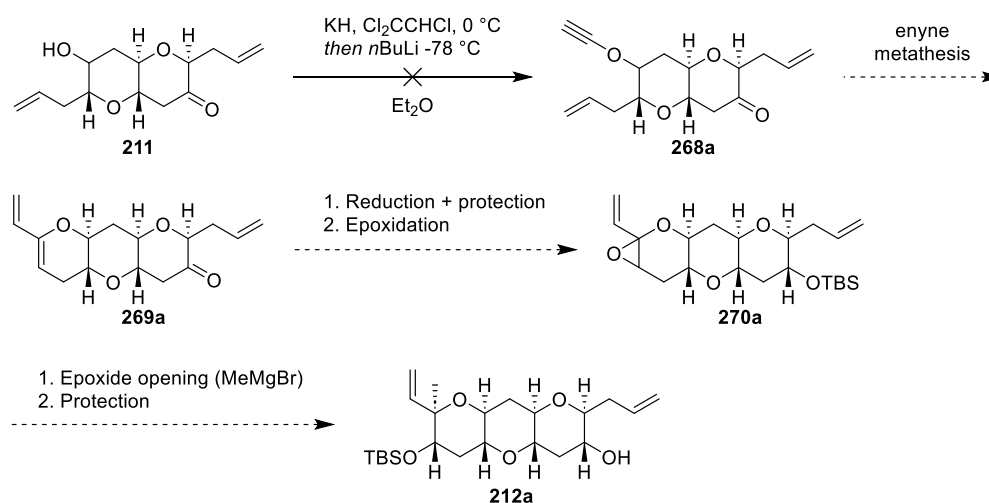
Following the procedure reported by Knowles *et al.*, ketone **223** could be converted to allylic alcohol **398**. First, conversion to alkyne **397** is done with *n*-BuLi and phenylacetylene. Knowles and coworkers then reduced the alkynes to alkenes by treatment with Red-Al. Unfortunately, for our system, this risks reducing the allyl side chain. Lindlar's catalyst could be used, though this would produce a *cis* alkene **397**. All alkenes in the substrate scope were of the *trans* conformation, and so it is unknown how this would impact the ring expansion. This ring expansion would introduce an unwanted aryl side chain, and so further manipulation would be necessary to access the desired fragments (Scheme 160).



Scheme 160. Potential route to 8-membered ring **399** via Ir-catalysed ring expansion

5.2.2 Total synthesis of gymnocin B

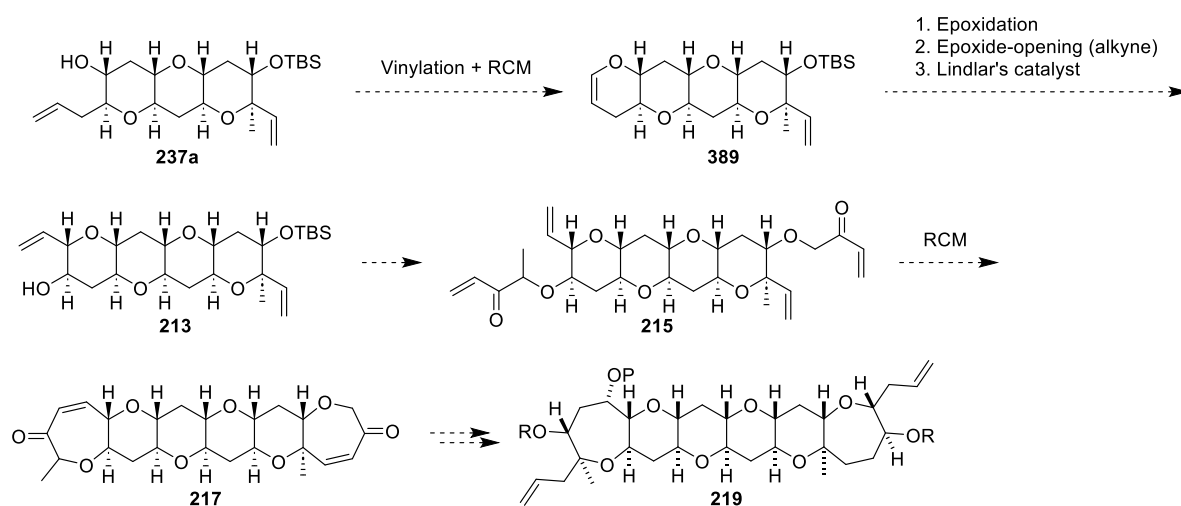
As discussed in Section 4.3.2, synthesis of enyne metathesis precursor **268** was unsuccessful. Successful enyne metathesis would have produced enol ether **269a**, which could have undergone epoxidation and epoxide-opening with a nucleophilic methyl reagent to product intermediate **212a** (Scheme 161).



Scheme 161. Future route to product intermediate **212a**

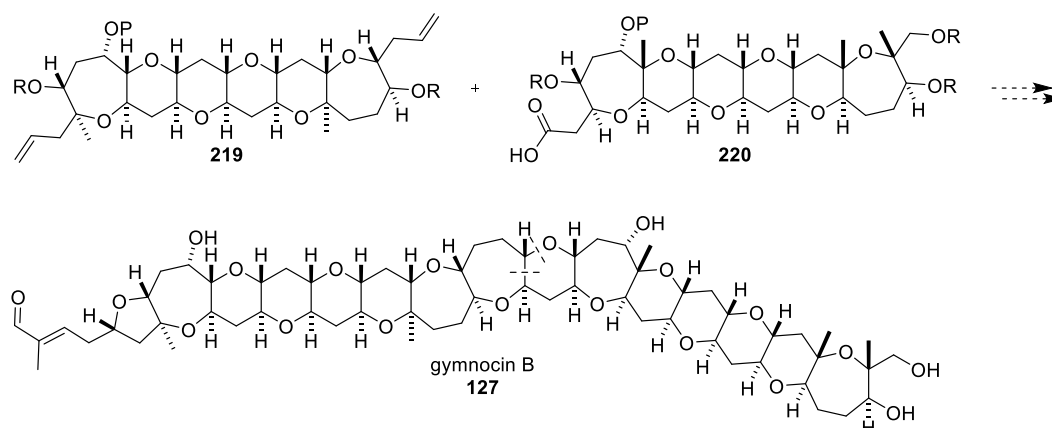
Due to time constraints, optimisation of this reaction not attempted. It is possible that this reaction would be successful with the correct solvent/temperature/equivalents, and future work should focus on finding the optimum reaction conditions.

Once fragment **212a** has been accessed, the synthesis route to gymnocin B discussed in Section 4.3.1 could be followed. **212a** could be converted into coupling partner **219** (Scheme 162).



Scheme 162. Synthesis of coupling partner **219** from intermediate **212a**

A very similar series of reactions can be used to synthesise coupling partner **220** from the enantiomer of **212a**. Coupling of **219** and **220**, a final ring closure, and addition of the 2-methyl-2-butenal side chain would afford gymnocin B **127** (Scheme 163).



Scheme 163. Coupling of **219** and **220** to produce gymnocin B **127**

6. Experimental

Organic solvents were dried using a Pure Solv™ 500 solvent purification system or purchased as anhydrous solvents from commercial suppliers. Reagents were obtained from commercial suppliers and used without further purification, unless otherwise stated.

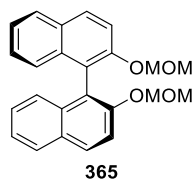
Flash column chromatography was performed with silica gel (Fluorochem LC60A, 35–70 micron) as the solid phase. Petroleum ether used for column chromatography was the 40–60 °C fraction. Thin layer chromatography (TLC) monitoring of reactions was performed with Merck silica gel 60 covered aluminium backed plated F254 which was visualised with UV light and developed with either potassium permanganate solution or Hanessian's stain.

IR spectra were recorded on a Shimadzu FTIR-8400S spectrometer, as a thin film (liquid) or powder (solid) at room temperature. HRMS were recorded by University of Glasgow analytical services staff on a Bruker micro TOFq (ESI), Jeol MStation JMS-700 (EI) or an Agilent 6546 LC/Q-TOF (ESI, APCI) mass spectrometer. Melting points were recorded using a Barnstead Electrothermal 9100 melting point apparatus. ¹H NMR spectra were obtained with a Bruker AVIII 400 MHz spectrometer at room temperature. ¹³C NMR spectra were recorded on a Bruker AVIII 400 MHz (101 MHz) spectrometer at room temperature. The signals were assigned using 2D NMR spectra (COSY, HSQC, HMBC). X-ray crystallography was carried out either at the University of Glasgow by Dr. Claire Wilson, or at the National Crystallography Service, Southampton

Chiral HPLC analysis was performed using a Shimadzu LC-20AD prominence liquid chromatograph with a CBM-20A prominence communications bus module, a DGU-20A5 prominence degasser and a SPD-M20A prominence diode array detector. A Diacel Chemical Industries chiralcel OD-H 5 µm 4.6 x 250 mm reverse phase analytical column was used with an isocratic mobile phase of HPLC grade isopropyl alcohol in HPLC grade hexane.

6.1 Synthesis of reagents

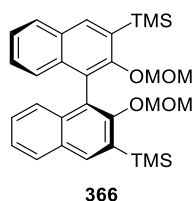
(S)-2,2'-Bis(methoxymethoxy)-1,1'-Binaphthyl 365



(S)-(-)-1,1'-Bi(2-naphthol) (1.5 g, 5.2 mmol) in anhydrous THF (10 mL) was added to a suspension of NaH (0.5 g, 60 % in oil, 12 mmol) in THF (15 mL) at 0 °C. The reaction was stirred at rt under argon atmosphere for 1 h. MOMCl (1.0 mL, 1.1 g, 13 mmol) was added dropwise and the reaction was stirred for a further 4 h. The reaction was quenched by the addition of NH₄Cl (sat. aq.). The phases were separated and the aqueous layer was extracted with CH₂Cl₂ (3 x 20 mL). The combined organic extracts were dried over MgSO₄, concentrated in vacuo, and purified by flash column chromatography on silica gel (petroleum ether/EtOAc, 10:1) to afford the product as a white solid (1.46 g, 74 %). m.p. 99 – 101 °C; ¹H NMR (400 MHz, CDCl₃) δ 7.94 (d, *J* = 8.0 Hz, 2H), δ 7.89 (d, *J* = 8.4 Hz, 2H), 7.58 (d, *J* = 9.6 Hz, 2H), 7.36 (m, 2H), 7.21 (m, 2H), 7.15 (d, *J* = 8.4 Hz, 2H), 5.08 (d, *J* = 7.2 Hz, 2H), 4.97 (d, *J* = 6.8 Hz, 2H), 3.14, s, 6H); ¹³C NMR (101 MHz, CDCl₃) δ 152.8, 134.2, 130.1, 129.6, 128.0, 126.5, 125.7, 124.3, 121.5, 117.5, 95.4, 56.0.

The spectroscopic data matched that previously reported in the literature.¹¹⁵

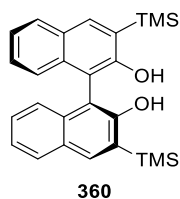
(S)-3,3'-bis(trimethylsilyl)-2,2'-bis(methoxymethoxy)-1,1'-binaphthyl 366



TMEDA (2.2 ml, 1.7 g, 15 mmol) and *n*-BuLi (1.8 M, 6.5 ml, 12 mmol) were added dropwise to **365** (1 g, 3 mmol) in anhydrous Et₂O (50 ml) at rt under argon atmosphere. The reaction was stirred for 30 min and TMSCl (2.2 ml, 1.9 g, 18 mmol) was added dropwise. The reaction was stirred for a further 18 h and quenched by the addition of NH₄Cl (sat. aq.). The phases were separated and the aqueous phase was extracted with EtOAc (3 x 20 mL). The combined organic extracts were dried over MgSO₄, concentrated in vacuo, and purified by flash column chromatography on silica gel (petroleum ether/EtOAc, 20:1) to afford the product as a colourless oil (0.99 g, 71 %). ¹H NMR (400 MHz, CDCl₃) δ 8.10 (s, 2H), 7.90 (d, *J* = 8.4 Hz, 2H), 7.42 – 7.36 (m, 2H), 7.31 – 7.24 (m, 4H), 4.48 (d, *J* = 4.4 Hz, 2H), 4.15 (d, *J* = 4.4 Hz, 2H), 2.95 (s, 6H), 0.45 (s, 18H); ¹³C NMR (101 MHz, CDCl₃) δ 158.5, 137.5, 136.1, 134.8, 130.8, 128.7, 127.4, 126.5, 125.0, 122.8, 98.2, 57.1, 0.1; (HRMS (ESI) [M+NH₄]⁺ calcd for C₃₀H₃₈O₄Si₂NH₄, 536.2647 found 536.2666.

The spectroscopic data matched that previously reported in the literature.¹¹⁶

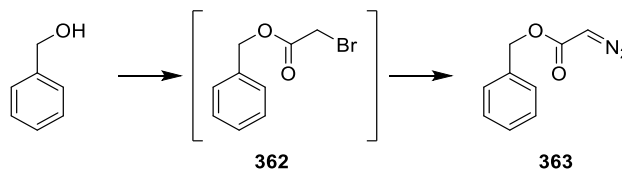
(S)-3,3'-bis(trimethylsilyl)-1,1'-binaphthyl-2,2'-diol 360



6 M HCl (22 ml) was added to a solution of **366** (0.5 g, 1 mmol) in THF (22 ml). The reaction was heated to 60 °C and stirred for 18 h. The reaction was cooled to rt and extracted with Et₂O (3 x 20 mL). The combined organic extracts were dried over MgSO₄, concentrated in vacuo, and purified by flash column chromatography on silica gel to afford the product as a white solid (60 mg, 14 %). ¹H NMR (400 MHz, CDCl₃) δ 8.05 (s, 2H), 7.86 (d, *J* = 8 Hz), 7.29 (m, 4H), 7.07 (d, *J* = 8.4 Hz, 2H), 0.39 (s, 18H). ¹³C NMR (101 MHz, CDCl₃) δ 157.1, 138.0, 134.5, 129.2, 128.7, 127.8, 124.2, 123.9, 109.7, -0.7. HRMS (APCI) [M+H]⁺ calcd for C₂₆H₃₁O₂Si₂, 432.1881 found 432.1880

The spectroscopic data matched that previously reported in the literature.¹⁰⁸

Benzyl diazoacetate **363**

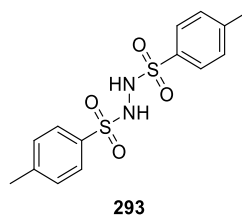


Bromoacetyl bromide (1.8 mL, 4.2 g, 21 mmol) was added dropwise to a solution of benzyl alcohol (1.9 mL, 2.0 g, 19 mmol), triethylamine (2.8 mL, 2.0 g, 20 mmol), and dimethylaminopyridine (0.23 g, 1.9 mmol) in CH₂Cl₂ (20 mL) at 0 °C. The reaction was stirred for 3 h and quenched by the addition of H₂O. The phases were separated and the aqueous phase was extracted with CH₂Cl₂ (3 x 15 mL). The combined organic extracts were washed with water (15 mL) and brine (15 mL), dried over MgSO₄, filtered, and concentrated in vacuo to afford benzyl bromoacetate **362** as a brown oil which was used crude in the next reaction.

N,N'-Ditosylhydrazine (4.45 g, 13.1 mmol) was added to crude bromoacetate **362** in THF (40 mL) at 0 °C. DBU (5.2 mL, 5.3 g, 6.6 mmol) was added dropwise and the reaction was stirred for 1 h. The reaction was quenched by the addition of NaHCO₃ (sat. aq.) and the phases were separated. The aqueous phase was extracted with EtOAc (3 x 20 mL). The combined organic phases were dried over MgSO₄ and concentrated in vacuo. The residue was purified by flash column chromatography on silica gel to afford benzyl diazoacetate **363** as a yellow oil (1.23 g, 38 %). ¹H NMR (400 MHz, CDCl₃) δ 7.45 – 7.28 (m, 5 H), 5.21 (s, 2 H), 4.80 (s, 1 H); ¹³C NMR (101 MHz, CDCl₃) δ 166.7, 136.0, 128.6, 128.3, 128.2, 66.5, 46.3.

The spectroscopic data matched that previously reported in the literature.¹¹⁷

***N,N'*-Ditosylhydrazine 293**



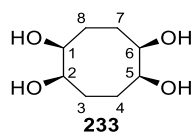
293

A mixture of *p*-toluenesulfonyl hydrazide (5.02 g, 27.0 mmol) and *p*-toluenesulfonyl chloride (7.70 g, 40.3 mmol) were stirred in CH₂Cl₂ (26 mL) at rt. Pyridine (3.2 ml, 3.1 g, 40 mmol) was added dropwise and the mixture was stirred for 1.5 h. The reaction mixture was cooled to 0 °C and Et₂O (20 ml) and H₂O (20 ml) were added. The solid product was collected by Buchner filtration and recrystallised from MeOH to afford the product as a crystalline solid (6.31 g, 69 %). m.p. 246 – 250 °C; ¹H NMR (400 MHz, d₆-DMSO) δ 8.86 – 8.63 (s, 2 H), 6.96 – 6.69 (d, 4 H), 6.64 – 6.45 (d, 4 H), 1.57 (s, 6 H); ¹³C NMR (101 MHz, DMSO) δ 143.4, 135.5, 129.4, 127.8, 21.0; HRMS (ESI) [M+NH₄]⁺ calcd for C₁₄H₁₆N₂O₄S₂NH₄, 363.0444 found 363.0447.

The spectroscopic data matched that previously reported in the literature.⁸⁵

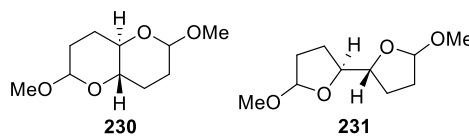
6.2 Experimental procedures

(1*R**,2*S**,5*R**,6*S**)-cyclooctane-1,2,5,6-tetrol **233**



1,5-Cyclooctadiene (8.8 g, 82 mmol) and OsO₄ (0.3 mL, 4% in H₂O, 0.05 mmol) were added to a solution of *N*-methylnmorpholine *N*-oxide monohydrate (24.2 g, 179 mmol) in THF (40 mL) and MeOH (40 mL) at 0 °C. The reaction was allowed to warm to rt over 30 min. 1,4- Diazabicyclo[2.2.2]octane (2.34 g, 20.8 mmol) was added and the solution was stirred for 1 hr. DABCO (110 mg, 0.98 mmol), OsO₄ (4% in H₂O, 0.3 mL 0.05 mmol), and K₂CO₃ (20 mg) were added. The reaction was stirred at rt for 60 hr. The precipitate was filtered under vacuum and washed with THF (50 mL). The precipitate was transferred to a flask, washing with MeOH (50 mL) and concentrated in vacuo to afford tetrol **233** as an off-white solid (13.0 g, 91 %). R_f = 0.26 (EtOAc/MeOH, 8:1); m.p. 175 – 178 °C; IR ν_{max} (solid) 3345, 2936, 2886, 1466, 1378, 1277, 1150, 1045, 1011, 961, 864, 829 cm⁻¹; ¹H NMR (400 MHz, MeOD) δ 3.78 (d, *J* = 8.8 Hz, 4H, CH-C₁, CH-C₂, CH-C₅, CH-C₆), 2.14 – 2.01 (m, 4H, CH₂-C_{3a}, CH₂-C_{4a}, CH₂-C_{7a}, CH₂-C_{8a}), 1.64 – 1.53 (m, 4H, CH₂-C_{3b}, CH₂-C_{4b}, CH₂-C_{7b}, CH₂-C_{8b}); ¹³C NMR (101 MHz, MeOD) δ 73.6 (C₁, C₂, C₅, C₆), 27.3 (C₃, C₄, C₇, C₈); HRMS (ESI+) [M+Na]⁺ calcd for C₈H₁₆NaO₄Na, 199.0941 found 199.0942.

(4aR,8aS)-2,6-dimethoxyoctahydropyrano[3,2-b]pyran 230 and (2R,2'S)-5,5'-dimethoxyoctahydro-2,2'-bifuran 231



Procedure 1:

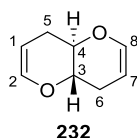
NaIO₄ (6.7 g, 31 mmol) in H₂O (55 mL) was added to a solution of tetrol **233** (4.94 g, 28.1 mmol) in H₂O (25 mL) at 0 °C. The reaction was stirred at 0 °C for 20 min and allowed to warm to room temperature for 20 min. *p*-TSA.H₂O (9.00 g, 47.4 mmol) in MeOH (140 mL) was added and the solution was stirred for 1 hr. A further portion of *p*-TSA.H₂O (1.80 g, 9.47 mmol) in MeOH (25 mL) was added and the reaction was stirred at rt for 18 h. The product was extracted with CH₂Cl₂ (multiple aliquots of 30 mL) in small portions and MeOH was added continuously as the extraction was performed. The combined organic extracts were dried over MgSO₄ and concentrated in vacuo to afford a mixture of the methyl acetals as a brown oil (4.52 g, 80 %).

Procedure 2:

NaIO₄ (4.28 g, 20.0 mmol) was added to a solution of tetrol **233** (3.20 g, 18.1 mmol) in H₂O (30 mL) at 0 °C. The mixture was stirred for 20 min and MeOH (40 mL) and 2M HCl (20 mL) were added. The mixture was stirred for 5 min and further MeOH (200 mL) was added. The reaction was allowed to warm to rt and stirred for 18 h and then diluted with H₂O (120 mL). The phases were separated and the aqueous phase was extracted with CH₂Cl₂ (3 x 100 mL). The combined organic extracts were combined, dried over MgSO₄, and concentrated in vacuo to afford acetals **230** and **231** (mixture, 3 g, 82 %).

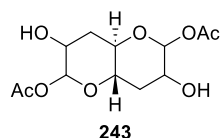
R_f (mixture) = 0.68 (pet. ether/EtOAc, 7:3); IR ν_{max} (oil) 2947, 2893, 2832, 2160, 2025, 1443, 1362, 1204, 1126, 1034, 953, 914, 891, 849 cm⁻¹; ¹H NMR (400 MHz, CDCl₃) (mixture) δ 5.01 (dt, J = 4.8, 1.2 Hz), 4.92 (dt, J = 4.3, 1.2 Hz), 4.61 (p, J = 1.5 Hz), 4.35 (ddd, J = 9.3, 3.5, 2.1), 4.06 – 3.96 (m), 3.91 (tt, J = 4.4, 2.0), 3.45 (s), 3.34 – 3.26 (m), 3.16 – 3.01 (m), 2.10 – 1.40 (m); ¹³C NMR (101 MHz, CDCl₃) δ 105.4, 104.3, 103.0, 98.0, 83.7, 82.1, 80.9, 79.5, 75.1, 74.5, 68.9, 68.4, 56.5, 54.8, 54.6, 54.5, 52.9, 33.0, 32.1, 31.9, 30.9, 30.5, 29.8, 29.5, 27.9, 27.5, 26.9, 25.5, 25.3, 24.4; HRMS (ESI+) [M+Na]⁺ calcd for C₁₀H₁₈NaO₄Na, 225.1097 found 225.1095.

(4*aR*,8*aS*)-4,4*a*,8,8*a*-tetrahydropyrano[3,2-*b*]pyran **232**



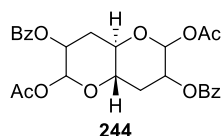
NaI (2.44 g, 16.3 mmol) and TMSCl (1.76 g, 2.05 mL, 16.2 mmol) were added to a solution of methyl acetals **230** and **231** (0.65 g, 3.2 mmol) in anhydrous MeCN (20 mL) at rt and stirred for 1 h under argon atmosphere. The mixture was cooled to 0 °C and HMDS (3.23 g, 4.20 mL, 20.1 mmol) was added. The mixture was stirred for 20 min and quenched with NaHCO₃. The phases were separated and the aqueous phase was extracted with pentane (2 x 70 mL). The combined organic extract were washed with Na₂S₂O₃ (70 mL) and H₂O (70 mL), dried over MgSO₄, and concentrated in vacuo (at <10 °C) to afford enol ether **232** as a low-melting point yellow solid (0.38 g, 86 %). IR ν_{max} (solution) 2916, 2855, 1647, 1443, 1339, 1289, 1234, 1153, 1103, 1065, 995, 841, 733 cm⁻¹; ¹H NMR (400 MHz, CDCl₃) δ 6.32 (ddd, *J* = 6.1, 2.6, 1.5 Hz, 2H, CH-C₂, CH-C₈), 4.70 (td, *J* = 5.6, 2.4 Hz, 2H, CH-C₃, CH-C₄), 3.87 – 3.76 (m, 2H, CH-C₃, CH-C₄), 2.37 – 2.23 (m, 2H, CH₂-C_{5a}, CH₂-C_{6a}), 2.12 – 1.99 (m, 2H, CH₂-C_{5b}, CH₂-C_{6b}). ¹³C NMR (101 MHz, CDCl₃) δ 143.3 (C₂, C₈), 98.4 (C₁, C₇), 71.8 (C₃, C₄), 26.8 (C₅, C₆). HRMS (ESI+) [M+H]⁺ calcd for C₈H₁₂O₂, 139.0754 found 139.0753.

(4a*R*,8a*S*)-3,7-dihydroxyoctahydropyrano[3,2-*b*]pyran-2,6-diyl diacetate **243**



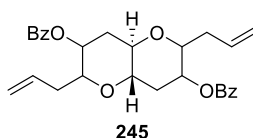
Acetic acid (7 mL) and *m*-CPBA (1.45 g, 8.38 mmol, 75% by weight) were added to a solution of enol ether **232** (0.53 g, 3.8 mmol) in anhydrous CH₂Cl₂ (15 mL) at 0 °C under argon atmosphere. The reaction was warmed to rt while stirring for 2 h. The reaction was concentrated in vacuo and purified by flash column chromatography on silica gel (gradient elution: petroleum ether/EtOAc 5:1, 1:1, then 100% EtOAc) to afford diol **243** as a white solid as a mixture of diastereomers (0.74 g, 67 %). *R*_f = 0.49 (EtOAc); m.p. 170 – 180 °C; IR ν_{max} (solid) 3430, 1721, 1373, 1246, 1180, 1134, 1045, 1018, 949, 844 cm⁻¹; ¹H NMR (400 MHz, MeOD) (mixture of diastereomers) δ 5.87 (d), 5.44 (d), 3.95 – 3.86 (m), 3.76 – 3.55 (m), 2.32 – 2.26 (m), 2.16 – 2.11 (m), 2.09 – 1.75 (m); ¹³C NMR (101 MHz, MeOD) δ 170.9, 94.6, 68.3, 68.0, 32.8, 20.9; HRMS (ESI+) [M+Na]⁺ calcd for C₁₂H₁₈NaO₈, 313.0894 found 313.0893

(4a*R*,8a*S*)-2,6-diacetoxyoctahydropyrano[3,2-*b*]pyran-3,7-diyl dibenzoate **244**



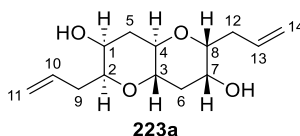
Benzoic anhydride (0.63 g, 2.8 mmol), triethylamine (0.36, 0.50 mL, 3.6 mmol), and 4-dimethylaminopyridine (0.03 g, 0.24 mmol) were added to a solution of diol **243** (0.24 g, 0.83 mmol) in anhydrous THF (15 mL) at rt under argon atmosphere. The mixture was stirred for 18 h and concentrated in vacuo. The residue was purified by flash column chromatography on silica gel (gradient elution: petroleum ether/EtOAc 5:1, then 3:1) to afford bisacetate **244** as a white solid as a mixture of diastereomers (83 %, 0.34 g). m.p. 110 – 117 °C; IR ν_{max} 1721, 1269, 1218, 1175, 1106, 1061, 1008, 965 cm^{-1} ; ^1H NMR (400 MHz, CDCl_3) (mixture of diastereomers) δ 8.20 – 7.79 (m, CH-Ph), 7.68 – 7.29 (m, CH-Ph) 6.13 – 5.95 (m), 5.94 – 5.75 (m), 5.29 – 4.96 (m), 3.88 – 3.69 (m), 2.79 – 2.48 (m), 2.29 (dd, $J = 31.4, 13.8$ Hz), 2.18 – 2.03 (m), 2.03 – 1.93 (m), 1.89 – 1.60 (m); ^{13}C NMR (101 MHz, CDCl_3) δ 165.4, 165.1, 133.7, 130.4, 129.9, 128.7, 93.9, 90.2, 71.8, 70.0, 69.5, 68.5, 33.8, 29.8, 22.5, 21.1; HRMS (ESI+) $[\text{M}+\text{Na}]^+$ calcd for $\text{C}_{26}\text{H}_{26}\text{O}_{10}\text{Na}$, 521.1418 found 521.1414.

(4a*R*,8a*S*)-2,6-diallyloctahydropyrano[3,2-*b*]pyran-3,7-diyl dibenzoate **245**



BF₃·OEt₂ (1.7 mL, 14 mmol) and TMSOTf (1.2 mL, 6.6 mmol) were stirred for 5 min in anhydrous CH₂Cl₂ at 0 °C under argon atmosphere. The solution was added to allyltrimethylsilane (2.2 mL, 1.6 g, 14 mmol) and bis-acetate **244** (0.67 g, 1.34 mmol) in anhydrous CH₂Cl₂ at 0 °C under argon atmosphere. The reaction was allowed to warm to rt and stirred for 18 h. The reaction was quenched by addition of NaHCO₃ (aq. sat., 100 mL) and the phases were separated. The aqueous phase was extracted with CH₂Cl₂ (2 x 150 mL). The combined organic extracts were dried over MgSO₄ and concentrated in vacuo. The residue was purified by flash column chromatography on silica gel to afford allyl benzoate **245** as a yellow oil as a mixture of diastereomers (68 %, 0.42 g). ¹H NMR (400 MHz, CDCl₃) (mixture of diastereomers) δ 8.19 – 7.93 (m, CH-Ph), 7.71 – 7.54 (m, CH-Ph), 7.51 – 7.38 (m, CH-Ph), 5.96 – 5.66 (m, CH), 5.39 – 4.83 (m, CH), 4.36 – 3.27 (m, CH), 2.90 – 2.22 (m, CH₂), 2.13 – 1.65 (m, CH₂); ¹³C NMR (101 MHz, CDCl₃) δ 171.2, 133.9, 133.7, 130.4, 129.9, 129.4, 128.7, 93.9, 90.2, 69.5, 68.5, 33.8, 29.8, 28.0, 24.0, 21.2, 21.1; LRMS (ESI+) [M+Na]⁺ found 485.1988.

(2R,3R,4aS,6S,7S,8aR)-2,6-diallyloctahydropyrano[3,2-b]pyran-3,7-diol 238a



Procedure 1:

K_2CO_3 (0.30 g, 2.2 mmol) was added to allyl benzoate **245** (0.20 g, 0.43 mmol) in MeOH (15 mL) at rt. The mixture was stirred for 18 h and extracted with CH_2Cl_2 (2 x 50 mL) and EtOAc (50 mL). The organic phase was dried over $MgSO_4$, concentrated in vacuo, and purified by flash column chromatography on silica gel (gradient elution: petroleum ether/EtOAc, 5:1, then 1:1) to afford diol **238** as a white solid (95 mg, 86%).

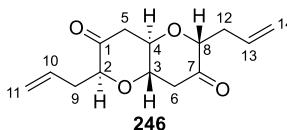
Procedure 2:

2,6-lutidine (0.51 g, 0.55 mL, 4.7 mmol) and chlorotrimethylsilane (0.45 g, 0.52 mL, 4.1 mmol) were added to diol **243** (0.54 g, 1.9 mmol) in anhydrous CH_2Cl_2 (15 mL) at 0 °C under argon atmosphere. The reaction was stirred for 30 min and allyltrimethylsilane (2.9 mL, 2.1, 18 mmol) was added. In a separate flask, $BF_3 \cdot OEt_2$ (2.4 mL, 2.8 g, 19 mmol) and TMSOTf (2.7 mL, 3.3 g, 15 mmol) were stirred in anhydrous CH_2Cl_2 (5 mL) at 0 °C under argon atmosphere for 10 min. This mixture was added to the main reaction flask and the reaction was stirred at 0 °C for 2 h. The reaction was quenched by careful addition of $NaHCO_3$ (aq. sat.). The phases were separated and the aqueous phase was extracted with CH_2Cl_2 (2 x 20 mL). The combined organic extracts were washed with H_2O (30 mL) and brine (40 mL). The combined aqueous washings were extracted with EtOAc (2 x 30 mL). The combined organic phases were dried over $MgSO_4$ and concentrated in vacuo. The residue was purified by flash column chromatography on silica gel (gradient elution: petroleum ether/EtOAc, 2:1, 1:1, 1:2, then 100 % EtOAc) to afford the allylated product **238** as an off-white solid (0.37 g, 78 %).

R_f = 0.33 (pet. ether/EtOAc 1:1); m.p. 125 – 132 °C; IR ν_{max} (solid) 3198, 2943, 2909, 1643, 1451, 1420, 1354, 1300, 1227, 1103, 1042, 991, 961, 914 cm^{-1} ; 1H NMR (400 MHz, MeOD) δ 5.91 – 5.78 (m, 2H, CH-C₁₀, CH-C₁₃), 5.16 – 5.03 (m, 4H, CH₂-C₁₁, CH₂-C₁₄), 3.98 – 3.85 (m, 4H, CH-C₂, CH-C₈, CH-C₁, CH-C₇), 3.23 – 3.15 (m, 2H, CH-C₃, CH-C₄), 2.61 – 2.49 (m, 2H, CH₂-C_{9a}, CH₂-C_{12a}), 2.37 – 2.28 (m, 2H, CH₂-C_{9b}, CH₂-C_{12b}), 1.94 (dt, J = 11.6, 3.6 Hz, 2H, CH₂-C_{5a}, CH₂-C_{6a}), 1.59 – 1.45 (m, 2H, CH₂-C_{5b}, CH₂-C_{6b}). ^{13}C NMR

(101 MHz, CDCl₃) δ 136.5 (C₁₀, C₁₃), 116.9 (C₁₁, C₁₄), 77.7 (C₂, C₈), 69.2 (C₃, C₄), 68.4 (C₁, C₇), 34.4 (C₅, C₆), 29.3 (C₉, C₁₂). HRMS (ESI+) [M+H]⁺ calcd for C₁₄H₂₄O₄, 255.1586 found 255.1591

(2R,4aS,6S,8aR)-2,6-diallyltetrahydropyrano[3,2-b]pyran-3,7(2H,6H)-dione 246



Procedure 1 (DMP oxidation):

Dess-Martin periodinane (0.13 g, 0.31 mmol) was added to diol **238** (32 mg, 0.13 mmol) in CH₂Cl₂ (5 mL) at rt and the mixture was stirred for 2 hr. TLC analysis indicated that the reaction was incomplete and further Dess-Martin periodinane (0.03 g, 0.1 mmol) was added. The reaction was stirred for a further 1 h. The reaction was quenched by the addition of Na₂SO₃ (aq. sat., 5 mL). The phases were separated and the aqueous phase was extracted with CH₂Cl₂ (2 x 10 mL). The combined organic extracts were dried over MgSO₄ and concentrated in vacuo. The product was purified by flash column chromatography on silica gel (petroleum ether/EtOAc, 5:1) to afford diketone **246** as a white solid (14 mg, 44 %).

Procedure 2 (IBX oxidation):

2-Iodoxybenzoic acid (54 mg, 0.19 mmol) was added to a solution of diol **238** (12 mg, 0.047) in anhydrous DMSO (2.5 mL) at rt under argon atmosphere. The mixture was stirred for 1.5 h and further 2-iodoxybenzoic acid (21 mg, 0.075 mmol) was added. The mixture was stirred for 18 h and quenched by the addition of NaHCO₃ (aq. sat.) and Na₂S₂O₃. The phases were separated and the aqueous phase was extracted with CH₂Cl₂ (2 x 20 mL) and EtOAc (2 x 20 mL). The organic extracts were washed with brine (20 mL), dried over MgSO₄, and concentrated in vacuo. The residue was purified by flash column chromatography on silica gel (petroleum ether/EtOAc, 5:1) to afford diketone **246** as a white solid (14 mg, 38 %).

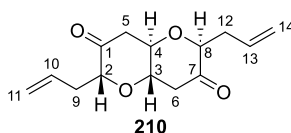
Procedure 3 (Albright-Goldman oxidation):

Acetic anhydride (0.67 g, 0.62 mL, 6.6 mmol) was added to diol **238** (0.14 g, 0.56 mmol) in anhydrous DMSO (1.55 mL) at rt under argon atmosphere. The mixture was stirred for 18 h. The mixture was cooled to 0 °C, diluted with EtOAc (5 mL) and the reaction was quenched by the addition of H₂O (5 mL) followed by NaHCO₃ (aq. sat.). The phases were separated and the aqueous phase was extracted with CH₂Cl₂ (3 x 15 mL). The combined organic extracts were washed with H₂O (2 x 20 mL), dried over MgSO₄, and

concentrated in vacuo. The residue was purified by flash column chromatography on silica gel (petroleum ether/EtOAc, 5:1) to afford diketone **246** as a yellow solid (64 %, 87 mg).

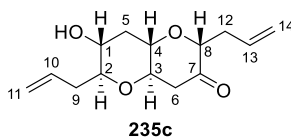
Rf = 0.54 (petroleum ether/EtOAc, 5:1); IR ν_{\max} (solid) 2921, 1720, 1257, 1236, 1103, 1079, 1010, 994, 979, 917, 904, 800 cm^{-1} ; ^1H NMR (400 MHz, CDCl_3) δ 5.81 – 5.70 (m, 2H, CH-C₁₀, CH-C₁₃), 5.19 – 5.11 (m, 4H, CH₂-C₁₁, CH₂-C₁₄), 4.16 – 4.08 (m, 2H, CH-C₂, CH-C₈), 3.97 – 3.88 (m, 2H, CH-C₃, CH-C₄), 2.92 (dd, J = 16.4, 4.4 Hz, 2H, CH₂-C_{5a}, CH₂-C_{6a}), 2.66 – 2.38 (m, 6H, CH₂-C_{5b}, CH₂-C_{6b}, CH₂-C₉, CH₂-C₁₂); ^{13}C NMR (101 MHz, CDCl_3) δ 206.3, 132.4, 118.9, 80.9, 68.7, 43.2, 34.5; HRMS (ESI+) $[\text{M}+\text{H}]^+$ calcd for $\text{C}_{14}\text{H}_{20}\text{O}_4$, 251.1278 found 251.1275.

(2R,4aR,6S,8aS)-2,6-diallyltetrahydropyrano[3,2-b]pyran-3,7(2H,6H)-dione **210**



1,8-Diazabicyclo[5.4.0]undec-7-ene (60 μ L, 61 mg, 0.40 mmol) was added to diketone **231** (136 mg, 0.54 mmol) in anhydrous CH_2Cl_2 (140 mL) at rt under argon atmosphere. The mixture was stirred for 72 h in the absence of light. The reaction was quenched by the addition of NH_4Cl (aq. sat.). The phases were separated and the aqueous phase was extracted with CH_2Cl_2 (2 x 50 mL). The combined organic extracts were washed with H_2O (100 mL), dried over MgSO_4 and concentrated in vacuo. The residue was purified by flash column chromatography on silica gel (petroleum ether/EtOAc, 5:1) to afford diketone **210** as a white solid (90 mg, 66 %). $R_f = 0.67$ (petroleum ether/EtOAc, 5:1); m.p. 123 – 130 $^\circ\text{C}$; IR ν_{max} (solid) 2920, 1724, 1435, 1358, 1296, 1234, 1096, 1049, 991, 914 cm^{-1} ; ^1H NMR (400 MHz, CDCl_3) δ 5.89 – 5.76 (m, 2H, CH- C_{10} , CH- C_{13}), 5.18 – 5.05 (m, 4H, CH_2 - C_{11} , CH_2 - C_{14}), 3.88 (dd, $J = 6.8, 3.2$ Hz, 2H, CH- C_2 , CH- C_8), 3.79 – 3.71 (m, 2H, CH- C_3 , CH- C_4), 3.05 (dd, $J = 15.6, 5.2$ Hz, 2H, CH- C_{5a} , CH- C_{6a}), 2.70 – 2.60 (m, 2H, CH- C_{9a} , CH- C_{12a}), 2.59 – 2.49 (m, 2H, CH- C_{5b} , CH- C_{6b}), 2.42 – 2.32 (m, 2H, CH- C_{9b} , C_{12b}). ^{13}C NMR (101 MHz, CDCl_3) δ 204.1 (C_1 , C_7), 133.7 (C_{10} , C_{14}), 118.0 (C_{11} , C_{14}), 82.4 (C_2 , C_8), 75.8 (C_3 , C_4), 45.0 (C_5 , C_6), 33.8 (C_9 , C_{12}). HRMS (ESI+) $[\text{M}+\text{H}]^+$ calcd for $\text{C}_{14}\text{H}_{20}\text{O}_4$, 251.1278 found 251.1278

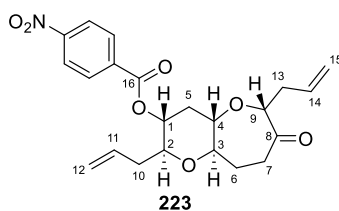
(2*R*,4*aR*,6*S*,7*R*,8*aS*)-2,6-diallyl-7-hydroxyhexahydropyrano[3,2-*b*]pyran-3(2*H*)-one
211c



[RhCl(COD)]₂ (47 mg, 0.01 mmol) and (*R*)-*i*PrPybox (115 mg, 0.04 mmol) were stirred in anhydrous THF (40 mL) at rt under argon atmosphere for 20 h. Silver tetrafluoroborate (5.7 mg, 0.029 mmol) was added and the mixture was stirred for 1 h. O₂ was bubbled through the reaction mixture and diketone **210** (480 mg, 0.19 mmol) in anhydrous THF (40 mL) was added, followed by diphenylsilane (0.71 mL, 52 μL, 0.28 mmol) and H₂O (35 μL, 35 mg, 0.18 mmol). The mixture was stirred for 18 h and then concentrated in vacuo. The residue was purified by flash column chromatography on silica gel (20:1 pentane/EtOAc, then 10:1 pentane/EtOAc, then 5:1 pentane/EtOAc, then 3:1 pentane/EtOAc) to afford the mono-alcohol **211c** as a white solid (317 mg, 66 %).

IR ν_{\max} (solid) 2877, 1709, 1639, 1429, 1311, 1218, 1100 cm⁻¹; ¹H NMR (400 MHz, MeOD) δ 5.98 – 5.78 (m, 2H, CH-C₁₀, CH-C₁₃), 5.19 – 5.04 (m, 4H, CH₂-C₁₁, CH₂-C₁₄), 3.82 (dd, *J* = 7.6, 4.4 Hz, 1H, CH-C₈), 3.61 – 3.52 (m, 1H, CH-C₁), 3.41 – 3.32 (m, 2H, CH-C₃, CH-C₄), 3.27 – 3.20 (m, 1H, CH-C₂), 2.95 – 2.88 (m, 1H, CH₂-C_{6a}), 2.68 – 2.28 (m, 6H, CH₂-C_{6b}, CH₂-C₁₂, CH₂-C₉, CH₂-C_{5a}), 1.67 – 1.62 (m, 1H, CH₂-C_{5a}); ¹³C NMR (101 MHz, CDCl₃) δ 204.9 (C₇), 134.5 (C₁₀), 133.8 (C₁₃), 117.5 (C_{11/14}), 117.4 (C_{11/14}), 82.6 (C₈), 80.9 (C₂), 76.4 (C_{3/4}), 75.3 (C_{3/4}), 69.2 (C₁), 45.0 (C₆), 38.3 (C₅), 36.4 (C_{9/12}), 33.7 (C_{9/12}); HRMS (ESI+) [M+H]⁺ calcd for C₁₄H₂₀O₄, 253.1434 found 253.1436

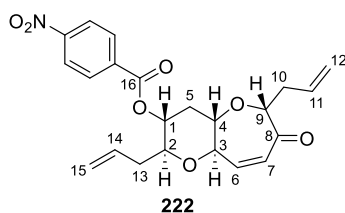
(2*S*,3*R*,4*aS*,6*R*,9*aR*)-2,6-diallyl-7-oxooctahydro-2*H*-pyrano[3,2-*b*]oxepin-3-yl 4-nitrobenzoate **223**



AlMe_3 (2M in hexanes, 0.1 mL, 0.2 mmol) and TMSCHN_2 (2M in hexanes, 0.1 mL, 0.2 mmol) were added to ketone **211c** (55 mg, 0.14 mmol) in anhydrous CH_2Cl_2 (9 mL) at -90°C . The mixture was stirred for 1.5 h and monitored by TLC. When all of the starting material had been consumed, the reaction was quenched by the addition of NaHCO_3 (sat. aq.). The phases were separated and the aqueous layer was extracted with CH_2Cl_2 (3 x 5 mL). The combined organic extracts were washed with H_2O (10 mL), brine (10 mL), dried over MgSO_4 , and concentrated in vacuo.

The crude isolated product was dissolved in THF (5 mL) at -78°C and TBAF (1M in THF, 0.11 mL) was added. The mixture was stirred for 2 h and the reaction was quenched by the addition of NH_4Cl (sat. aq.). The phases were separated and the aqueous layer was extracted with CH_2Cl_2 (3 x 5 mL). The combined organic extracts were dried over MgSO_4 and concentrated in vacuo. The residue was purified by flash column chromatography on silica gel to afford the product **223** as a white solid. IR ν_{max} (solid) 2871, 1716, 1606, 1525, 1347, 1270, 1098 cm^{-1} ; ^1H NMR (400 MHz, CDCl_3) δ 8.31 (d, $J = 8.9$ Hz, 2H, Ar-CH), 8.19 (d, $J = 8.9$ Hz, 2H, Ar-CH), 5.91 – 5.71 (m, 2H, CH- C_{11} , C- C_{14}), 5.12 – 4.97 (m, 4H, CH_2 - C_{12} , CH_2 - C_{15}), 4.89 – 4.80 (m, 1H, CH- C_1), 3.91 (dd, $J = 8.0, 4.4$ Hz, 1H, CH- C_9), 3.60 – 3.53 (m, 1H, CH- C_2), 3.44 – 3.35 (m, 1H, CH- C_3), 3.23 – 3.13 (m, 1H, CH- C_4), 2.64 (dt, $J = 12, 4.4$ Hz), 1H, CH_2 - C_{5a}), 2.89 – 2.80 (m, 1H, CH_2 - C_{7a}), 2.48 – 2.18 (m, 6H, CH_2 - C_{10} , CH_2 - C_{13} , CH_2 - C_{6a} , CH_2 - C_{7b}), 1.75 (m, 1H, CH_2 - C_{5b}), 1.64 – 1.55 (m, 1H, CH_2 - C_{6b}); ^{13}C NMR (101 MHz, CDCl_3) δ 214.96 (C_8), 163.77 (C_{16}), 150.92 (Ar-C), 135.38 (Ar-C), 133.74 (C_{11}), 133.30 (C_{14}), 130.95 (Ar-C), 123.85 (Ar-C), 118.13 (C_{12}), 117.66 (C_{15}), 87.01 (C_9), 80.99 (C_3), 80.16 (C_4), 78.47 (C_2), 71.90 (C_1), 37.25 ($\text{C}_{10/13}$), 36.82 (C_7), 36.7 (C_5), 36.47 ($\text{C}_{10/13}$), 29.17 (C_6); HRMS (APCI) $[\text{M}]^-$ calcd for $\text{C}_{22}\text{H}_{24}\text{NO}_7$, 415.1637 found 415.1634

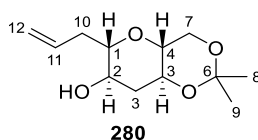
(2*S*,3*R*,4*aS*,6*R*,9*aR*)-2,6-diallyl-7-oxo-3,4,4*a*,6,7,9*a*-hexahydro-2*H*-pyrano[3,2-*b*]oxepin-3-yl 4-nitrobenzoate **222**



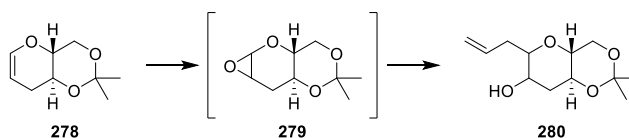
LHDMS (1M in THF, 60 μ L, 0.060 mmol) and triethylamine (22 μ L, 16 mg, 0.16 mmol) were to a solution of **223** (10 mg, 0.024 mmol) in anhydrous THF (0.5 mL) under argon atmosphere at -78 $^{\circ}$ C. The mixture was stirred for 40 min and TMSCl (17 μ L, 15 mg, 0.13 mmol) was added. The mixture was stirred for 1 h at -78 $^{\circ}$ C and then 1 h at room temperature. The reaction was quenched by the addition phosphate buffer (aq., pH = 7.4) and extracted with EtOAc (3 x 2 mL). The combined organic extracts were dried over MgSO_4 and concentrated in vacuo.

The crude residue was dissolved in anhydrous MeCN (0.5 mL) under argon atmosphere and $\text{Pd}(\text{OAc})_2$ (10 mg, 0.04 mmol) was added. The reaction mixture was stirred at room temperature for 4 hours, filtered, and purified by flash column chromatography on silica gel to afford enone **222** (3 mg, 30 %). IR ν_{max} (film) 1724, 1526, 1266, 1099, 736, 718 cm^{-1} ; ^1H NMR (400 MHz, CDCl_3) 8.31 (d, $J = 8.8$ Hz, 2H), 8.19 (d, $J = 8.8$ Hz, 2H), 6.53 – 6.45 (m, 1H, CH- C_7), 6.05 – 5.98 (m, 1H, CH- C_6). 5.92 – 5.72 (m, 2H, CH- C_{11} , CH- C_{13}), 5.13 – 4.99 (m, 4H, CH_2 - C_{12} , CH_2 - C_{15}), 4.93 – 4.85 (m, 1H, CH- C_1), 4.26 (dd, $J = 7.8, 4$ Hz, 1H, CH- C_9), 4.00 (tt, $J = 8.8, 2.8$ Hz, 1H, CH- C_3), 3.70 – 3.52 (m, 2H, CH- C_4 , CH- C_2), 2.77 – 2.67 (m, 1H, CH_2 - C_{5a}), 2.62 – 2.54 (m, 1H, CH_2 - C_{10a}), 2.50 – 2.24 (m, 3H, CH_2 - C_{13} , CH_2 - C_{10b}), 1.87 – 1.78 (m, 1H, CH_2 - C_{5b}); ^{13}C NMR (101 MHz, CDCl_3) δ 203.9 ($\text{C}_{8/16}$), 202.9 ($\text{C}_{8/16}$), 143.3 (C_7), 133.5 (C_{14}), 133.4 (C_{11}), 131.0 (CH-Ar), 128.6 (C_6), 123.9 (CH-Ar), 118.0 (C_{12} , C_{15}), 87.0 (C_9), 80.3 (C_3), 79.1 (C_2), 76.6 (C_4), 71.5 (C_1), 37.7 (C_{10}), 36.4 (C_{13}), 36.3 (C_5); HRMS (APCI) $[\text{M}+\text{H}]^+$ calcd for $\text{C}_{22}\text{H}_{24}\text{NO}_7$, 414.1547 found 415.1548

(4aR,6S,7R,8aS)-Hexahydro-2,2-dimethyl-6-(prop-2-en-1-yl)-pyrano[3,2-d]-1,3-dioxin-7-ol 280



Procedure 1:



A solution of *m*-CPBA (17.2 g, 87.8 mmol, 70 – 75 % by weight) and KF (10.2 g, 176 mmol) was stirred in anhydrous CH₂Cl₂ (400 mL) under argon atmosphere for 30 min. A solution of enol ether **278** (6.0 g, 35 mmol) in anhydrous CH₂Cl₂ (100 mL) was added slowly. The reaction mixture was stirred for 3 h. The mixture was filtered through a pad of MgSO₄ and the filtrate was concentrated in vacuo to afford epoxide **279** as a colourless oil.

The crude epoxide was dissolved in anhydrous THF (50 mL) and added to a solution of allylmagnesium chloride (2M in THF, 90 mL, 180 mmol) in anhydrous THF (450 mL) at 0 °C under argon atmosphere. The mixture was stirred for 3 h and the reaction was quenched by addition of H₂O (500 mL). The product was extracted into EtOAc (3 x 300 mL). The combined organic extracts were dried over MgSO₄ and concentrated in vacuo. The residue was purified by flash column chromatography on silica gel (petroleum ether/EtOAc, 5:1, then 1:1) to afford a diastereomeric mix of alcohol **280** as a yellow oil (2.18 g, 27 %).

Procedure 2:

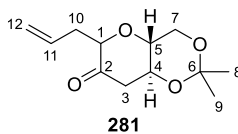
NaBH₄ (8 mg, 0.2 mmol) was added to a solution of ketone **277** (30 mg, 0.13 mmol) in an EtOH/CH₂Cl₂ mixture (1:1, 2 mL) at 0 °C. The solution was stirred for 1 h and the reaction was quenched by addition of H₂O. The phases were separated and the aqueous phase was extracted with EtOAc (3 x 2 mL). The combined organic extracts were dried over MgSO₄ and concentrated in vacuo to afford alcohol **280** (25 mg, 83 %).

¹H NMR (400 MHz, CDCl₃) δ 5.93 – 5.80 (m, 1H, CH-C₁₆), 5.15 – 5.00 (m, 2H, CH₂-C₁₂), 3.84 (dd, *J* = 16, 5.6 Hz, 1H, CH₂-C_{7a}), 3.63 (t, *J* = 10.4 Hz, 1H, CH₂-C_{7b}), 3.55 – 3.41 (m,

2H, CH-C₃, CH-C₂), 3.21 – 3.07 (m, 2H, CH-C₁, CH-C₄), 2.59 – 2.50 (m, 1H, CH₂-C_{10a}), 2.28 – 2.19 (m, 2H, CH₂-C_{10b}, CH₂-C_{3a}), 1.52 – 1.42 (m, 1H, CH₂-C_{3b}), 1.45 (s, 3H, CH₃-C₈), 1.36 (s, 3H, CH₃-C₉); ¹³C NMR (101 MHz, CDCl₃) δ 134.7 (C₁₁), 117.2 (C₁₂), 99.3 (C₆), 81.8 (C₁), 74.3 (C₄), 69.4 (C₅), 69.1 (C₃), 62.8 (C₇), 38.7 (C₃), 36.4 (C₁₀), 29.3 (C₉), 19.2 (C₈); HRMS (APCI) [M+H]⁺ calcd for C₁₂H₂₁O₄, 229.1436 found 229.1436

The spectroscopic data matched that previously reported in the literature.⁸⁴

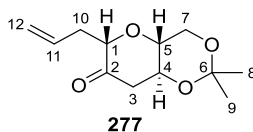
(4a*R*,8a*S*)-Hexahydro-2,2-dimethyl-6-(prop-2-en-1-yl)-pyrano[3,2-*d*]-1,3-dioxin-7-one **281**



Acetic anhydride (5.85 g, 5.42 mL, 57.4 mmol) was added to alcohol **280** (2.18 g, 9.54 mmol) in anhydrous DMSO (27.1 mL) at rt under argon atmosphere. The reaction mixture was stirred for 18 h. The mixture was cooled to 0 °C, diluted with EtOAc (20 mL) and the reaction was quenched by the addition of H₂O (20 mL) followed by NaHCO₃ (aq. sat.). The phases were separated and the aqueous phase was extracted with CH₂Cl₂ (3 x 40 mL). The combined organic extracts were washed with H₂O (2 x 20 mL), dried over MgSO₄, and concentrated in vacuo. The residue was purified by flash column chromatography on silica gel (petroleum ether/EtOAc, 10:1) to afford a diastereomeric mixture of ketone **281** as a yellow solid (1.58 g, 73 %). ¹H NMR (400 MHz, CDCl₃) (mixture of diastereomers) δ 5.91 – 5.68 (m), 5.16 – 4.97 (m), 3.99 (dd, *J* = 10.8, 5.2 Hz), 3.92 – 3.83 (m), (t, *J* = 10.4 Hz), 3.52 – 3.42 (m), 2.81 (dd, *J* = 15.2, 5.6 Hz), 2.66 – 2.56 (m), 2.53 – 2.40 (m), 1.48 (s), 1.45 (s), 1.39 (s), 1.37 (s); ¹³C NMR (101 MHz, CDCl₃) δ 206.6, 204.5, 133.8, 132.6, 118.8, 117.7, 99.4, 99.3, 83.4, 81.8, 73.2, 70.0, 69.4, 69.0, 66.8, 62.9, 62.6, 45.4, 43.7, 34.5, 33.9, 29.2, 19.2.

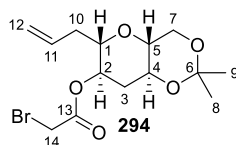
The spectroscopic data matched that previously reported in the literature.⁸⁴

(4a*R*,6*S*,8a*S*)-Hexahydro-2,2-dimethyl-6-(prop-2-en-1-yl)-pyrano[3,2-*d*]-1,3-dioxin-7-one **277**



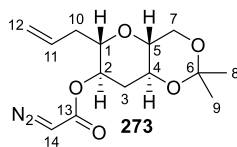
DBU (0.24 mL, 0.24 g, 1.6 mmol) was added to a solution of ketone **281** (1.44 g, 6.31 mmol) in anhydrous CH₂Cl₂ (70 mL) under argon atmosphere at room temperature. The mixture was stirred for 24 h and the reaction was quenched by the addition of NH₄Cl (aq. sat.). The phases were separated and the aqueous phase was extracted with CH₂Cl₂ (3 x 30 mL). The combined organic extracts were dried over MgSO₄ and concentrated in vacuo. The residue was purified by flash column chromatography on silica gel (petroleum ether/EtOAc, 10:1) to afford ketone **277** as a white solid (0.90 g, 63 %). IR ν_{\max} (film) 2920, 1722, 1400, 1250, 1037, 844 cm⁻¹; ¹H NMR (400 MHz, CDCl₃) δ 5.88 – 5.75 (m, 1H, CH-C₁₁), 5.16 – 5.02 (m, 2H, CH₂-C₁₂), 4.03 (dd, *J* = 10.8, 5.6 Hz, 1H, CH₂-C_{7a}), 3.96 – 3.86 (m, 2H, CH-C₁, CH-C₄), 3.79 (t, *J* = 10.4 Hz, CH₂-C_{7b}), 3.55 – 3.47 (m, 1H, CH-C₅), 2.85 (dd, *J* = 15.6, 5.6 Hz, 1H, CH₂-C_{3a}), 2.70 – 2.60 (m, 1H, CH₂-C_{10a}), 2.48 (dd, *J* = 15.6, 11.6 Hz, 1H, CH₂-C_{3b}), 2.41 – 2.32 (m, 1H, CH₂-C_{10b}), 1.52 (s, 3H, CH₃-C₈), 1.43 (CH₃-C₉); ¹³C NMR (101 MHz, CDCl₃) δ 204.7 (C₂), 133.8 (C₁₁), 117.8 (C₁₂), 99.4 (C₆), 83.5 (C₁), 73.3 (C₅), 69.5 (C₄), 62.7 (C₇), 45.5 (C₃), 33.9 (C₁₀), 29.1 (C₉), 19.3 (C₈); HRMS (APCI) [M+Na]⁺ calcd for C₁₂H₁₈O₄Na, 249.1097 found 249.1096

(4aR,6S,7R,8aS)-6-allyl-2,2-dimethylhexahydropyrano[3,2-d][1,3]dioxin-7-yl 2-bromoacetate **294**



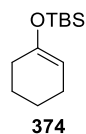
Bromoacetic acid (23 mg, 0.17 mmol), DCC (34 mg, 0.16 mmol) and DMAP (10 mg, 0.082 mmol) were added to a solution of alcohol **280a** (25 mg, 0.11 mmol) in anhydrous CH_2Cl_2 (1 mL) under argon atmosphere at room temperature. The mixture was stirred for 1.5 h. The reaction mixture was concentrated in vacuo and the residue was purified by flash column chromatography on silica gel (pentane/EtOAc, 10:1) to afford bromoacetate **294** (20 mg, 38 %). IR ν_{max} (film) 2360, 2341, 1737, 1379, 1272, 1199, 1100, 985, 920, 855 cm^{-1} ; ^1H NMR (400 MHz, CDCl_3) δ 5.88 – 5.76 (m, 1H, CH- C_{11}), 5.12 – 5.04 (m, 2H, CH_2 - C_{12}), 4.76 – 4.68 (m, 1H, CH- C_2), 3.93 – 3.87 (m, 1H, CH_2 - C_{7a}), 3.84 – 3.76 (m, 2H, CH_2 - C_{14}), 3.69 (t, J = 10.8 Hz, 1H, CH_2 - C_{7b}), 3.66 – 3.58 (m, 1H, CH- C_4), 3.52 – 3.45 (m, 1H, C_1), 3.25 – 3.16 (m, 1H, C_5), 2.45 – 2.35 (m, 2H, CH_2 - C_{3a} , CH_2 - C_{10a}), 2.27 – 2.16 (m, 1H, CH_2 - C_{10b}), 1.62 – 1.52 (m, 1H, CH_2 - C_{10b}), 1.49 (s, 3H, CH_3 - C_8), 1.40 (s, 3H, CH_3 - C_9); ^{13}C NMR (101 MHz, CDCl_3) δ 166.4, 133.7, 117.8, 99.5, 78.8, 74.6, 72.0, 68.6, 62.8, 36.2, 35.0, 29.3, 25.6, 19.3; HRMS (APCI) $[\text{M}+\text{H}]^+$ calcd for $\text{C}_{14}\text{H}_{22}\text{BrO}_5$, 349.0645 found 349.0646

(4aR,6S,7R,8aS)-6-allyl-2,2-dimethylhexahydropyrano[3,2-d][1,3]dioxin-7-yl 2-diazoacetate **273**



N,N'-Ditosylhydrazine **293** (1.01 g, 2.97 mmol) and DBU (1.1 mL, 1.1 g, 7.2 mmol) were added to a solution of bromoacetate **294** (0.52 mg, 1.5 mmol) in anhydrous THF (25 mL) under argon atmosphere at 0 °C. The mixture was stirred for 10 min and the reaction was quenched by the addition of NaHCO₃ (aq. sat.). The phases were separated and the aqueous layer was extracted with CH₂Cl₂ (3 x 20 mL). The combined organic extracts were dried over MgSO₄ and concentrated in vacuo. The residue was purified by flash column chromatography on silica gel (pentane/EtOAc, 10:1) to afford diazoacetate **273** as a white solid (170 mg, 44%). IR ν_{\max} (solid) 2110, 1692, 1380, 1351, 1232, 1176, 1089, 1049, 988, 915, 857 cm⁻¹; ¹H NMR (400 MHz, CDCl₃) δ 5.88 – 5.76 (m, 1H, CH-C₁₆), 5.11 – 5.02 (m, 2H, CH₂-C₁₂), 4.81 – 4.71 (m, 2H, CH-C_{2a}, CH-C₁₄), 3.92 – 3.85 (m, 1H, CH₂-C_{7a}), 3.69 (t, *J* = 10.8 Hz, 1H, CH₂-C_{7b}), 3.65 – 3.56 (CH-C₄), 3.44 – 3.37 (1H, CH-C₁) 3.24 – 3.14 (CH-C₅), 2.42 – 2.32 (2H, CH₂-C_{3a}, CH₂-C_{10a}), 2.24 – 2.14 (CH₂-C_{10b}), 1.60 – 1.50 (1H, CH₂-C_{3b}), 1.48 (s, 3H, CH₃-C₈), 1.40 (s, CH₃-C₉); ¹³C NMR (101 MHz, CDCl₃) δ 133.9, 117.5, 99.5, 79.2, 74.6, 70.7, 68.7, 62.8, 46.6, 36.3, 35.7, 29.3, 19.3; HRMS (APCI) [M+H]⁺ calcd for C₁₄H₂₁N₂O₅, 297.1445 found 297.1444

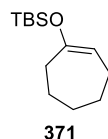
tert-Butyl(cyclohexenyloxy)dimethylsilane 374



Triethylamine (3.5 mL, 2.5 g, 25 mmol) was added to a solution of cyclohexanone (1 g, 10 mmol) in CH₂Cl₂ (60 mL) under argon atmosphere at room temperature. The reaction was stirred for 1 h and TBSOTf (2.6 mL, 3.0 g, 11 mmol) was added. The reaction was stirred for 2 h and quenched with NH₄Cl (aq. sat.). The phases were separated and the aqueous phases was extracted with CH₂Cl₂ (3 x 20 mL). The combined organic phases were dried over MgSO₄ and concentrated in vacuo. The residue was purified by flash column chromatography on silica gel (100 % hexanes) to afford silyl enol ether **374** as a colourless oil (1.45 g, 68 %). ¹H NMR (400 MHz, CDCl₃) δ 4.89 – 4.84 (m, 1H), 2.05 – 1.95 (m, 4H), 1.70 – 1.61 (m, 2H), 1.55 – 1.46 (m, 2H), 0.92 (s, 9H), 0.13 (s, 6H); ¹³C NMR (101 MHz, CDCl₃) δ 150.7, 104.5, 29.9, 25.8, 24.0, 23.4, 22.6, 18.2, -4.2.

The spectroscopic data matched that previously reported in the literature .¹¹⁸

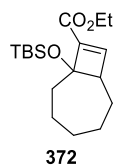
Tert-butyl(cyclohept-1-en-1-yloxy)dimethylsilane 371



Triethylamine (1.5 mL, 1.1 g, 11 mmol) was added to a solution of cycloheptanone (0.5 g, 5.1 mmol) in CH₂Cl₂ (25 mL) under argon atmosphere at room temperature. The reaction was stirred for 1 h and TBSOTf (0.93 mL, 1.1 g, 4.0 mmol) was added. The reaction was stirred for 2 h and quenched with NH₄Cl (aq. sat.). The phases were separated and the aqueous phases was extracted with CH₂Cl₂ (3 x 10 mL). The combined organic phases were dried over MgSO₄ and concentrated in vacuo. The residue was purified by flash column chromatography on silica gel (100 % pentane, then pentane/EtOAc, 10:1) to afford silyl enol ether **371** as a colourless oil (0.58 g, 58 %). ¹H NMR (400 MHz, CDCl₃) δ 5.00 (t, *J* = 6.8 Hz, 1H), 2.24 – 2.19 (m, 2H), 2.00 – 1.94 (m, 2H), 1.71 – 1.62 (m, 2H), 1.60 – 1.48 (m, 4H), 0.92 (s, 9H), 0.11 (s, 6H); ¹³C NMR (101 MHz, CDCl₃) δ 156.3, 108.7, 35.7, 31.6, 27.9, 25.9, 25.5, 25.3, 18.1, -4.3; HRMS (APCI) [M+H]⁺ calcd for C₁₃H₂₇OSi, 227.1826 found 227.1828.

The spectroscopic data matched that previously reported in the literature.¹¹⁹

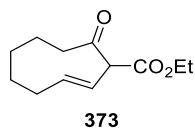
Ethyl l-(tert-Butyldi-methylsilyloxy)bicyclo[5.2.0]non-8-ene-9-carboxylate **372**



Silyl enol ether **371** (100 mg, 0.44 mmol) in CH_2Cl_2 (1 mL) was added dropwise to a solution of freshly distilled titanium tetrachloride (73 μL , 0.13 g, 0.69 mmol) and ethyl propiolate (67 μL , 0.065 g, 0.67 mmol) in CH_2Cl_2 (1.5 mL) at $-78\text{ }^\circ\text{C}$ under Ar atmosphere. The reaction was stirred for 15 minutes and quenched with H_2O (2 mL). The phases were separated and the aqueous layer was extracted with CH_2Cl_2 (3 x 2 mL). The combined organic phases were dried over MgSO_4 , filtered, and concentrated in vacuo to afford the crude product. The product was purified by flash column chromatography to afford cyclobutene **372** as a colourless oil (40 mg, 28 %). IR ν_{max} (film) 2361, 2341, 1700, 1252, 836, 778 cm^{-1} ; ^1H NMR (400 MHz, CDCl_3) δ 6.90 (d, J = 1.2 Hz, 1H), 4.19 (m, 2H), 2.78 (m, 1H), 1.29 (t, J = 7.2 Hz, 3H), 0.88 (s, 9H), 0.05 (s, 3H), 0.02 (s, 3H); ^{13}C NMR (101 MHz, CDCl_3) δ 162.3, 149.8, 143.6, 82.9, 60.1, 57.1, 36.3, 32.2, 29.9, 27.6, 26.4, 25.9, 23.8, 18.4, 14.5, -2.8, -3.1; HRMS (APCI) $[\text{M}+\text{H}]^+$ calcd for $\text{C}_{18}\text{H}_{33}\text{O}_3\text{Si}$, 325.2193 found 325.2195

The spectroscopic data matched that previously reported in the literature ¹¹¹

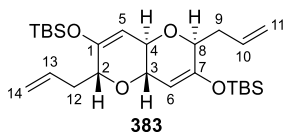
Ethyl 2-Oxocyclonon-8-ene-1-carboxylate **373**



A solution of cyclobutene **372** (35 mg, 0.1 mmol), acetic acid (0.5 mL), phosphoric acid (50 μ L), THF (0.5 mL) and H₂O (0.25 mL) was refluxed for 5 h. The reaction was extracted with Et₂O (3 x 2 mL). The combined organic phases were dried over MgSO₄ and concentrated in vacuo. The residue was purified by flash column chromatography on silica gel (hexanes/EtOAc, 10:1) to afford **373** (15 mg, 60 %). ¹H NMR (400 MHz, CDCl₃) δ 5.91 – 5.79 (m, 1H), 5.58 (dd, J = 10.0 Hz, 1H), 4.28 – 4.18 (m, 2H), 4.13 (d, J = 10.0 Hz, 1H), 2.85 (td, J = 12.8, 3.2 Hz, 1H), 1.29 (t, J = 7.2 Hz); ¹³C NMR (101 MHz, CDCl₃) δ 204.0, 168.4, 138.5, 119.9, 64.8, 61.2, 38.0, 33.5, 29.7, 26.3, 24.4, 14.2.

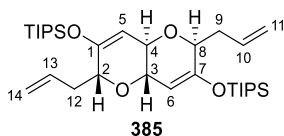
The spectroscopic data matched that previously reported in the literature. ¹¹¹

(((2*R*,4*aR*,6*S*,8*aS*)-2,6-diallyl-2,4*a*,6,8*a*-tetrahydropyrano[3,2-*b*]pyran-3,7-diyl)bis(oxy))bis(tert-butyldimethylsilane) **383**



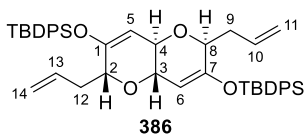
LHMDS (1M in THF, 0.8 mL, 0.8 mmol) and Et₃N (0.44 mL, 0.32 g, 3.1 mmol) were added to a solution of TBSOTf (0.18 mL, 0.21 g, 0.78 mmol), diketone **210** (0.05 g, 0.20 mmol), and 4Å MS in THF (2 mL) at -78 °C. The reaction was stirred for 2.5 h and quenched with NaHCO₃ (sat. aq.). The phases were separated and the aqueous layer was extracted with CH₂Cl₂ (3 x 5 mL). The combined organic layers were dried over MgSO₄, concentrated in vacuo, and purified by flash column chromatography on silica gel (100% petroleum ether, then petroleum ether/EtOAc, 10:1) to afford the product as a white solid (30 mg, 31 %). IR ν_{max} (solid) 2954, 2856, 1651, 1470, 1360, 1290, 1253, 1210, 1096, 850 cm⁻¹; ¹H NMR (400 MHz, CDCl₃) δ 5.94 – 5.80 (m, 2H, CH-C_{13/10}), 5.15 – 5.02 (m, 4H, CH₂-C_{11/14}), 4.98 (s, 2H, CH-C_{5/6}), 4.11 (br. s, 2H, CH-C_{2/8}), 3.85 (s, 2H, CH-C_{3/4}), 2.58 – 2.47 (m, 2H, CH-C_{9*a*/12*a*}), 2.42 – 2.31 (m, 2H, CH-C_{9*b*/12*b*}), 0.92 (s, 18H), 0.19 (s, 12 H); ¹³C NMR (101 MHz, CDCl₃) δ 152.1 (C_{1/7}), 134.6 (C_{10/13}), 117.2 (C_{11/14}), 103.7 (C_{5/6}), 77.4 (C_{2/8}), 72.8 (C_{3/4}), 36.8 (C_{9/12}), 25.8, -4.4; HRMS (APCI) [M+H]⁺ calcd for C₂₆H₄₇O₄Si₂, 479.3007 found 479.3003

(((2*R*,4*aR*,6*S*,8*aS*)-2,6-diallyl-2,4*a*,6,8*a*-tetrahydropyrano[3,2-*b*]pyran-3,7-diyl)bis(oxy))bis(triisopropylsilane) **385**



LHMDS (1M in THF, 0.6 mL, 0.6 mmol) and Et₃N (0.35 mL, 0.25 g, 2.5 mmol) were added to a solution of TIPSOTf (0.16 mL, 0.18 g, 0.60 mmol), diketone **210** (0.03 g, 0.12 mmol), and 4A MS in THF (1 mL) at -78 °C. The reaction was stirred for 5 h and quenched with NaHCO₃ (sat. aq.). The phases were separated and the aqueous layer was extracted with CH₂Cl₂ (3 x 2 mL). The combined organic layers were dried over MgSO₄, concentrated in vacuo, and purified by flash column chromatography on silica gel (pentane/EtOAc, 8:1) to afford the product as a white solid (60 mg, 88 %). IR ν_{\max} (film) 2944, 2866, 1651, 1461, 1286, 1210, 1098, 994, 909, 880, 828 cm⁻¹; ¹H NMR (400 MHz, CDCl₃) δ 5.95 – 5.82 (m, 2H, CH-C_{13/10}), 5.15 – 5.01 (m, 4H, CH₂-C_{11/14}), 4.98 (s, 2H, CH-C_{5/6}), 4.14 (br. s, 2H, CH-C_{2/8}), 3.83 (s, 2H, CH-C_{3/4}), 2.59 – 2.49 (m, 2H, CH₂-C_{9*a*/12*a*}), 2.46 – 2.37 (m, 2H, CH₂-C_{9*b*/12*b*}), 1.28 – 1.17 (m, 6 H), 1.12 – 1.06 (m, 36 H); ¹³C NMR (101 MHz, CDCl₃) δ 152.1 (C_{1/7}), 134.7 (C_{10/13}), 117.0 (C_{11/14}), 103.2 (C_{5/6}), 77.4 (C_{2/8}), 72.7 (C_{3/4}), 36.9 (C_{9/12}), 17.9, 12.5; HRMS (ESI) [M+H]⁺ calcd for C₂₃H₅₉O₄Si₂, 563.3946 found 563.3948.

(((2*R*,4*aR*,6*S*,8*aS*)-2,6-diallyl-2,4*a*,6,8*a*-tetrahydropyrano[3,2-*b*]pyran-3,7-diyl)bis(oxy))bis(tert-butyldiphenylsilane) **386**



LHMDS (1M in THF, 0.5 mL, 0.5 mmol) and Et₃N (0.28 mL, 0.20 g, 2.0 mmol) were added to a solution of TBDPSOTf (0.12 mL, 0.14 g, 0.5 mmol), diketone **210** (0.025 g, 0.1 mmol), and 4A MS in THF (1 mL) at -78 °C. The reaction was stirred for 5 h and quenched with NaHCO₃ (sat. aq.). The phases were separated and the aqueous layer was extracted with CH₂Cl₂ (3 x 2 mL). The combined organic layers were dried over MgSO₄, concentrated in vacuo, and purified by flash column chromatography (pentane/EtOAc, 10:1) to afford the product as a white solid (24 mg, 32 %). ¹H NMR (400 MHz, CDCl₃) δ 7.59 – 7.44 (m, Ar-CH), 7.30 – 7.15 (m, Ar-CH), 5.81 – 5.49 (m, 2H, CH-C_{10/13}), 4.70 – 4.60 (m, 2H, CH-C_{5/6}), 4.07 (br. s, 2H, CH-C_{2/8}), 3.72 (CH-C_{3/4}), 2.42 – 2.27 (m, 2H, CH₂-C_{9*a*/12*a*}), 2.26 – 2.14 (m, 2H, CH₂-C_{9*b*/12*b*}), 0.92 – 0.86 (m, 9H); ¹³C NMR (101 MHz, CDCl₃) δ 135.6, 134.8, 134.4, 129.7, 127.7, 116.9, 95.5, 75.7, 72.9, 36.9, 26.5

7. References

- (1) Lin, Y.-Y.; Risk, M.; Ray, S. M.; Van Engen, D.; Clardy, J.; Golik, J.; James, J. C.; Nakanishi, K. Isolation and Structure of Brevetoxin B from the “Red Tide” Dinoflagellate *Ptychodiscus Brevis* (*Gymnodinium Breve*). *J. Am. Chem. Soc.* **1981**, *103* (22), 6773–6775. <https://doi.org/10.1021/ja00412a053>.
- (2) Sittihan, S.; Jamison, T. F. Total Synthesis of the Marine Ladder Polyether Gymnocin B. *J. Am. Chem. Soc.* **2019**, *141* (28), 11239–11244. <https://doi.org/10.1021/jacs.9b04696>.
- (3) Hort, V.; Abadie, E.; Arnich, N.; Dechraoui Bottein, M.-Y.; Amzil, Z. Chemodiversity of Brevetoxins and Other Potentially Toxic Metabolites Produced by *Karenia* Spp. and Their Metabolic Products in Marine Organisms. *Mar. Drugs* **2021**, *19* (12), 656. <https://doi.org/10.3390/md19120656>.
- (4) *Effects of Florida’s Red Tide on Marine Animals | FWC*. <https://myfwc.com/research/redtide/general/marine-animals/> (accessed 2024-11-10).
- (5) Fuwa, H. Synthesis-Driven Stereochemical Assignment of Marine Polycyclic Ether Natural Products. *Mar. Drugs* **2021**, *19* (5), 257. <https://doi.org/10.3390/md19050257>.
- (6) *Fish Poisoning*. <https://www.hopkinsmedicine.org/health/conditions-and-diseases/fish-poisoning> (accessed 2024-05-29).
- (7) Traylor, J.; Murray, B. P.; Singhal, M. Ciguatera Toxicity. In *StatPearls*; StatPearls Publishing: Treasure Island (FL), 2024.
- (8) Satake, M.; Campbell, A.; Van Wagoner, R. M.; Bourdelais, A. J.; Jacocks, H.; Baden, D. G.; Wright, J. L. C. Brevisin: An Aberrant Polycyclic Ether Structure from the Dinoflagellate *Karenia Brevis* and Its Implications for Polyether Assembly. *J. Org. Chem.* **2009**, *74* (3), 989–994. <https://doi.org/10.1021/jo802183n>.
- (9) Nakanishi, K. The Chemistry of Brevetoxins: A Review. *Toxicon* **1985**, *23* (3), 473–479. [https://doi.org/10.1016/0041-0101\(85\)90031-5](https://doi.org/10.1016/0041-0101(85)90031-5).
- (10) Lee, M. S.; Repeta, D. J.; Nakanishi, K.; Zagorski, M. G. Biosynthetic Origins and Assignments of Carbon 13 NMR Peaks of Brevetoxin B. *J. Am. Chem. Soc.* **1986**, *108* (24), 7855–7856. <https://doi.org/10.1021/ja00284a072>.
- (11) Baldwin, J. E. Rules for Ring Closure. *J. Chem. Soc. Chem. Commun.* **1976**, No. 18, 734. <https://doi.org/10.1039/c39760000734>.

- (12) Baldwin, J. E.; Thomas, R. C.; Kruse, L. I.; Silberman, L. Rules for Ring Closure: Ring Formation by Conjugate Addition of Oxygen Nucleophiles. *J. Org. Chem.* **1977**, *42* (24), 3846–3852. <https://doi.org/10.1021/jo00444a011>.
- (13) Wang, L.; Parnell, A.; Williams, C.; Bakar, N. A.; Challand, M. R.; van der Kamp, M. W.; Simpson, T. J.; Race, P. R.; Crump, M. P.; Willis, C. L. A Rieske Oxygenase/Epoxide Hydrolase-Catalysed Reaction Cascade Creates Oxygen Heterocycles in Mupirocin Biosynthesis. *Nat. Catal.* **2018**, *1* (12), 968–976. <https://doi.org/10.1038/s41929-018-0183-5>.
- (14) Dechraoui, M.-Y.; Naar, J.; Pauillac, S.; Legrand, A.-M. Ciguatoxins and Brevetoxins, Neurotoxic Polyether Compounds Active on Sodium Channels. *Toxicon* **1999**, *37* (1), 125–143. [https://doi.org/10.1016/S0041-0101\(98\)00169-X](https://doi.org/10.1016/S0041-0101(98)00169-X).
- (15) European Chemicals Agency. *Guidance on the Application of the CLP Criteria: Guidance to Regulation (EC) No 1272/2008 on Classification, Labelling and Packaging (CLP) of Substances and Mixtures.*; Publications Office: LU, 2024.
- (16) *Ciguatoxins and other marine biotoxins | EFSA.* <https://www.efsa.europa.eu/en/topics/ciguatoxins-and-other-marine-biotoxins> (accessed 2024-05-03).
- (17) Chinain, M.; Gatti, C. M. i.; Darius, H. T.; Quod, J.-P.; Tester, P. A. Ciguatera Poisonings: A Global Review of Occurrences and Trends. *Harmful Algae* **2021**, *102*, 101873. <https://doi.org/10.1016/j.hal.2020.101873>.
- (18) Watkins, S. M. Neurotoxic Shellfish Poisoning. *Mar. Drugs* **2008**, *6* (3), 430–455. <https://doi.org/10.3390/md20080021>.
- (19) Gold, E. P.; Jacocks, H. M.; Bourdelais, A. J.; Baden, D. G. Brevenal, a Brevetoxin Antagonist from *Karenia Brevis*, Binds to a Previously Unreported Site on Mammalian Sodium Channels. *Harmful Algae* **2013**, *26*, 12–19. <https://doi.org/10.1016/j.hal.2013.03.001>.
- (20) Bourdelais, A. J.; Campbell, S.; Jacocks, H.; Naar, J.; Wright, J. L. C.; Carsi, J.; Baden, D. G. Brevenal Is a Natural Inhibitor of Brevetoxin Action in Sodium Channel Receptor Binding Assays. *Cell. Mol. Neurobiol.* **2004**, *24* (4), 553–563.
- (21) Alfonso, A.; de la Rosa, L.; Vieytes, M. R.; Yasumoto, T.; Botana, L. M. Yessotoxin, a Novel Phycotoxin, Activates Phosphodiesterase Activity: Effect of Yessotoxin on cAMP Levels in Human Lymphocytes. *Biochem. Pharmacol.* **2003**, *65* (2), 193–208. [https://doi.org/10.1016/S0006-2952\(02\)01454-5](https://doi.org/10.1016/S0006-2952(02)01454-5).

- (22) Suárez Korsnes, M.; Espenes, A. Yessotoxin as an Apoptotic Inducer. *Toxicon* **2011**, *57* (7), 947–958. <https://doi.org/10.1016/j.toxicon.2011.03.012>.
- (23) Beavon, I. R. G. The E-Cadherin–Catenin Complex in Tumour Metastasis: Structure, Function and Regulation. *Eur. J. Cancer* **2000**, *36* (13), 1607–1620. [https://doi.org/10.1016/S0959-8049\(00\)00158-1](https://doi.org/10.1016/S0959-8049(00)00158-1).
- (24) Ronzitti, G.; Callegari, F.; Malaguti, C.; Rossini, G. P. Selective Disruption of the E-Cadherin–Catenin System by an Algal Toxin. *Br. J. Cancer* **2004**, *90* (5), 1100–1107. <https://doi.org/10.1038/sj.bjc.6601640>.
- (25) Konishi, M.; Yang, X.; Li, B.; Fairchild, C. R.; Shimizu, Y. Highly Cytotoxic Metabolites from the Culture Supernatant of the Temperate Dinoflagellate *Protoceratium Cf. Reticulatum*. *J. Nat. Prod.* **2004**, *67* (8), 1309–1313. <https://doi.org/10.1021/np040008c>.
- (26) Tobío, A.; Alfonso, A.; Madera-Salcedo, I.; Botana, L. M.; Blank, U. Yessotoxin, a Marine Toxin, Exhibits Anti-Allergic and Anti-Tumoural Activities Inhibiting Melanoma Tumour Growth in a Preclinical Model. *PLoS ONE* **2016**, *11* (12), e0167572. <https://doi.org/10.1371/journal.pone.0167572>.
- (27) George, J.; Baden, D. G.; Gerwick, W. H.; Murray, T. F. Bidirectional Influence of Sodium Channel Activation on NMDA Receptor–Dependent Cerebrocortical Neuron Structural Plasticity. *Proc. Natl. Acad. Sci. U. S. A.* **2012**, *109* (48), 19840–19845. <https://doi.org/10.1073/pnas.1212584109>.
- (28) Nagai, H.; Murata, M.; Torigoe, K.; Satake, M.; Yasumoto, T. Gambieric Acids, New Potent Antifungal Substances with Unprecedented Polyether Structures from a Marine Dinoflagellate *Gambierdiscus Toxicus*. *J. Org. Chem.* **1992**, *57* (20), 5448–5453. <https://doi.org/10.1021/jo00046a029>.
- (29) Potera, C. Florida Red Tide Brews Up Drug Lead for Cystic Fibrosis. *Science* **2007**, *316* (5831), 1561–1562. <https://doi.org/10.1126/science.316.5831.1561>.
- (30) Nicolaou, K. C.; Prasad, C. V. C.; Somers, P. K.; Hwang, C. K. Activation of 7-Endo over 6-Exo Epoxide Openings. Synthesis of Oxepane and Tetrahydropyran Systems. *J. Am. Chem. Soc.* **1989**, *111* (14), 5335–5340. <https://doi.org/10.1021/ja00196a044>.
- (31) Yoshikawa, K.; Inoue, M.; Hirma, M. Synthesis of the LMN-Ring Fragment of the Caribbean Ciguatoxin C-CTX-1. *Tetrahedron Lett.* **2007**, *48* (12), 2177–2180. <https://doi.org/10.1016/j.tetlet.2007.01.103>.

- (32) Sakai, T.; Mizuno, S.; Sone, A.; Hori, Y.; Yamazaki, W.; Takazawa, K.; Mori, Y. Biomimetic Construction of a Syn-2,7-Dimethyloxepane Ring via 7-Endo Cyclization. *J. Org. Chem.* **2022**, *87* (1), 579–594. <https://doi.org/10.1021/acs.joc.1c02600>.
- (33) Katcher, M.; Jamison, T. F. Studies toward Brevisulcena F via Convergent Strategies for Marine Ladder Polyether Synthesis. *Tetrahedron* **2018**, *74* (11), 1111–1122. <https://doi.org/10.1016/j.tet.2018.01.039>.
- (34) Parker, R. E.; Isaacs, N. S. Mechanisms Of Epoxide Reactions. *Chem. Rev.* **1959**, *59* (4), 737–799. <https://doi.org/10.1021/cr50028a006>.
- (35) Armbrust, K. W.; Beaver, M. G.; Jamison, T. F. Rhodium-Catalyzed Endo-Selective Epoxide-Opening Cascades: Formal Synthesis of (-)-Brevisin. *J. Am. Chem. Soc.* **2015**, *137* (21), 6941–6946. <https://doi.org/10.1021/jacs.5b03570>.
- (36) Kelley, E. H.; Jamison, T. F. Synthesis of the EFG Framework of Tamulamides A and B. *Org. Lett.* **2019**, *21* (19), 8027–8030. <https://doi.org/10.1021/acs.orglett.9b03015>.
- (37) Sasaki, M.; Fuwa, H. Total Synthesis and Complete Structural Assignment of Gambieric Acid A, a Large Polycyclic Ether Marine Natural Product. *Chem. Rec.* **2014**, *14* (4), 678–703. <https://doi.org/10.1002/tcr.201402052>.
- (38) Inanaga, J.; Hirata, K.; Saeki, H.; Katsuki, T.; Yamaguchi, M. A Rapid Esterification by Means of Mixed Anhydride and Its Application to Large-Ring Lactonization. *Bull. Chem. Soc. Jpn.* **1979**, *52* (7), 1989–1993. <https://doi.org/10.1246/bcsj.52.1989>.
- (39) Sato, K.; Sasaki, M. Studies toward the Total Synthesis of Gambieric Acids, Potent Antifungal Polycyclic Ethers: Convergent Synthesis of the CDEFG-Ring System. *Org. Lett.* **2005**, *7* (12), 2441–2444. <https://doi.org/10.1021/ol050760k>.
- (40) Mori, Y.; Yaegashi, K.; Furukawa, H. A New Strategy for the Reiterative Synthesis of *Trans*-Fused Tetrahydropyrans via Alkylation of Oxiranyl Anion and 6- *Endo* Cyclization. *J. Am. Chem. Soc.* **1996**, *118* (34), 8158–8159. <https://doi.org/10.1021/ja961454s>.
- (41) Leeuwenburgh, M. A.; Litjens, R. E. J. N.; Codée, J. D. C.; Overkleeft, H. S.; van der Marel, G. A.; van Boom, J. H. Radical Cyclization of Sugar-Derived β -(Alkynyloxy)Acrylates: Synthesis of Novel Fused Ethers. *Org. Lett.* **2000**, *2* (9), 1275–1277. <https://doi.org/10.1021/ol0000408>.

- (42) Elustondo, F.; Chintalapudi, V.; Clark, J. S. A Short Sequence for the Iterative Synthesis of Fused Polyethers. *Helv. Chim. Acta* **2019**, *102* (9), e1900161. <https://doi.org/10.1002/hlca.201900161>.
- (43) Satake, M.; Shoji, M.; Oshima, Y.; Naoki, H.; Fujita, T.; Yasumoto, T. Gymnocin-A, a Cytotoxic Polyether from the Notorious Red Tide Dinoflagellate, *Gymnodinium Mikimotoi*. *Tetrahedron Lett.* **2002**, *43* (33), 5829–5832. [https://doi.org/10.1016/S0040-4039\(02\)01171-1](https://doi.org/10.1016/S0040-4039(02)01171-1).
- (44) Tsukano, C.; Sasaki, M. Total Synthesis of Gymnocin-A. *J. Am. Chem. Soc.* **2003**, *125* (47), 14294–14295. <https://doi.org/10.1021/ja038547b>.
- (45) Satake, M.; Tanaka, Y.; Ishikura, Y.; Oshima, Y.; Naoki, H.; Yasumoto, T. Gymnocin-B with the Largest Contiguous Polyether Rings from the Red Tide Dinoflagellate, *Karenia* (Formerly *Gymnodinium*) *Mikimotoi*. *Tetrahedron Lett.* **2005**, *46* (20), 3537–3540. <https://doi.org/10.1016/j.tetlet.2005.03.115>.
- (46) Dodds, D. R.; Jones, J. Bryan. Enzymes in Organic Synthesis. 38. Preparations of Enantiomerically Pure Chiral Hydroxydecalones via Stereospecific Horse Liver Alcohol Dehydrogenase Catalyzed Reductions of Decalindiones. *J. Am. Chem. Soc.* **1988**, *110* (2), 577–583. <https://doi.org/10.1021/ja00210a044>.
- (47) *What are the Limitations of Enzymes in Synthetic Organic Chemistry? - Reetz - 2016 - The Chemical Record - Wiley Online Library.* <https://onlinelibrary.wiley.com/doi/10.1002/tcr.201600040> (accessed 2024-07-17).
- (48) Ni, Y.; Holtmann, D.; Hollmann, F. How Green Is Biocatalysis? To Calculate Is To Know. *ChemCatChem* **2014**, *6*. <https://doi.org/10.1002/cctc.201300976>.
- (49) Hirao, A.; Itsuno, S.; Owa, M.; Nagami, S.; Mochizuki, H.; Niakahama, Z. S.; Yamazaki, N. Asymmetric Reduction of Aromatic Ketones with Reagents Prepared from Sodium Borohydride and Various Carboxylic Acids in the Presence of 1,2:5,6-Di-O-Isopropylidene- α -D-Glucopyranose.
- (50) Corey, E. J.; Bakshi, R. K.; Shibata, S. Highly Enantioselective Borane Reduction of Ketones Catalyzed by Chiral Oxazaborolidines. Mechanism and Synthetic Implications. *J. Am. Chem. Soc.* **1987**, *109* (18), 5551–5553. <https://doi.org/10.1021/ja00252a056>.
- (51) Spivey, A. C.; Andrews, B. I.; Brown, A. D.; Frampton, C. S. First Asymmetric Desymmetrisation of a Centrosymmetric Molecule: CBS Reduction of a 2-

- Pyridone [4 + 4]-Photodimer Derivative. *Chem. Commun.* **1999**, No. 24, 2523–2524. <https://doi.org/10.1039/a908059g>.
- (52) Holland, J. M.; Lewis, M.; Nelson, A. First Desymmetrization of a Centrosymmetric Molecule in Natural Product Synthesis: Preparation of a Key Fragment in the Synthesis of Hemibrevetoxin B. *Angew. Chem. Int. Ed Engl.* **2001**, *40* (21), 4082–4084. [https://doi.org/10.1002/1521-3773\(20011105\)40:21<4082::AID-ANIE4082>3.0.CO;2-T](https://doi.org/10.1002/1521-3773(20011105)40:21<4082::AID-ANIE4082>3.0.CO;2-T).
- (53) Prasad, A. V. K.; Shimizu, Y. The Structure of Hemibrevetoxin-B: A New Type of Toxin in the Gulf of Mexico Red Tide Organism. *J. Am. Chem. Soc.* **1989**, *111* (16), 6476–6477. <https://doi.org/10.1021/ja00198a098>.
- (54) Plakas, S. M.; Dickey, R. W. Advances in Monitoring and Toxicity Assessment of Brevetoxins in Molluscan Shellfish. *Toxicon* **2010**, *56* (2), 137–149. <https://doi.org/10.1016/j.toxicon.2009.11.007>.
- (55) Nakata, T. Synthetic Study of Marine Polycyclic Ethers: Total Synthesis of Hemibrevetoxin B. *J. Synth. Org. Chem. Jpn.* **1998**, *56* (11), 940–951.
- (56) Dodd, K.; Morton, D.; Worden, S.; Narquizian, R.; Nelson, A. Desymmetrisation of a Centrosymmetric Molecule by Carbon–Carbon Bond Formation: Asymmetric Aldol Reactions of a Centrosymmetric Dialdehyde. *Chem. – Eur. J.* **2007**, *13* (20), 5857–5861. <https://doi.org/10.1002/chem.200700277>.
- (57) Sheldrake, H. M.; Jamieson, C.; Pascu, S. I.; Burton, J. W. Synthesis of the Originally Proposed Structures of Elatenyne and an Enyne from *Laurencia Majuscula*. *Org. Biomol. Chem.* **2008**, *7* (2), 238–252. <https://doi.org/10.1039/B814953D>.
- (58) Naito, H.; Kawahara, E.; Maruta, K.; Maeda, M.; Sasaki, S. The First Total Synthesis of (+)-Bullatacin, a Potent Antitumor Annonaceous Acetogenin, and (+)-(15,24)-Bis-Epi-Bullatacin. *J. Org. Chem.* **1995**, *60* (14), 4419–4427. <https://doi.org/10.1021/jo00119a019>.
- (59) Poss, C. S.; Rychnovsky, S. D.; Schreiber, S. L. Two-Directional Chain Synthesis: An Application to the Synthesis of (+)-Mycotycin A. *J. Am. Chem. Soc.* **1993**, *115* (8), 3360–3361. <https://doi.org/10.1021/ja00061a057>.
- (60) Clark, J. S.; Popadyne, M. Stereoselective Synthesis of the I–L Fragment of the Pacific Ciguatoxins. *Toxins* **2020**, *12* (12), 740. <https://doi.org/10.3390/toxins12120740>.

- (61) Clark, J. S.; Romiti, F.; Sieng, B.; Paterson, L. C.; Stewart, A.; Chaudhury, S.; Thomas, L. H. Synthesis of the A–D Ring System of the Gambieric Acids. *Org. Lett.* **2015**, *17* (19), 4694–4697. <https://doi.org/10.1021/acs.orglett.5b02093>.
- (62) Chintalapudi, V.; Wilson, C.; Clark, J. S. Synthesis of the I–K Fused Polyether Array of CTX3C and Related Ciguatoxins by Use of a Gold-Catalyzed Cyclization Reaction. *Org. Lett.* **2024**, *26* (4), 775–780. <https://doi.org/10.1021/acs.orglett.3c03782>.
- (63) Elwood, J. Convergent and Bidirectional Strategies Towards the Total Synthesis of Hemibrevetoxin B, University of Glasgow, 2020.
- (64) Myers, E. L.; Butts, C. P.; Aggarwal, V. K. BF₃·OEt₂ and TMSOTf: A Synergistic Combination of Lewis Acids. *Chem. Commun.* **2006**, No. 42, 4434–4436. <https://doi.org/10.1039/B611333H>.
- (65) Sirol, S.; Courmarcel, J.; Mostefai, N.; Riant, O. Efficient Enantioselective Hydrosilylation of Ketones Catalyzed by Air Stable Copper Fluoride–Phosphine Complexes. *Org. Lett.* **2001**, *3* (25), 4111–4113. <https://doi.org/10.1021/ol0169170>.
- (66) Nishiyama, H.; Kondo, M.; Nakamura, T.; Itoh, K. Highly Enantioselective Hydrosilylation of Ketones with Chiral and C₂-Symmetrical Bis(Oxazolynyl)Pyridine–Rhodium Catalysts. *Organometallics* **1991**, *10* (2), 500–508. <https://doi.org/10.1021/om00048a029>.
- (67) Schroeder, M. Osmium Tetraoxide Cis Hydroxylation of Unsaturated Substrates. *Chem. Rev.* **1980**, *80* (2), 187–213. <https://doi.org/10.1021/cr60324a003>.
- (68) Meyer, S. D.; Schreiber, S. L. Acceleration of the Dess–Martin Oxidation by Water. *J. Org. Chem.* **1994**, *59* (24), 7549–7552. <https://doi.org/10.1021/jo00103a067>.
- (69) Albright, J. D.; Goldman, L. Indole Alkaloids. III.1 Oxidation of Secondary Alcohols to Ketones. *J. Org. Chem.* **1965**, *30* (4), 1107–1110. <https://doi.org/10.1021/jo01015a038>.
- (70) Brunner, H.; Kürzinger, A. Enantioselective Hydrosilylation of Ketones by Diphenylsilane with [Rh(Cod)Cl]₂/Pyridinethiazolidine Catalysts. *J. Organomet. Chem.* **1988**, No. 346, 413–424.
- (71) Nishiyama, H.; Park, S.-B.; Itoh, K. Stereoselectivity in Hydrosilylative Reduction of Substituted Cyclohexanone Derivatives with Chiral Rhodium-

- Bis(Oxazolinyl)Pyridine Catalyst. *Tetrahedron Asymmetry* **1992**, 3 (8), 1029–1034. [https://doi.org/10.1016/S0957-4166\(00\)86036-X](https://doi.org/10.1016/S0957-4166(00)86036-X).
- (72) Ojima, I.; Nihonyanagi, M.; Kogure, T.; Kumagai, M.; Horiuchi, S.; Nakatsugawa, K.; Nagai, Y. Reduction of Carbonyl Compounds via Hydrosilylation: I. Hydrosilylation of Carbonyl Compounds Catalyzed by Tris(Triphenylphosphine)Chlororhodium. *J. Organomet. Chem.* **1975**, 94 (3), 449–461. [https://doi.org/10.1016/S0022-328X\(00\)86954-5](https://doi.org/10.1016/S0022-328X(00)86954-5).
- (73) Zheng, G. Z.; Chan, T. H. Regiocontrolled Hydrosilation of .Alpha.,.Beta.-Unsaturated Carbonyl Compounds Catalyzed by Hydridotetrakis(Triphenylphosphine)Rhodium(I). *Organometallics* **1995**, 14 (1), 70–79. <https://doi.org/10.1021/om00001a015>.
- (74) Schneider, N.; Finger, M.; Haferkemper, C.; Bellemin-Lapponnaz, S.; Hofmann, P.; Gade, L. H. Metal Silylenes Generated by Double Silicon–Hydrogen Activation: Key Intermediates in the Rhodium-Catalyzed Hydrosilylation of Ketones. *Angew. Chem. Int. Ed.* **2009**, 48 (9), 1609–1613. <https://doi.org/10.1002/anie.200804993>.
- (75) Duckett, S. B.; Perutz, R. N. Mechanism of Homogeneous Hydrosilation of Alkenes by (η^5 -Cyclopentadienyl)Rhodium. *Organometallics* **1992**, 11 (1), 90–98. <https://doi.org/10.1021/om00037a022>.
- (76) Nagashima, H.; Tatebe, K.; Ishibashi, T.; Nakaoka, A.; Sakakibara, J.; Itoh, K. Unusual Rate Enhancement in the RhCl(PPh₃)₃-Catalyzed Hydrosilylation by Organosilanes Having Two Si-H Groups at Appropriate Distances: Mechanistic Aspects. *Organometallics* **1995**, 14 (6), 2868–2879. <https://doi.org/10.1021/om00006a036>.
- (77) Woolford, S. A Bi-Directional Centrosymmetric Approach Towards the Total Synthesis of Marine Polyether Natural Products, University of Glasgow, 2023.
- (78) Barnett, K. W.; Beach, D. L.; Garin, D. L.; Kaempfe, L. A. Effect of Oxygen on Rhodium-Catalyzed Ring Openings of Bicycloalkenes. *J. Am. Chem. Soc.* **1974**, 96 (22), 7127–7128. <https://doi.org/10.1021/ja00829a065>.
- (79) Beach, D. L.; Garin, D. L.; Kaempfe, L. A.; Barnett, K. W. Rhodium Catalyzed Reactions of Bicyclic Hydrocarbons. Products, Mechanism, and the Nature of the Catalyst. *J. Organomet. Chem.* **1977**, 142 (2), 211–223. [https://doi.org/10.1016/S0022-328X\(00\)94344-4](https://doi.org/10.1016/S0022-328X(00)94344-4).

- (80) da Rosa, R. G.; de Campos, J. D. R.; Buffon, R. The Effect of Water on the Rhodium-Catalyzed Carbonylation of Isopropylallylamine. *J. Mol. Catal. Chem.* **2000**, *153* (1), 19–24. [https://doi.org/10.1016/S1381-1169\(99\)00347-7](https://doi.org/10.1016/S1381-1169(99)00347-7).
- (81) Majumder, U.; Cox, J. M.; Johnson, H. W. B.; Rainier, J. D. Total Synthesis of Gambierol: The Generation of the A–C and F–H Subunits by Using a C-Glycoside Centered Strategy. *Chem. – Eur. J.* **2006**, *12* (6), 1736–1746. <https://doi.org/10.1002/chem.200500993>.
- (82) Moyano, A.; Charbonnier, F.; Greene, A. E. Simple Preparation of Chiral Acetylenic Ethers. *J. Org. Chem.* **1987**, *52* (13), 2919–2922. <https://doi.org/10.1021/jo00389a048>.
- (83) Mamalis, D. Methodology Studies on One and Two Carbon Ring Expansion on Polyether Polycyclic Natural Products. MRes Thesis, University of Glasgow, 2020.
- (84) Popadyne, M.; Gibbard, H.; Clark, J. S. Bidirectional Synthesis of the IJK Fragment of Ciguatoxin CTX3C by Sequential Double Ring-Closing Metathesis and Tsuji–Trost Allylation. *Org. Lett.* **2020**, *22* (9), 3734–3738. <https://doi.org/10.1021/acs.orglett.0c01238>.
- (85) Toma, T.; Shimokawa, J.; Fukuyama, T. N,N'-Ditosylhydrazine: A Convenient Reagent for Facile Synthesis of Diazoacetates. *Org. Lett.* **2007**, *9* (16), 3195–3197. <https://doi.org/10.1021/ol701432k>.
- (86) House, H. O.; Blankley, C. J. Preparation and Decomposition of Unsaturated Esters of Diazoacetic Acid. *J. Org. Chem.* **1968**, *33* (1), 53–60. <https://doi.org/10.1021/jo01265a011>.
- (87) Corey, E. J.; Myers, A. G. Efficient Synthesis and Intramolecular Cyclopropanation of Unsaturated Diazoacetic Esters. *Tetrahedron Lett.* **1984**, *25* (33), 3559–3562. [https://doi.org/10.1016/S0040-4039\(01\)91075-5](https://doi.org/10.1016/S0040-4039(01)91075-5).
- (88) Regitz, M. New Methods of Preparative Organic Chemistry. Transfer of Diazo Groups. *Angew. Chem. Int. Ed. Engl.* **1967**, *6* (9), 733–749. <https://doi.org/10.1002/anie.196707331>.
- (89) Lin, L.-Z.; Che, Y.-Y.; Bai, P.-B.; Feng, C. Sulfinate-Engaged Nucleophilic Addition Induced Allylic Alkylation of Allenates. *Org. Lett.* **2019**, *21* (18), 7424–7429. <https://doi.org/10.1021/acs.orglett.9b02728>.
- (90) *Carbene-Mediated Functionalization of the Anomeric C–H Bond of Carbohydrates: Scope and Limitations - Boultadakis-Arapinis - 2013 - Chemistry*

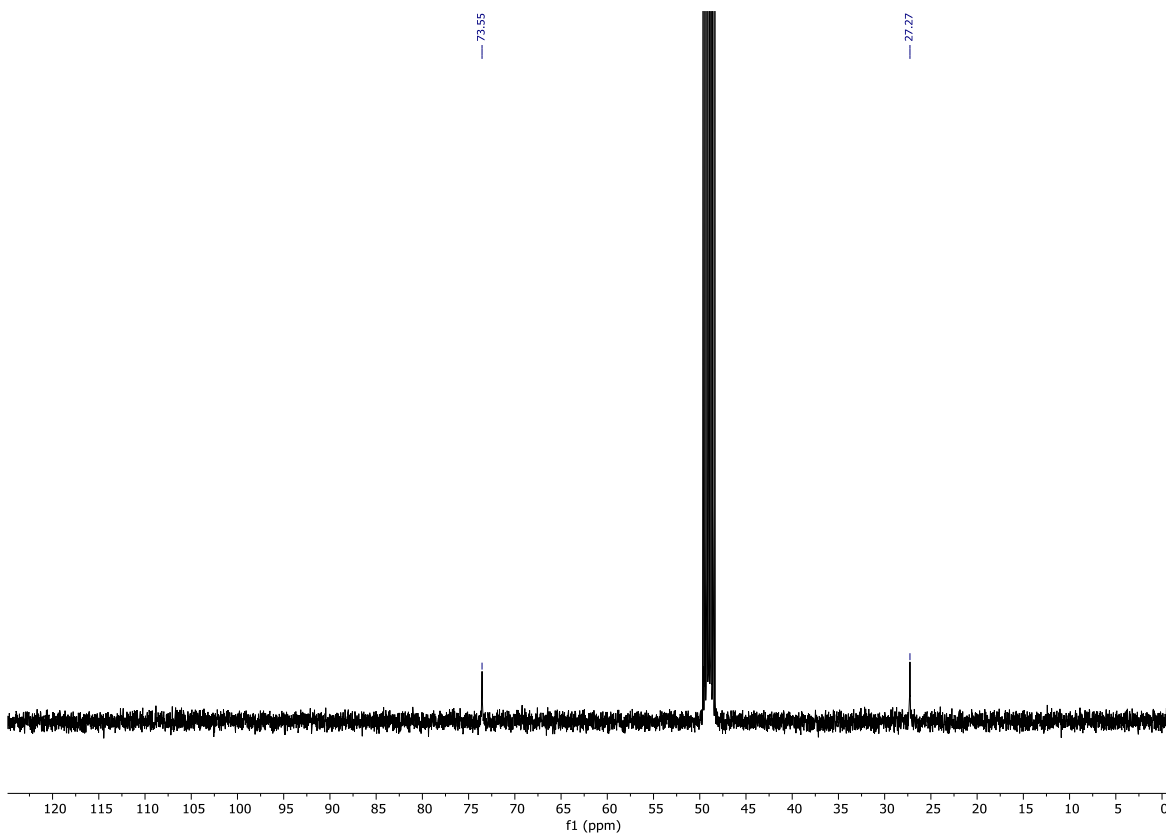
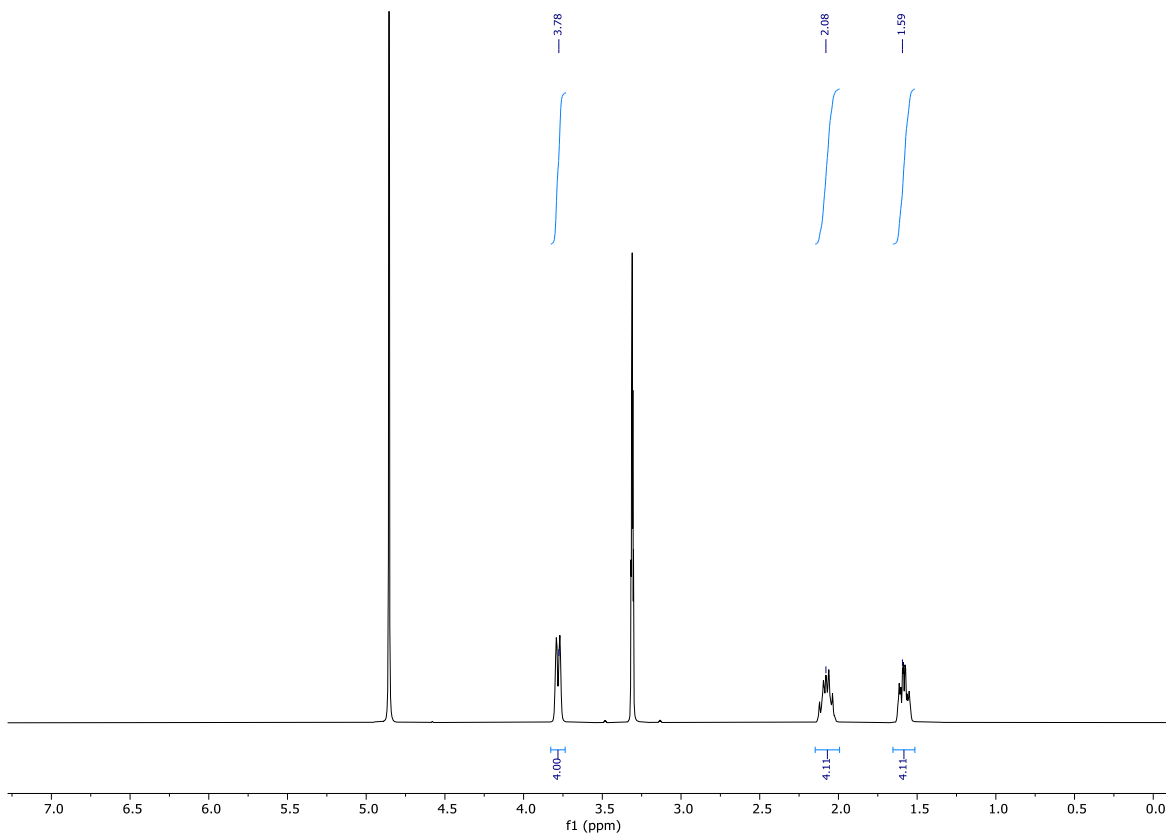
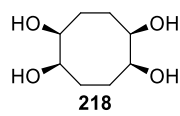
- *A European Journal - Wiley Online Library*. <https://chemistry-europe.onlinelibrary.wiley.com/doi/10.1002/chem.201203725> (accessed 2024-09-10).
- (91) Wong, F. M.; Wang, J.; Hengge, A. C.; Wu, W. Mechanism of Rhodium-Catalyzed Carbene Formation from Diazo Compounds. *Org. Lett.* **2007**, *9* (9), 1663–1665. <https://doi.org/10.1021/ol070345n>.
- (92) Andrews, M. A.; Gould, G. L.; Klaeren, S. A. Decarbonylation of Unprotected Aldose Sugars by Chlorotris(Triphenylphosphine)Rhodium(I). A New Descent of Series Approach to Alditols, Deoxyalditols, and Glycosylalditols. *J. Org. Chem.* **1989**, *54* (22), 5257–5264. <https://doi.org/10.1021/jo00283a017>.
- (93) Boultadakis-Arapinis, M.; Lescot, C.; Micouin, L.; Lecourt, T. Gram-Scale Quaternarization of the Anomeric Position of Carbohydrates: Dramatic Effects of Molecular Sieves on Rhodium(II)-Mediated Decomposition of Diazo Sugars. *Synthesis* **2012**, *44* (24), 3731–3734. <https://doi.org/10.1055/s-0032-1317013>.
- (94) d'Angelo, J.; Desmaële, D.; Dumas, F.; Guingant, A. The Asymmetric Michael Addition Reactions Using Chiral Imines. *Tetrahedron Asymmetry* **1992**, *3* (4), 459–505. [https://doi.org/10.1016/S0957-4166\(00\)80251-7](https://doi.org/10.1016/S0957-4166(00)80251-7).
- (95) Desmaële, D.; Pain, G.; d'Angelo, J. Enantioselective Synthesis of 2,2-Dialkyltetrahydropyran-3-Ones via the Asymmetric Michael Addition Reaction Using Chiral Imines. *Tetrahedron Asymmetry* **1992**, *3* (7), 863–866. [https://doi.org/10.1016/S0957-4166\(00\)82185-0](https://doi.org/10.1016/S0957-4166(00)82185-0).
- (96) Buchner, E.; Curtius, Th. Synthese von Ketonensäureäthern Aus Aldehyden Und Diazoessigäther. *Berichte Dtsch. Chem. Ges.* **1885**, *18* (2), 2371–2377. <https://doi.org/10.1002/cber.188501802118>.
- (97) Schlotterbeck, F. Umwandlung von Aldehyden in Ketone Durch Diazomethan. (Erwiderung an Hrn. H. Meyer). *Berichte Dtsch. Chem. Ges.* **1907**, *40* (2), 1826–1827. <https://doi.org/10.1002/cber.19070400285>.
- (98) Mosettig, E.; Burger, A. Ring Enlargement with Diazomethane in the Hydroaromatic Series. *J. Am. Chem. Soc.* **1930**, *52* (8), 3456–3463. <https://doi.org/10.1021/ja01371a070>.
- (99) Sakai, T.; Ito, S.; Furuta, H.; Kawahara, Y.; Mori, Y. Mechanism of the Regio- and Diastereoselective Ring Expansion Reaction Using Trimethylsilyldiazomethane. *Org. Lett.* **2012**, *14* (17), 4564–4567. <https://doi.org/10.1021/ol302032w>.

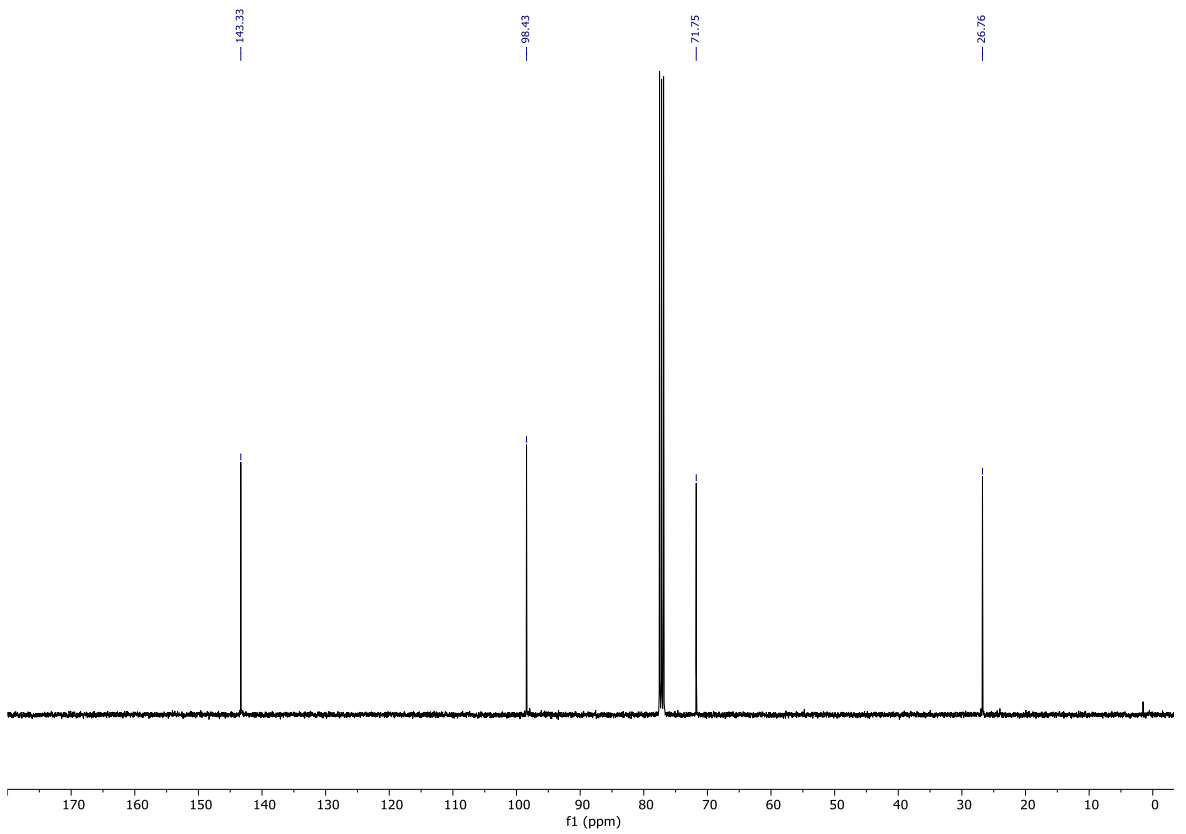
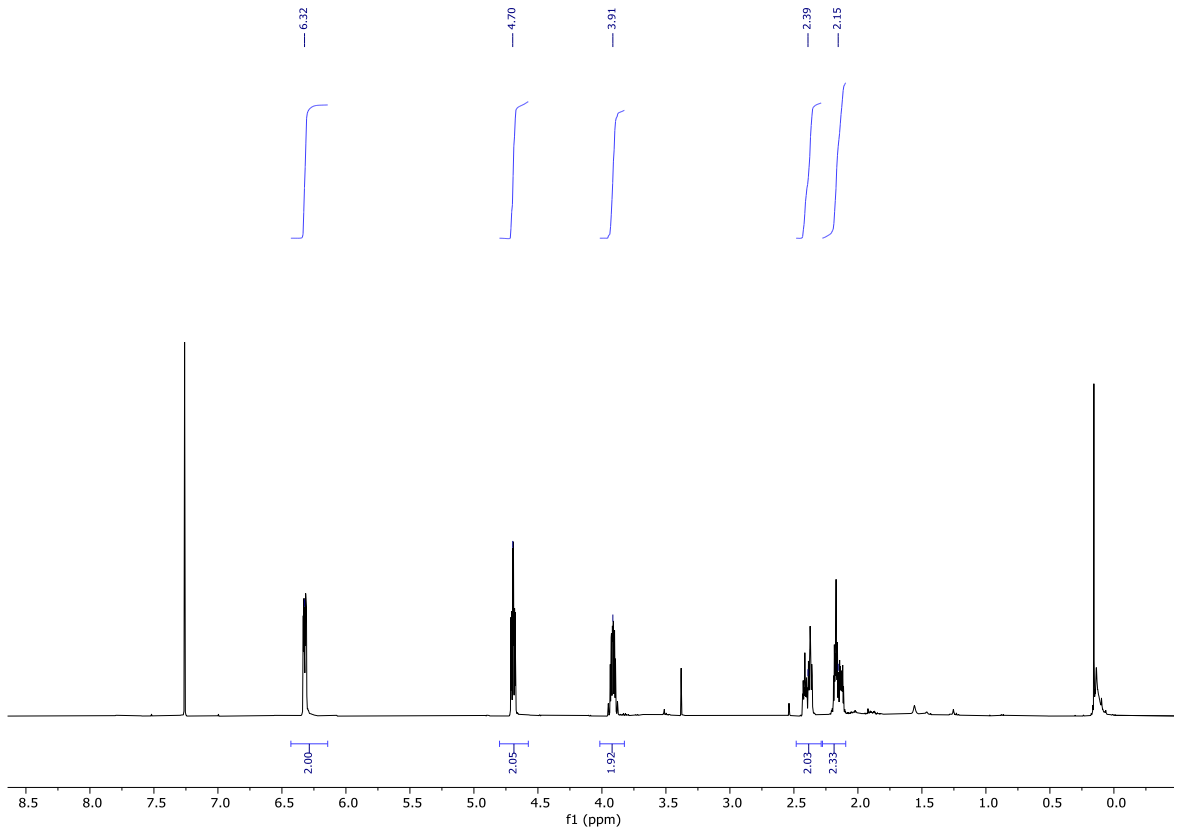
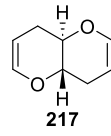
- (100) Gutsche, C. D. The Reaction of Diazomethane and Its Derivatives with Aldehydes and Ketones. In *Organic Reactions*; Denmark, S. E., Ed.; Wiley, 2011; pp 364–430. <https://doi.org/10.1002/0471264180.or008.08>.
- (101) Gutsche, C. David. Ring Enlargements. I. The Ring Enlargement of 2-Chlorocyclohexanone and 2-Phenylcyclohexanone. *J. Am. Chem. Soc.* **1949**, *71* (10), 3513–3517. <https://doi.org/10.1021/ja01178a075>.
- (102) Sakai, T.; Sugimoto, A.; Mori, Y. A Convergent Strategy for the Synthesis of Polycyclic Ethers by Using Oxiranyl Anions. *Org. Lett.* **2011**, *13* (21), 5850–5853. <https://doi.org/10.1021/ol202467z>.
- (103) Mori, Y.; Yaegashi, K.; Furukawa, H. Formal Total Synthesis of Hemibrevetoxin B by an Oxiranyl Anion Strategy. *J. Org. Chem.* **1998**, *63* (18), 6200–6209. <https://doi.org/10.1021/jo980320p>.
- (104) Furuta, H.; Hasegawa, Y.; Mori, Y. Total Synthesis of Gambierol. *Org. Lett.* **2009**, *11* (19), 4382–4385. <https://doi.org/10.1021/ol9017408>.
- (105) Brook, A. G. Molecular Rearrangements of Organosilicon Compounds. *Acc. Chem. Res.* **1974**, *7* (3), 77–84. <https://doi.org/10.1021/ar50075a003>.
- (106) Zhong, L.-P.; Feng, R.; Wang, J.-J.; Li, C.-C. Asymmetric Total Synthesis of Twin Bufogargarizins A and B. *J. Am. Chem. Soc.* **2023**, *145* (4), 2098–2103. <https://doi.org/10.1021/jacs.2c13494>.
- (107) Ito, Y.; Hirao, T.; Saegusa, T. Synthesis of .Alpha.,.Beta.-Unsaturated Carbonyl Compounds by Palladium(II)-Catalyzed Dehydrosilylation of Silyl Enol Ethers. *J. Org. Chem.* **1978**, *43* (5), 1011–1013. <https://doi.org/10.1021/jo00399a052>.
- (108) Hashimoto, T.; Naganawa, Y.; Maruoka, K. Desymmetrizing Asymmetric Ring Expansion of Cyclohexanones with α -Diazoacetates Catalyzed by Chiral Aluminum Lewis Acid. *J. Am. Chem. Soc.* **2011**, *133* (23), 8834–8837. <https://doi.org/10.1021/ja202070j>.
- (109) Han, M.-Y.; Xie, X.; Zhou, D.; Li, P.; Wang, L. Organocatalyzed Direct Aldol Reaction of Silyl Glyoxylates for the Synthesis of α -Hydroxysilanes. *Org. Lett.* **2017**, *19* (9), 2282–2285. <https://doi.org/10.1021/acs.orglett.7b00811>.
- (110) Brannock, K. C.; Burpitt, R. D.; Goodlett, V. W.; Thweatt, J. G. Enamine Chemistry. VI. Reactions with Propiolates¹. *J. Org. Chem.* **1964**, *29* (4), 818–823. <https://doi.org/10.1021/jo01027a011>.

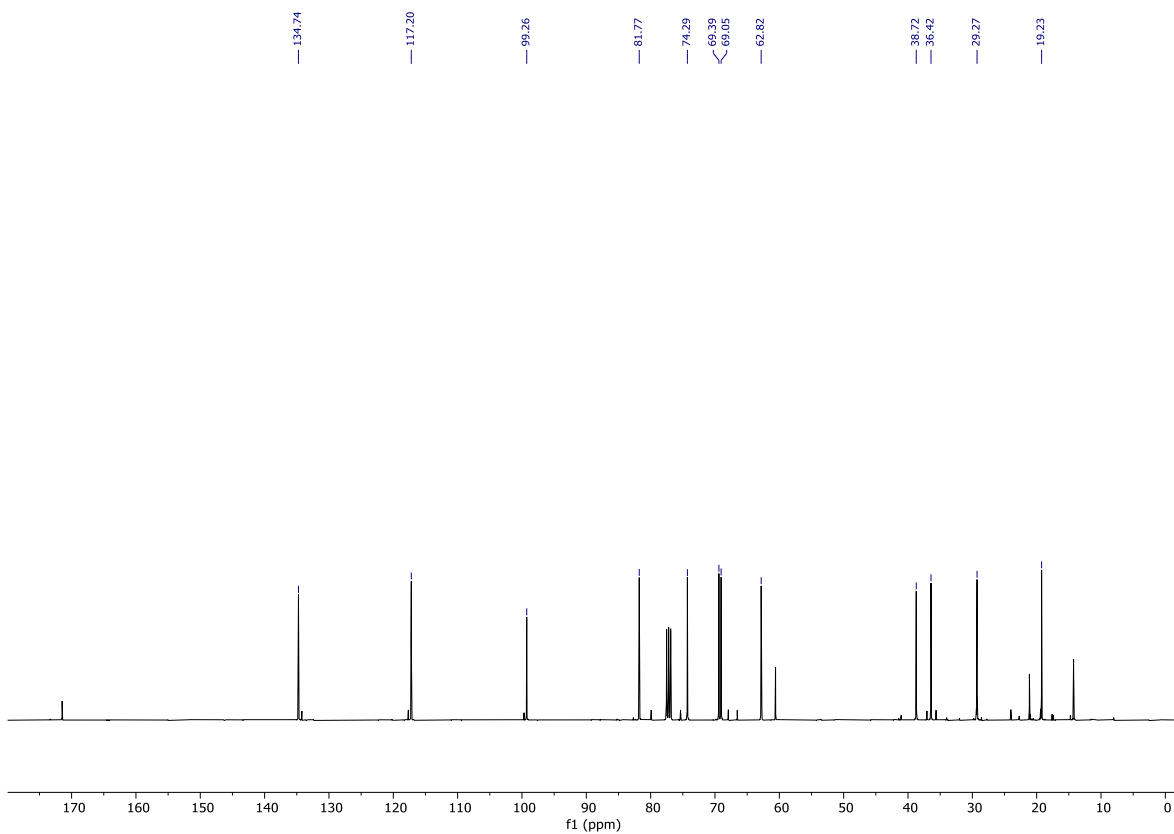
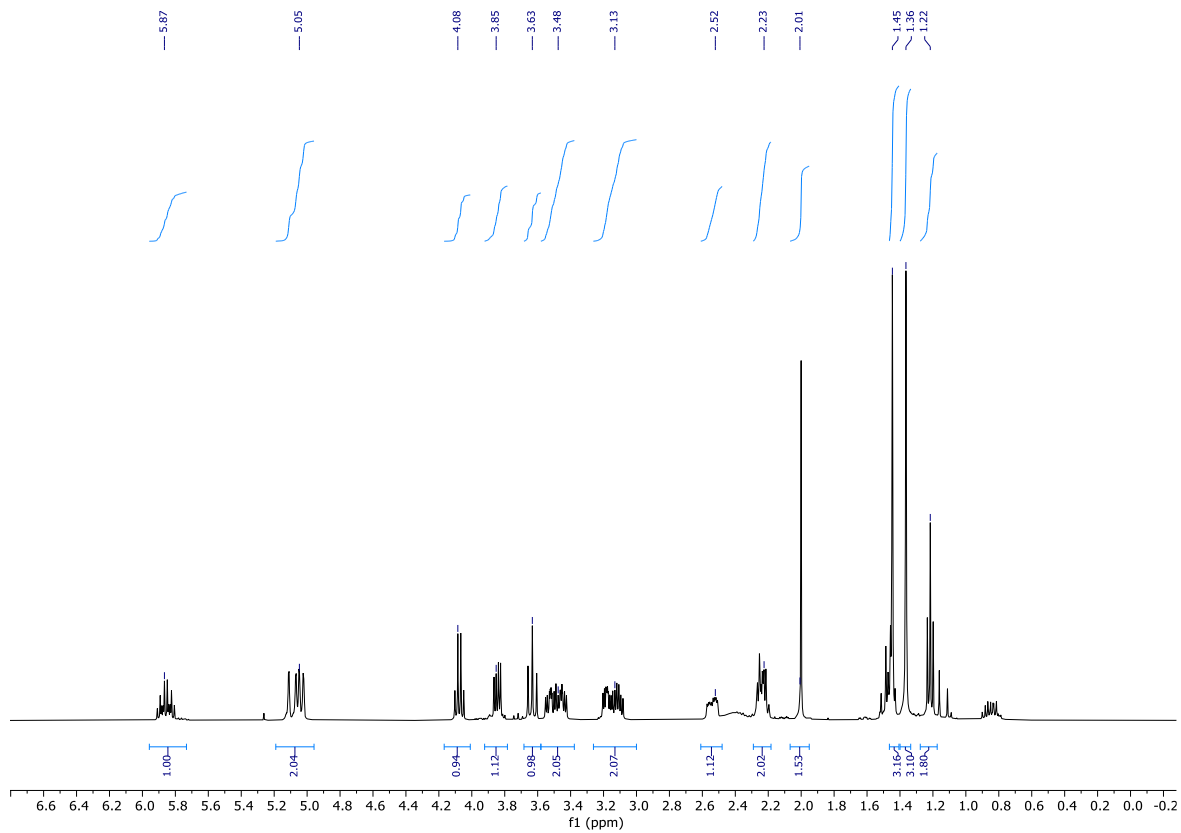
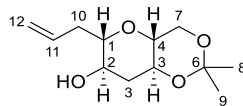
- (111) Clark, R. D.; Untch, K. G. [2 + 2] Cycloaddition of Ethyl Propiolate and Silyl Enol Ethers. *J. Org. Chem.* **1979**, *44* (2), 248–253. <https://doi.org/10.1021/jo01316a020>.
- (112) Mislin, G.; Miesch, M. Synthesis of Polyfunctionalized Bicyclo[5.3.1]Undecadiene Ring Systems Using a Two-Carbon Ring-Expansion of Cyclobutene Intermediates. *Eur. J. Org. Chem.* **2001**, *2001* (9), 1753–1759. [https://doi.org/10.1002/1099-0690\(200105\)2001:9<1753::AID-EJOC1753>3.0.CO;2-E](https://doi.org/10.1002/1099-0690(200105)2001:9<1753::AID-EJOC1753>3.0.CO;2-E).
- (113) Moebius, D. C.; Kingsbury, J. S. Catalytic Homologation of Cycloalkanones with Substituted Diazomethanes. Mild and Efficient Single-Step Access to α -Tertiary and α -Quaternary Carbonyl Compounds. *J. Am. Chem. Soc.* **2009**, *131* (3), 878–879. <https://doi.org/10.1021/ja809220j>.
- (114) Zhao, K.; Yamashita, K.; Carpenter, J. E.; Sherwood, T. C.; Ewing, W. R.; Cheng, P. T. W.; Knowles, R. R. Catalytic Ring Expansions of Cyclic Alcohols Enabled by Proton-Coupled Electron Transfer. *J. Am. Chem. Soc.* **2019**, *141* (22), 8752–8757. <https://doi.org/10.1021/jacs.9b03973>.
- (115) Wu, T. R.; Shen, L.; Chong, J. M. Asymmetric Allylboration of Aldehydes and Ketones Using 3,3'-Disubstitutedbinaphthol-Modified Boronates. *Org. Lett.* **2004**, *6* (16), 2701–2704. <https://doi.org/10.1021/ol0490882>.
- (116) Simonin, C.; Awale, M.; Brand, M.; van Deursen, R.; Schwartz, J.; Fine, M.; Kovacs, G.; Häfliger, P.; Gyimesi, G.; Sithampari, A.; Charles, R.-P.; Hediger, M. A.; Reymond, J.-L. Optimization of TRPV6 Calcium Channel Inhibitors Using a 3D Ligand-Based Virtual Screening Method. *Angew. Chem. Int. Ed.* **2015**, *54* (49), 14748–14752. <https://doi.org/10.1002/anie.201507320>.
- (117) Zhao, J.; Li, P.; Xu, Y.; Shi, Y.; Li, F. Nickel-Catalyzed Transformation of Diazoacetates to Alkyl Radicals Using Alcohol as a Hydrogen Source. *Org. Lett.* **2019**, *21* (23), 9386–9390. <https://doi.org/10.1021/acs.orglett.9b03610>.
- (118) Loy, N. S. Y.; Choi, S.; Kim, S.; Park, C.-M. Synthesis of Pyrroles and Oxazoles Based on Gold α -Imino Carbene Complexes.
- (119) Kang, T.; Cao, W.; Hou, L.; Tang, Q.; Zou, S.; Liu, X.; Feng, X. Chiral Zinc(II)-Catalyzed Enantioselective Tandem α -Alkenyl Addition/Proton Shift Reaction of Silyl Enol Ethers with Ketimines. *Angew. Chem. Int. Ed.* **2019**, *58* (8), 2464–2468. <https://doi.org/10.1002/anie.201810961>.

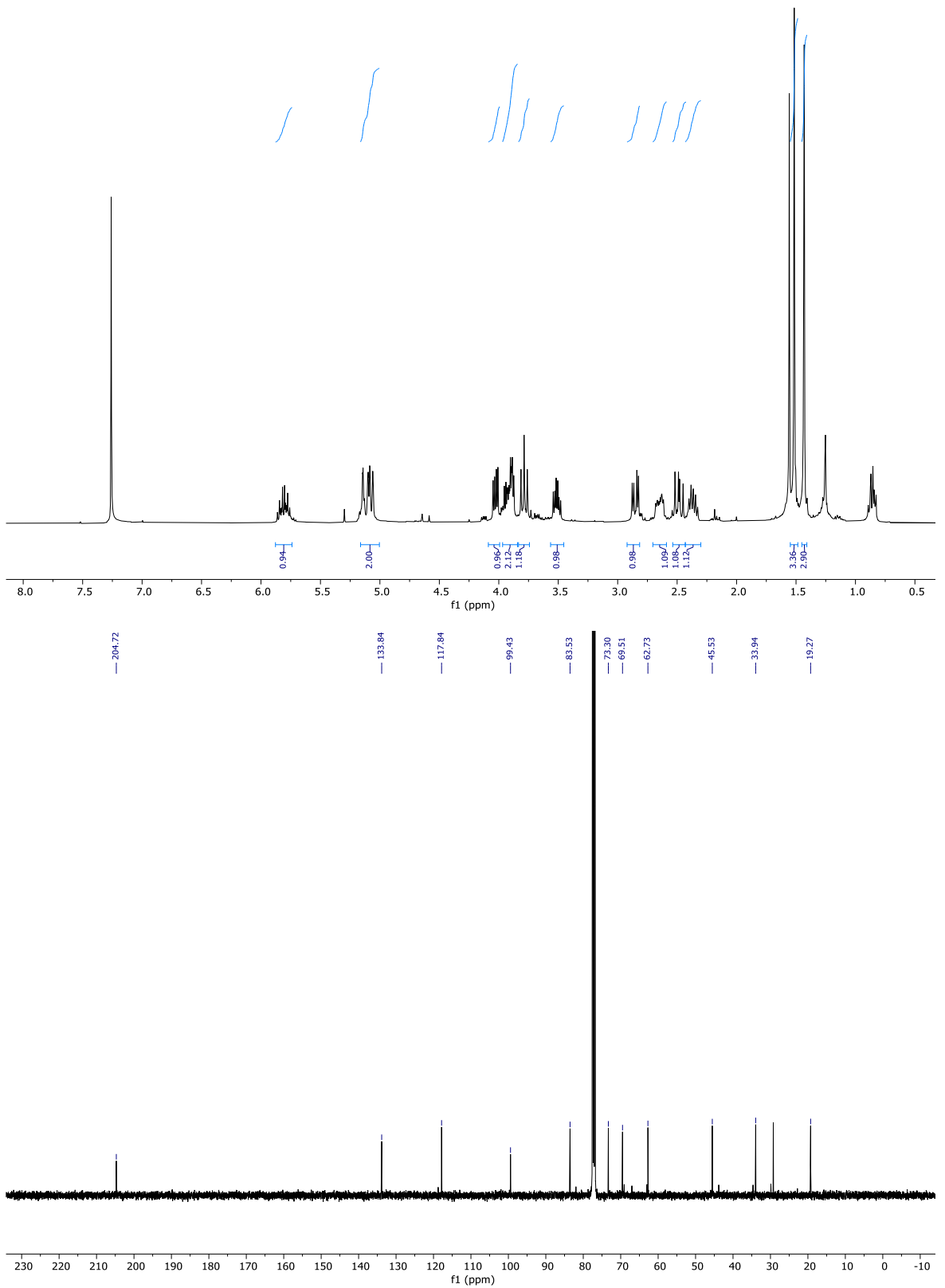
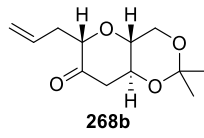
8. Appendix

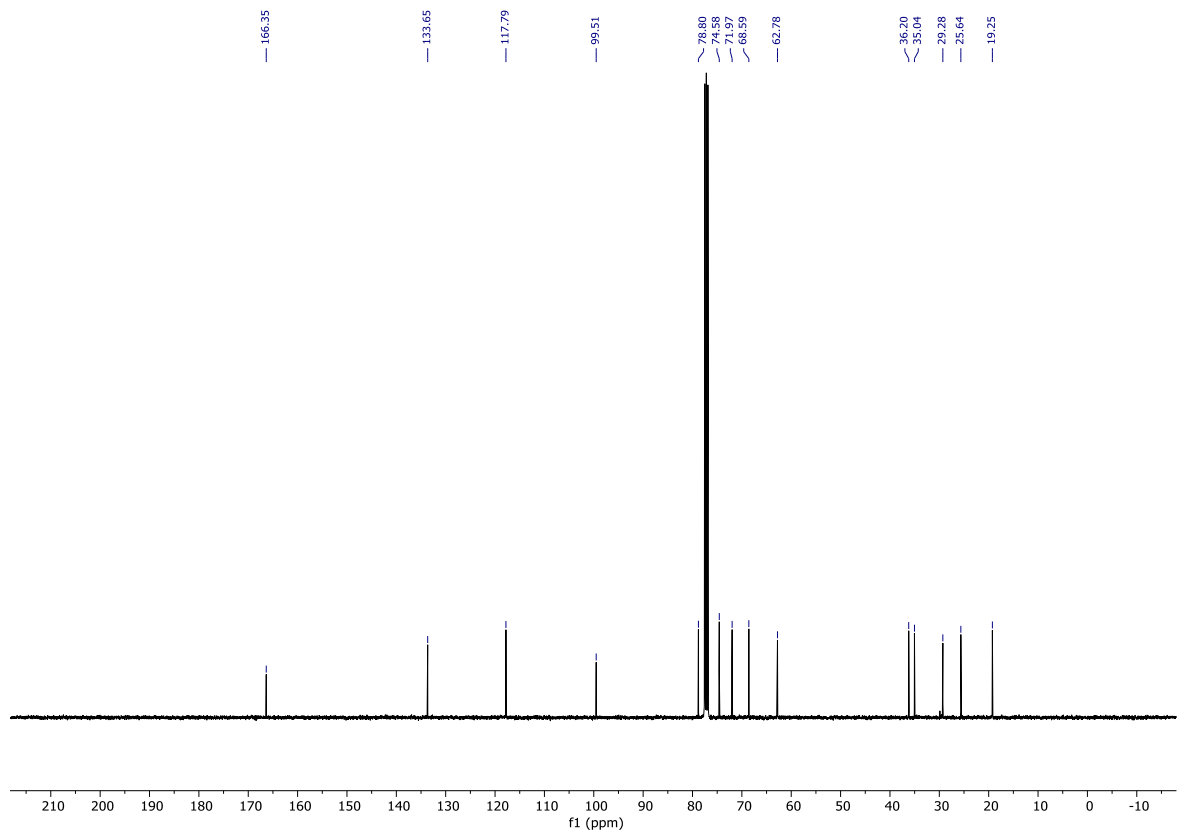
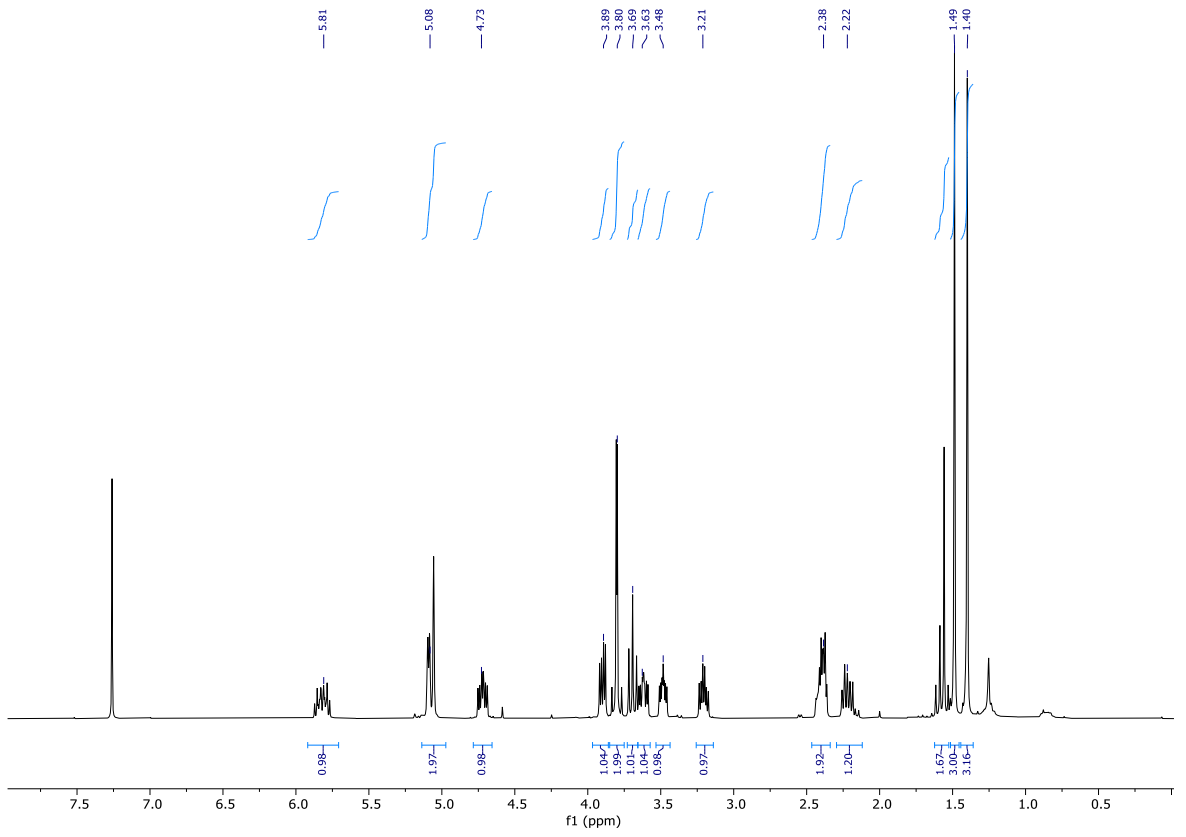
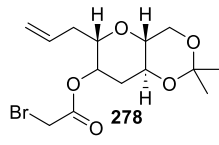
8.1 ^1H and ^{13}C NMR Data

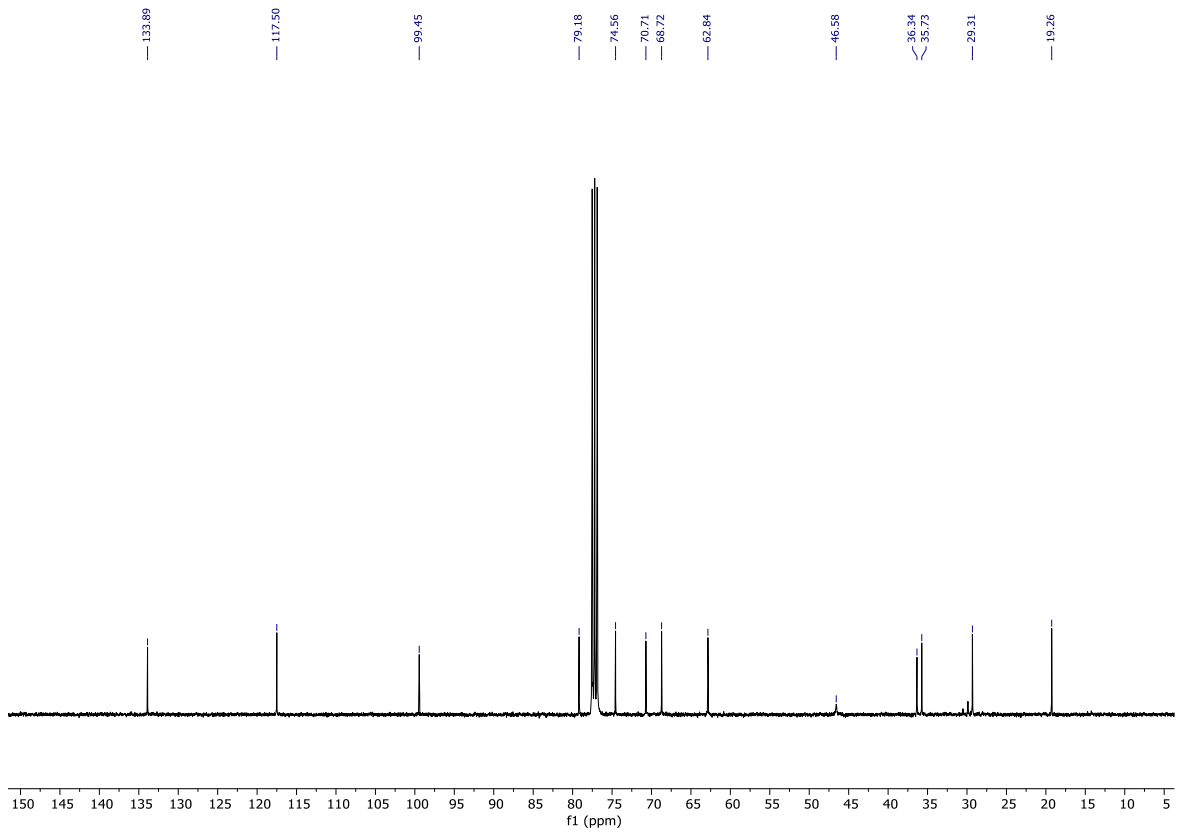
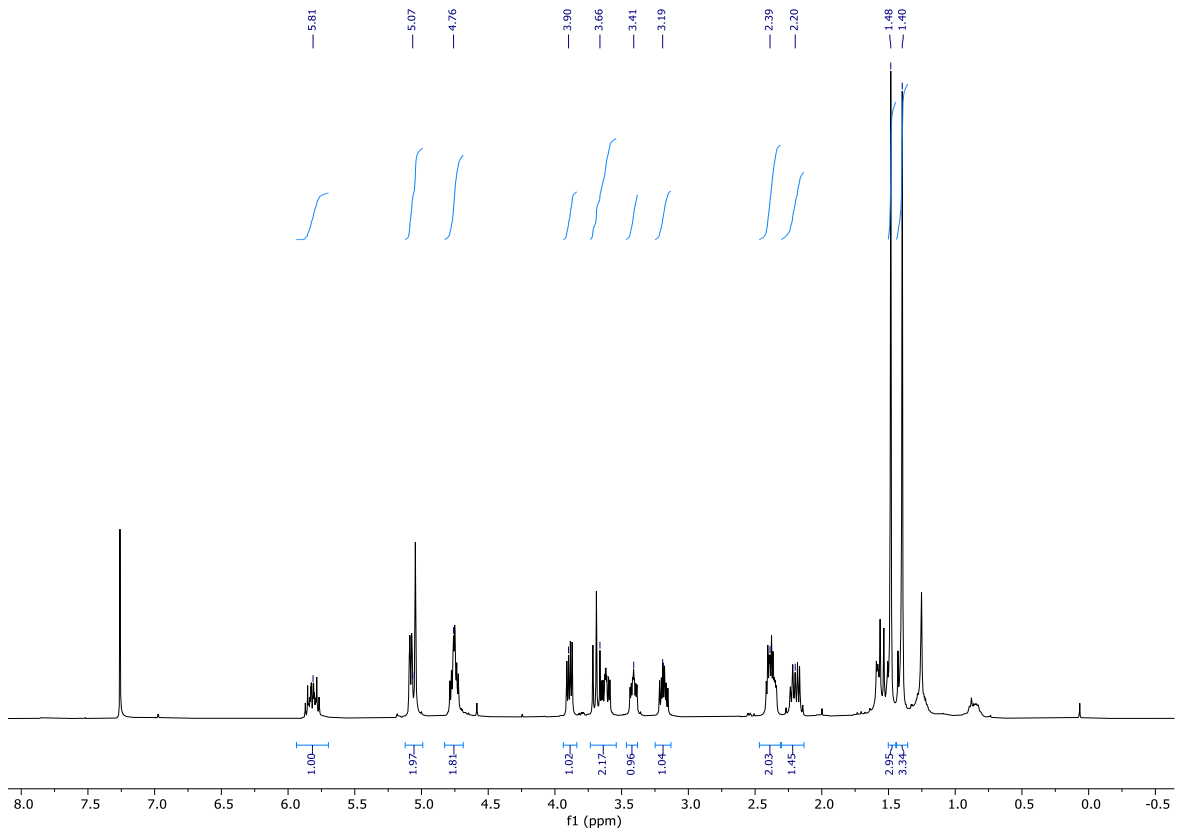
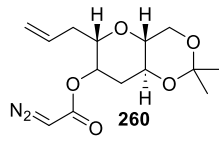


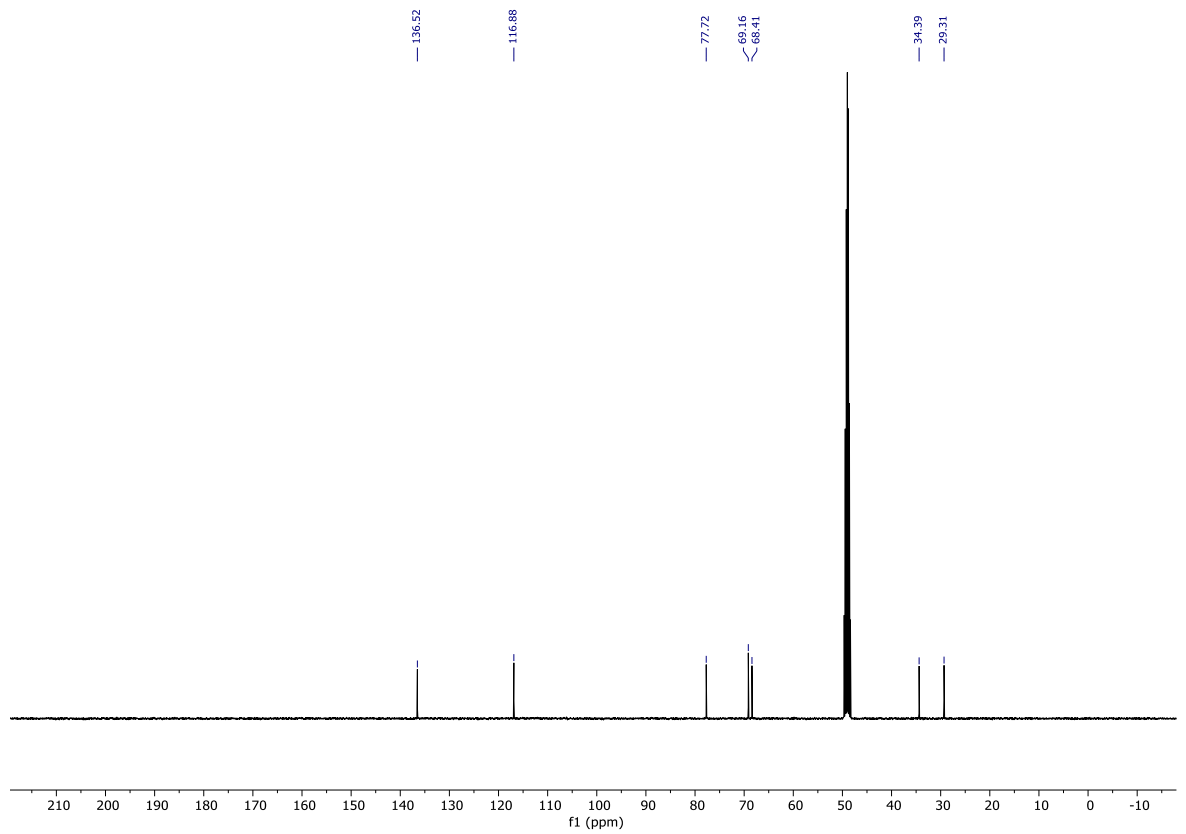
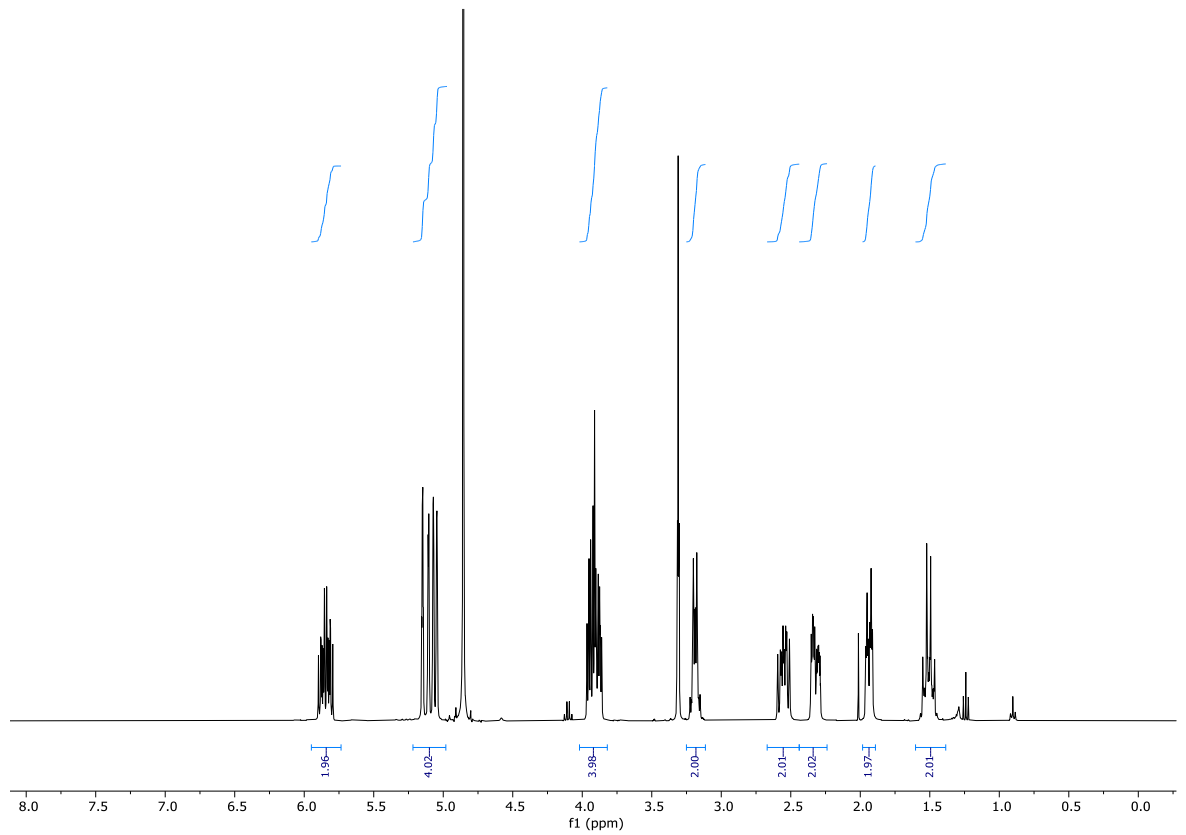
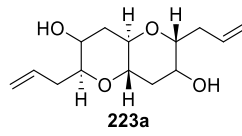


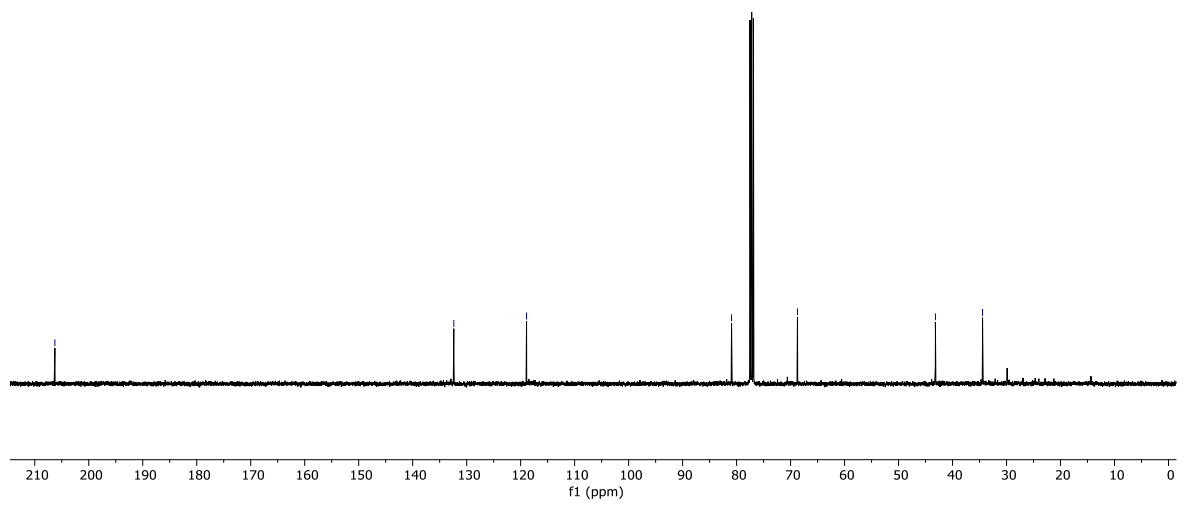
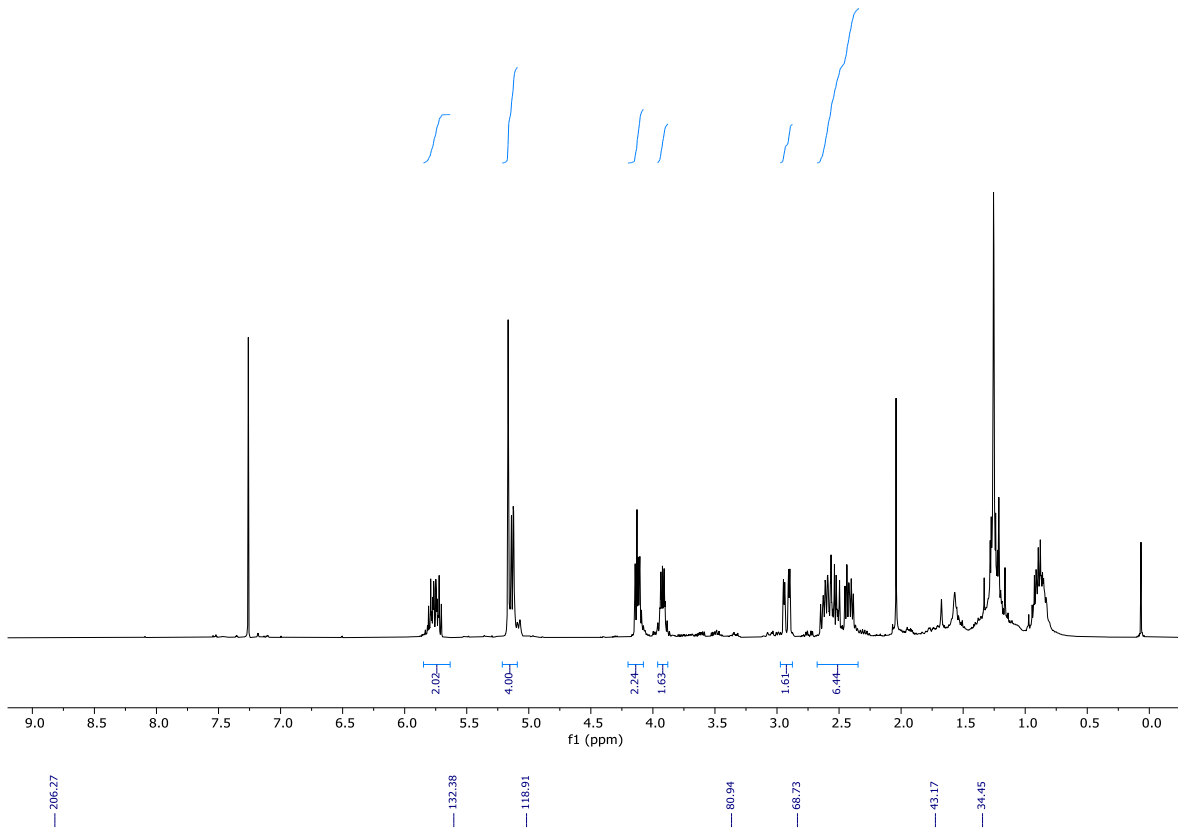
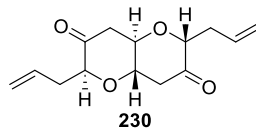


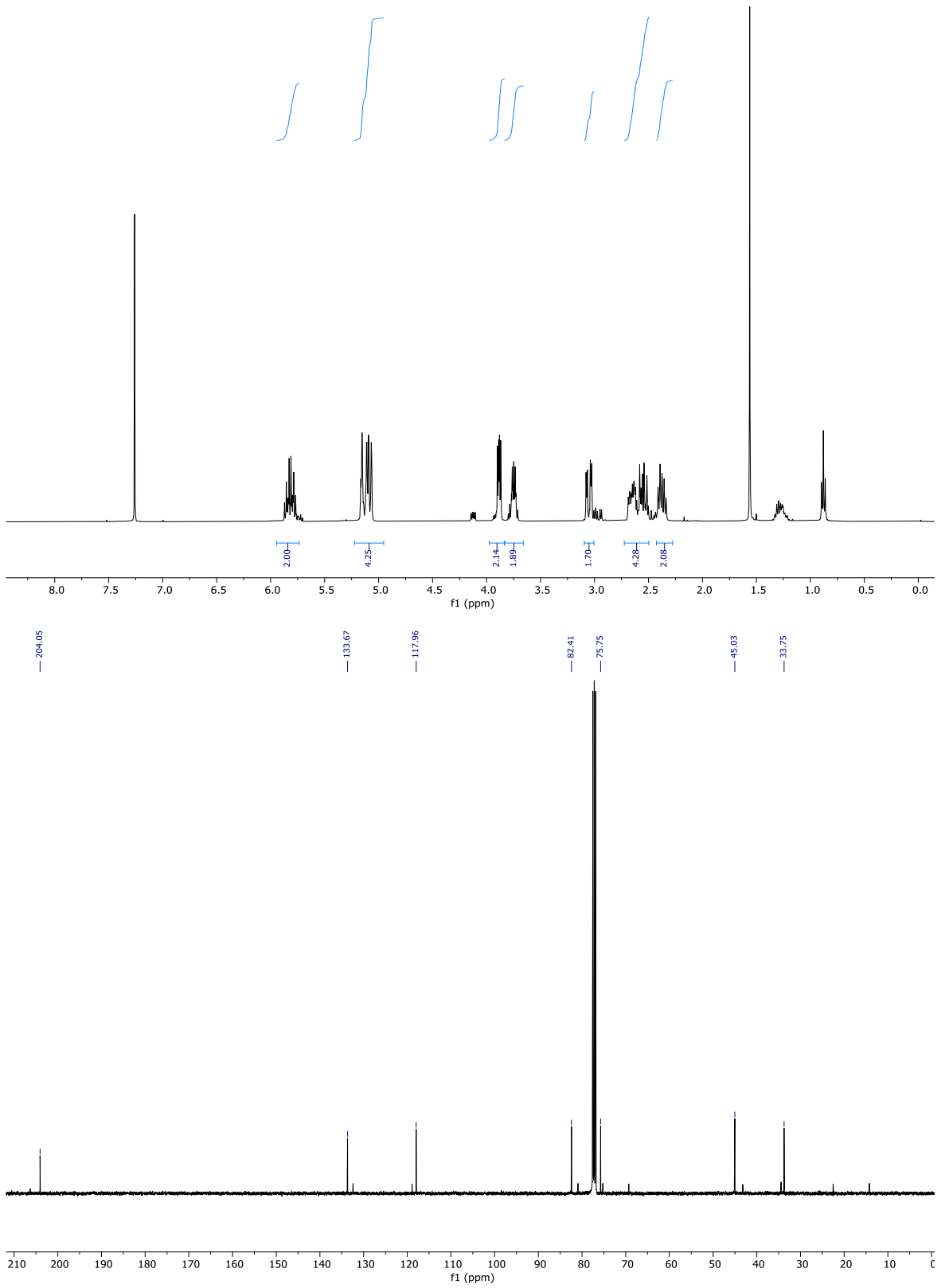
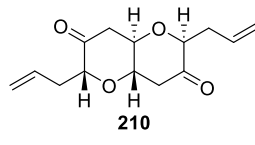


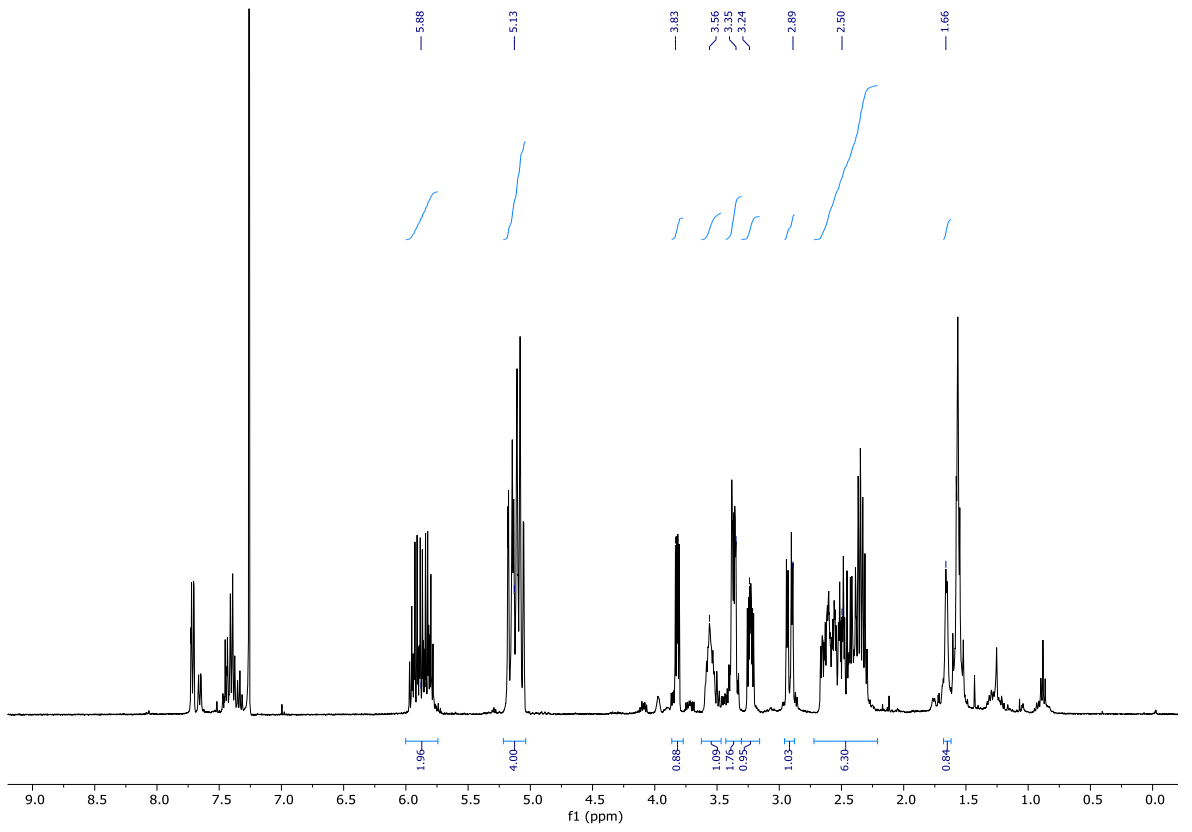
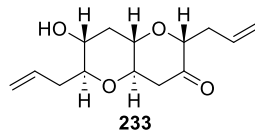


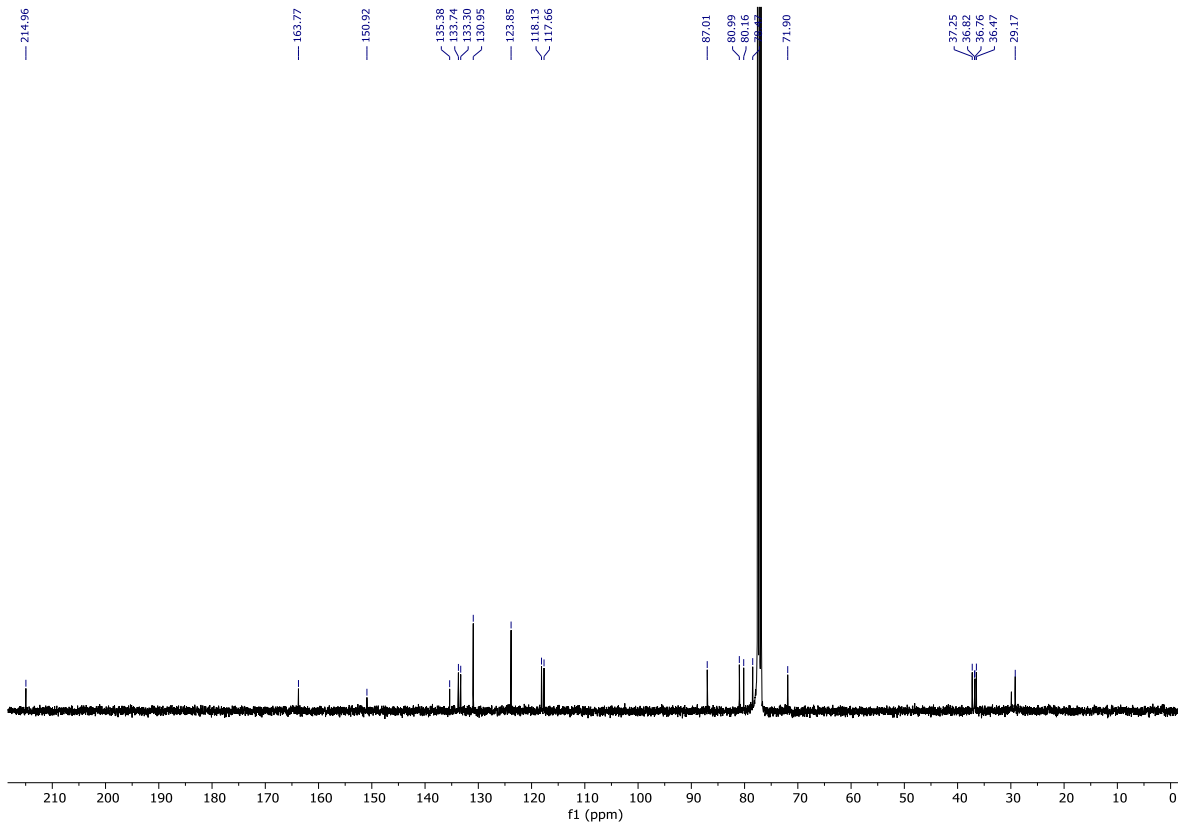
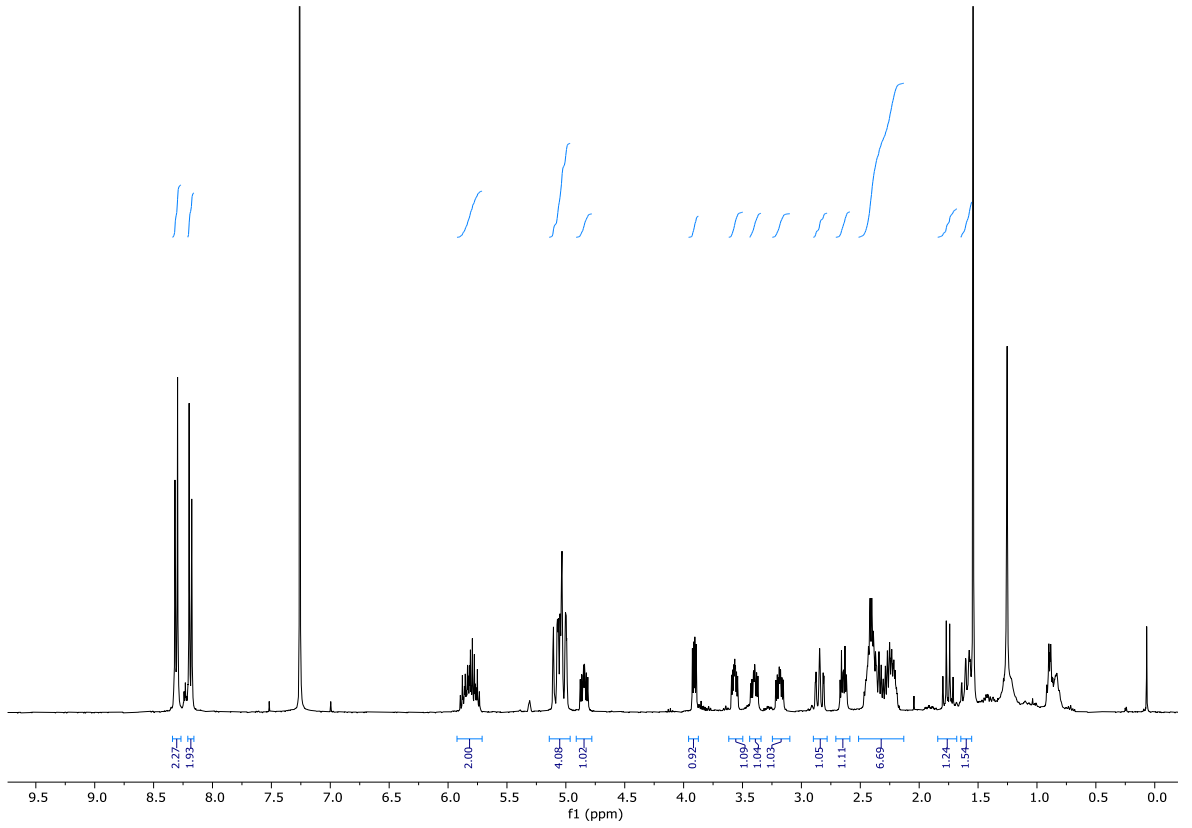
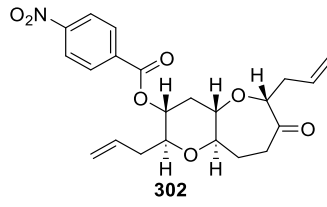


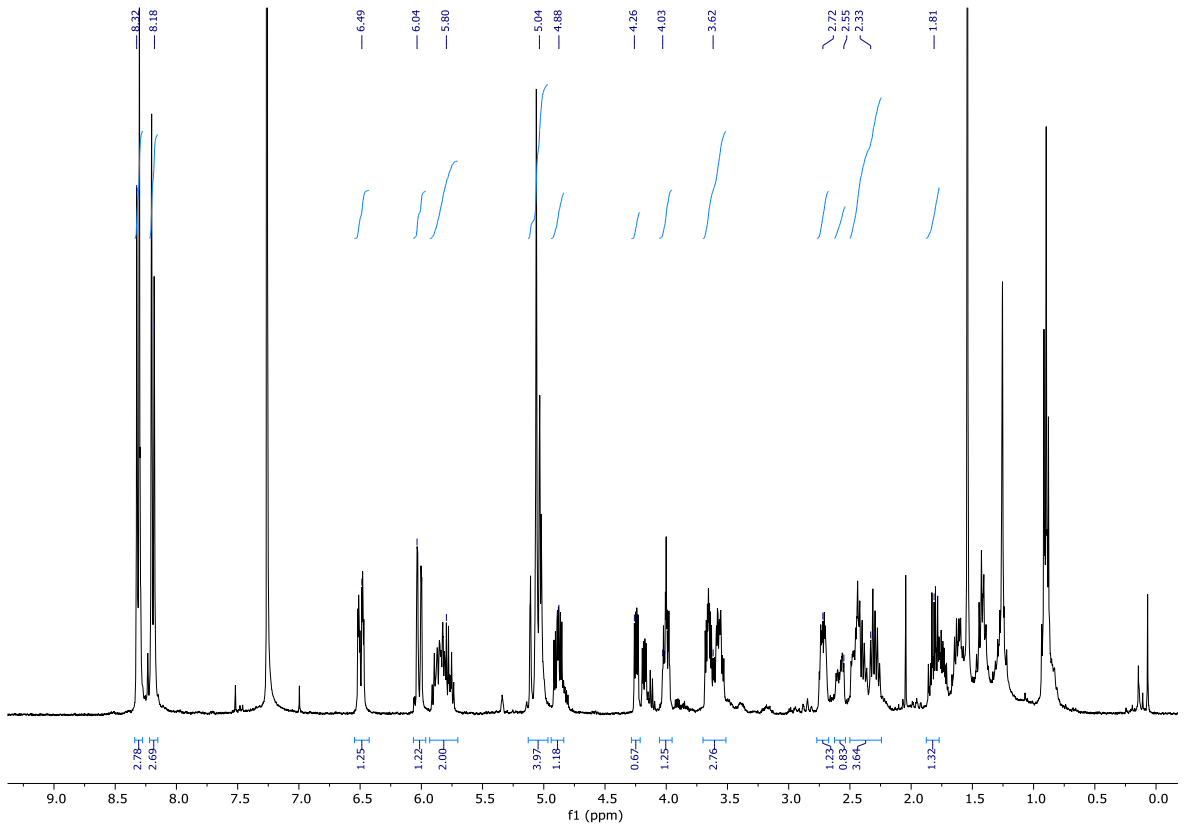
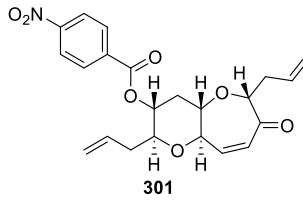


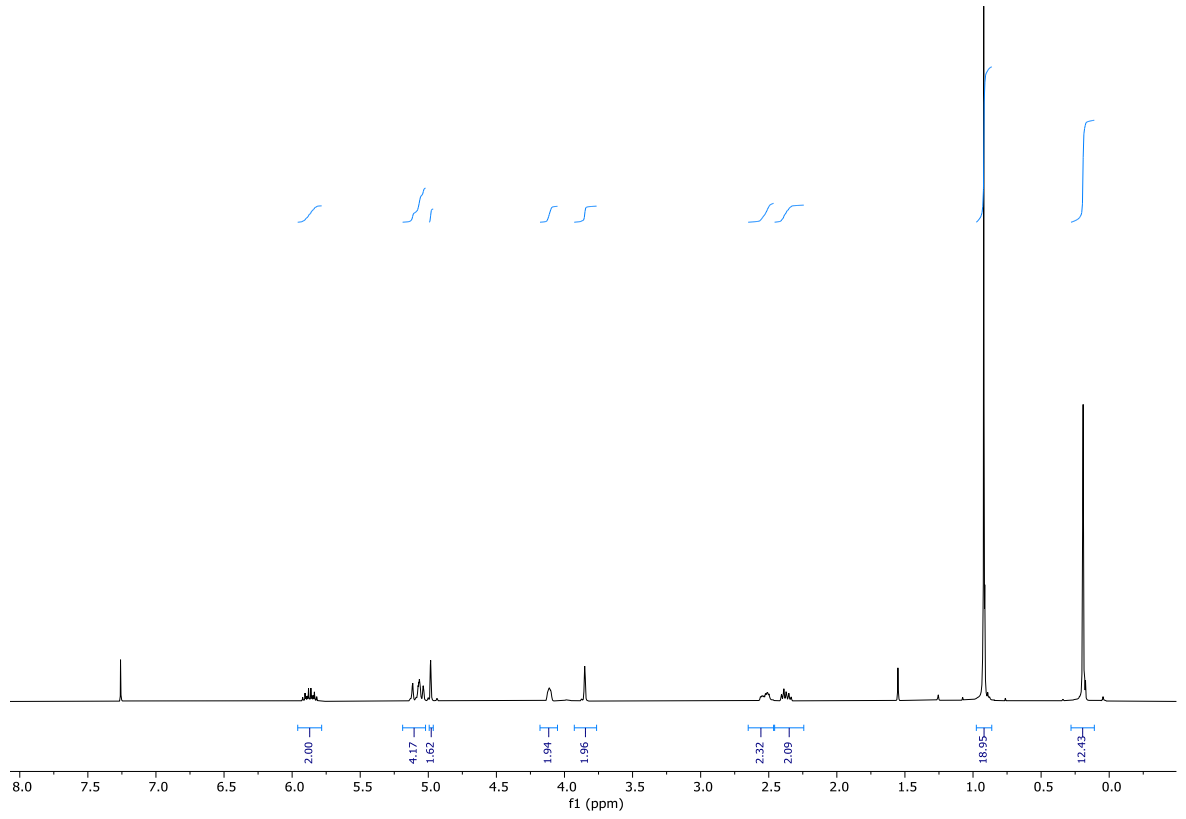
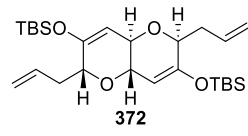




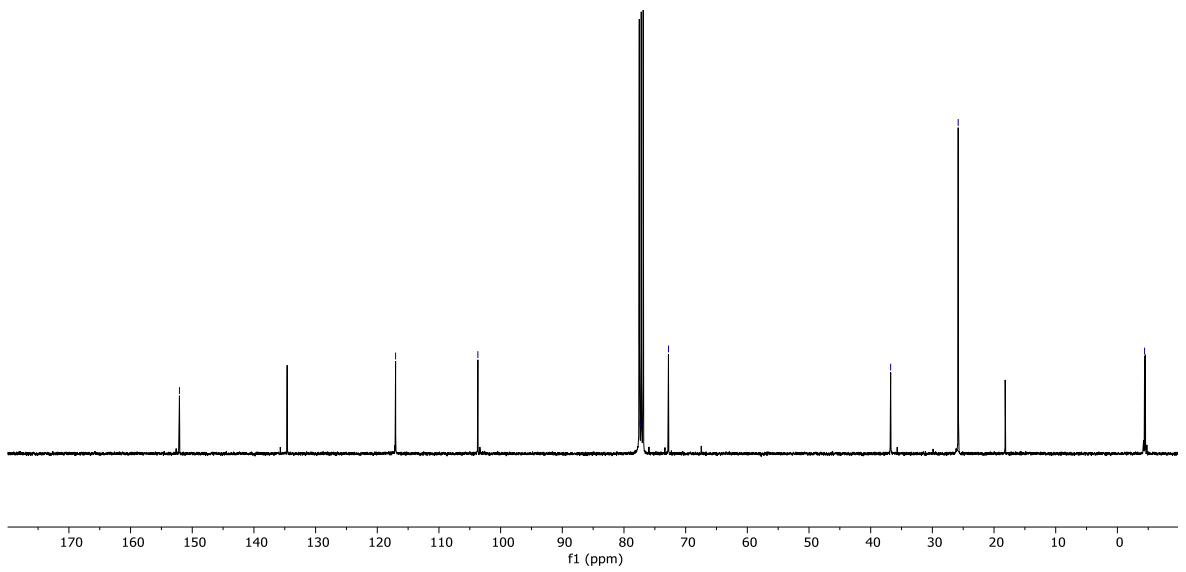


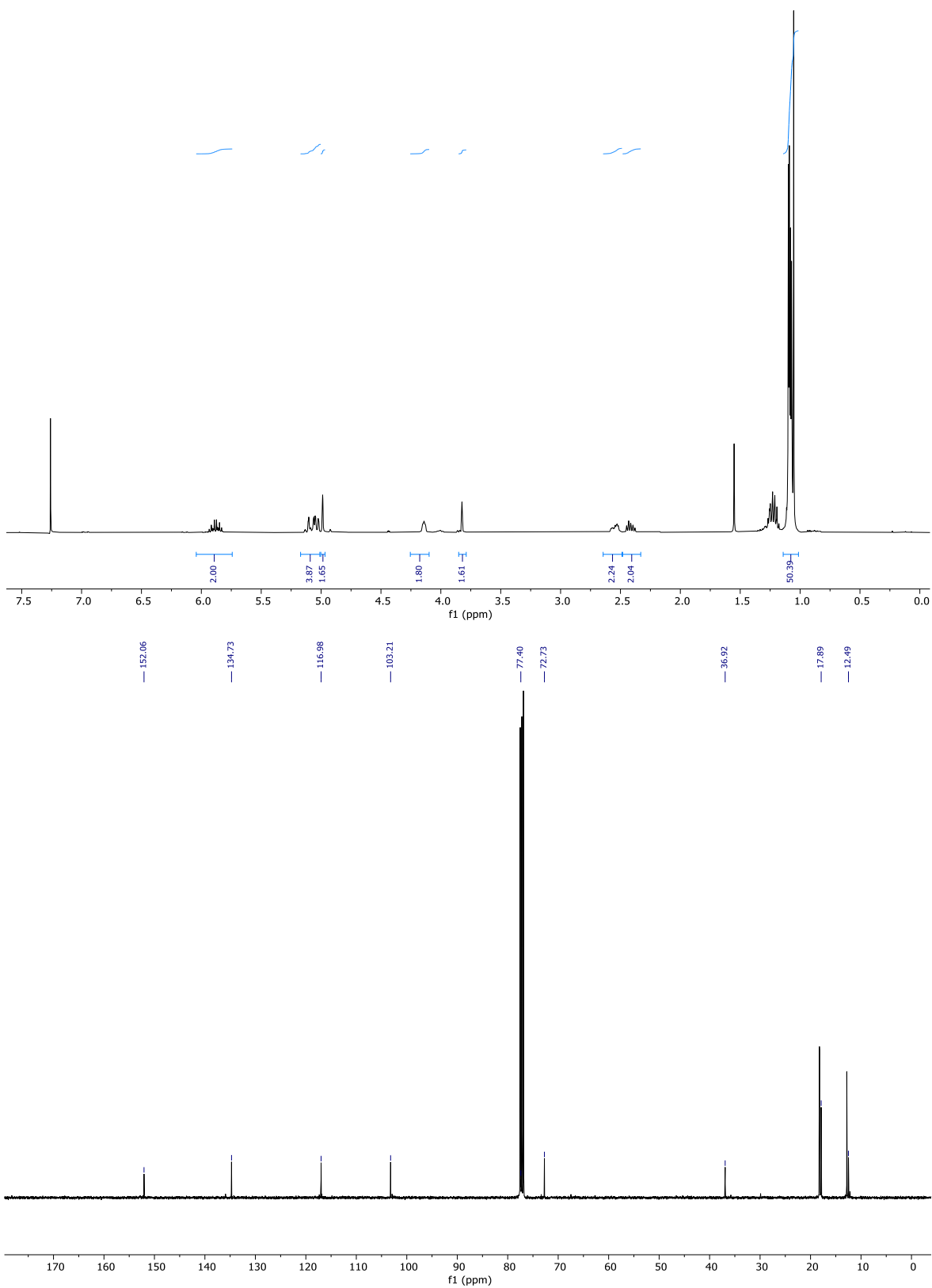
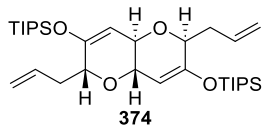




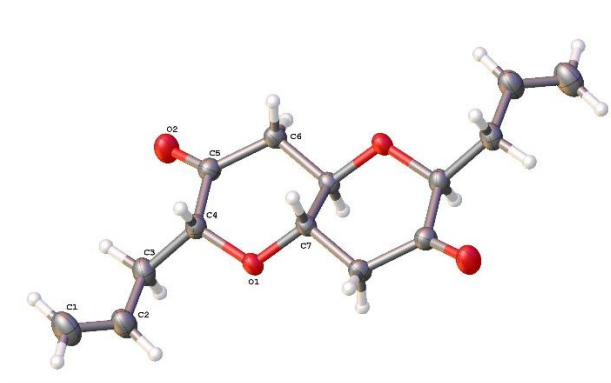


— 152.07 — 117.03 — 103.69 — 77.40 — 72.79 — 36.76 — 25.81 — -4.41





8.2 X-ray crystal structure data



Crystal data

$C_{14}H_{18}O_4$	$D_x = 1.302 \text{ Mg m}^{-3}$
$M_r = 250.28$	Mo K α radiation, $\lambda = 0.71073 \text{ \AA}$
Orthorhombic, <i>Pbca</i>	Cell parameters from 9903 reflections
$a = 9.3231 (6) \text{ \AA}$	$q = 3.1\text{--}28.3^\circ$
$b = 7.2728 (5) \text{ \AA}$	$m = 0.10 \text{ mm}^{-1}$
$c = 18.8340 (13) \text{ \AA}$	$T = 295 \text{ K}$
$V = 1277.04 (15) \text{ \AA}^3$	Block, colourless
$Z = 4$	$0.44 \times 0.43 \times 0.14 \text{ mm}$
$F(000) = 536$	

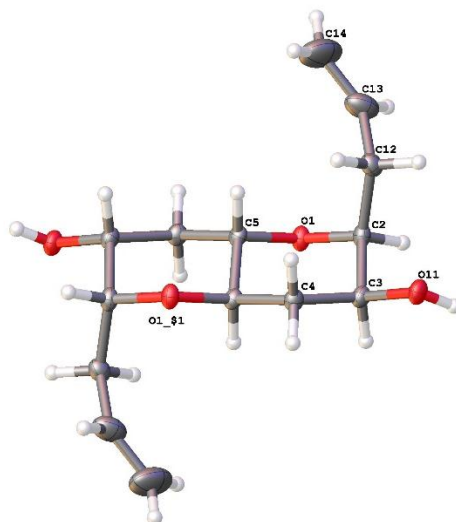
Data collection

Bruker D8 VENTURE diffractometer	1588 independent reflections
Radiation source: microfocus sealed tube, INCOATEC Ims 3.0	1401 reflections with $I > 2\sigma(I)$
Multilayer mirror optics monochromator	$R_{\text{int}} = 0.040$
Detector resolution: $7.4074 \text{ pixels mm}^{-1}$	$q_{\text{max}} = 28.3^\circ$, $q_{\text{min}} = 2.2^\circ$
f and w scans	$h = -12^{\circ}12$
Absorption correction: multi-scan SADABS2016/2 (Bruker,2016/2) was used for absorption correction. $wR2(\text{int})$ was 0.1170 before and 0.0652 after correction. The Ratio of minimum to maximum transmission is 0.9032. The $l/2$ correction factor is Not present.	$k = -9^{\circ}9$
$T_{\text{min}} = 0.674$, $T_{\text{max}} = 0.746$	$l = -25^{\circ}25$

14244 measured reflections	
----------------------------	--

Refinement

Refinement on F^2	Primary atom site location: dual
Least-squares matrix: full	Hydrogen site location: inferred from neighbouring sites
$R[F^2 > 2s(F^2)] = 0.054$	H-atom parameters constrained
$wR(F^2) = 0.161$	$w = 1/[s^2(F_o^2) + (0.0787P)^2 + 0.8406P]$ where $P = (F_o^2 + 2F_c^2)/3$
$S = 1.09$	$(D/s)_{\max} < 0.001$
1588 reflections	$D\tilde{n}_{\max} = 0.44 \text{ e } \text{\AA}^{-3}$
82 parameters	$D\tilde{n}_{\min} = -0.19 \text{ e } \text{\AA}^{-3}$
0 restraints	



Crystal data

$C_{14}H_{22}O_4$	$D_x = 1.111 \text{ Mg m}^{-3}$
$M_r = 254.31$	Mo $K\alpha$ radiation, $\lambda = 0.71073 \text{ \AA}$
Trigonal, $R\bar{3}$	Cell parameters from 2226 reflections
$a = 28.4925 (16) \text{ \AA}$	$q = 2.5\text{--}26.3^\circ$
$c = 4.8658 (3) \text{ \AA}$	$m = 0.08 \text{ mm}^{-1}$
$V = 3420.9 (4) \text{ \AA}^3$	$T = 123 \text{ K}$
$Z = 9$	Rod, colourless
$F(000) = 1242$	$0.31 \times 0.04 \times 0.04 \text{ mm}$

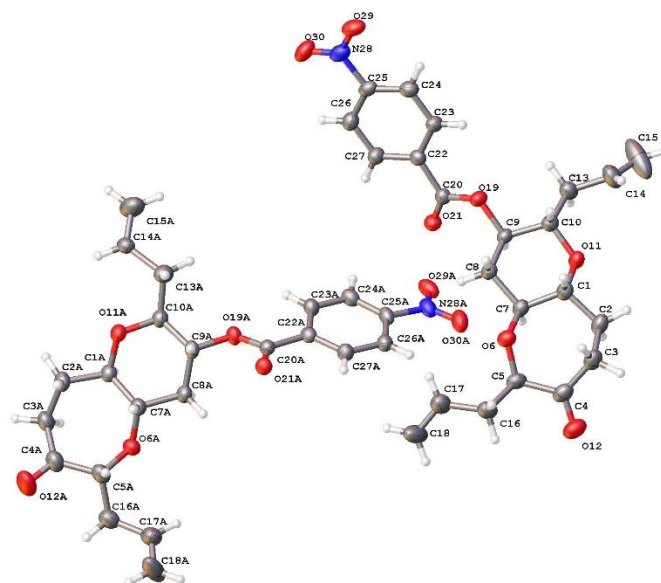
Data collection

Bruker D8 VENTURE diffractometer	1537 independent reflections
Radiation source: microfocus sealed tube, INCOATEC Ims 3.0	1306 reflections with $I > 2\sigma(I)$
Multilayer mirror optics monochromator	$R_{\text{int}} = 0.041$
Detector resolution: $7.4074 \text{ pixels mm}^{-1}$	$q_{\text{max}} = 26.4^\circ$, $q_{\text{min}} = 2.5^\circ$
f and w scans	$h = -35^{\circ}22$
Absorption correction: multi-scan SADABS2016/2 (Bruker,2016/2) was used for absorption correction. $wR2(\text{int})$ was 0.0653 before and 0.0499 after correction. The Ratio of minimum to maximum transmission is 0.8265. The $l/2$ correction factor is Not present.	$k = -21^{\circ}35$

$T_{\min} = 0.616, T_{\max} = 0.745$	$l = -4^{\circ}6$
3908 measured reflections	

Refinement

Refinement on F^2	0 restraints
Least-squares matrix: full	Hydrogen site location: mixed
$R[F^2 > 2s(F^2)] = 0.054$	H atoms treated by a mixture of independent and constrained refinement
$wR(F^2) = 0.181$	$w = 1/[s^2(F_o^2) + (0.150P)^2 + 9.9404P]$ where $P = (F_o^2 + 2F_c^2)/3$
$S = 0.79$	$(D/s)_{\max} < 0.001$
1537 reflections	$D\tilde{\rho}_{\max} = 0.30 \text{ e } \text{\AA}^{-3}$
86 parameters	$D\tilde{\rho}_{\min} = -0.26 \text{ e } \text{\AA}^{-3}$



Crystal data

$C_{22}H_{25}NO_7$	$Z = 2$
$M_r = 415.43$	$F(000) = 440$
Triclinic, $P1$	$D_x = 1.318 \text{ Mg m}^{-3}$
$a = 4.8182 (2) \text{ \AA}$	Cu $K\alpha$ radiation, $\lambda = 1.54184 \text{ \AA}$
$b = 12.4928 (3) \text{ \AA}$	Cell parameters from 12784 reflections
$c = 17.5741 (4) \text{ \AA}$	$q = 2.5\text{--}74.1^\circ$
$a = 96.115 (2)^\circ$	$m = 0.82 \text{ mm}^{-1}$
$b = 95.436 (2)^\circ$	$T = 293 \text{ K}$
$\gamma = 90.552 (2)^\circ$	Plate, colourless
$V = 1046.88 (6) \text{ \AA}^3$	$0.18 \times 0.08 \times 0.02 \text{ mm}$

Data collection

Rigaku 007HF diffractometer equipped with Arc)Sec VHF Varimax confocal mirrors and a UG2 goniometer and HyPix 6000HE detector	14542 measured reflections
Radiation source: Rotating anode, Rigaku 007 HF	14542 independent reflections
Mirror monochromator	13049 reflections with $I > 2s(I)$
Detector resolution: $10 \text{ pixels mm}^{-1}$	$q_{\text{max}} = 75.8^\circ$, $q_{\text{min}} = 2.5^\circ$
profile data from w -scans	$h = -6^{\circ}6$

Absorption correction: multi-scan <i>CrysAlis PRO</i> 1.171.42.80a (Rigaku Oxford Diffraction, 2023) Empirical absorption correction using spherical harmonics, implemented in SCALE3 ABSPACK scaling algorithm.	$k = -15^{\circ}15$
$T_{\min} = 0.073, T_{\max} = 1.000$	$l = -21^{\circ}21$

Refinement

Refinement on F^2	H-atom parameters constrained
Least-squares matrix: full	$w = 1/[s^2(F_o^2) + (0.1466P)^2 + 0.1856P]$ where $P = (F_o^2 + 2F_c^2)/3$
$R[F^2 > 2s(F^2)] = 0.069$	$(D/s)_{\max} = 0.001$
$wR(F^2) = 0.206$	$D\tilde{n}_{\max} = 0.41 \text{ e } \text{\AA}^{-3}$
$S = 1.09$	$D\tilde{n}_{\min} = -0.32 \text{ e } \text{\AA}^{-3}$
14542 reflections	Extinction correction: <i>SHELXL2018/3</i> (Sheldrick 2018), $F_c^* = kFc[1 + 0.001 \times Fc^2 / \sin(2q)]^{-1/4}$
583 parameters	Extinction coefficient: 0.019 (4)
58 restraints	Absolute structure: refined for each of the twin components
Hydrogen site location: inferred from neighbouring sites	Absolute structure parameter: 0.06 (9)

Special details

<i>Geometry.</i> All esds (except the esd in the dihedral angle between two l.s. planes) are estimated using the full covariance matrix. The cell esds are taken into account individually in the estimation of esds in distances, angles and torsion angles; correlations between esds in cell parameters are only used when they are defined by crystal symmetry. An approximate (isotropic) treatment of cell esds is used for estimating esds involving l.s. planes.
<i>Refinement.</i> Refined as a 4-component twin.